Seismic Hazard, Tectonics, and Geomorphology of the Southern Sierra Nevada Range and Southern Walker Lane Belt, California

FRIENDS OF THE PLEISTOCENE

PACIFIC CELL FIELD TRIP

SEPTEMBER 15 TO 18, 2011

Introduction

Welcome, all Friends of the Pleistocene, back to the Golden State of California for the 2011 Pacific Cell FOP Field Trip. We're glad you have all joined us on this trip, and feel especially honored to take our turn as the stewards of this elite and venerable non-institution. We hope you enjoy what we have to share and find this little corner of California as interesting (and fun) as we do.

The foundation and inspiration for this trip is our desire to share several years of data collection and analysis performed by consulting geologists at Fugro William Lettis & Associates and URS Corporation (in collaboration with geologists from AMEC and Kleinfelder) to characterize seismic hazard at the Isabella Project, a set of two earth fill dams operated by the U.S. Army Corps of Engineers. We owe a special thanks to the Corps, particularly Ronn Rose and David Serafini, for generously allowing the findings from this project to be presented on this trip.

Main and Auxiliary dams of the US Army Corps of Engineers Isabella Project (Kozlowicz)

This year's FOP is the product of many collaborators and trip presenters who have all donated their time and resources to make this trip happen. The organizers are:

Andy Lutz	(lutz@lettisci.com)	Keith Kelson	(k.kelson@fugro.com)
Colin Amos	(cbamos@berkeley.edu)	Dave Simpson	(david_simpson@urscorp.com)
Angela Jayko	(ajayko@usgs.gov)	Ben Kozlowicz	(benjamin_kozlowicz@urscorp.com)

We would like to take responsibility for the contents of this guidebook. If contributions are not correctly formatted or displayed, please blame Andy. However, we are not responsible for the content of individual contributions beyond our own.

Many thanks to those that contributed content to the guidebook and are presenting the field trip stops:

Cooper Brossy	(c.brossy@fugro.com)	Andrea Figueroa	(figgygeo@gmail.com)
Paul Hancock	(pack@qnet.com)	Rob Negrini	(rnegrini@csub.edu)
Jeff Knott	(jknott@fullerton.edu)	Jay Rehor	(jay_rehor@urscorp.com)
Janet Sowers	(j.sowers@fugro.com)	Ashley Streig	(streig@uoregon.edu)
Rob Turner	(r.turner@fugro.com)	Jeff Unruh	(unruh@lettisci.com)
Dave Wagner	(dave.wagner@suddenlink.net)		

Tremendous thanks are due to a number of people who helped us get this field trip off the ground, including Scott Hinkle for donating his backhoe and time, Dell McCollough for allowing us to re-excavate a trench on his property, Paul Hancock for his logistical help on the east side, and the Coso Operating Company, USFS, and BLM for camping access to their properties.

So with that said, here's to many more good times with great friends and great rocks!

Let's go to the FOP!

Itinerary and Table of Contents

The plan for this weekend is to field trip across the southern Sierra Nevada and visit locations where we can review some of the tectonic and geomorphic features that record the late Quaternary history of this range. Some stops will necessarily be overviews, but we've included plenty of places to get your hands and boots dirty as well.

The roads along this trip are generally quite good, and a 2-wheel-drive vehicle should suffice everywhere except maybe **Stop 1-3**, so please follow our logistical suggestions below. Also, parking will be a little tight for **Stops 1-3** and **2-1**, so try to coordinate with each other and check out the notes below.

Thursday September 15, 2011			
Thursday Night Camp: **Keyesville Recreation Area** [35.6317°, -118.5005°]	Note: Cookstove permits available online at: www.fs.fed.us/r5/sequoia/passespermits/campfire_permit/campfire-index.html		Page 6
Friday September 16, 2011 **(Route map on page 9)**			
Location	**Speaker(s)**	**Title**	
Kern River Gorge: From Thursday camp to **Stop 1-1**		Road Log A-A′	Page 12
Stop 1-1: **Kern Gorge fault** Rancheria Rd at CA-178 [35.4197°, -118.8325°]	Andy Lutz	(**1-1a**) Opening welcome and Regional overview of strain patterns in the southern Sierra Nevada	Page 13
	Andrea Figueroa Jeff Knott	(**1-1b**) Tectonic geomorphology of the western Sierra Nevada Mountains	Page 22
		(**1-1c**) Modeling the effects of the San Andreas, Garlock faults and Sierra Nevada Frontal fault zone on the uplift of the Sierra Nevada Mountains	Page 28
	Rob Negrini	(**1-1d**) Bits and Pieces: Kern River Sediments below the Modern Fan Apex	Page 35
	Keith Kelson	(**1-1e**) Scope of the seismic hazard characterization of the Kern Canyon fault for the Isabella Project, California	Page 44
Kern River Gorge: **Stop 1-1** to **Stop 1-2**		Road Log B-B′	Page 49
Stop 1-2: **Bernie Drive paleoseismic site** Bernie Dr at Reeder Dr [35.6049°,-118.4920°]	Andy Lutz	(**1-2a**) Paleoseismic record of earthquakes along the Lake Isabella section of the Kern Canyon fault	Page 51

Note: Before proceeding to Stop 1-3, please consider leaving all low clearance and low occupancy vehicles at the clearing located on your right 0.5 miles after we turn off the dirt road. From there it's a very short drive to Stop 1-3, so try to fill seats.			
Kern Valley to Kern Canyon: **Stop 1-2** to **Stop 1-3**		Road Log C-C′	Page 58
Stop 1-3: **Corral Creek paleoseismic site** [35.8556°, -118.4380°]	Ashley Streig Cooper Brossy Keith Kelson	(**1-3a**) Record of Kern Canyon fault earthquakes at the Corral Creek paleoseismic site	Page 60
	Janet Sowers	**(1-3b)** Soil-Profile Development Principles Applied to an Investigation of the Kern Canyon Fault at Corral Creek, Kern County, California	Page 66
	Jay Rehor	**(1-3c)** History of human occupation in the Kern River Valley	Page 69
Friday Night Camp: **Corral Creek Dispersed Camping Area**	Cookstove permits available online at: www.fs.fed.us/r5/sequoia/passespermits/campfire_permit/campfire-index.html		Page 7
Saturday September 17, 2011 **(Route map on page 10)** **Location**	**Speaker(s)**	**Title**	
Upper Kern Canyon: From camp to Stop 2-1		Road Log D-D′	Page 72
Note: Before departing for Stop 2-1, consider teaming back up with your carpool from yesterday afternoon or with some new friends. Parking at Stop 2-1 is also a little tricky, and it's easy because we'll be driving back by camp on our way to Stop 2-2.			
Stop 2-1: **Kern Canyon Overlook** [36.0409°, -118.4893°]	Keith Kelson	(**2-1a**) Structural and Geomorphic Control on Landscape Evolution by the Kern Canyon Fault near the Little Kern River Valley, Tulare County, California	Page 74
	Colin Amos	(**2-1b**) Late Quaternary slip rate on the Kern Canyon fault at Soda Spring	Page 84
Lower Kern Canyon: **Stop 2-1** to **Stop 2-2**		Road Log E-E′	Page 90
Stop 2-2: **Isabella Project Auxiliary Dam** Barlow Drive, Lake Isabella [35.6440°, -118.4738°]	Keith Kelson	(**2-2a**) Assessment of seismic hazard to the Isabella Project dams	Page 92
	Andy Lutz	(**2-2b**) Fault displacement hazard analysis for the Isabella Project Auxiliary Dam	Page 99
	Dave Simpson	(**2-2c**) Status of the Isabella Project	n/a
Kern Valley to Little Lake via the Kern Plateau: **Stop 2-2** to **Stop 2-3**		Road Log F-F′	Page 111
Stop 2-3: **Little Lake fault zone** US-395 at Little Lake [35.9276°/-117.9089°]	Colin Amos	(**2-3a**) Late Quaternary tectonic, geomorphic, and volcanic interactions in the Little Lake Area	Page 114
	Colin Amos	(**2-3b**) Fossil Falls overlook	n/a

	Dave Wagner	(**2-3c**) Sneak preview of Sunday's optional Stop 3-2	n/a
Little Lake to Rose Valley: **Stop 2-3** to **Stop 2-4**		Road Log G-G′	Page 113
Stop 2-4: **The Black Mat!** Coso Junction [36.0541°, -117.9322°]	Angela Jayko	(**2-4a**) Rose Valley Black Mat, Caltrans Quarry Pit	Page 120
	Angela Jayko	(**2-4b**) Anadonta and gastropod ^{14}C ages from the Salt Wells Spillway, China Lake, CA	Page 123
	Angela Jayko	(**2-4c**) Closed basins and abandoned sills along the late Pleistocene Owens River	Page 125
	Sandy Rogers	(**2-4d**) The Borden Collection and the insights it provides on ancient lifeways in Rose Valley, Eastern California, CA	Page 127
Saturday Night Camp: **Coso Ranch**	Now it's time for a little liquid courage as you think up your proposal to lead next year's trip at tonight's business meeting. *FOP needs you!*		Page 8
Sunday September 18, 2011 **(Route map on page 11)**			
Location	**Speaker(s)**	**Title**	
Rose Valley to Owens Valley: Saturday camp to **Stop 3-1**		Road Log H-H′	Page 130
Stop 3-1: **Owens Valley fault** South shore Lake Owens [36.3194°, -117.9633°]	Angela Jayko	(**3-1a**) Historic shorelines and the 1872 Owens Valley earthquake: A rupture segment east of Dirty Socks Spring	Page 131
	Angela Jayko Paul Hancock	(**3-1b**) Late Pleistocene lake deposits and the 1872 rupture south of HWY 190	Page 135
Note: If you're headed home on northbound US-395, or if you aren't in a rush for FOP to end, you are encouraged to visit Stop 3-2 with Dave. We understand if you can't make it (hence the preview on Saturday afternoon).			
Stop 3-2: **Oak Creek** Independence	Dave Wagner	(**3-2**) The Oak Creek Debris Flows of July 12, 2008, Independence, Inyo County, CA	Page 141
End of the 2011 FOP field trip. Thanks for the great times, see you all next year!			

Thursday Night Camp: Keyesville Recreation Area

In line with the grand FOP tradition you are cordially invited to the kick-off camp at the Keyesville Recreation Area in Lake Isabella, California. Appropriately, we'll be camping on an old (mid-Pleistocene to Pliocene?) bedrock terrace of the ancestral Kern River. A couple points to keep in mind:

- Please be careful getting here, especially if you're driving up out of Bakersfield, and especially if you're driving after nightfall. Kern Valley residents (and geologists who work here) know this road well and drive at speeds commensurate with their familiarity. Stay alert and stay alive—this is a dangerous, windy road with no sympathy for texting.
- Access to the Kern River is available here, but please know that this river runs swift and deep at all times of the year. Merle Haggard wrote a song about this.
- Bring your own drinking water, there is none here.
- Get yourself a fire permit if you plan to use a cookstove here. You can do this online at: www.fs.fed.us/r5/sequoia/passespermits/campfire_permit/campfire-index.html.
- This is a dry area and we're visiting during fire season: please lessen the hazard by enjoying our group campfire instead of building your own.

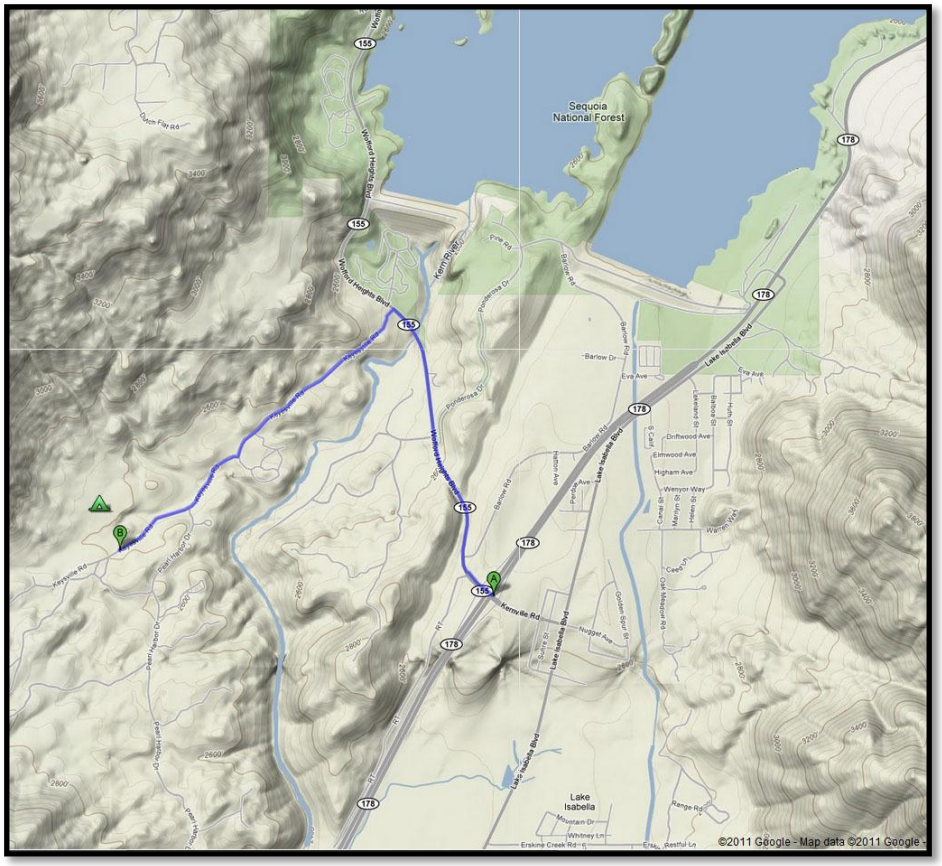

Directions:

From the town of Lake Isabella, travel north from the junction of CA-178 and CA-155 for 1.0 mi.

Turn left into Keyesville Recreation Area (Keyesville Road) after crossing over the Kern River.

Continue on Keyesville Road for 1.0 mi and turn right off the pavement onto Foot Hills Loop Road.

Cross a dry wash and head uphill, bearing generally to the left until you reach a broad, flat area.

Keep to the left and find your friends on the south side of the meadow.

[35.6317°, -118.5005°].

Friday Night Camp: Corral Creek Dispersed Camping Area

On Friday night we'll be camping in Kern Canyon proper. Here's what to expect:

- Since we're a large group in a narrow canyon, camping will be…conslidated. That's okay, we're all friends here. If we run out of room, we can overflow to the Corral Creek Picnic Area which is roughly 0.3 mi to the south on Sierra Highway. Watch for traffic on your walk to the main camp.
- Access to the Kern River is available here, but mind the strong current and slippery rocks and roaring rapids.
- Bring your own drinking water, there's no plumbing on this little gravel bar.
- Get yourself a fire permit if you plan to use a cookstove here. You can do this online at: www.fs.fed.us/r5/sequoia/passespermits/campfire_permit/campfire-index.html.
- This is a dry area and we're visiting during fire season: please lessen your impact on the land by enjoying our group campfire instead of building your own.

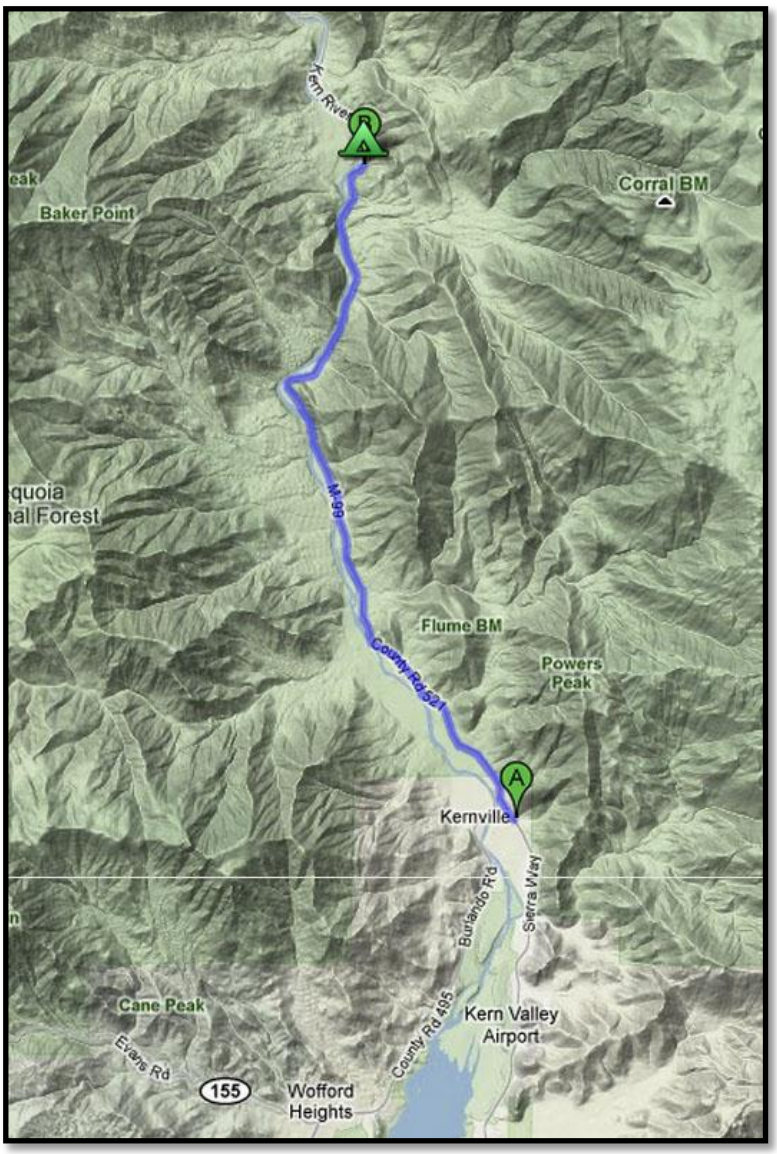

Directions:

From the town of Kernville, go north from the junction of County Road 495 (Kernville Road) and Mountain Highway 99 (Sierra Way).

Drive for 8.7 mi and turn left off pavement into the Corral Creek Dispersed Camping Area.

[35.8618°, -118.4481°].

Saturday Night Camp: Coso Ranch

On Saturday night we'll be camping in Rose Valley on the Coso Ranch. Many thanks to Chris Ellis at the Coso Operating Company for generously arranging our access to this site.

This is a dry area and we're visiting during fire season: please lessen your impact on the land by enjoying our group campfire instead of building your own.

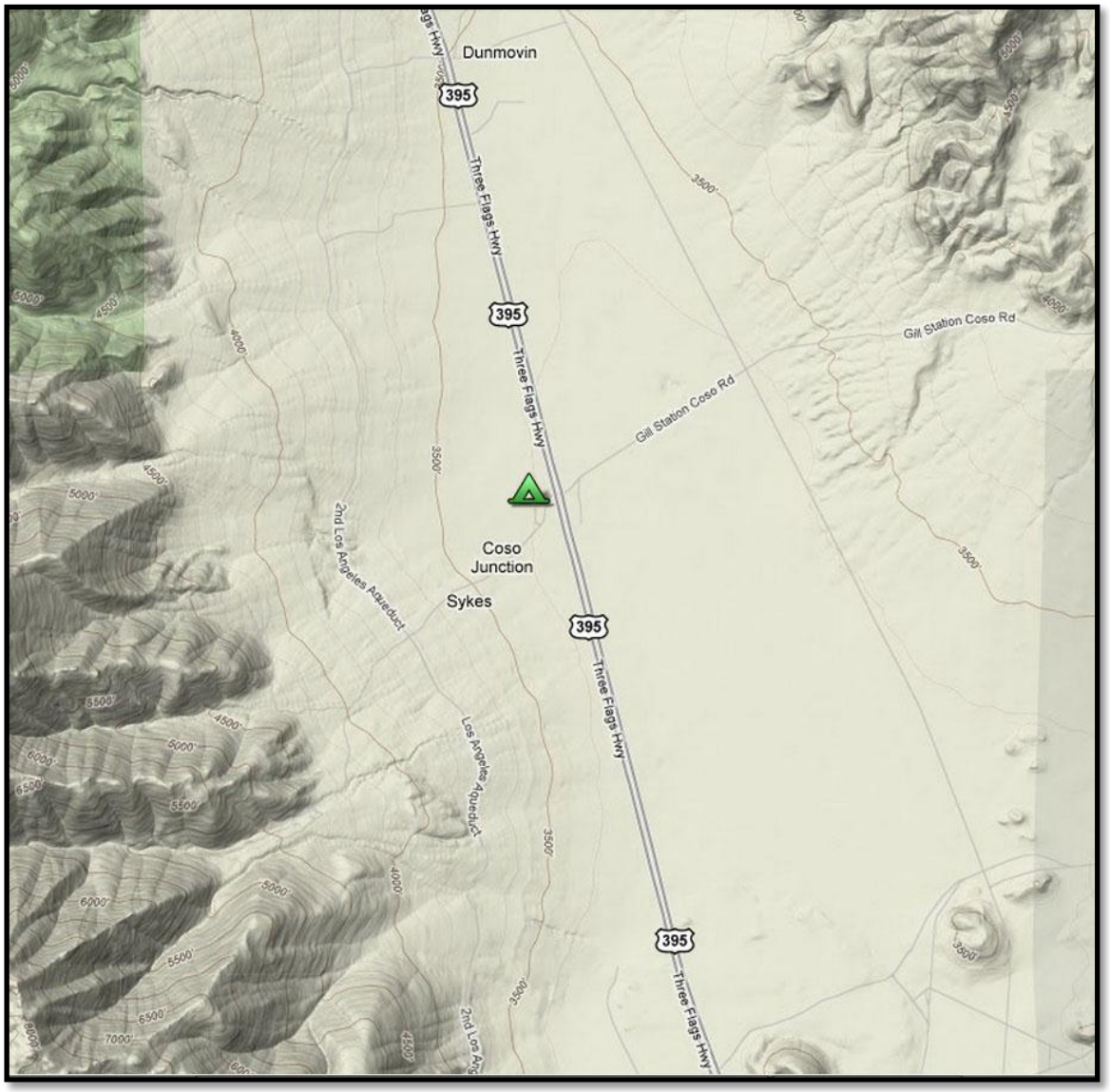

Directions

On the west side of US-395 at Coso Junction is Sykes Road.

Go west on Sykes Road for about 0.2 mi, then turn right into the Coso Ranch.

[36.0440°, -117.9512°]

Route for Day 1:

Stop 1-1: Kern Gorge fault
Stop 1-2: Bernie Drive paleoseismic site
Stop 1-3: Corral Creek trench site
Friday night camp: Corral Creek Camping Area

Let's hit the road out of Keyesville at 8:30 a.m. The drive to **Stop 1-1** takes about 45 minutes and we'll be there about 2 hours. Along our way down the Kern Gorge you'll see some fabulous geomorphology—some of these features are described on Road Log A-A′ (p. 12).

The drive back up canyon to **Stop 1-2** is about 50 minutes long. Road Log B-B′ is basically the reverse of A-A′ with parking instructions and a note about the Erskine Creek debris flow (p. 49). Bring your lunch.

Stop 1-3 is really worth the logistical hassle of getting us all up there, so please bear with. It'll take about 50 minutes to get there. The road up to **Stop 1-3** from the highway is not well graded in key places, and for a stretch it is a one-lane road. We need everyone to help consolidate our group by leaving low-occupancy and 2-wheel-drive vehicles at parking area just up the hill from the highway. See Road Log C-C′ for directions and things to see along the way (p. 58).

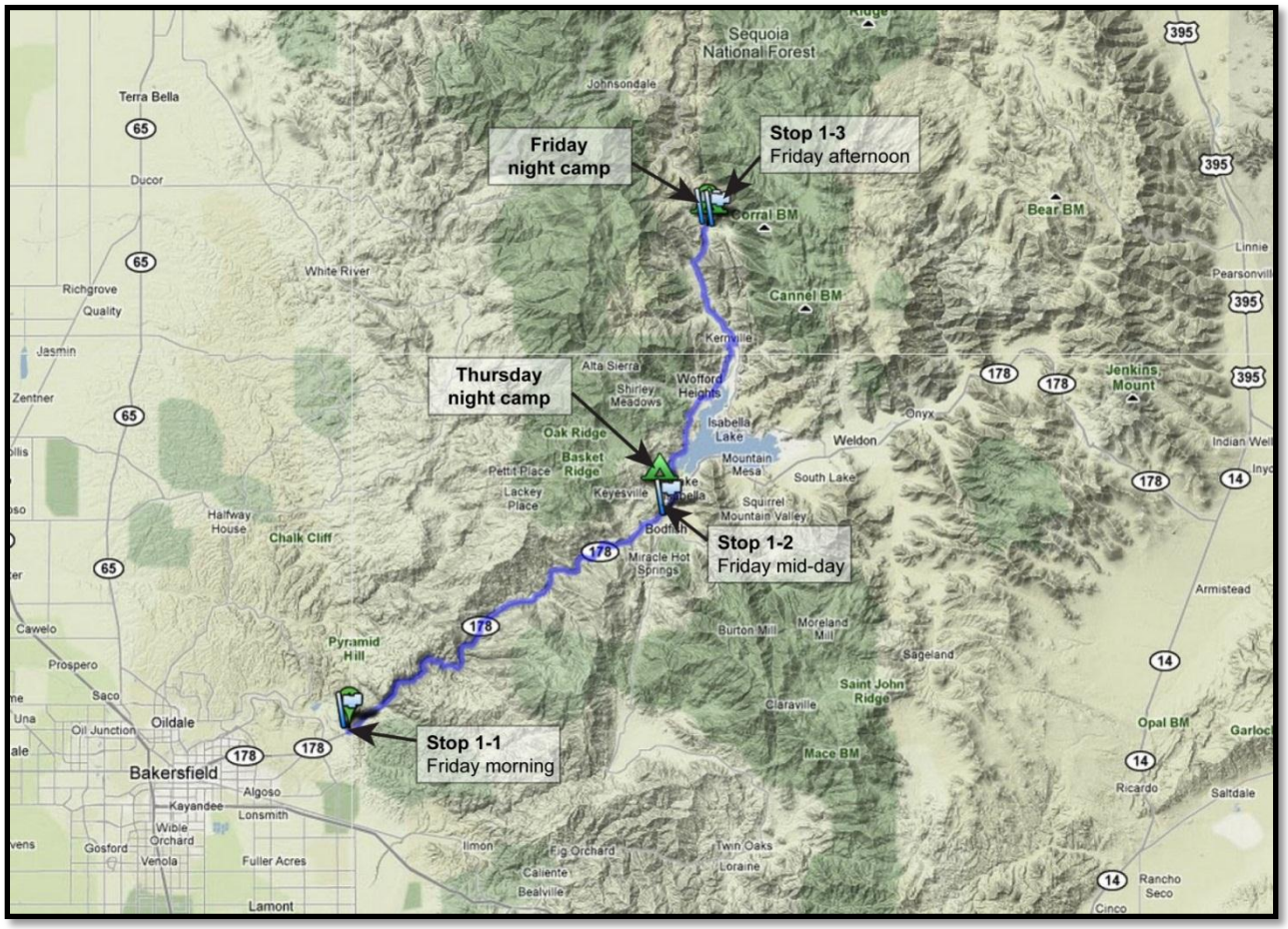

Route Map for Day 2:

Stop 2-1: Rincon overlook
Stop 2-2: Isabella Project Auxiliary Dam
Stop 2-3: Little Lake fault zone
Stop 2-4 (optional): Black Mat site
Saturday night camp: Coso Ranch

Let's leave camp at 8:30 a.m. and head up to see the upper Kern Canyon and some really big views (50 minutes; Road Log D-D′, p. 72). If your ride to the Corral Creek trenches worked well yesterday, then team up again for the first stop to conserve parking space—we'll drive back by camp on the way to **Stop 2-2**.

Heading down canyon, Road Log E-E′ (p. 90) is more or less the reverse of Road Logs C-C′ and D-D′, but maybe you were sleeping or texting or something. See you at **Stop 2-2** for lunch in about 90 minutes.

The trip from **Stop 2-2** to **Stop 2-3** is a fun little road that heads up out of Kern Valley up into the Chimney Creek catchment and onto the Kern Plateau via Chimney Peak Scenic Byway. The payoff is when we descend to Indian Wells Valley via Nine Mile Canyon (Road Log F-F′, p. 111).

Road Log G-G′ (p. 113) gets you to optional **Stop 2-4**, only which we'll visit if there's time left in the day. It's right across the road from camp, about 15 minutes and 9.4 miles.

Route Map for Day 3:

Stop 3-1: Owens Valley fault

Stop 3-2 (optional): Oak Creek Debris Flow

It's been a late night, so let's leave camp at 9:00 a.m.—our first stop is just up the road on the south side of Owens Lake (50 minutes; Road Log H-H′, p. 130). If you'd like to continue on to the north to **Stop 3-2** after this, have a chat with Dave Wagner and he'll give you some info about where to meet up. **Stop 3-2** is just outside of Independence, about an hour's drive from southern Owens Lake.

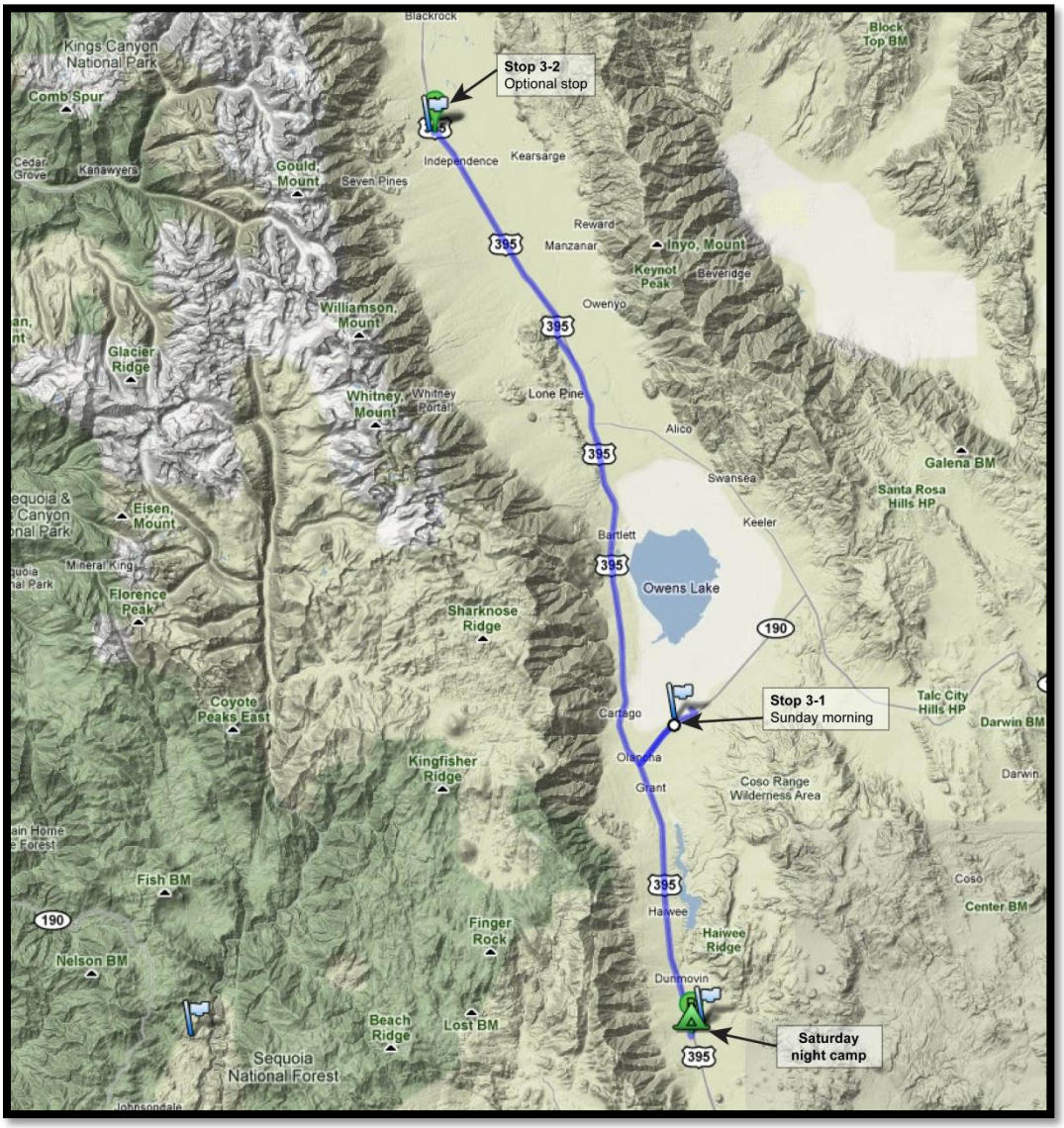

Road Log A-A′

Kernville Recreation Area (Thursday night camp) to Kern Gorge fault (Stop 1-1)

32.3 miles, 45 minutes

Mileage		Lat./Long.
0.0	**Turn RIGHT from Foot Hills Loop Road onto Keyesville Drive (reset odometer)**	**35.6315° -118.4969°**
1.0	**Turn RIGHT onto Wofford Heights Blvd (CA-155)**	**35.6411° -118.4838°**
1.9	Crossing over onto the hanging wall of the Kern Canyon fault (KCF) and into Hot Springs Valley	35.6290° -118.4796°
2.0	**Turn RIGHT onto CA-178 (toward Bakersfield)**	**35.6282° -118.4789°**
2.3	On the right is a high bedrock scarp produced by the Kern Canyon fault, which continues into the distance ahead through a prominent saddle with distinctly different vegetation patterns to the east and west.	35.6234° -118.4821°
3.4	Crossing back onto the footwall of the KCF—to the left are bedrock terraces (elev. 750 m) truncated to the east by the KCF	35.6171° -118.4861°
5.0	Overpass bridges a once-contiguous bedrock terrace (elev. 770 m)	35.5984° -118.5136°
5.3	Several additional lower bedrock terraces to the right (elev. 745 m)	35.5962° -118.5170°
5.9	To the left is the Borel Powerhouse and Penstocks (Kern River No. 2), built from 1897-1904 by the Kern River Co. and now operated by So.Cal. Edison	35.5889° -118.5247°
8.6	The canyon is slightly narrower and the prominent bedrock terrace sets observed in the previous few miles are generally absent, but the river profile does not show any inflections here	35.5760° -118.5616°
13.7	The Kern River Gorge opens slightly between here and mile 17.6—some deeply incised bedrock terraces (elev. 610 and 635 m) are preserved along the north canyon wall (right side)	35.5428° -118.6188°
17.6	The gorge narrows again here and the river starts it's descent into the steepest reach below Isabella Dam—again, bedrock terraces are absent.	35.5217° -118.6726°
18.1	Between here and the mouth of the gorge note a steady increase in relief along over-steepened river margins that rise to meet convex-upward hillslope shoulders and record several tens of meters of incision, increasing to hundreds of meters—this is the top of the Kern River Gorge proper	35.5000° -118.6942°

22.3	The river takes an anomalous 90° turn to the west-northwest where it intersects a bedrock lineament oriented subparallel to the Kern Gorge fault—several low boulder terraces have accumulated because the river gradient is not being steepened as rapidly by incision, consistent with north-northeast-directed tilting of this part of the range…or…dextral displacement?	35.4743° -118.7120°
24.8	The river turns back to the prevailing west-southwestern direction and the longitudinal profile shows another slight nickpoint here	35.4802° -118.7478°
25.0	Remnant boulder terrace along right side of gorge, about 8 m above river	35.4779° -118.7511°
27.6	Kern Gorge Powerhouse (Kern River No. 1), built from 1902-1907 by the Kern River Company and now operated by Southern California Edison—when first online this was the largest hydroelectric facility in the world, providing electric power for Los Angeles. Steep rock debris chute above it across the river.	35.4605° -118.7786°
29.3	Crossing the Kern Gorge fault and Bakersfield city limits	35.4402° -118.7947°
32.0	**Turn RIGHT on Rancheria Road**	**35.4165° -118.8315°**
32.3	**Drive a couple few hundred meters further and park along the right shoulder**	**35.4197° -118.8325°**

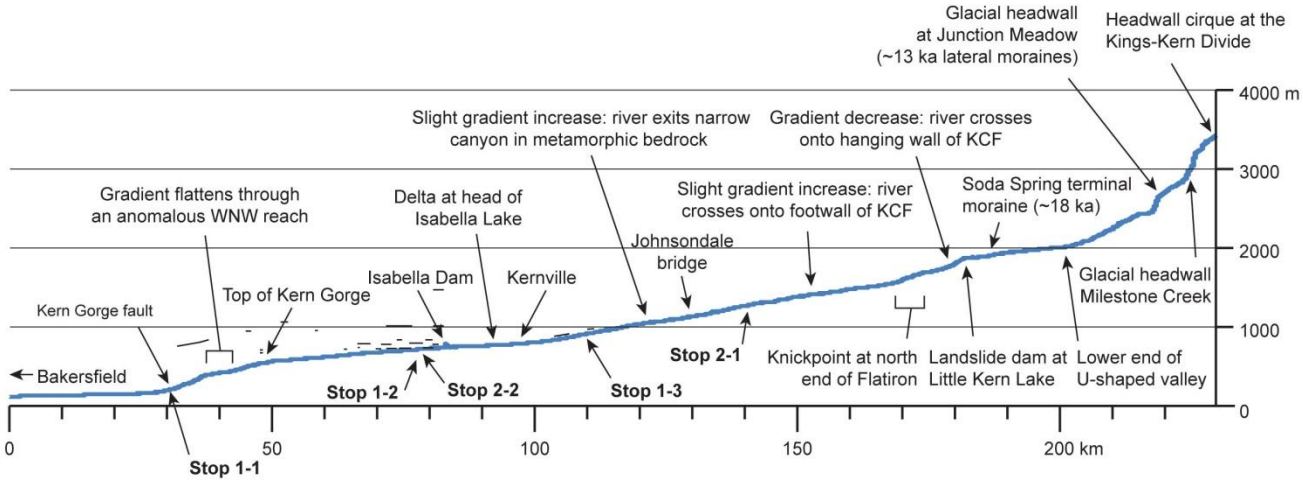

Longitudinal Profile of the Kern River. Profile starts arbitrarily at the Golden State Avenue (CA-204) overcrossing in Bakersfield. Small black lines are approximate locations of bedrock terraces. Vertical exaggeration is 15x.

Stop 1-1a:
Regional overview of strain patterns in the southern Sierra Nevada

Jeff Unruh, *Fugro Consultants**

*currenly: Lettis Consultants International

Introduction

Like most places in California, the existing geologic data that inform our understanding of the southern Sierra Nevada is vast and defies any attempt to summarize into a short talk. However, we consultants have some experience approximating the impossible (scaled of course to the available time and budget, which in this case are zero on both counts), and so in this spirit we've put together a short introduction of a few inter-related topics that we'll be returning to over the course of the trip. These areas of focus are (1) forcing mechanisms driving deformation of the southern Sierra Nevada, including delamination of the mantle lithosphere and regional plate-boundary strain diffusing from the southern Walker Lane fault system into the southern Sierra Nevada, and (2) timing of uplift of the southern Sierra, primarily through an understanding of erosional landscapes preserved in the mountains we'll be travelling through.

The Sierra Nevada and Central Valley are considered at a very broad scale to act as a rigid microplate moving independently block within the broad zone of distributed deformation between the Pacific Plate and the stable interior of North America (Figure 1). This microplate is located between the San Andreas transform system and the Walker Lane fault system which together accommodate most of the North American-Pacific plate boundary motion at a ratio of roughly 3:1, respectively. Although this is accurate at the plate boundary scale, data collected by many workers over the past few decades indicate that the southern Sierra Nevada shares a common late Cenozoic uplift history with the rest of the range but is also responding to regional forces that drive seismogenic deformation.

Large scale vertical tectonics: foundering of the mantle lithosphere

Tomographic analysis of modern seismicity indicates that the southeastern Sierra Nevada range south of about 37° latitude is characterized by elevated levels of background seismicity that coincide with the presence of relatively thin crust (about 35 km) and higher heat flow (32 to 57 mW/m^2) than the foothills to the west, where crustal thickness is approximately 41 km and heat flow values range from 18 to 21 mW/m^2 (Ruppert et al., 1998; Saltus and Lachenbruch, 1991). This zone of thicker crust coincides with the position of a narrow, vertically elongate zone of high P-wave velocity in the upper mantle located west of (and below, obviously) Isabella Lake, known as the Isabella anomaly (Benz and Zandt, 1993), and interpreted as a cold and acoustically fast section of lower lithosphere that has separated from the crust and is descending into the asthenosphere (Saleeby et al., 2003; Boyd et al., 2004; Jones et al., 2004; Zandt et al., 2004). The three-dimensional geometry of this feature is suggested by the tomographic data presented in Figure 2 (Unruh and Hauksson, *submitted to Geosphere*). Zandt et al. (2004) interpret a local depression in the Moho above the Isabella anomaly (as interpreted by Ruppert et al., 1998 and Fliedner et al., 2000) as a zone of crustal thickening

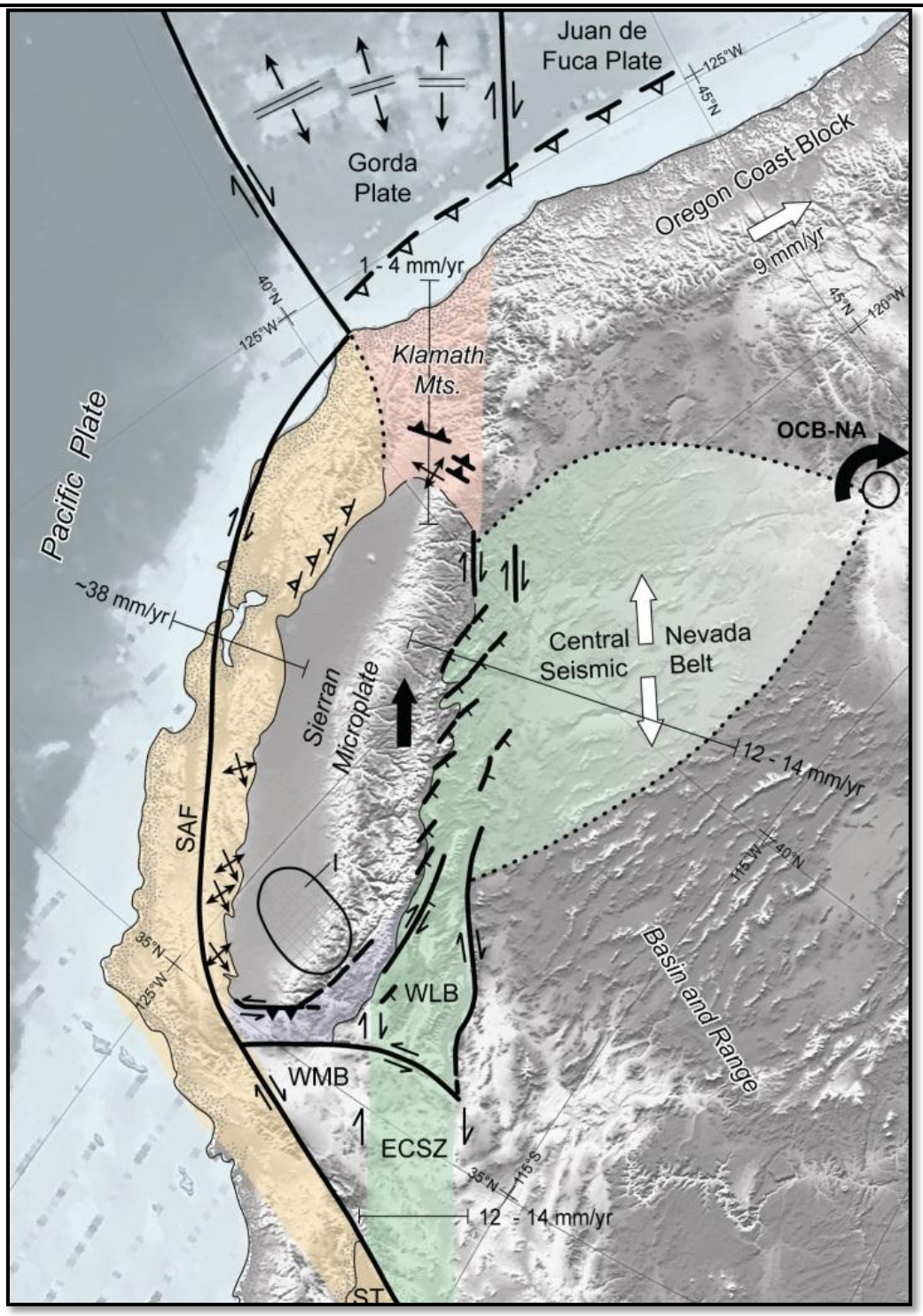

Figure 1. Oblique Mercator map of the western US using the Euler pole for Sierran-North American motion as a basis for projection (modified from Unruh et al., 2003). All vertical lines are parallel to motion of the Sierran microplate with respect to stable North America. Pacific-North American plate motion branches in the northern Salton trough (ST) where roughly 75% of Pa-NA plate motion (yellow) is accommodated by the San Andreas fault (SAF) and related structures and the remaining 25% of the plate motion (green) is transferred across the Mojave block by the Eastern California shear zone (ECSZ) to the Walker Lane belt (WLB) on the east side of the Sierra Nevada. Deformation in the WLB spreads eastward into the central Nevada seismic belt and drives northward motion of the Oregon coast block as clockwise rotation around an Euler pole in eastern Oregon/western Idaho (OCBNA). Some WLB motion steps west across the northern Sierra crest to the southern Cascadia subduction zone and drives crustal shortening in the northern Sacramento Valley (pink band). Note: I = Isabella anomaly

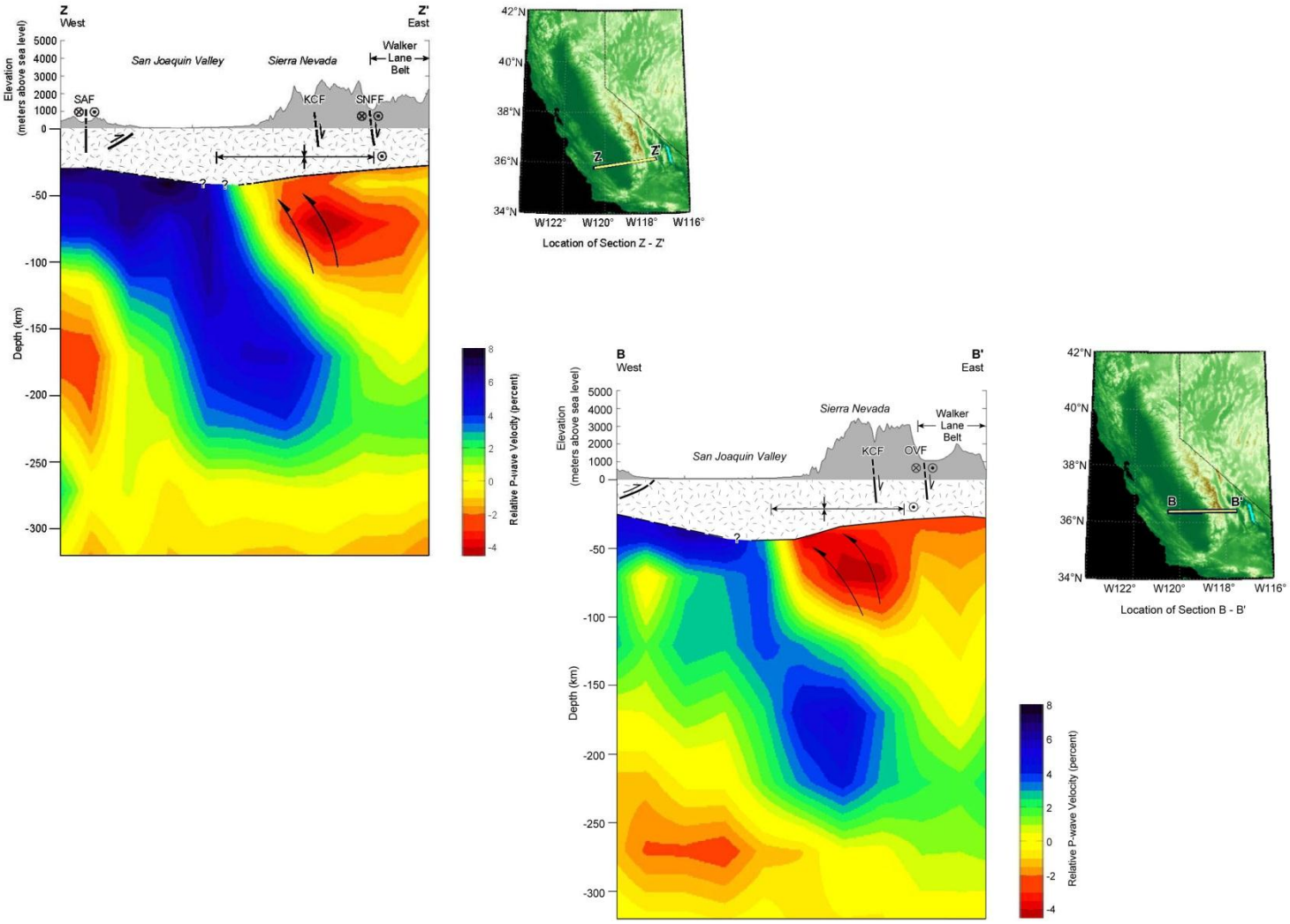

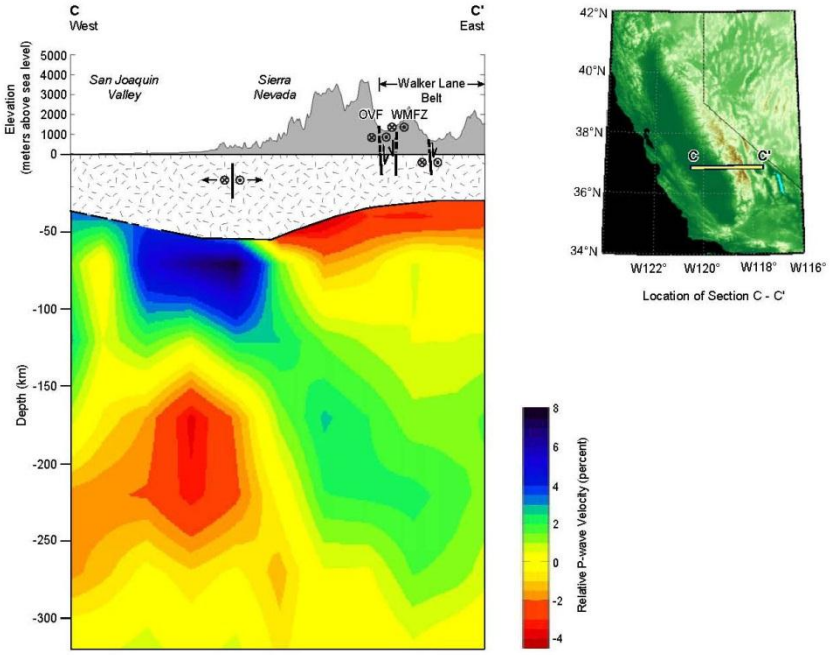

Figure 2. Cross sections of the crust and upper mantle (adapted from Unruh and Hauksson, *submitted to* Geosphere) across the southern Sierra Nevada and San Joaquin Valley showing vertically exaggerated surface topography and positions of the Kern Canyon fault and major faults of the southern Walker Lane belt. Warm colors of the 3D tomographic model (courtesy Craig Jones, Univ. Colorado Boulder) represent zones of low P-wave velocity interpreted in sections X-X′ and B-B′ to represent upwelling of material from the asthenosphere. Cool colors represent high P-wave velocity zones interpreted as foundering eclogitic mantle lithosphere. Section C-C′ is located further north and shows that the mantle drip tapering by about latitude N37°.

above the descending lithosphere. In this model, late Cenozoic uplift of the southern Sierra is driven by the buoyancy of upwelling asthenosphere, which is replacing the descending lithosphere. This interpretation is consistent with evidence for Quaternary subsidence of terminal basins at the south end of the San Joaquin Valley (e.g., Tulare Lake) (Saleeby and Foster, 2004), and that distinctive differences exist in the material properties of the lithosphere beneath the southeastern Sierra Nevada.

Crustal strain patterns in the southern Sierra Nevada

Now shifting our focus slighty higher onto the seismogenic crust we will describe the spatial variation in strain pattern as characterized through kinematic analyses of background microseismicity. The majority of historical earthquakes in the southern Sierra Nevada have occurred along a broad, north-trending band of epicenters generally parallel to and east of the Kern River Canyon, (e.g., the Southern Sierra Nevada Seismic Zone of Jennings, 1994), and a broad band of epicenters trending east-northeast across the southern tail of the range (e.g., the Scodie lineament of Bawden et al., 1999) (Figure 3). The results of kinematic analyses of focal mechanisms (e.g., Unruh et al., 1996.; 1997; 2002; 2003) from groups of earthquakes across the southern Sierra Nevada and San Joaquin Valley provide a snapshot of spatial segregation within the regional deformation field. Figure 4 depicts the horizontal components of the seismogenic deformation as smooth trajectories drawn parallel to the trends of d1 (maximum extension) principal strains and d3 (maximum shortening) principal strains. The seismogenic deformation field is plotted on horizontal two-dimensional sections derived from a three-dimensional tomographic model of P-wave velocities in the crust and upper mantle. The sections used as base maps show lateral velocity variations at depths of 70 km and 170 km. Where both the maximum extensional and shortening strains are sub-horizontal, the trajectories form a grid-like pattern, and the style of crustal deformation is characterized by distributed shearing and strike-slip faulting (i.e., the southern Walker Lane belt). If one of the principal strains is steeply plunging, then it has very little to no horizontal expression and is instead characterized by sub-horizontal extension and vertical shortening (i.e., net crustal thinning and net vertical deformation)—these are areas where only solid maximum-extension trajectories are shown. Specific areas of crustal thinning are shown bounded on Figure 4 with dotted lines and the dominant direction of extension within each area is indicated.

As shown in Figure 4, seismogenic deformation in the southern Walker Lane belt is characterized by WNW-ESE extension and NNE-SSW shortening, consistent with NNW-directed dextral shear approximately parallel to Sierran-North American Plate motion. Deformation in the southern Walker Lane belt is dominated by strike-slip faulting and distributed shear (e.g., Airport Lake fault, Little Lake fault, Owens Valley fault, Panamint Valley fault) with localized zones of extension and shortening related to releasing and restraining slip transfer. The western Sierra foothills east of Fresno are also characterized by horizontal plane strain and shearing, with the principal strains generally parallel to trends in the Walker Lane belt.

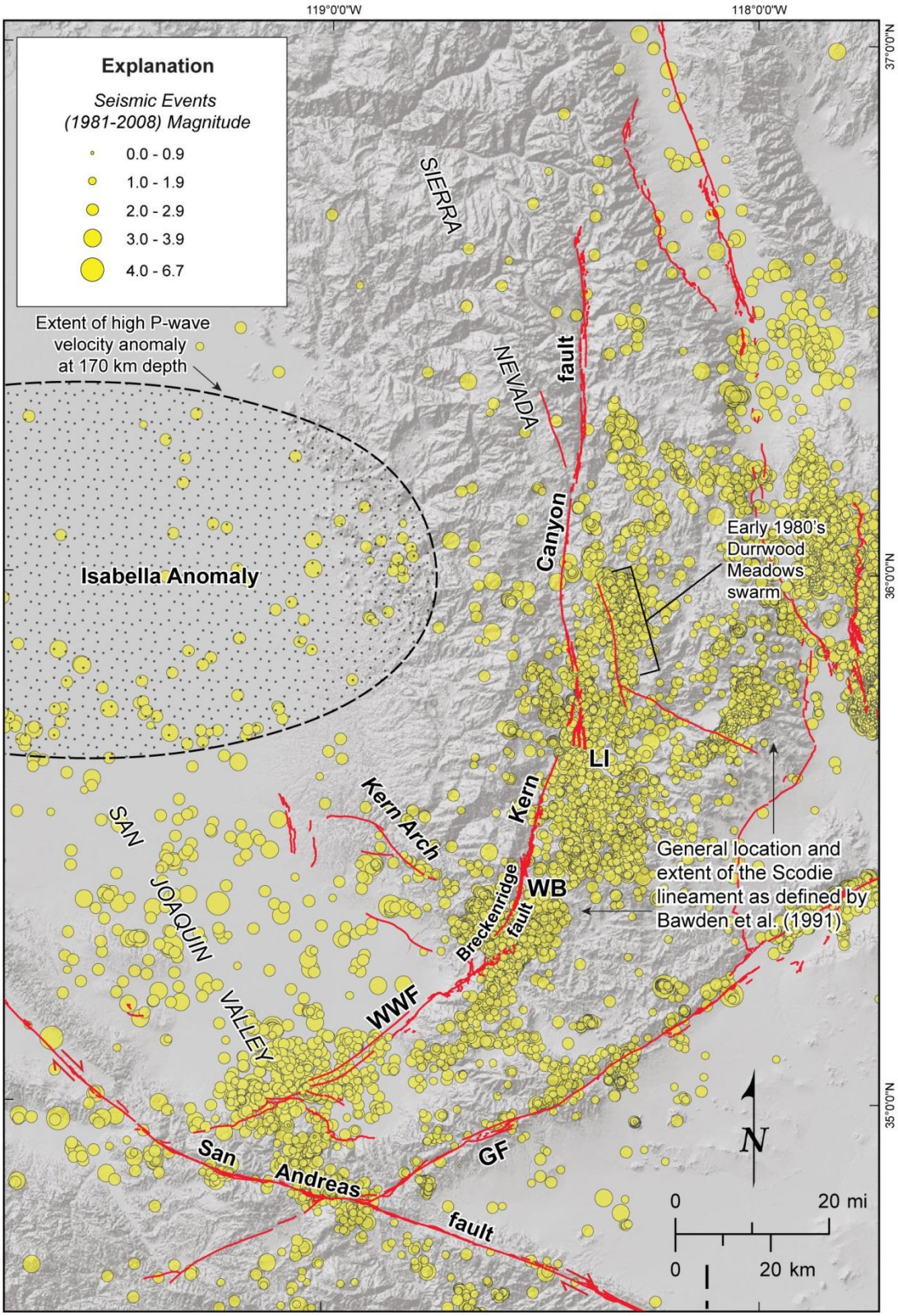

Figure 3. Earthquakes recorded by the Northern and Southern California Seismic Networks for which focal mechanisms have been calculated using the algorithm FPFIT (data provided courtesy of E. Hauksson, Caltech). LI=Lake Isabella;WB=Walker Basin; GF=Garlock fault; WWF=White Wolf fault

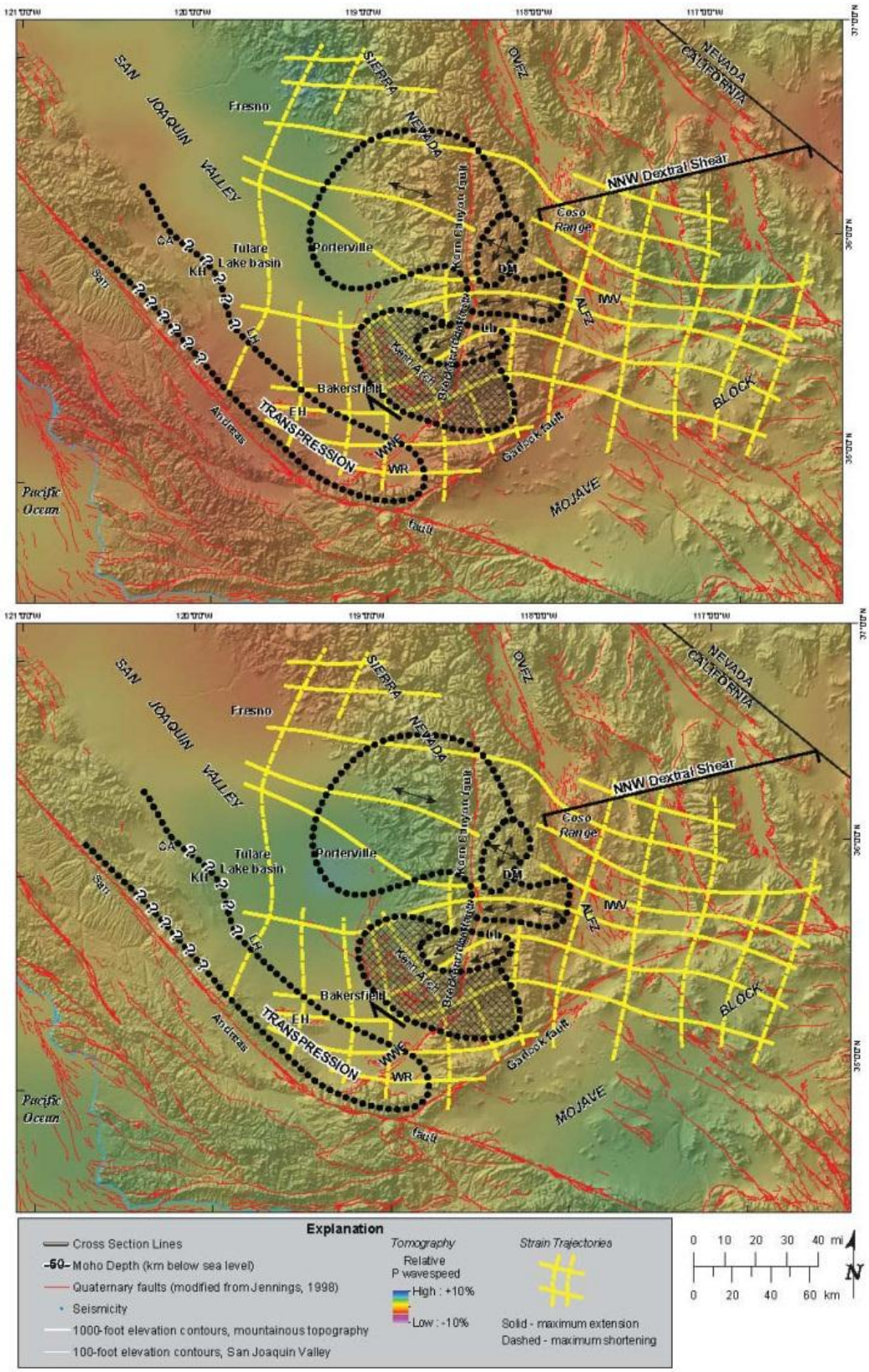

Figure 4. Seismogenic deformation field showing major areas of crustal shearing, extension, and transpression plotted on 70 km (above) and 170 km (below) depth sections through the 3D tomographic model (data courtesy Craig Jones, Univ. Colorado Boulder). Color variations indicate lateral variations in P-wave velocity. LI = Lake Isabella; KCF= Kern Canyon fault; BF = Breckenridge fault; GF = Garlock fault; WWF = White Wolf fault; DM = Durrwood Meadows

Seismogenic deformation between Durrwood Meadows and Walker Basin is characterized by horizontal extension and vertical crustal thinning. This zone of crustal extension includes the north-trending Sierra Nevada seismicity lineament continues from the interior of the Sierra westward across the Kern Canyon fault and to the western Sierran slope, including part of the eastern San Joaquin Valley between Porterville and Fresno. The style and direction of this extension varies locally across southern Sierra Nevada, for example, the crust beneath the western Sierra between Porterville and the northern Kern Canyon fault is characterized by WNW-ESE-directed extension, and the direction of extension underneath the southern end of the Kern Plateau (just north of Isabella Lake) is approximately east-west. An approximately 40-km-long NNE-trending domain east of the Kern Canyon fault that encompasses the mid-1980s Durrwood Meadows earthquake swarm is characterized by extension in two perpendicular horizontal directions (orthogonal pair of arrows on Figure 4) and accommodates extreme thinning and “pancaking” of the crust (Unruh and Hauksson, 2009). The Breckenridge fault and the Kern Canyon fault south of Isabella Lake is characterized by WSW-ENE-directed extension that appears unconnected to the larger, contiguous zone of WSW-ENE-directed extension to the north.

The principal strains in the southwestern Sierra Nevada at the latitude of Walker Basin (shown by cross-hatching on Figure 4) are rotated distinctly counterclockwise from regional trends to the east and west. Both principal strains are subhorizontal indicating that the deformation is characterized by crustal shearing. In this strain regime, vertical faults optimally oriented to accommodate dextral shear would predictably strike WNW-ESE, that is, about 45° to 60° more westerly than the San Andreas fault or dextral faults in the Walker Lane belt.

In contrast to the deformation character described thus far, analysis of focal mechanisms delineate a narrow zone of transpressional deformation directly east of the San Andreas fault (Figure 4). East of this zone, deformation in the central part of the southern San Joaquin Valley is characterized by horizontal plane strain and dextral shear subparallel to the San Andreas fault.

References

Boyd, O.S., Jones, C.H., and Sheehan, A.F., 2004. Foundering lithosphere imaged beneath southern Sierra Nevada, California, USA. Science 305: 660–662.

Fliedner, M., Klemperer, S.L., and Christensen, N.I., 2000. Three-dimensional seismic model of the Sierra Nevada arc, California, and its implications for crustal and upper mantle composition. Journal of Geophysical Research 105: 10,899–10, 921.

Jennings, C.W., 1994. Fault activity map of California and adjacent areas, with locations of recent volcanic eruptions. California Division of Mines and Geology geologic data map no. 6, scale 1:750,000 with explanatory text, 92 pp.

Jones, C.H., Farmer, G.L., and Unruh, J.R., 2004. Tectonics of Pliocene removal of lithosphere of the Sierra Nevada, California. Geological Society of America Bulletin 116: 1408–1422.

Ruppert, S., Fliedner, M.M., and Zandt, G., 1998. Thin crust and active upper mantle beneath the southern Sierra Nevada in the western United States. Tectonophysics 286: 237–252.

Saleeby, J., and Foster, Z., 2004. Topographic response to mantle lithosphere removal in the southern Sierra Nevada region, California. Geology 32(3): 245–248.

Saleeby, J.B., Ducea, M.N., and Clements-Knott, D., 2003. Production and loss of high-density batholithic root: Southern Sierra Nevada, California. Tectonics 22(6): 24 pp.(doi:10.1029/2002TC001374).

Unruh, J., and Hauksson, E., 2009. Seismotectonics of an evolving intracontinental plate boundary: Southeastern California. In: Late Cenozoic structure and evolution of the Great Basin-Sierra Nevada transition, ed. by Oldow, J.S., and Cashman, P.H. Geological Society of America Special Paper 447: 351–372.

Unruh, J.R., Twiss, R.J., and Hauksson, E., 1996. Seismogenic deformation field in the Mojave block and implications for the tectonics of the eastern California shear zone. Journal of Geophysical Research 101(B4): 8335–8362.

Unruh, J.R., Twiss, R.J., and Hauksson, E., 1997. Kinematics of post-seismic relaxation from aftershocks of the 1994 Northridge, California, earthquake. Journal of Geophysical Research 102: 24,589–24,603.

Unruh, J.R., Hauksson, E., Monastero F.C., Twiss, R.J., and Lewis, J.C., 2002. Seismotectonics of the Coso Range-Indian Wells Valley region, California: Transtensional deformation along the southeastern margin of the Sierran microplate. In: Geologic evolution of the Mojave Desert and Southwestern Basin and Range, ed. by Glazner, A.F., Walker, J.D., and Bartley, J.M. Boulder, Colorado: Geological Society of America Memoir 195: 277– 294.

Unruh, J., Humphrey, J., and Barron, A., 2003. Transtensional model for the Sierra Nevada frontal fault system: Eastern California. Geology 31: 327–330.

Saltus, R.W., and Lachenbruch, A.H., 1991. Thermal evolution of the Sierra Nevada: Tectonic implications of new heat flow data. Tectonics 10: 325–344.

Zandt, G., Gilbert, H., Owens, T.J., Ducea, M., Saleeby, J., and Jones, C.H., 2004. Active foundering of a continental arc root beneath the southern Sierra Nevada, California. Nature 431: 41–46.

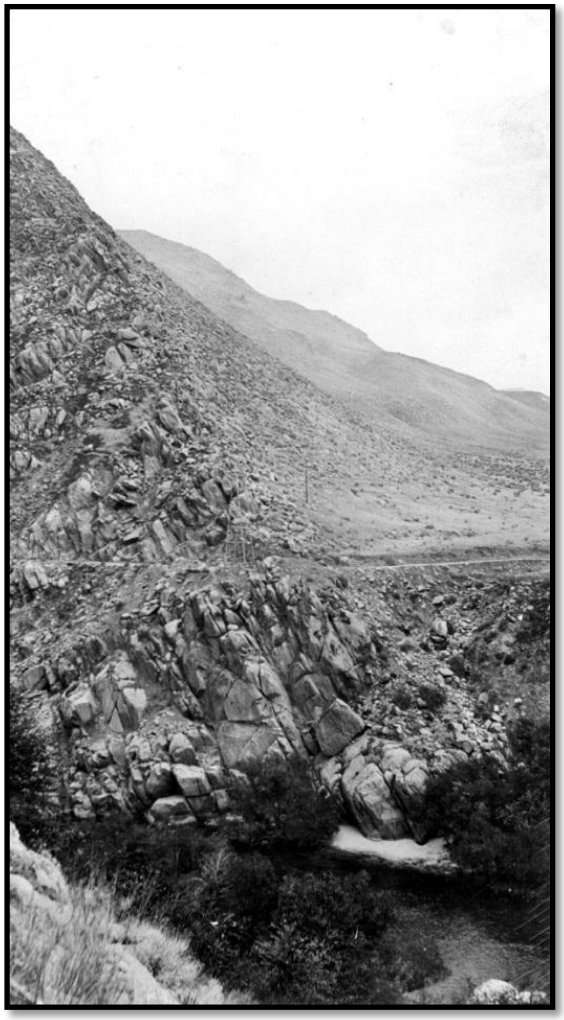

Photographs of the Kern Gorge fault at the Kern River by G.K. Gilbert taken in 1903 (Gilbert, 1928)

Stop 1-1b:
Tectonic geomorphology of the western Sierra Nevada Mountains, CA

Andrea Figueroa, *California State University, Fullerton*

Jeffrey Knott, *California State University, Fullerton*

Abstract

Hypotheses regarding uplift of the Sierra Nevada Mountains (Sierra), California, USA, vary from a single, westward tilting block to rapid Pliocene and/or Quaternary uplift by various mechanisms. To test these hypotheses, we examined geomorphic indices of the western Sierra. We interpret longitudinal profiles of the larger westerly flowing rivers, mountain front sinuosity, valley floor-to-width to height ratio, and relief ratio to show that there are two tectonically active segments of the western Sierra mountain front. Relative tectonic activity is greatest in the southern Sierra near the Kern River Gorge fault. In the central Sierra, the geomorphology indicates lower, but still active, tectonic activity that we hypothesize is consistent with Pliocene delamination. We hypothesize that the locus of tectonism in the south is most consistent with post-Pliocene interaction of the San Andreas, Garlock, and Sierra Nevada Frontal fault zones.

Introduction

Several different hypotheses for the style and mechanism of late Cenozoic Sierra Nevada Mountains, California, USA (Sierra) surface uplift are proposed (e.g., Huber, 1981; Unruh, 1991; Wakabayashi and Sawyer, 2001; Stock et al., 2004). In this study, we apply geomorphic indices to the western mountain front and west-flowing rivers of the Sierra (Fig. 1). We chose geomorphic indices based on their likelihood to record perturbations or reach equilibrium over late Cenozoic time scales.

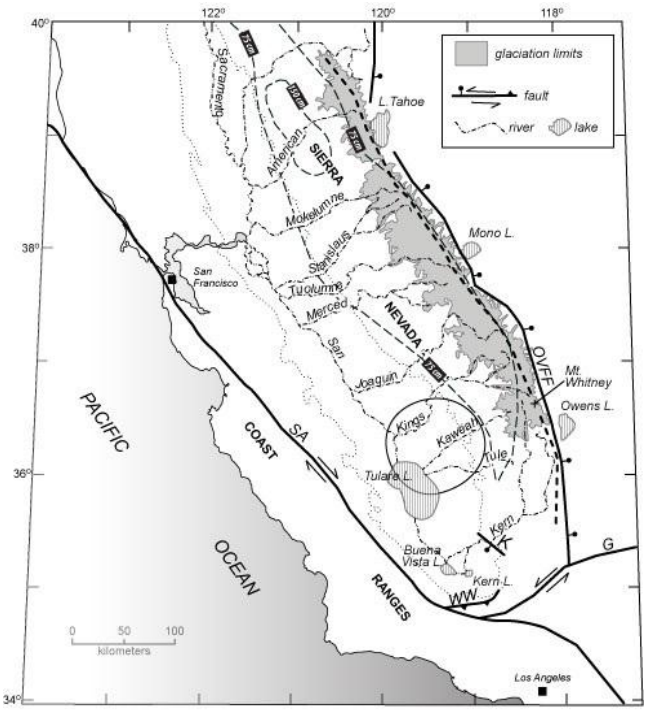

Figure 1. Sierra Nevada and vicinity. Dotted line is edge of San Joaquin and Sacramento River valleys. Long dash line is approximate location of Sierra crest with Mt. Whitney the highest point. The circle is the approx. location of the mantle drip (Saleeby and Saleeby, 2004). Major faults are San Andreas (SA), Garlock (G), Owens Valley frontal fault (OWFF), White Wolf (WW) and Kern River Gorge (K). Ball and bar and barb are on hanging wall for normal and thrust faults, respectively. Strike-slip motion shown by arrows. Precipitation contours for 150 cm/yr and 75 cm/yr are generalized from National Atlas (www.nationalatlas.gov). Limits of glaciation is Tahoe stage of Blackwelder (1931) taken from Atwater et al. (1986).

The most frequently cited mechanism is westerly tilting attributed to normal faulting along the east side of the Sierras (e.g., Huber, 1981; Unruh, 1991). Huber (1981) proposed that the Sierras experienced uniform westward tilting of the entire Sierra from north to south (Fig. 2e).

Wakabayashi and Sawyer (2001) supported this hypothesis by noting that relatively uniform uplift rates inferred from river incision are seen from the Yuba River south to the San Joaquin River (Fig. 1).

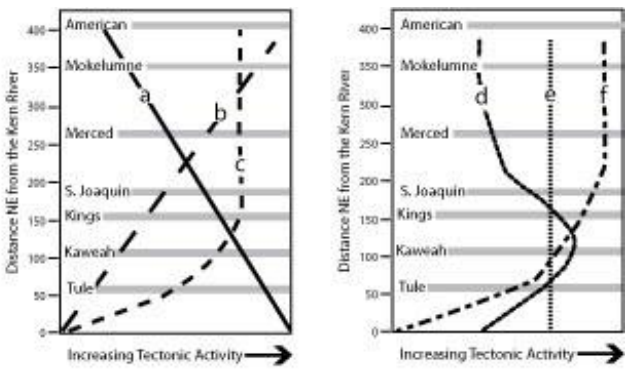

Figure 2. Hypothetical relations between tectonic geomorphic indices and differing tectonic uplift scenarios: a) delamination caused by Basin and Range extension (Ducea and Saleeby, 1998; Liu and Shen, 1998; Manley et al., 2000; Niemi, 2003); b) northward migration of the Mendicino triple junction (Crough, 1977); c) delamination in the central and northern Sierras (Farmer, 2002); d) mantle drip (Saleeby, 2004); e. uniform uplift related to slip on the Owens Valley frontal fault (Wakabayashi and Sawyer, 2001); f) climate-driven isostatic rebound (Small and Anderson, 1995).

Alternatively, Sierran uplift may be in response to the northward migration of the Mendocino triple junction (Crough and Thompson, 1977; Jones et al., 2004). According to this hypothesis, because the triple junction moved from south to north, the southern Sierra have been rising the longest and have therefore experienced the most total uplift (Fig. 2b).

Niemi (2003) proposed that Sierra uplift initiated because of westward migration of Basin and Range extension. Basin and Range extension is thought to have propagated NW since the Miocene and continued through the Quaternary.

Uplift may also be related to delamination of the upper mantle from the lower crust (Ducea and Saleeby, 1998; Liu and Shen, 1998; Manley et al., 2000; Niemi, 2003). As the lower crust delaminated and sank into the mantle, rising asthenosphere induced uplift (Ducea and Saleeby, 1998; Liu and Shen, 1998). The delamination is modeled as a singular event initiated in the late Miocene or early Pliocene (Manley et al., 2000) with the subsequent tectonic impact decreasing through the Quaternary (Fig. 2a).

The locus of delamination is found in the central Sierras near the Kings, Kaweah and Tule Rivers (Farmer et al., 2002; Saleeby and Foster, 2004). The delamination and subsequent mantle instability would have generated a mantle drip structure in the mantle below the Tulare Basin (Saleeby and Foster, 2004). This mantle drip may be pulling down the crust near the Kings, Kaweah, and Tule Rivers (Fig. 2d), generating a basin in this region of the San Joaquin Valley. If Pliocene delamination is driving uplift, then the greatest tectonic activity would be found in the central Sierras (Fig. 2c); however, the effects of any Pliocene delamination in would have decreased through the Quaternary.

Another hypothesis infers that tilting of the Sierras may be in response to isostatic rebound from high rates of glacial erosion (Montgomery, 1994; Small and Anderson, 1995). According to Small and Anderson (1995), this hypothesis predicts that the greatest amounts of denudation, and therefore isostatic response, occurred in areas with the greatest glaciation. As a result, the southernmost Sierra near the Kern River would have had the least glaciation as it has lower elevations and precipitation and, consequently, relatively lower uplift rates (Fig. 2f).

Methods

Digital elevation models (DEMs) were used to calculate geomorphic indices. All river length measurements were made using Rivertools, as

were all river longitudinal profiles. Mapinfo v7.0 was used in the measurement and calculation of all other values

Tectonic activity induces topographic and base-level changes in fluvial systems that may be used to decipher relative tectonic activity among mountain ranges (e.g., Bull and McFadden, 1977) and segmentation along a single mountain range (e.g., Wells et al., 1988). Quantification of geomorphic response to tectonic activity may be done by using geomorphic indices (Bull, 1984). In this study the following indices were used: mountain front sinuosity (Bull and McFadden, 1977), valley floor width to height ratio and relief ratio (Bull and McFadden, 1977; Rockwell et al., 1985; Wells et al., 1988). In addition, river profiles were created because they record long term system equilibrium (Ritter et al. 2001).

Results

Both the mountain-front sinuosity and valley floor width to height ratio are the lowest near the Kern River and increase with increasing latitude (Fig. 3A and B). The highest relief ratios are found at the Tule and Kaweah Rivers, respectively (Fig. 3C).

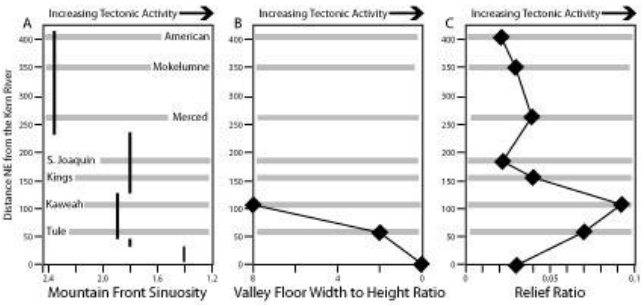

Figure 3. Plots of (A) mountain front sinuosity, (B) valley floor width to height ratio and (C) relief ratio versus distance northeast of the Kern River. Gray bars indicate rivers shown on Fig. 1 and as labeled on A.

The longitudinal profile of the main fork of the Kern River (Fig. 4A) is fault controlled above Lake Isabella (Webb, 1955; Nadin and Saleeby, 2005). The Kern River reach below Lake Isabella has a convex upward profile showing at least 600 m of incision below equilibrium at the mountain front where the Kern River Gorge fault is found.

The Tule River has an overall concave upward shape (Fig. 5A). A knickpoint indicates at least 200 m of incision is found near the river mouth. The Kaweah River also has a concave upward longitudinal profile (Fig. 5B), but a knickpoint is found at the confluence with a tributary, showing that the river is not completely in equilibrium. The Kaweah River knickpoint (Fig. 5C) is also at an elevation of 2000 m, within the glaciated portion of the Sierra.

The Kings River has an overall concave upward profile, but several knickpoints are found at the confluence between tributaries and the trunk streams in both the middle and south forks, and at the confluence between the two forks (Fig. 5C). The one knickpoint with a low enough elevation to rule out as glacial in origin shows at least 200 m of incision. The San Joaquin longitudinal is largely a result of three reservoirs along the river's course.

The Merced River longitudinal profiles are a good example of the effects of glaciation. The main (north) fork of the Merced has several prominent knickpoints that are the result of glacial downcutting near Yosemite Valley (Fig. 6B).

Discussion

Variations in the geomorphic indices along the western Sierra suggest different uplift histories and base level changes with latitude. We divide the western Sierra into three areas based on tectonic geomorphology: (i) north of the Kings River, (ii) the Tule-Kaweah-Kings area and (iii) the Kern River area – south of the Tule River.

The mountain front north of the Kings River is inactive. The mountain front sinuosity and basin relief ratios are >2, which is consistent with an

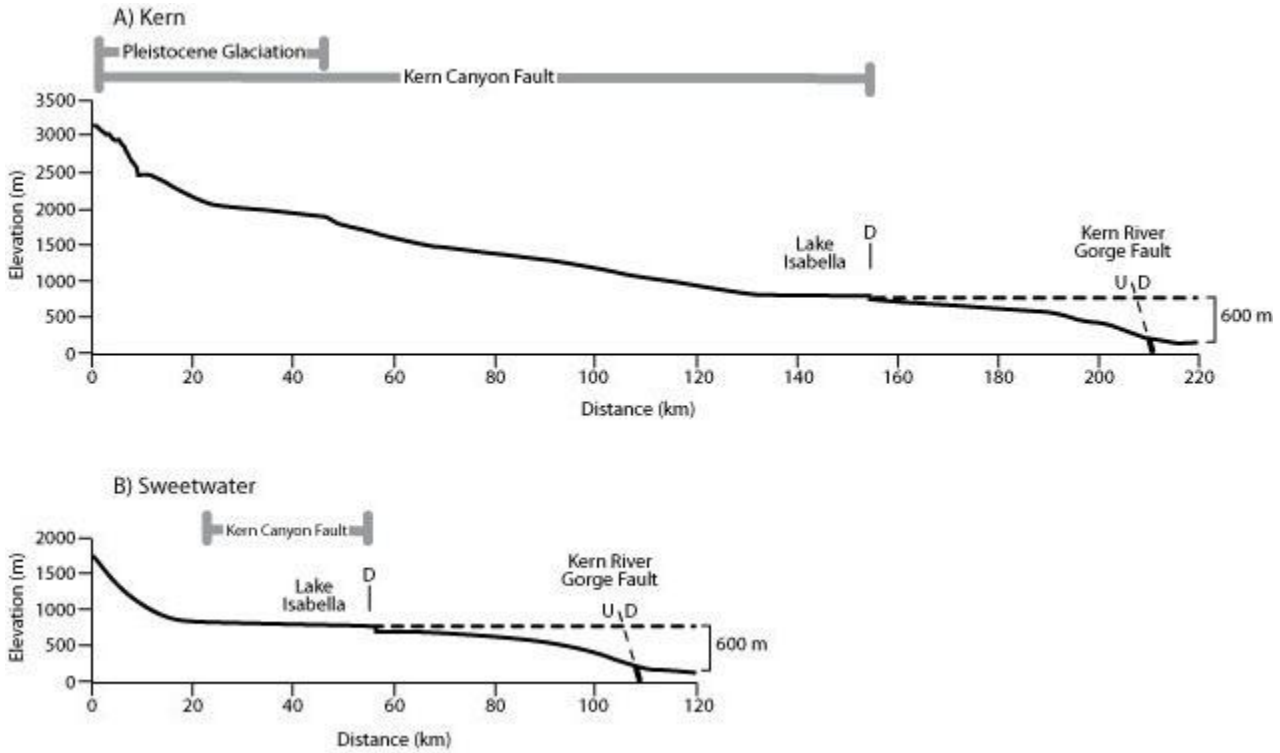

Figure 1. Longitudinal profiles of the Kern River (A) and its tributary Sweetwater Creek (B). Distances are measured downstream from the basin divide. Gray bars below profile show the lateral extent of Pleistocene glaciation and reaches influenced by the Kern Canyon fault. Dam location (D) and relative movement (U=upthrown block; D=downthrown block) of fault are also shown.

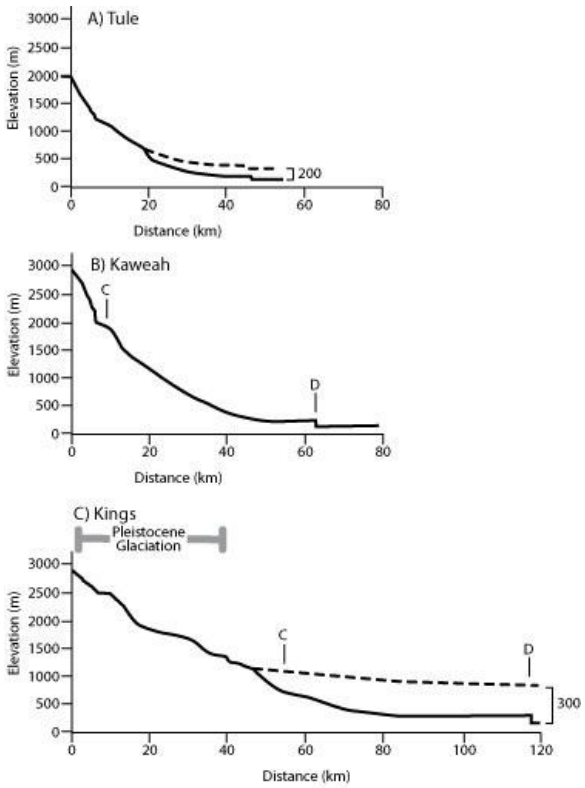

Figure 2. Profiles of Tule, Kaweah and Kings Rivers.

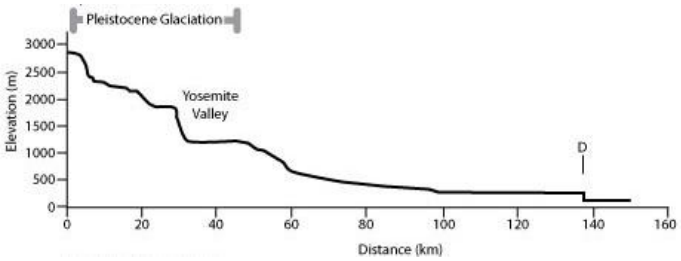

Figure 6. Profile of Merced River with relict glacial topography.

inactive mountain front using the criteria of Bull and McFadden (1977). Longitudinal profiles of rivers in this region show a concave up profile that approximate an equilibrium profile.

In the Tule-Kaweah-Kings River area the mountain front sinuosity is 1.8-1.9. The Tule and Kings Rivers also have knickpoints in their longitudinal profiles are unrelated to glaciation. This region also has higher basin relief ratios consistent with greater tectonic activity.

The Tule-Kaweah-Kings mountain front qualifies as a class 2, or an active mountain front using Bull and McFadden's criteria; however, the mountain front sinuosity and relief ratio are not consistent. The Tule-Kaweah-Kings River area coincides with anomalous topography (more linear mountain front) and the mantle drip (Fig. 1) related to Pliocene crustal delamination (Saleeby and Foster, 2004). Volcanism in the Tule-Kaweah-Kings area is geochemically consistent with lithospheric delamination (Farmer et al., 2002). Along the Kings River, Stock et al. (2004) described the Kings River as experiencing more rapid Pliocene incision followed by slower uplift during the Quaternary, possibly related to the Pliocene crustal delamination. We interpret these knickpoints to be evidence of Quaternary tectonic activity along the mountain front. Although we have no analogs, we suggest that the geomorphology, which indicates an active mountain front, but at a comparatively low uplift rate, might be the result of a singular isostatic pulse of uplift related to Pliocene delamination whose expression has been subsequently subdued by Quaternary erosion.

The lowest mountain front sinuosity values along the western Sierra mountain front (1.3) is found in the southernmost area near the Kern River. The valley floor width to height ratio is close to 0. The longitudinal profile of the lower Kern River is convex up and shows ~600 m of incision below an equilibrium profile. All of these geomorphic ratios are consistent with an active, class 1 mountain front according to Bull and McFadden (1977). The 600 m of uplift is consistent with the basement uplift estimated by Hart et al. (1984) for the Kern River Gorge fault at the mountain front. The relief ratio of the Kern River is relatively low; however, this may reflect structural control of the basin. Farmer et al. (2002) interpreted geochemical data from the Kern volcanic field as inconsistent with delamination in the Kern River area. As a result, we interpret the geomorphology as consistent with active uplift along the Kern River Gorge fault.

To explain the two-fold tectonics of the southern Sierra, we hypothesize that the Pliocene delamination and mantle drip generated rapid uplift in the Tule-Kaweah-Kings River region (Saleeby and Foster, 2004). Isostatic response to delamination was relatively rapid and has since decreased (Saleeby and Foster, 2004; Stock et al., 2004). Subsequently, we suggest that uplift of the southern Sierra over the last 5 Ma is related to San Andreas plate margin tectonics has caused rapid subsidence in the Tulare Basin and incision of the lower reaches of the Kern River along the Kern Gorge Fault (Fig. 7). This combination of mechanisms is consistent with the geomorphic indices.

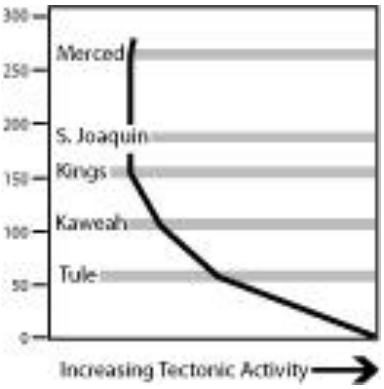

Figure 7. Hypotheticall summation of geomorphic indices.

Conclusions

A combination of Pliocene lower crust/upper mantle delamination followed by late Pliocene to present San Andreas plate boundary deformation is most consistent with Sierra geomorphology. The delamination and mantle drip hypotheses explain the lack of crustal root in the central Sierras, as well as the higher elevations in the Kings River region. Because delamination occurred in the Pliocene, the effects have waned during the Quaternary. This is consistent with uplift rates in the central and northern Sierras (Stock et al., 2004). The higher tectonic activity in the southwestern Sierras and southern San Joaquin Valley is a consequence of San Andreas, Garlock, and Sierra Nevada Frontal fault interactions (Figueroa et al., this volume; Figueroa, 2005) beginning in the late Pliocene and continuing to the present.

References

Bull, W.B., 1984. Tectonic geomorphology. Journal of Geological Education 32, 310-324.

Bull, W.B., McFadden, L.D., 1977. Tectonic geomorphology north and south of the Garlock fault, California. In: Doehring, D.C. (Ed.), Geomorphology in Arid Regions, Proceedings 8th Annual Geomorphology Symposium, State University of New York, Binghamton, NY, pp. 115-137.

Crough, S.T., Thompson, G.A., 1977. Upper mantle origin of Sierra Nevada uplift. Geology 5, 396-399.

Ducea, M., Saleeby, J.B., 1998. A case for delamination of the deep batholithic crust beneath the Sierra Nevada, California. International Geology Review 40(1), 78-93.

Farmer, G.L., Glazner, A.F., Manley, C.R., 2002. Did lithospheric delamination trigger late Cenozoic potassic volcanism in the southern Sierra Nevada, California. Geological Society of America Bulletin 114(6), 754-768.

Figueroa, A.M., 2005. Elastic modeling and tectonic geomorphic investigation of the Late Cenozoic Sierra Nevada (California) uplift. M.S. Thesis, California State University-Fullerton, CA.

Hart, E.W., Bryant, W.A., Smith, T.C., 1984. Summary Report: Fault Evaluation Program, 1983 Area (Sierra Nevada Region). California Division of Mines and Geology, Sacramento, CA.

Huber, N.K., 1981. Amount and Timing of Late Cenozoic Uplift and Tilt of the Central Sierra Nevada, California-Evidence from the upper San Joaquin River Basin. U.S. Geological Survey Professional Paper 1197, Washington, D.C., pp. 1-28.

Jones, C.H., Farmer, G.L., Unruh, J., 2004. Tectonics of Pliocene removal of lithosphere of the Sierra Nevada, California. Geological Society of America Bulletin 116 (11/12), 1408-1422.

Liu, M., and Shen, Y., 1998. Sierra Nevada uplift: a ductile link to mantle upwelling under the Basin and Range province. Geology 26 (4), 299-302

Manley, C.R., Glazner, A.F., Farmer, G.L., 2000. Timing of volcanism in the Sierra Nevada of California: evidence for Pliocene delamination of the batholithic root? Geology 28(9), 811-814.

Monastero, F.C., Walker, J.D., Katzenstein, A.M., Sabin, A.E., 2002. Neogene evolution of the Indian Wells Valley, east-central California. In: Glazner, A.F., Walker, J.D.,Bartley, J.M. (Eds.), Geologic Evolution of the Mojave Desert and Southwestern Basin and Range. Geological Society of America Memoir 195, Boulder, CO, pp. 199-228.

Montgomery, D. R. 1994 Valley incision and the uplift of mountain peaks. Journal of Geophysical Research 99(B7), 13,913-13,921.

Nadin, E., Saleeby, J., 2005. Recent motion on the Kern Canyon fault, southern Sierra Nevada. EOS, Transactions of the American Geophysical Union 86(52).National Atlas of the United States, 2010. http://www.nationalatlas.gov/printable/images/pdf/precip/pageprecip_ca3.pdf.

Niemi, N.A., 2003. Active faulting in the southern Sierra Nevada: initiation of a new Basin and Range normal fault? Geological Society of America Abstracts with Program 35(6), 581.

Ritter, D.F., Kochel, R.C., Miller, J.R., 2002. Process Geomorphology. Waveland Press, Long Grove, IL.

Saleeby, J., Foster, Z., 2004. Topographic response to mantle lithosphere removal in the southern Sierra Nevada region, California. Geology 32(3), 245-248.

Small, E.E., Anderson, R.S., 1995. Geomorphically driven Late Cenozoic rock uplift in the Sierra Nevada, California. Science 270, 277-280.

Stock, G.M., Anderson, R.S., Finkel, R.C., 2004. Pace of landscape evolution in the Sierra Nevada, California revealed by cosmogenic dating of cave sediments. Geology 32(3), 193-196.

Unruh, J.R., 1991. The uplift of the Sierra Nevada and implications for the late Cenozoic epeirogeny in the western Cordillera. Geological Society of America Bulletin 103, 1395-1404.

Wakabayashi, J., Sawyer, T.L., 2001. Stream incision, tectonics, uplift and evolution of topography of the Sierra Nevada, California. Journal of Geology 109, 539-562.

Webb, R.W., 1955. Kern Canyon lineament. In: G.B. Oakeshott, G.B., Jenkins, O.P. (Eds.), Earthquakes in Kern County, California, during 1952. California Division of Mines and Geology Bulletin 171, pp. 35-36.

Wells, S.G. Bullar, T.F., Menges, C.M., Drake, P.G., Kara, P.A., Kelson, K.I., Ritter, J.B., Wesling, J.R., 1988. Regional variations in tectonic geomorphology along a segmented convergent plate boundary, Pacific coast of Costa Rica. Geomorphology 1, 239-365.

Stop 1-1c:

Modeling the effects of the San Andreas, Garlock faults and Sierra Nevada frontal fault zone on the uplift of the Sierra Nevada mountains, California

Andrea Figueroa, *California State University, Fullerton*

David Bowman, *California State University, Fullerton*

Jeffrey Knott, *California State University, Fullerton*

Abstract

Hypotheses that explain the mechanism of uplift for the Sierra and subsidence of the adjacent San Joaquin Valley have largely failed to consider the influence of the San Andreas Fault (SAF). To examine the influence of the SAF, Garlock and Sierra Nevada Frontal Fault Zone (SNFFZ) on late Cenozoic Sierra uplift dislocation models of regional crustal deformation were constructed and run using geologically determined slip rates. Slip on only the SNFFZ generates the observed mountain front-piedmont intersection, but not the observed subsidence of the San Joaquin Valley. Models with combined slip on the Garlock, SAF and vertical slip on the SNFFZ generate the observed greater subsidence in the southern San Joaquin. Based on modeling, pre-Cenozoic uplift along the SNFFZ could define the large-scale crustal blocks and relict topography. The post-5 Ma Sierra and San Joaquin Valley deformation may be produced by a complex interaction between SAF and Garlock strike-slip motion and SNFFZ normal faulting, with SNFFZ strike-slip faulting having little influence.

Introduction

The Sierra Nevada Mountains of eastern California (Sierra) were a prominent topographic high in the early Cenozoic that has undergone a lesser, yet significant, late Cenozoic uplift (Bateman and Wahrhaftig, 1966; House et al., 2001; Huber, 1981; Poage and Chamberlain, 2002; Unruh, 1991; Wakabayashi and Sawyer, 2001). However, controversy continues regarding the mechanism driving the late Cenozoic uplift (Small and Anderson, 1995; Unruh, 1991; Wakabayashi and Sawyer, 2001; Wernicke et al., 1996).

The question proposed herein is: Can the fault geometry and slip rates produce the southern Sierra and San Joaquin valley topography? In this paper, a 3D crustal dislocation model is presented that describes strain generated by the interaction of the SAF – Garlock – SNFFZ fault systems. The goal of the modeling is to use various time-dependent fault slip rates and fault interaction to replicate the modern topography.

Methods

Modeling Physical Parameters

Faults are modeled as dislocations in an elastic half-space (Okada, 1992). In this large-scale model the lithosphere is assumed to behave in an elastic fashion (Hubert-Ferrari at al., 2003). Faults are areas where dislocations are imposed on the model. The resulting elastic deformation is calculated. Fault locations are from Jennings (1994).

San Andreas Fault

In the model, the SAF is a vertical (Eberhart-Phillips et al., Snay et al., 196; Zhu 2000), right lateral fault with variable slip rates. For modeling purposes, the SAF slip rate is estimated to be 10 mm/yr pre-5 Ma and 30 mm/yr after 5 Ma

(Atwater, 1970; Atwater and Stock, 1998; Eberhart-Phillips et al., 1990; Jones and Wesnousky, 1992; Niemi and Hall, 1992; Petersen and Wesnousky, 1994; Sedlock and Hamilton, 1991; Snay et al., 1996 Weldon and Sieh, 1985; Wesnousky, 1986; Zhu, 2000).

Garlock Fault

In the model, the Garlock fault is a vertical (Astiz and Allen, 1983), left-lateral strike slip fault extending at least 265 km eastward from the SAF (Figures 2 and 3; (Hutton et al., 1991). A slip rate of 10 mm/yr was assigned to the Garlock fault since estimates of slip rate vary from 7 to 13 mm/yr (Clark et al., 1984; Eberhart-Phillips et al., 1990; McGill and Sieh 1993; Petersen and Wesnousky, 1994; Smith, 1962; Smith et al., 2002; Snay et al., 1996). It is assumed in the model that slip on the Garlock fault began at 5 Ma when the slip rate on the SAF increased (Hill and Dibblee, 1953).

Sierra Nevada Frontal Fault Zone (SNFFZ)

The SNFFZ was modeled as one continuous fault with an easterly dip of 70º. This dip angle and direction is consistent with the 80 ± 15º dip estimated from 1872 rupture (Beanland and Clark, 1982).

Normal Slip Component of SNFFZ. If late Cenozoic uplift of the Sierra is the result of normal faulting along the SNFFZ, then the beginnings of SNFFZ normal faulting and Sierra uplift should be simultaneous. Estimates of the initiation of late Cenozoic uplift vary from 10 Ma to 5 Ma, while onset of normal faulting ranges from 2.3 to 7 Ma (Bachman, 1978; Monastero et al., 2002; Reheis and Sawyer, 1997).

The vertical component of slip, as measured on normal and oblique faults, varies from 0.1 to 2.5 mm/yr (Berry, 1997; Clark and Gillespie, 1993; Clark et al., 1984; Martel et al., 1987; Zehfuss et al., 2001). River incision and tilted strata in the San Joaquin Valley reveal a longer-term rate of 0.28º per million years for the last 5 Ma (Unruh, 1991). To produce this tilt requires a 0.5-mm/yr vertical slip rate on the SNFFZ. Thus, a model slip rate of 0.5 mm/yr was chosen.

Strike Slip and Oblique Slip on the SNFFZ. Oblique (dextral, normal) motion is common along the SNFFZ (Table 2). The transition from vertical to oblique motion within the SNFFZ occurred after the onset of normal faulting between 3.5 and 2 Ma and propagated northward (Monastero et al., 2002). Estimates of the dextral slip rate on the Owens Valley fault (southern section of SNFFZ) range from 1.5 to 8.5 mm/yr (Beanland and Clark, 1982; Gan et al., 2000; Lee et al., 2001a; Lee et al., 2000; Lee et al., 2001b; Reheis and Dixon, 1996) with most values close to 2 mm/yr. For the model, a right-lateral strike-slip rate of 2 mm/yr was chosen.

Table 1. Model Slip Rates. Slip rates (mm/year) for fault zones used for each model version.

Model Conditions	San Andreas	Garlock	SNFFZ Lateral	SNFFZ Normal	Figure
Only uplift	0	0	0	0.5	1a
No SNFFZ activity	30	10	0	0	1b
5 - 3 Ma	30	10	0	0.5	1c
3 Ma to present	30	10	2	0.5	1d

Model Construction

Modeling of elastic deformation was done using Nutcracker v6.3 (http://geology.fullerton.edu/bowman/downloads.html). The model was constructed to cover the area 35.2º N 121.2º W to 38.8º N to 117.8º W. All calculations of elastic deformation in response to slip on the faults were done at a grid spacing of 5 km.

Model Results

Scenario A

Many studies have proposed that uplift of the Sierra is the result of normal slip on the SNFFZ along the east side of the range (e.g., Huber, 1981; 1987; Wakabayashi and Sawyer, 2001). To test this hypothesis, Scenario A included 0.5 mm/yr of west-side-up slip on the SNFFZ and no lateral slip on the SAF, SNFFZ and Garlock faults (Figure 1a). Scenario A shows both uniform uplift perpendicular to SNFFZ and uniform subsidence in the San Joaquin Valley parallel to the axis of the modern valley. However, drawbacks to Scenario A are that it does no uplift along the SAF nor does it produce greater subsidence in the southern San Joaquin Valley.

Scenario B

Scenario B models deformation generated by slip on the Garlock and SAF alone (Table 1) with no slip on the SNFFZ. As such, Scenario B tests whether the SAF and Garlock faults, without the SNFFZ, could generate Sierra uplift or San Joaquin valley subsidence. Scenario B produces a region of subsidence in the southern San Joaquin Valley that extends across the southern Sierras (Figure 1b). Uplift produced by this model is found along the SAF extending eastward into the northern San Joaquin Valley; however, Scenario B does not produce uplift of the Sierras.

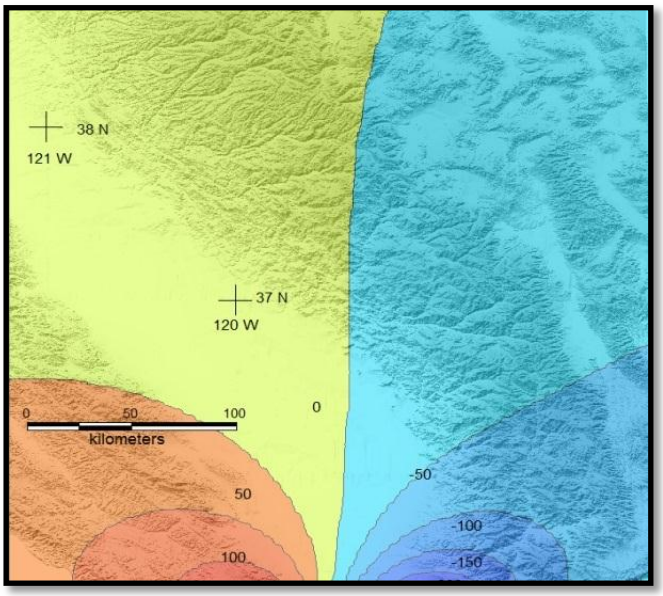

Figure 3a. Model results with normal slip on SNFFZ only. Contours show elevation change in meters. Yellow tints are uplift; green and blue tints are subsidence.

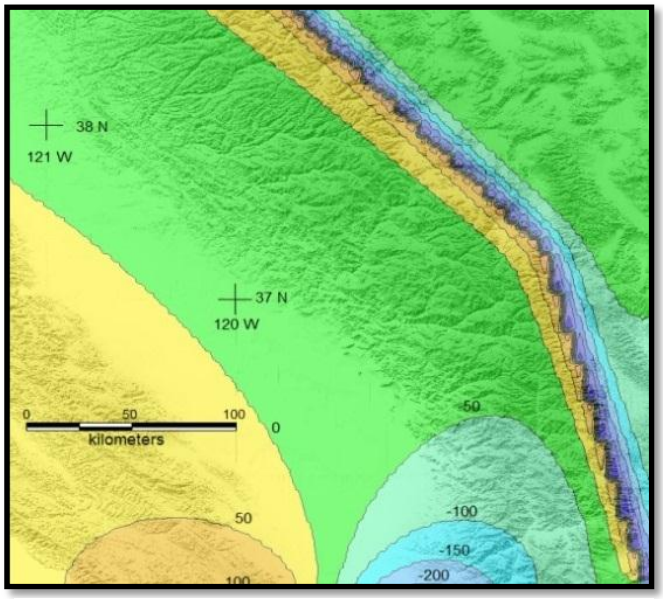

Figure 1b. Model results with strike slip on SAF and Garlock.

Scenario C

Scenario C models the 5-3 Ma tectonic conditions by using slip rates of 30 mm/yr for the SAF, 10 mm/yr for the Garlock, and 0.5 mm/yr of west side up slip for the SNFFZ (Figure 1c). In Scenario C, the southern Sierra has a narrower

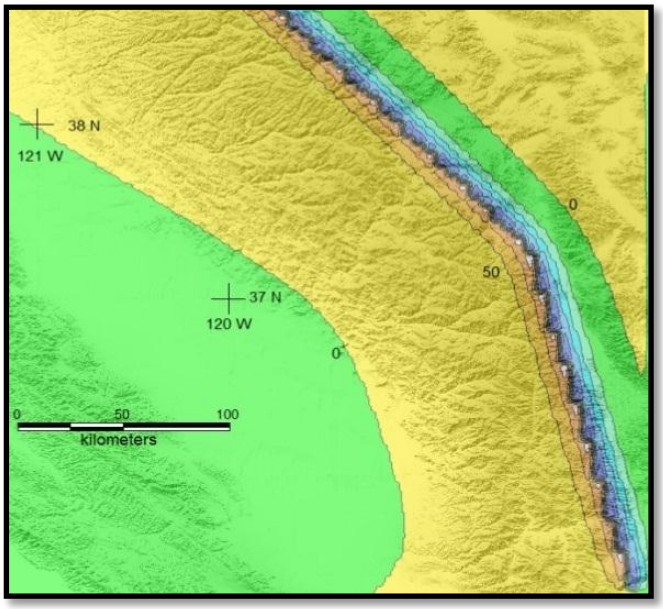

Figure 1c. Model results with slip rates from 5-3 Ma – see Table 1 for rates.

area of uplift compared to the northern Sierras. Subsidence is generated in the southern Sierra and San Joaquin Valley, and there is uplift of the region along the SAF.

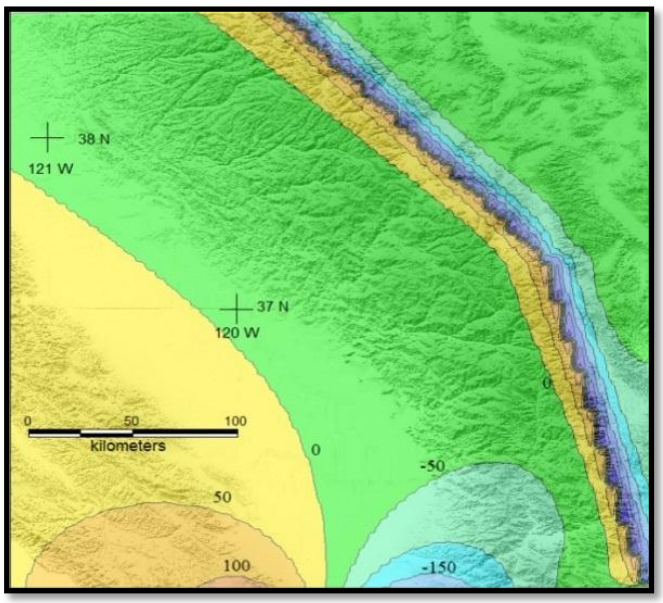

Figure 1d. 3 Ma to present model results with lateral slip on SNFFZ.

Scenario D

Scenario D depicts crustal deformation similar to Scenario C with the addition of 2 mm/yr of dextral slip along the SNFFZ. The 2 mm/yr of strike slip motion on the SNFFZ (Figure 1d) results in a more restricted subsidence in the southern San Joaquin Valley along with the accompanying greater area of uplift of the southern Sierra and along the SAF.

Discussion

Many studies have invoked uplift along the SNFFZ as the key mechanism producing the late Cenozoic Sierra and San Joaquin topography (e.g., Huber, 1981; 1987; Unruh, 1991; Wakabayashi and Sawyer, 2001). Scenario A uses uplift by normal slip on the SNFFZ only; however, critically absent is the generation of the topographic low in the southern San Joaquin Valley. Scenario A accurately predicts the variation in width of the Sierra with latitude, which is likely a relict topographic feature generated by pre-5 Ma slip on the SNFFZ.

Jones et al. (2004) hypothesized that the uplift of the Coast Ranges, which are at the western margin of the model, are the result of compressive stresses formed as a consequence of Sierra uplift. If this were correct, then there would be a topographic expression of the Coast Ranges with simple SNFFZ uplift (Figure 1a); however, the Coast Ranges are not produced by Scenario A. In contrast, scenarios involving SAF slip produce uplift similar to the present-day Coast Ranges, even without SNFFZ normal slip (Scenario B).

Scenario B, models topography generated by SAF and Garlock slip alone and does not produce the observed greater uplift of the southern Sierra. The absence of southern Sierra uplift is critical to dismissing this model as an unrealistic mechanism for Sierra topography. Scenario B does, however, show that the

SAF/Garlock system could cause extension in the southernmost Sierra in the location of the modern day Kern Gorge Fault.

Scenarios C and D create a greater topographic low in the southern San Joaquin Valley compared with the north. This is consistent with the division of the San Joaquin Valley into two different sub-basins at the Kings River. The Kings River alluvial plain is split with part of its water flowing to the south into the Tulare Basin and part flowing north to San Francisco Bay and the Pacific Ocean (Davis and Green, 1962). The Tulare structural basin has been actively subsiding (Naeser, 1984) at a rate of 0.4 mm/yr for the last 0.6 Ma (Atwater et al., 1986; Davis and Green, 1962). The location of the Tulare Basin is located to the north of the locus of subsidence predicted in the model. This is most likely due to the fact that the White Wolf Fault is not included in the model. The White Wolf Fault is subparallel to the Garlock fault with the same sense of motion. If it were included in this model it would likely shift the locus of subsidence in the model to the actual location of the Tulare Basin. The greater flexure shown in the southern Sierra in this model is also consistent with the dipping of Tertiary sediments which varies from 1º -2º in the northern Sierras and 4º - 6º in the Bakersfield area (Bartow, 1991).

Conclusions

An elastic model of the Sierra crust with SAF, Garlock and SNFFZ geometry and slip rate inputs accurately predicts regional topography. The model scenario with 30 mm/yr of slip on the SAF, 10 mm/yr on the Garlock and 0.5 mm/yr of vertical slip on the SNFFZ most closely resembles the uplift of the Sierra and Coast Ranges, and subsidence of the San Joaquin Valley. Model scenarios indicate that SNFFZ uplift alone does not generate the Coast Ranges or San Joaquin Valley subsidence. The modeling supports Webb's (1955) hypothesis that the kinematics of the southern Sierra are affected by the San Andreas and Garlock faults.

References

Astiz, L., and Allen, C. R., 1983, Seismicity of the Garlock Fault, California: Bulletin of the Seismological Society of America, v. 73, no. 6, p. 1721-1734.

Atwater, B. F., Adam, D. P., Bradbury, J. P., Forester, R. M., Mark, R. K., Lettis, W. R., Fisher, G. R., Gobalet, K. W., and Robinson, S. W., 1986, A fan dam for Tulare Lake, California, and implications for the Wisconsin glacial history of the Sierra Nevada: Geological Society of America Bulletin, v. 97, p. 97-109.

Atwater, T., 1970, Implications of plate tectonics for the Cenozoic tectonic evolution of western North America: Bulletin of the Geological Society of America, v. 81, p. 3513-3536.

Atwater, T., and Stock, J., 1998, Pacific-North American plate tectonics of the Neogene southwestern United States: An update, *in* Ernst, W. G., and Nelson, C. A., eds., Integrated Earth and Environmental Evolution of the Southwestern United States, the Clarence A Hall, Jr Volume: Columbia, Bellwether Publishing, Ltd.

Bachman, S. B., 1978, Pliocene-Pleistocene break-up of the Sierra Nevada-White-Inyo Mountains block and formation of Owens Valley: Geology, v. 6, p. 461-463.

Bartow, J. A., 1991, The Cenozoic evolution of the San Joaquin Valley, California: U.S.G.S. Professional Paper, v. 1501, p. D1-D40.

Bateman, P. C., and Wahrhaftig, C., 1966, Geology of the Sierra Nevada, *in* Bailey, E., ed., Geology of Northern California, California Division of Mines and Geology, p. 107-172.

Beanland, S., and Clark, M. M., 1982, The Owens Valley Fault Zone, eastern California, and surface faulting associated with the 1872 earthquake: U.S. Geological Survey Bulletin.

Berry, M. E., 1997, Geomorphic analysis of late Quaternary faulting on Hilton Creek, Round Valley and Coyote warp faults, east-central Sierra Nevada, California, USA: Geomorphology, v. 20, p. 177-195.

Clark, M. M., and Gillespie, A., 1993, Variations in Late Quaternary behavior along and among range-front faults of the Sierra Nevada, California: Geological Society of America, 89th annual Cordillearan Section meeting and 46th annual Rocky Mountain Section meeting Abstracts with Programs, v. 35, no. 5, p. 21.

Clark, M. M., Harms, K. K., Lienkaemper, J. J., Harwood, D. S., Lajoie, K. R., Matti, J. C., Perkins, J. A., Rymer, M. J., Sarna-Wojcicki, A. M., Sharp, R. V., Sims, J. D., Tinsley, J. C., and Ziony, J. I., 1984, Preliminary slip-rate table and map of Late-Quaternary Faults of California: U.S. Geological Survey Open-File Report 84-106, Open File Report 84-106.

Davis, G. H., and Green, J. H., 1962, Structural control of interior drainage, southern San Joaquin Valley, California: U.S.G.S. Professional Paper 450-D. Short Papers in Geology, Hydrology, and Topogrpahy Articles, p. 120-17989-94.

Eberhart-Phillips, D., Lisowski, M., and Zoback, M. D., 1990, Crustal strain near the big bend of the San Andreas Fault: Analysis of the Los Padres-Tehachapi Trilateration Networks, California: Journal of Geophysical Research, v. 95, no. B2, p. 1139-1153.

Gan, W., Svarc, J. L., Savage, J. C., and Prescott, W. H., 2000, Strain accumulation across the Eastern California Shear Zone at latitude 36 30'N: Journal of Geophysical Research, v. 105, no. B7, p. 16,229-16,236.

Hill, M. L., and Dibblee, T. W. J., 1953, San Andreas, Garlock, and Big Pine Faults, California: Bulletin of the Geological Society of America, v. 64, p. 443-458.

Huber, N. K., 1981, Amount and timing of Late Cenozoic uplift and tilt of the central Sierra Nevada, California--Evidence from the upper San Joaquin River Basin: Geological Survey Professional Paper, v. 1197, p. 1-28.

-, 1987, The Geologic Story of Yosemite National Park: U.S. Geological Survey, 1595.

Hubert-Ferrari, A., King, G., Mangihetti, I., Armijo, R., Meyer, B., and Tapponnier, P., 2003, Long-term elasticity in the continental lithosphere; modeling the Aden Ridge propagation and the Anatolian extrusion process: Geophysical Journal International, v. 153, no. 111-132.

Hutton, L. K., Jones, L. M., Hauksson, E., and Given, D. D., 1991, Seismotectonics of southern California, *in* Engdahl, D. B., Zoback, M. D., and Blackwell, D. D., eds., Neotectonics of North America: Boulder, Colorado, Geological Society of America, p. 133-152.

Jones, C. H., Farmer, G. L., and Unruh, J. R., 2004, Tectonics of Pliocene removal of lithosphere of the Sierra Nevada, California: Geological Society of America Bulletin, v. 116, no. 11/12, p. 1408-1422.

Jones, C. H., and Wesnousky, S. G., 1992, Variations in strength and slip rate along the San Andreas Fault system: Science, v. 256, p. 83-85.

Lee, J., Rubin, C. M., and Calvert, A., 2001a, Quaternary faulting history along the Deep Springs fault, California: Geological Society of America Bulletin, v. 113, no. 7, p. 855-869.

Lee, J., Rubin, C. M., Miller, M., Spencer, J., Lewis, O., and Dixon, T. H., 2000, Kinematics of the Eastern California shear zone north of the Garlock Fault: Geological Society of America 2000 Annual Meeting Abstracts with Programs, v. 32, no. 7, p. 105.

Lee, J., Spencer, J., and Owen, L., 2001b, Holocene slip rates along the Owens Valley fault, California: Implications for the recent evolution of the Eastern California Shear Zone: Geology, v. 29, no. 9, p. 819-822.

Martel, S. J., Harrison, T. M., and Gillespie, A. R., 1987, Late Quaternary vertical displacment rate across the Fish Springs Fault, Owens Valley Fault Zone, California: Quaternary Research, v. 27, p. 113-129.

McGill, S. F., and Sieh, K. E., 1993, Holocene slip rate of the central Garlock Fault in southeastern Searles Valley, California: Journal of Geophysical Research, v. 98, no. B8, p. 14,217-14,231.

Monastero, F. C., Walker, J. D., Katzenstein, A. M., and Sabin, A. E., 2002, Neogene evolution of the Indian Wells Valley, east-central California, *in* Glazner, A. F., Walker, J. D., and Bartley, J. M., eds., Geologic Evolution of the Mojave Desert and Southwestern BAsin and Range: Boulder, Colorado, Geological Society of America Memoir 195, p. 199-228.

Naeser, N. D., 1984, Thermal history determined by fission-track dating for three sedimentary basins in California and Wyoming: Geological Society of America, 97th meeting Abstracts with Programs, v. 16, no. 6, p. 607.

Niemi, N. A., 2003, Active faulting in the southern Sierra Nevada: initiation of a new basin and range normal fault?: U.S. Geological Society Annual Meeting.

Niemi, T. M., and Hall, N. T., 1992, Late Holocene slip rate and recurrence of greate earthquakes on the San Andreas fault in northern California: Geology, v. 20, p. 195-198.

Okada, Y., 1992, Internal deformation due to shear and tensile faults in a half-space: Bulletin of the Seismological Society of America, v. 82, p. 1018-1040.

Petersen, M. D., and Wesnousky, S. G., 1994, Review-Fault slip rates and earthquake hisotires for active faults in southern California: Bulletin of the Seismological Society of America, v. 84, no. 5, p. 1608-1649.

Reheis, M. C., and Dixon, T. H., 1996, Kinematics of the Eastern California shear zone: evidence for slip transfer from Owens and Saline Valley fault zones to Fish Lake Valley fault zone: Geology, v. 24, no. 4, p. 339-342.

Reheis, M. C., and Sawyer, T. L., 1997, Late Cenozoic history and slip rates of the Fish Lake Valley, Emigrant Peak, and Deep Springs fault zones, Nevada and California: Geological Society of America Bulletin, v. 109, no. 3, p. 280-299.

Sedlock, R. L., and Hamilton, D. H., 1991, Late Cenozoic evolution of southwestern California: Journal of Geophysical Research, v. 96, no. B2, p. 2325-2351.

Smith, E. I., Sanchez, A., Keenan, D. L., and Monastero, F. C., 2002, Stratigraphy and geochemistry of volcanic rocks in the Lava Mountains, California: Implications for the Miocene development of the Garlock fault, *in* Glazner, A. F., and Bartley, J. M., eds., Geological Evolution of the Mojave Desert and Southwestern Basin and Range: Boulder, Colorado, p. 151-160.

Smith, G. I., 1962, Large lateral displacment on Garlock Fault, California, as measured from offset dike swarm: Bulletin of the American Association of Petroleum Geolgists, v. 46, no. 1, p. 85-104.

Snay, R. A., Cline, M. W., Phillip, C. R., Jackson, D. D., Feng, Y., Shen, Z.-K., and Lisowski, M., 1996, Crustal velocity field near the big bend of California's San Andreas fault: Journal of Geophysical Research, v. 101, no. B2, p. 3173-3185.

Unruh, J. R., 1991, The uplift of the Sierra Nevada and implications for the late Cenozoic epeirogeny in the western Cordillera: Geological Society of America Bulletin, v. 103, p. 1395-1404.

Wakabayashi, J., and Sawyer, T. L., 2001, Stream incision, tectonics, uplift and evolution of topography of the

Sierra Nevada, California: Journal of Geology, v. 109, p. 539-562.

Webb, R. W., 1955, Kern Canyon Lineament, *in* Oakeshott, G. B., and Jenkins, O. P., eds., Earthquakes in Kern County, California, during 1952, Bulletin, p. 35-36.

Weldon, R. J., and Sieh, K. E., 1985, Holocene rate of slip and tentative recurrence interval for large earthquakes on the San Andreas fault, Cajon Pass, southern California: Geological Society of America Bulletin, v. 96, p. 793-812.

Wesnousky, S. G., 1986, Earthquakes, Quaternary faults and seismic hazard in California: Journal of Geophysical Research, v. 91, no. B12, p. 12,587-12,631.

Zehfuss, P. H., Bierman, P. R., Gillespie, A., Burke, R., and Caffee, M., 2001, Slip rates on the Fish Springs fault, Owens Valley, California, deduced from cosmogenic 10 Be and 26 Al and soil development on fan surfaces: Geological Society of America Bulletin, v. 113, no. 2, p. 241-255.

Zhu, L., 2000, Crustal structure across the San Andreas Fault, southern California from teleseismic converted waves: Earth and Planetary Science Letters, v. 179, p. 183-190.

Stop 1-1d:
Bits and Pieces: Kern River Sediments below the Modern Fan Apex

Rob Negrini, *California State University, Bakersfield*

The Kern River in the San Joaquin Valley

After it emerges from the Panorama Bluffs at ~129 masl, the modern channel of the Kern River drops 40 m in elevation on its way down its alluvial fan to Buena Vista lake, a local terminal basin (Figure 1). When Buena Vista Lake reaches a depth of only a few meters, it spills over into a north-directed channel along the distal edge of the KRF. This channel ends up at Tulare Lake (lake bottom elevation = 55 m). Prior to irrigation-related diversion, the surface of Tulare Lake rises to a sill at 64 m before spilling over into the San Joaquin River drainage and then on towards San Francisco Bay (Figure 1).

The Modern Kern River Fan

The KRF is an extremely large (2,000 km^2) alluvial fan that has been built out into the valley for at least the past million years (Figure 2) (Bartow, 1991). What we know of its subsurface is limited to geophysical logs and cuttings; very little core exists. As a result, its age is poorly constrained. A single sample taken from a depth of 185 mbgs in a core from Well (KWB17M2) exhibited reversed magnetic polarity (Marble and Negrini, 2008). This preliminary observation supports the idea that the fan is at least a million years old. However, the majority of magnetic samples taken from this core did not pass basic paleomagnetic stability tests, thus extensive resampling of the core will have to be undertaken to better constrain the magnetostratigraphy of the fan sediments.

A Middle Pleistocene-aged Delta Prograding into Buena Vista Lake

As expected for an alluvial fan depositional environment, it's extremely difficult to correlate units across the fan except at its distal reaches (Wilson, 1993; Negrini et al., 2004; 2006a). One such correlateable distal unit is a 50-100 meter-thick unit likely deposited as part of a prograding delta into a Buena Vista Lake at a time when a more extensive lake was at the edge of a less extensive fan (Figure 3). The base of this distal unit is found at depths ranging from 100-200 m below ground surface. It thickens basinward, has a coarsening upward grain-size distribution and occupies a trough whose geometry appears to be constrained by a graben bounded by NE-SW striking normal faults. The deposit extends outward onto an extensive fine-grained unit found at a depth of ~300 m below the modern Buena Vista Lake basin and correlated by some to the Corcoran Clay (e.g., Croft, 1972; Page, 1986; Negrini et al., 2009). A volcanic ash is found in this clay layer in cuttings from Well BV27C (Powers et al., 2008). The major element geochemistry of its glass shards is a match to the Bishop Ash, though correlation to older Bishop-like ashes are not precluded by these data. The Bishop Ash is the favored correlation because the overlying sediments contain paleoenvironmental indicators of dramatic climate swings consistent with those of the past several thousands of years in northern hemisphere. For example, the presence of the ostracodes *C. lacustris* and *P. pustolosa* and mountain tree pollen suggest that an extremely fresh and cold lake had fir, alder, and mountain mohagany growing on its margins on the floor of the San Joaquin Valley five times since the deposition of the volcanic ash (Powers et al., 2008).

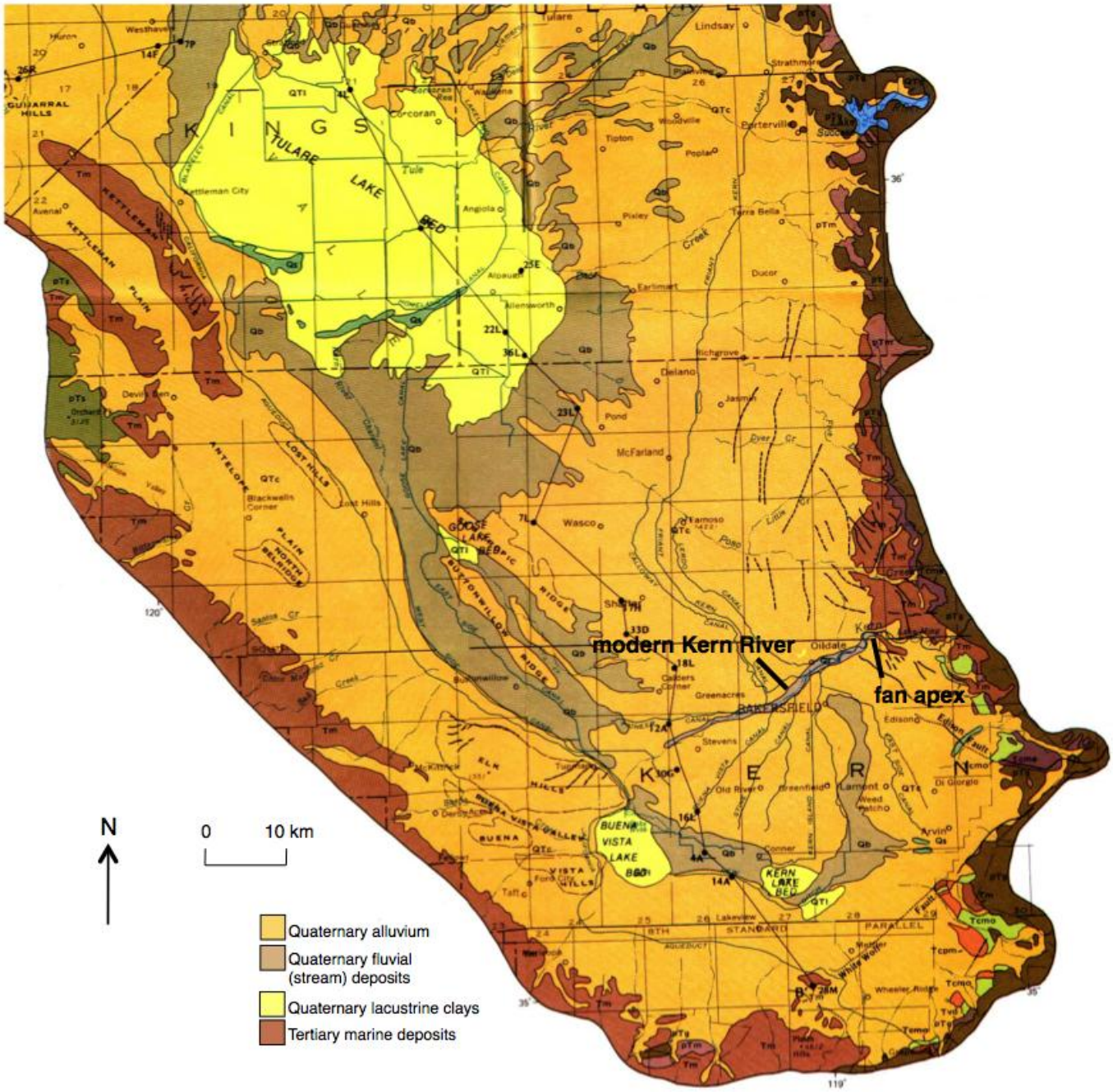

Figure 1. Simplified geologic map of southern San Joaquin Valley (after Page, 1986).

The Corcoran Clay and Lake Clyde

The Corcoran Clay is a unit found throughout the Central Valley of California (Frink and Kues, 1954; Croft, 1972; Sarna-Wojcicki, 1995; Harden, 2004). The age of the Corcoran Clay is constrained by the Matuyama/Brunhes magnetic polarity transition(774 ± 3 ka; Sarna-Wojcicki et al., 2000), the Bishop Ash (759 ± 2 ka; Sarna-Wojcicki et al., 2000), and the Lava Creek B ash (639 ± 2; Lanphere et al., 2002), all found in association with the Clay in a core taken from north of the Kern River Alluvial Fan near the town of Wasco, California (Davis et al., 1977; Sarna-Wojcicki, 1995). Because of its widespread distribution, the Corcoran Clay suggests the existence of a Central Valley-wide

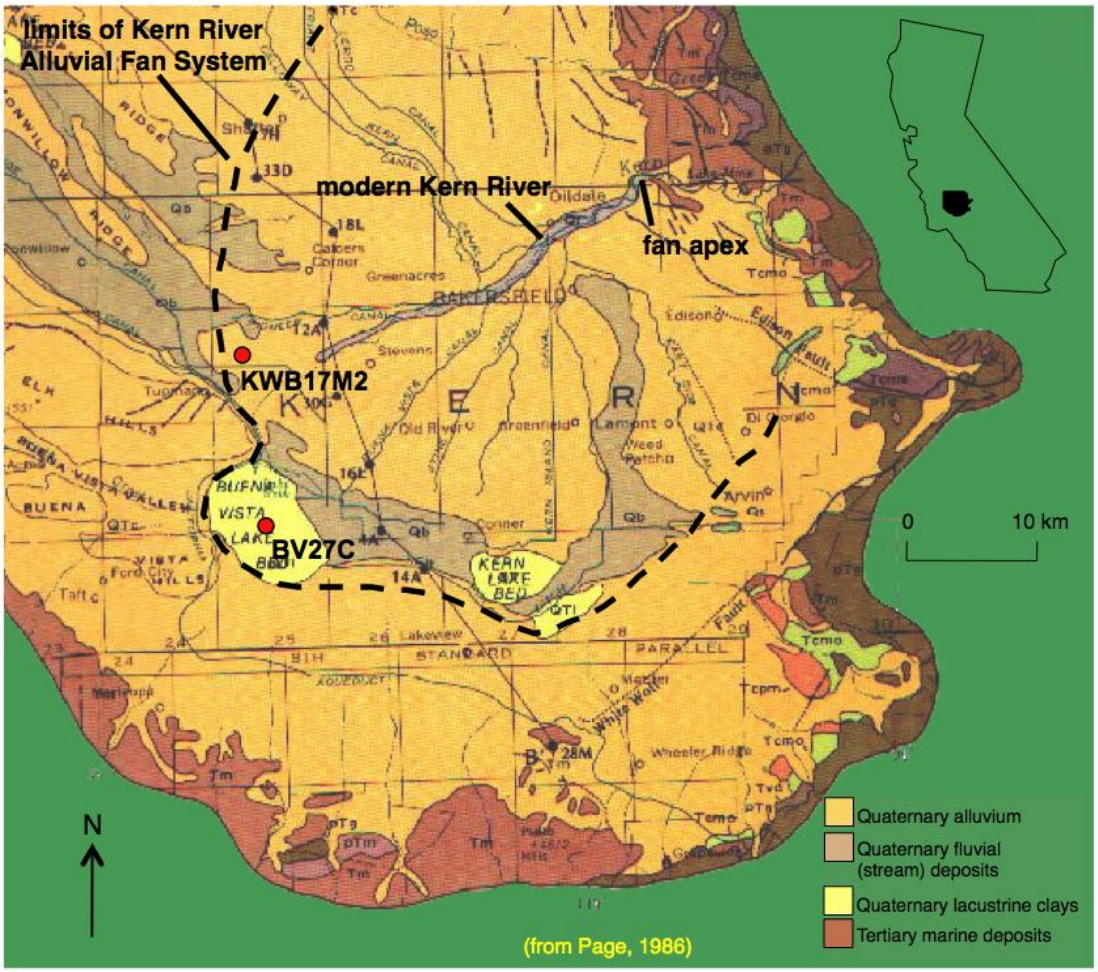

Figure 2. Limits of the Kern River Fan and locations of wells KWB17M2 and BV27C.

lake named Lake Clyde, a lake that is thought to have drained after incision of the present channel connecting the Central Valley to San Francisco Bay during a time of extremely low sea levels and high pluvial lake levels corresponding to Marine Isotope Stage (MIS) 16 (Sarna-Wojcicki (1995). If this is the case, then the prograding delta unit described above may have principally built out into Lake Clyde in response to this dramatic increase in discharge and lowering of base level.

Tulare Lake

Tulare Lake occupies a basin with an area as large as 1600 km^2 when its surface waters are at the historic highstand elevation of 67 meters above sea level (masl) (Atwater et al., 1986). The basin bottom, exposed at present due to agricultural irrigation diversion, is at 55 masl. Thus Tulare Lake reached a maximum depth of ~12 meters in historic times after which it spilled over a sill generated by the confluence of alluvial fans from the Sierra Nevada and the Coast Ranges and then overflowed into the San Joaquin River system (Atwater et al., 1986). The lake system has a number of geomorphic features typical of a long-lived lacustrine system (Currey, 1994). These include an extensive lake-bottom plain, a highstand shoreline, sand spits/bars deposited by longshore drift, and a series of sand deposits that are perhaps reworked delta deposits associated with the Kern River, which enters the basin at the southern end (Figures 4 and 5).

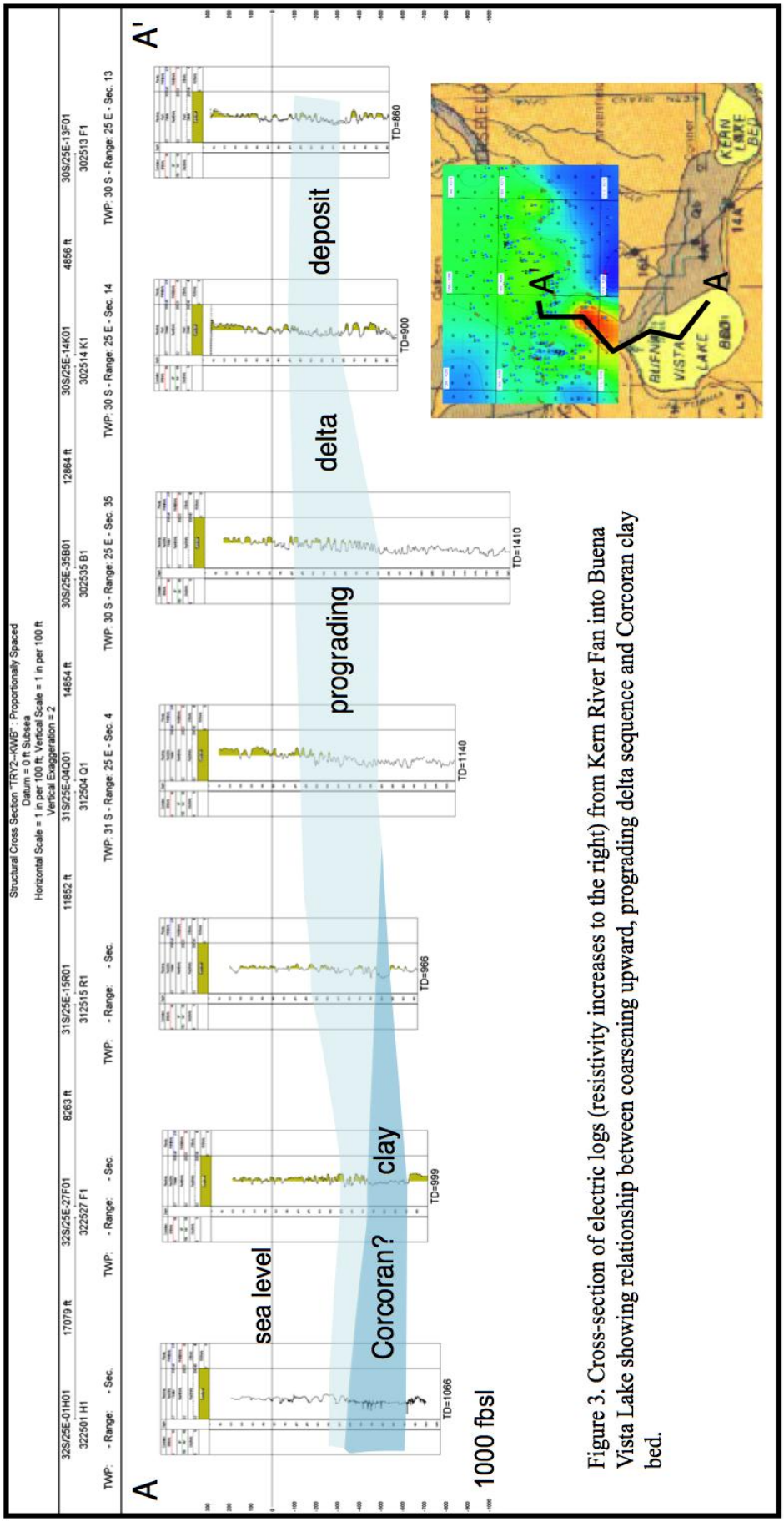

Figure 3. Cross-section of electric logs (resistivity increases to the right) from Kern River Fan into Buena Vista Lake showing relationship between coarsening upward, prograding delta sequence and Corcoran clay bed.

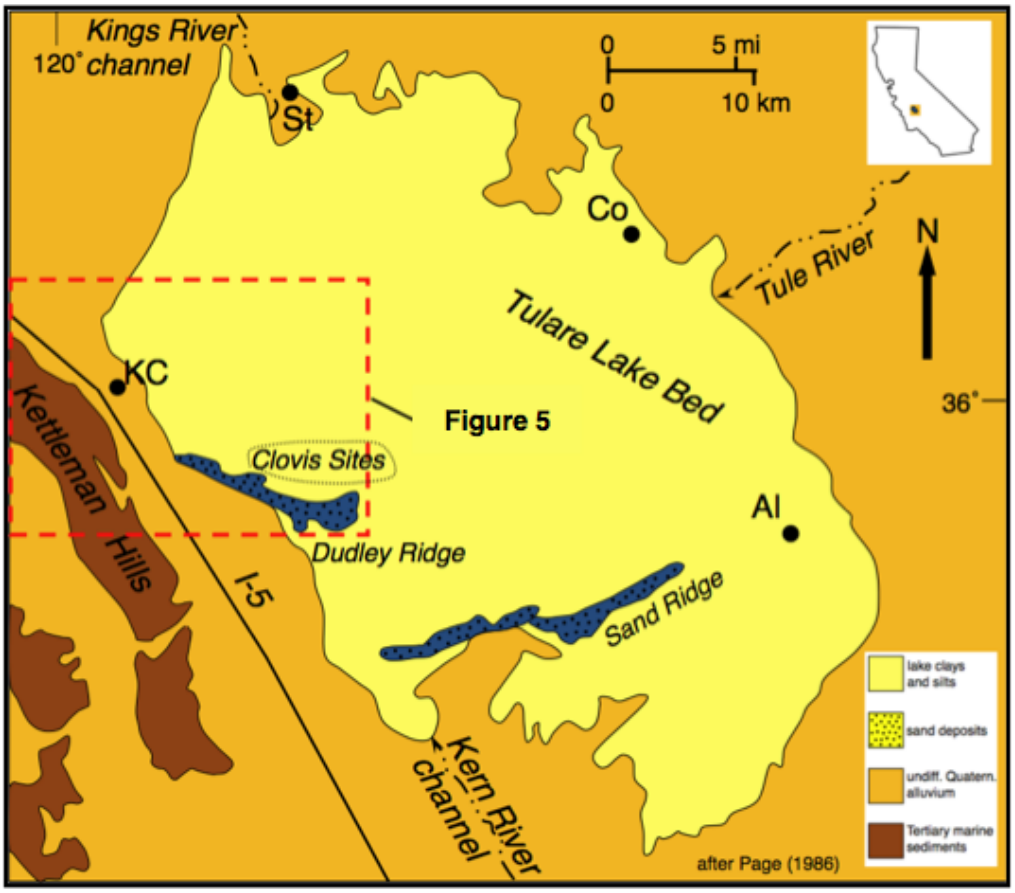

Figure 4. Simplified map of implified geologic map of Tulare Lake. Area studied to date is included in Figure 3 (after Page, 1986; Negrini et al., 2006).

Tulare Lake Level during the Holocene

Building on a previous study by Atwater et al. (1986), Negrini et al. (2006) demonstrated that the surface elevation of Tulare Lake over the past 10,000 years (Figure 6) was consistent with other lacustrine, paludal, and tree-ring based records of paleoclimate throughout south-central California including a record generated from the sediments of Owens Lake (Benson et al., 2002), a body of water that also sources streams flowing from the Sierra Nevada. The reproducibility of these results demonstrates the feasibility of a high resolution surface level history of Tulare Lake that represents climate-driven changes in precipitation over the past several thousand years, an improvement that would require a much larger number of trench and core locations and better age control.

At present, the record in Figure 6 gives only a rough estimate for the surface elevation of Tulare Lake as indicated in part by the many question marks. This is not surprising because this record is based on occurrences of sediments from only three elevations represented by two trench locations and one core location. The problem with such a limited set of sample elevations is as follows. Lake-surface elevation is estimated most dependably by inferring a higher elevation for the lake surface than the elevation of sediments deposited in that lake as found in trenches, cores or outcrops. For example, the presence in the "higher elevation trench" of a clay deposit (blue line) thick enough

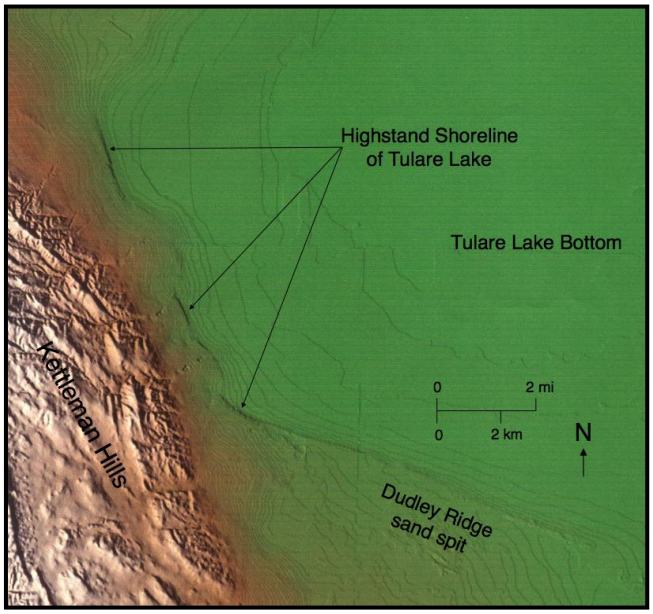

Figure 5. Digital elevation map of the northwestern portion of Tulare Lake and environs. Highstand shorelines are marked by prominent slopes. Younger alluvial fans are superimposed on shorelines. The Dudley Ridge sand spit formed by longshore drift of sands deposits transported to the southeast by winds that are predominantly out of the northwest (Preston, 1981; Negrini et al., 1986).

to represent ~ 1,000 years of time strongly suggests a deep, long lived lake during a time interval centered at ~9,000 cal yr BP, a lake that had to have had a surface elevation above the clay layer elevation of 62 masl. Although it seems reasonable that the surface of such a long-lived lake would occupy the elevation of the overflow sill for much of this time interval, in fact, the upper limit of the lake surface elevation is not constrained. This shortcoming can only be overcome by investigating the nature of coeval sediments in trenches or cores taken at higher elevations. One would then expect to see coeval sediments coarsening upward from trench to trench until the elevation of the sediments approached the surface elevation of the lake at that time. Increasing the number of trenches and/or cores in this manner would also improve lake-level estimates because this increase would lead to a greater likelihood of finding sedimentary features that are particularly diagnostic of water depth at the time of formation (e.g., mudcracks).

Connecting lake level to stream runoff

Building on earlier results from Harding (1949), Atwater et al. (1986) devised a hydrologic balance model that allowed them to calculate Tulare Lake surface elevations through time using stream runoff as the principal input. This model successfully generated an accurate reconstruction of observed lake level for the 25-30 yr time period starting when lake-level records were first kept and ending when lake-lake level was dramatically altered by irrigation-related stream diversion (Figure 7).

The calculated lake level is the end result of calculated water volume, which mostly depends upon a stream runoff contribution that is corrected for evaporation and infiltration and direct precipitation onto the lake. The range of calculated elevations within the gray band reflects uncertainties mostly in the less well known corrections. Because the upper bound of the calculated elevations provides the best fit to the observed elevations (Figure 7) and, the more uncertain corrections subtract from the calculated lake level (e.g., infiltration), the true corrections are likely closest to their minimum values (see Table 2 of Atwater et al., 1986).

The comparison shown in Figure 8 suggests that a relationship between Tulare Lake runoff and regional climate change does indeed exist. A positive Pacific Decadal Oscillation index corresponds to warmer eastern Pacific Ocean waters offshore California, which, in turn, predicts more rainfall in the southwestern U.S. including the central and southern Sierra (e.g., Barron et al., 2010 and references therein). The lone radiocarbon date shown in Figure 6 suggests that the lake began to rise as the long-term PDO index shifted to positive values and

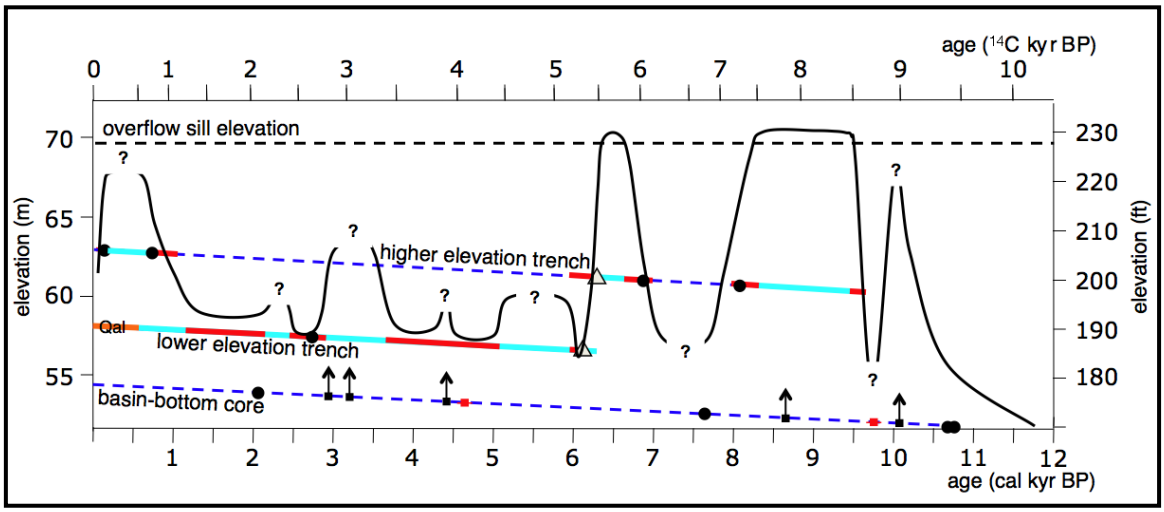

Figure 6. Tulare Lake-level record of Negrini et al. (2006) based on sediments trenched basinward of the highstand shoreline shown in Figure 3 and supplemented with pollen-based interpretation of a basin center core by Davis (1999). Solid blue lines indicate age of deeper water sediments (silts and clays). Red lines indicate sandy sediments. Orange line represents end of lacustrine-dominated sediment record of lower elevation trench due to encroachment of late Holocene alluvium fan. Open triangles denote mudcracks. Upward arrows denote deep water indicators in basin-center core record (e.g., laminated silts/clays or high concentrations of pelagic algae). Red squares show sediments with high concentrations of littoral pollen (so shallower lake). Location of radiocarbon dates are shown as solid black circles.

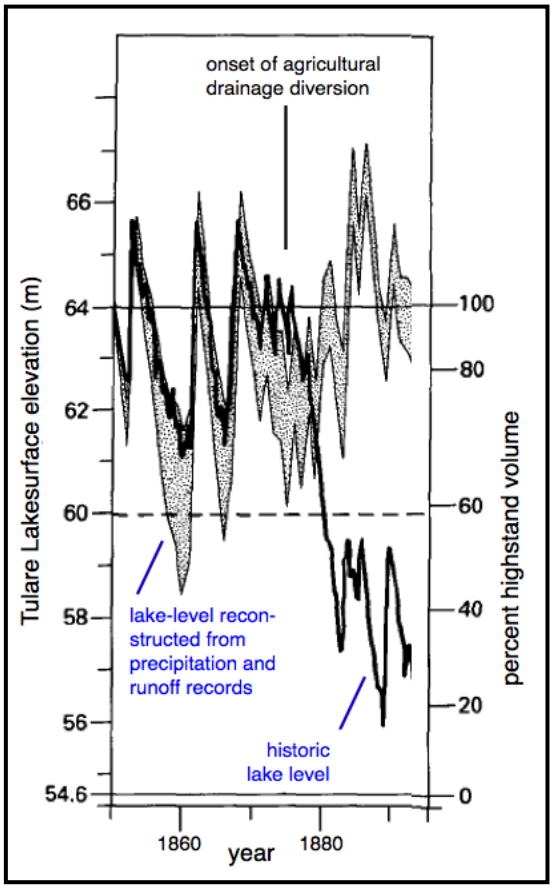

Figure 7. Comparison of observed Tulare Lake surface elevations (bold black line) with elevations calculated from hydrologic parameters (stippled gray band). Note that calculated and observed elevations diverge after the runoff was diverted for irrigation. Since the beginning of the 20th century (not shown) the lake has been dry (i.e., all of the stream flow has been captured for irrigation). (after Atwater et al., 1986).

became very deep (massive clays) during the extreme positive PDO anomaly starting in the mid-15th century. Note that other paleoclimate records exist, which estimate the sea surface temperatures (e.g., Barron et al., 2010) corresponding to the PDO index. Although this result is intriguing, the existing Tulare Lake level record is at this point too under constrained to make a definitive correlation.

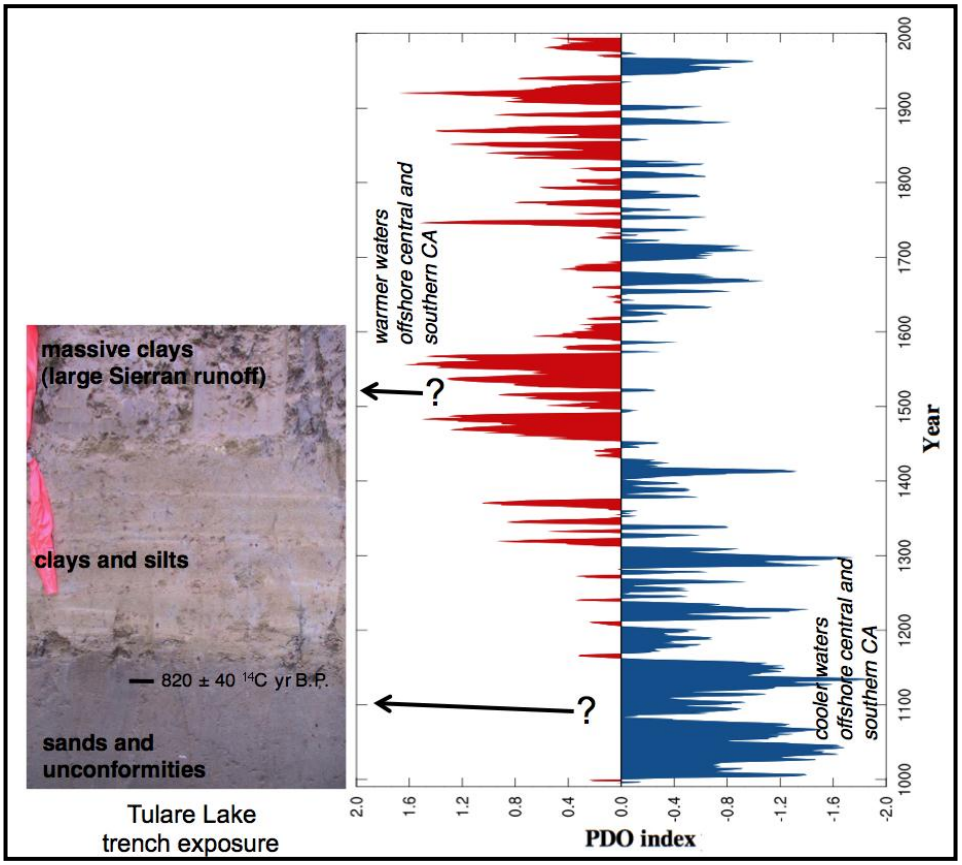

Figure 8. On the left is an exposure from a trench at an elevation corresponding to a one-half-full Tulare Lake. Thus the lake was relatively high when the clay and silts and particularly the massive clays were deposited. On the right is the tree-ring-based reconstruction of the Pacific Decadal Oscillation index from McDonald and Case (2005).

References

Atwater, B.F., Adam, D.P., Bradbury, J.P., Forester, R.M., Mark, R.K., Lettis, W.L., Fisher, G.R., Gobalet, K.W., Robinson, S.W., 1986. A fan dam for Tulare Lake, California, and implications for the Wisconsin Glacial history of the Sierra Nevada. Bulletin of the Geological Society of America 97, 97–109.

Barron, J.A., 2010. Santa Barbara Basin diatom and silicoflagellate response to global climate anomalies during the past 2200 years, Quaternay International, 215: 34-44.

Bartow, J.A., 1991. The Cenozoic evolution of the San Joaquin Valley, California, U.S. Geol. Surv. Prof. Paper 1501, 40 pp.

Benson, L., Kashgarian, M., Rye, R., Lund, S., Paillet, F., Smoot, J., Kester, C., Mensing, S., Meko, D., Lindstro¨ m, S., 2002. Holocene multidecadal and multicentennial droughts affecting Northern California and Nevada. Quaternary Science Reviews 21, 659–682.

Croft, M.G., 1972. Subsurface geology of the Late Tertiary and Quaternary water-bearing deposits of the southern part of the San Joaquin Valley, California, U.S. Geol. Surv. Water-Supply Paper 1999H, 29 p.

Currey, D.R., 1994. Hemiarid Lake basins: geomorphic patterns. In: Abrahams, D., Parsons, A.J. (Eds.), Geomorphology of Desert Environments. Chapman & Hall, New York, pp. 422–444.

Dale R.H., J.J. French, G.V. Gordon, 1966, Ground-water geology and hydrology of the Kern River alluvial fan area, California, U.S. Geol. Surv. Water Res. Div. Open-File Report.

Davis, O.K., 1999. Pollen analysis of Tulare Lake, California: Great Basin-like vegetation in central California during the full-glacial and early Holocene. Review of Palaeobotany and Playnology 107: 249–257.

Davis, P., J. Smith, G.J. Kukla, N.D. Opdyke, 1977. Paleomagnetic study at a nuclear power plant near Bakersfield, California, Quaternary Research, v. 7, pp. 380-397.

Frink, J.W., H.A. Kues, 1954. Corcoran clay - A Pleistocene lacustrine deposit in the San Joaquin Valley, California, American Association Petroleum Geologist Bulletin, v. 38, pp. 2357-2371.

Harden, D., 2004. California Geology, Prentice Hall, 576 p.

Harding, S.T., 1949. Inflow to Tulare Lake from its tributary streams: Hanford, California, Tulare Lake Basin Water Storage District, 129 p.

Lanphere, M.A., Champion, D.E., Christiansen, R.L., Izett, G.A., Obradovich, J.D., 2002. Revised ages for tuffs of the Yellowstone Plateau volcanic field: assignment of the Huckleberry Ridge Tuff to a new geomagnetic polarity event. Geological Society of America Bulletin 114, 559-568.

MacDonald, G.M., Case, R.A., 2005. Variations in Pacific Decadal Oscillation over the past millennium. Geophysical Research Letters 32, L08703.

Marble, R., R. Negrini, 2008. Dating Kern River Alluvial Fan sediments with magnetostratigraphy: Initial magnetization stability tests, poster presentation at May, 2008 monthly meeting of the San Joaquin Geological Society, Bakerfield, CA

Negrini, R., D. Baron, R. Horton, J. Gillespie, K. Blake, J. Huff, 2004. Section 2. CSU Bakersfield contributions, in 3-D Characterization and Monitoring of the Aquifer Attributes in the Kern Water Bank, final report submitted to CA Dept. Water Resources for AB303 Local Groundwater Assistance grant, Kern Water Bank Authority, Bakersfield, CA.

Negrini, R., D. Baron, R. Horton, J. Gillespie, P. Wigand, M. Palacios-Fest, L. Boockoff, M. Casterline, E. Powers, R. Nunneley, K. O'Sullivan, 2006a. Section 2. CSU Bakersfield contributions, in Hydrogeology of the Kern Fan Element and Implications on Local Groundwater Management of Kern Water Bank, final report submitted to CA Dept. Water Resources for AB303 Local Groundwater Assistance grant, Kern Water Bank Authority, Bakersfield, CA.

Negrini, R.M., P.E. Wigand, S. Draucker, K. Gobalet, J.K. Gardner, M.Q. Sutton, R.M. Yohe II., 2006b. The Rambla Highstand Shoreline and the Holocene lake level history of Tulare Lake, California. Quaternary Science Reviews, 25: 1599-1618.

Negrini, R., D. Baron, J. Gillespie, R. Horton, A. Draucker, N. Durham, J. Huff, P. Philley, C. Register, 2009. A middle Pleistocene lacustrine delta in the Kern River depositional system: Structural control, regional stratigraphic context, and impact on groundwater quality, *in* Contributions to the Geology of the San Joaquin Basin, California, Miscellaneous Publication #48, Pacific Section AAPG.

Page, R.W., 1986. Geology of the fresh ground-water basin of the central valley, California, with texture maps and sections, U.S. Geol. Surv. Prof. Paper 1401C, 54 p.

Preston, W.L., 1981. Vanishing Landscapes: Land and Life in the Tulare Lake Basin. University of California Press, Berkeley, CA.

Powers, E., R. Negrini, P. Wigand, M. Palacios-Fest, and N. Foit, 2008. The Corcoran Clay at great depths in the southern San Joaquin Valley, CA, Pacific Section AAPG annual meeting, Bakersfield, CA.

Reheis, M.C., A.M. Sarna-Wojcicki, R.L. Reynolds, C.A. Repenning, and M.D. Mifflin, 2002. Pliocene to middle Pleistocene lakes in the Great Basin: Ages and Connections, In Hershler, R., D.B. Madsen, D.R. Currey, (eds.), Great Basin Aquatic Systems History, Smithsonian Contributions to the Earth Sciences, No. 3, Smithsonian Press, Washington, D.C.

Sarna-Wojcicki, A.M., 1995. Age, areal extent, and paleoclimatic effects of "Lake Clyde," a mid-Pleistocene lake that formed the Corcoran Clay, Great Valley, California. Glacial History of the Sierra Nevada, California: a Symposium in Memorial to Clyde Wahrhaftig.

Sarna-Wojcicki, A.M., Pringle, M.S., and Wijbrans, Jan, 2000, New 40Ar/39Ar age of the Bishop Tuff from multiple sites and sediment rate calibration for the Matuyama-Brunhes boundary. Journal of Geophysical Research, v. 105, B9, p. 21,431-21,443.

Wilson, R.I., 1993. Paleoenvironmental Analysis of the Shallow Sediments within the Kern Water Bank Project Area of the Southern San Joaquin Valley, Western Kern County, California: Implications for Local Hydrogeology, M.S. Thesis, CSU Fresno.

Stop 1-1e:

Scope of the seismic hazard characterization of the Kern Canyon fault for the Isabella Project, California

Keith Kelson, *Fugro Consultants*
Andrew Lutz, *Fugro Consultants**
Cooper Brossy, *Fugro Consultants*
Robert Turner, *Fugro Consultants*
David Serafini, *US Army Corps of Engineers*
Dave Simpson, *URS Corporation*
Ben Kozlowicz, *URS Corporation*
Ozgur Kozaci, *Fugro Consultants*
Ronn Rose, *US Army Corps of Engineers*

*currently: Lettis Consultants International

Findings presented at the Kern Canyon fault stops along the 2011 FOP field trip are a partial presentation of the results of a comprehensive characterization of the previously poorly understood Kern Canyon fault (KCF), which is a primary seismogenic source in the southern Sierra Nevada in Tulare and Kern counties, California. The investigation performed by URS Corporation and Fugro William Lettis & Associates was designed to provide direct input for assessing the seismic stability of the Isabella Project Main Dam and Auxiliary Dam, owned and operated by the U.S. Army Corps of Engineers. Our investigation involved regional geologic and seismologic analyses and detailed geologic and paleoseismic data collection at multiple sites along the fault to characterize the KCF as a potential seismic source for the Isabella Lake dams. The results of these investigations are being used to assess the viability of potential remedial alternatives.

The north-striking KCF is primary geologic structure within the southern Sierra Nevada, continuing for more than 135 km from the Walker Basin on the south to the Kings-Kern Divide in the High Sierra on the north (Figure 1). Until recently, the KCF was thought to be inactive, based on early interpretations that a 3.5-million-year-old basalt flow (located about 60 km north of Auxiliary dam) is not displaced by the fault (Webb, 1946). However, the KCF is associated with prominent geomorphic expression (Page, 2005; URS, 2006), and initial findings from this investigation documented geomorphic evidence of displacement within the past approximately 15,000 years (URS, 2007, 2008; Kelson et al., 2009). Prior to this assessment, there were no data on fault activity, slip rate, coseismic displacement, or sense of fault slip; in other words, critical information needed to complete an adequate seismic source characterization did not exist for use in either a probabilistic seismic hazard analysis (PSHA) or a deterministic seismic hazard analysis (DSHA).

The KCF is now judged as a capable fault per Corps criteria, and an active fault per California Division of Safety of Dams criteria (Fraser, 2001). The Corps classifies the Auxiliary dam in Dam Safety Action Class (DSAC) 1, which is the highest rating, based on a high probability of failure and severe consequence from failure. Because the fault extends beneath the right abutment of the Auxiliary Dam, assessing fault activity and determining the likely amount of coseismic rupture are critical for dam safety considerations. Information on fault activity and segmentation is essential for estimating maximum earthquake magnitude and conducting strong ground-motion analyses, and data on the timing of large paleoearthquakes on the Kern Canyon fault are critical for calculating probabilistic strong ground motions. This investigation provided a basis for characterizing seismic hazard at the Isabella dams, and for

understanding regional seismic hazard for the entire southern Sierra Nevada. As a result of the recognition of fault activity and the possibility of fault rupture beneath the Auxiliary dam, detailed information was developed on the location, width, and distribution of expected coseismic deformation specifically at the Auxiliary dam.

The primary purposes of our investigation were to (a) develop well-constrained seismic source characteristics for the KCF for use in analyses of strong ground motions for the dams and appurtenant structures, and (b) characterize potential fault-rupture hazards at the Auxiliary dam. Our effort built upon previous seismic characterizations based on regional or preliminary information (e.g., URS, 2006) and provides the first clear demonstration of recent fault activity and the first quantitative evaluation of the location, width, and expected amount of coseismic displacement beneath the Auxiliary dam. The scope of work included: (1) evaluating available pre-existing geologic and geophysical data and Corps project files, (2) geomorphic mapping of the entire Kern Canyon and Breckenridge faults from aerial photography and LiDAR-derived imagery, (3) paleoseismic trenching and/or shallow drilling at six sites north and south of Lake Isabella, (4) estimating numerical and relative ages of faulted and unfaulted deposits using radiocarbon, optically stimulated luminescence, cosmogenic exposure, and relative soil-profile development analyses, (5) analyzing instrumental seismicity and regional seismotectonic models, (6) developing reasonable earthquake rupture scenarios and determining maximum earthquake magnitudes, and (7) providing seismic source characteristics for DSHA and PSHA calculations of strong ground motions.

These office- and field-based investigations were synthesized developed a new seismic source characterization for the KCF, essentially starting from scratch because of an absence of well-constrained paleoseismic data. The geologic field analyses were conducted at various levels of technical detail according to site-specific geologic conditions, in order to develop well-constrained information along the entire 135-km-long KCF, as well as the Breckenridge fault at the southern end of the KCF. For example, in readily accessible areas containing well-bedded alluvial stratigraphy overlying the fault, we completed detailed paleoseismic trenching and shallow drilling to target specific geologic features indicative of past earthquakes. On the other hand, parts of the KCF that extend through rugged, high-mountain topography (e.g., in the Golden Trout Wilderness) are not accessible for paleoseismic trenching or drilling, and called for acquisition and analysis of detailed LiDAR-based topographic data and detailed geologic and geomorphic mapping of specific fault-related features. As the investigation progressed, we adapted data collection activities to accommodate the evolving understanding of fault characteristics, various logistical restrictions (e.g., wilderness permits), and the need to balance expenditures with anticipated results. In our opinion, this comprehensive investigation is unusual not only because it characterizes a fault for which very little was known, but also because the fault is long (over 140 km), relatively active (even by California standards), and accommodates a significant amount of deformation across a large part of the state (the southern Sierra Nevada). In addition to developing new data on the KCF as a seismic source, the results of this analysis are useful for understanding regional seismotectonics, defining the distribution of paleoseismic rupture on a relatively long normal fault, and understanding patterns of alluvial and glacial deposition during and after the late Pleistocene-Holocene climatic change in the southern Sierra Nevada.

The project team developed specific geologic and paleoseismic data to define three physical sections of the KCF and one section of the adjacent Breckenridge fault. The project team used these data to interpret the likely fault-rupture scenarios on various combinations of these fault sections. A total of 16 paleoseismic trenches were excavated at six sites as part of this study. In addition to these excavations and other detailed investigations along all four fault sections, the project team completed detailed and reconnaissance-level studies along nearly the entire KCF and the adjacent Breckenridge fault to evaluate the lengths of the fault sections and the probable total length of possible late-Quaternary ruptures on the KCF-Breckenridge fault system. Coseismic displacement has occurred along all or most of the KCF during the late Quaternary (e.g., since 125 ky). Field-based geologic and stratigraphic data suggest coseismic displacements of about 2.2 to 6.0 ft (0.67 to 1.8 m) and a late-Quaternary slip rate of about 0.3 ± 0.1 mm/yr. Possible fault-rupture segments are interpreted using the results obtained from the paleoseismic investigations, the geomorphic and geologic mapping, and the analysis of instrumental seismicity. The paleoseismic evidence suggests both single-section and longer, multi-section rupture behaviors. The available information was used to assign preliminary weightings for nine possible rupture scenarios, which can be used in the deterministic seismic hazard analysis (DSHA) and the probabilistic seismic hazard analysis (PSHA) calculations. The segmentation models suggest that 55 percent of the earthquakes on the KCF involve ruptures that are more than 50 km long and that continue beneath the Auxiliary Dam. Such ruptures are probably in the range of moment magnitude (**M**) 6.5 to 7.5 and will likely generate surface faulting beneath the Auxiliary Dam embankment. Of the scenarios that involve rupture of the fault section that passes beneath the Auxiliary Dam, the weighted mean magnitude is about **M**6.7. It is judged that the Maximum Credible Earthquake (MCE) on the KCF is **M**7.5, but an earthquake of this magnitude is an extremely unlikely event.

References

Kelson, K.I., and 10 others, 2009, Recent advancements in understanding seismic source characteristics of the Kern Canyon fault, southern Sierra Nevada [abstr]: Association of Engineering and Environmental Geologists Annual Meeting, South Lake Tahoe, CA.

Kelson, K.I., Simpson, D.T., Rose, S.R., and Serafini, D.C., 2010, Seismic hazard characterization of the Kern Canyon fault for Isabella Dam, California: Proceedings, United States Society on Dams 2010 30th Annual Meeting, Sacramento, April, 2010, p. 295-310: http://ussdams.com/proceedings/2010Proc/295-310.pdf

Page, W.D., 2005, Reconnaissance along the Kern Canyon fault and inspection of the Little Kern basalt flow, Kern County, California: Report to URS Corporation, Oakland, Calif., 6 pp. plus figures.

URS Corporation, 2006, Kern Canyon Fault Assessment Study. Technical Memorandum, Isabella Dam – Dam Safety Assurance Program, Lake Isabella, CA: Consultant's report prepared for Dam Safety Assurance Program, U.S. Army Corps of Engineers, Sacramento, California, 6 p., plus figures.

URS Corporation, 2007, Quaternary study of the Rincon section of the Kern Canyon fault, California: Consultant's report prepared for Dam Safety Assurance Program, U.S. Army Corps of Engineers, Sacramento, California, 6 p. plus figures.

URS Corporation, 2008, Kern Canyon fault Assessment Phase II, Kern and Tulare Counties, California: Consultant's report prepared for Dam Safety Assurance Program, U.S. Army Corps of Engineers, Sacramento, California (dated March 21, 2008).

Webb, R.W., 1946, The geomorphology of the Middle Kern River Basin, southern Sierra Nevada, California: Geological Society of America Bulletin, v. 57, p. 355-382.

Table 1. Summary of investigations and results along fault sections of the Kern Canyon fault system

				Investigations							Results				
Fault Section	**Length (km)**	**Section Boundary**	**Investigation Sites**	Geologic / Geomorphic Mapping	Trenching	Drilling	Age Dating	Seismicity Analysis	Geophysical Data Review	Geotech Data Review	Fault Pattern	Fault Activity	Earthquake Chronology	Fault Slip Rate	Coseismic Displacement
Harrison Pass				X							X	X			
North Kern Canyon	56 + 15		Junction Meadow	X			X				X	X			
			Soda Spring	X			X				X	X		X	
Flatiron				X							X	X			
South Kern Canyon	47 + 10		Sinombre Creek	X			X				X	X		X	
			Rincon Spring	X	X		X				X	X	X	X	X
			Brush Creek	X	X		X				X	X	X	X	X
			Brin Creek	X			X				X	X		X	
			Corral Creek	X	X	X	X				X	X	X	X	X
Kernville				X					X		X	X			
Lake Isabella	32 + 10		Barlow Drive	X	X	X	X		X	X	X	X	X	X	X
			Bernie/Silicz	X	X	X	X			X	X	X	X	X	X
			Havilah North	X	X		X				X	X	X	X	X
Piute Pass				X				X			X	X			
Breckenridge	19 + 6		Oak Tree Estates	X			X	X			X	X		X	
Julia Lake				X				X			X	X			

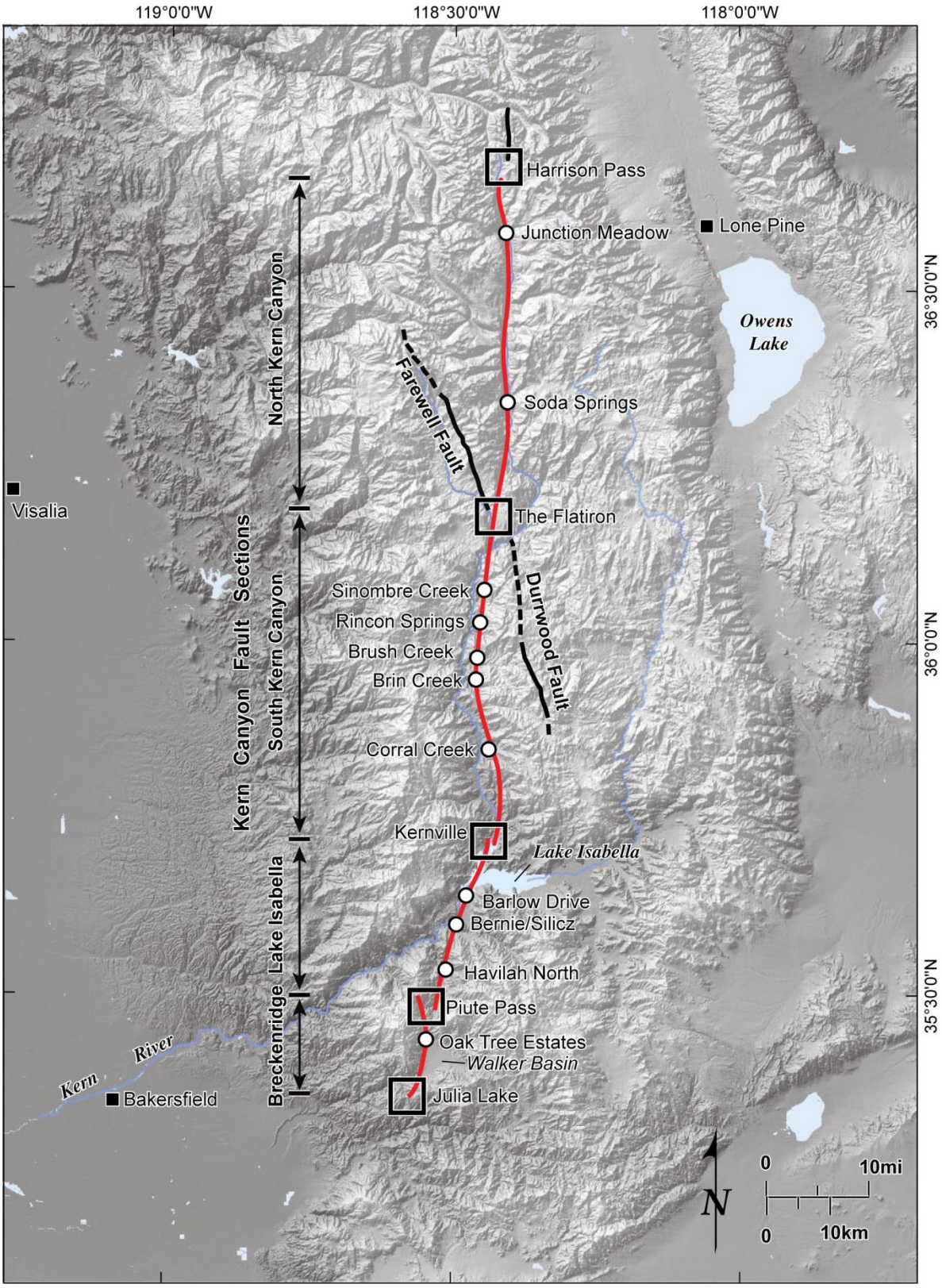

Figure 1. Hillshade rendering of the southern Sierra Nevada and surrounding region, showing location of the Isabella dams, primary fault sections of the Kern Canyon fault, and detailed investigation sites.

Road Log B-B′

Kern Gorge fault (Stop 1-1) to Bernie Drive paeloseismic site (Stop 1-2)

30.1 miles, 45 minutes

Mileage		Lat./Long.
0.0	**Turn LEFT onto CA-178 toward Lake Isabella (reset odometer)**	**35.4197° -118.8325°**
2.7	Crossing the Kern Gorge fault and Bakersfield city limits	35.4402° -118.7947°
4.4	Kern Gorge Powerhouse (Kern River No. 1), built from 1902-1907 by the Kern River Company and now operated by Southern California Edison—when first online this was the largest hydroelectric facility in the world, providing electric power for Los Angeles. Steep rock debris chute above it across the river.	35.4605° -118.7786°
7.2	The river takes an anomalous 90° turn to the east-southeast where it intersects a bedrock lineament oriented subparallel to the Kern Gorge fault—the longitudinal profile shows another slight nickpoint here and several low boulder terraces have accumulated because the river gradient is not being steepened as rapidly by incision, consistent with north-northeast-directed tilting of this part of the range…or…dextral displacement?	35.4802° -118.7478°
9.7	The river turns back to the prevailing east-northeastern direction	35.4743° -118.7120°
13.9	This is effectively the top of the Kern Gorge—between the mouth of the gorge and here the relief decreases along over-steepened river margins that rise to meet convex-upward hillslope shoulders. Several tens of meters of incision are recorded here, increasing to hundreds of meters at the mouth of the gorge.	35.5000° -118.6942°
14.4	The Kern River Gorge opens slightly between here and mile 18.3—some deeply incised bedrock terraces (elev. 610 and 635 m) are preserved along the north canyon wall (right side)	35.5217° -118.6726°
26.1	To the right is the Borel Powerhouse and Penstocks (Kern River No. 2), built from 1897-1904 by the Kern River Co. and now operated by So.Cal. Edison	35.5889° -118.5247°
26.7	Several lower bedrock terraces to the left (elev. 745 m)	35.5962° -118.5170°
26.9	Overpass bridges a once-contiguous bedrock terrace (elev. 770 m)	35.5980° -118.5157°
28.5	As you cross the Kern River you are about to cross over onto the footwall of the KCF—to the left are bedrock terraces (elev. 750 m) truncated to the east by the KCF	35.6073° -118.4955°

28.7	**Take exit 42 toward Bodfish/Lake Isabella**	**35.6087°** **-118.4924°**
29.0	**Turn RIGHT onto Elizabeth Norris Road** You may see some remaining evidence along the road here of a long run-out debris flow that descended Erskine Creek on July 12, 2008, the same day as the Oak Creek debris flow that Dave Wagner will present at Stop 3-2 on Sunday. These debris flows were triggered by heavy rainfall from two separate monsoonal storm cells that formed the same day roughly 100 km apart	**35.6108°** **-118.4886°**
29.4	**Turn RIGHT onto Lake Isabella Boulevard**	**35.6089°** **-118.4835°**
29.9	**Take the 2nd RIGHT onto Chain Avenue**	**35.6029°** **-118.4860°**
30.0	**Take the 1st RIGHT onto Reeder Drive**	**35.6030°** **-118.4899°**
30.1	**Locate street parking in the vicinity of Reeder Drive and Bernie Drive. Walk up Bernie Drive to Stop 1-2**	**35.6045°** **-118.4894°**

Stop 1-2a:

Paleoseismic record of earthquakes along the Lake Isabella section of the Kern Canyon fault

Andrew Lutz, *Fugro Consultants* *
Keith Kelson, *Fugro Consultants*
John Baldwin, *Fugro William Lettis & Associates**
Ronn Rose, *U.S. Army Corps of Engineers*
**currently: Lettis Consultants International*
Ozgur Kozaci, *Fugro Consultants*
Dave Simpson, *URS Corporation*
Robert Turner, *Fugro Consultants*

Abstract

The Kern Canyon fault is a major N-S striking crustal structure that has accommodated extensional deformation within the southern Sierra Nevada range via dominantly east-down faulting since at least the middle Pleistocene. A 34-km-long portion of this fault, the Lake Isabella section, strikes N10°W between the towns of Kernville and Havilah and is characterized along much of its length by linear, east-facing bedrock scarps that impound Holocene and late Pleistocene alluvial and colluvial deposits in the Hot Spring and Havilah Valleys. The southern boundary of this fault section is a 3 km right step-over to the Breckenridge fault in Walker Basin. The northern boundary with the South Kern Canyon section of the Kern Canyon fault is a 3 to 4 km right step-over that corresponding with a prominent change in strike (35°) and a distinct disruption in the continuity of fault-related geomorphic features. Detailed geomorphic mapping along the Lake Isabella section documents clear evidence for the occurrence of multiple late Quaternary surface-rupturing earthquakes, and paleoseismic and radiometric age data from one site in Havilah Valley and two sites in Hot Spring Valley indicate at least two and as many as three Holocene surface-rupturing earthquakes that faulted colluvial and alluvial deposits.

Faulted colluvial deposits at the Havilah Valley site provide evidence for at least two Holocene surface ruptures and one Late Pleistocene surface rupture and a minimum vertical slip rate of 0.1 to 0.3 mm/yr since about 15 ka. Faulted and warped alluvial deposits near the south end of Hot Spring Valley (Bernie/Silicz site) indicate at least two and possibly three Holocene surface ruptures and a vertical slip rate of 0.2 to 0.4 mm/yr since 30 ka. Faulted and warped colluvial deposits near the north end of Hot Spring Valley (at the Isabella Project Auxiliary Dam) show evidence for two to three Holocene to possibly late Pleistocene surface ruptures and a vertical slip rate of 0.1 to 0.3 mm/yr since 20 ka.

A paleoearthquake chronology for the Lake Isabella section of the Kern Canyon fault was developed by correlating paleoseismic data among these three sites. The most-recent surface-rupturing earthquake occurred at about 3.6 ka and the penultimate earthquake occurred between about 5.5 and 4.4 ka. Comparison of this event chronology with the South Kern Canyon section of the Kern Canyon fault indicates that these two fault sections ruptured independently during their most recent surface ruptures and may have ruptured together during their penultimate surface rupture. Trench evidence shows that the two Holocene ruptures along the Lake Isabella section produced average vertical displacements of about 0.9 to 1.1 m.

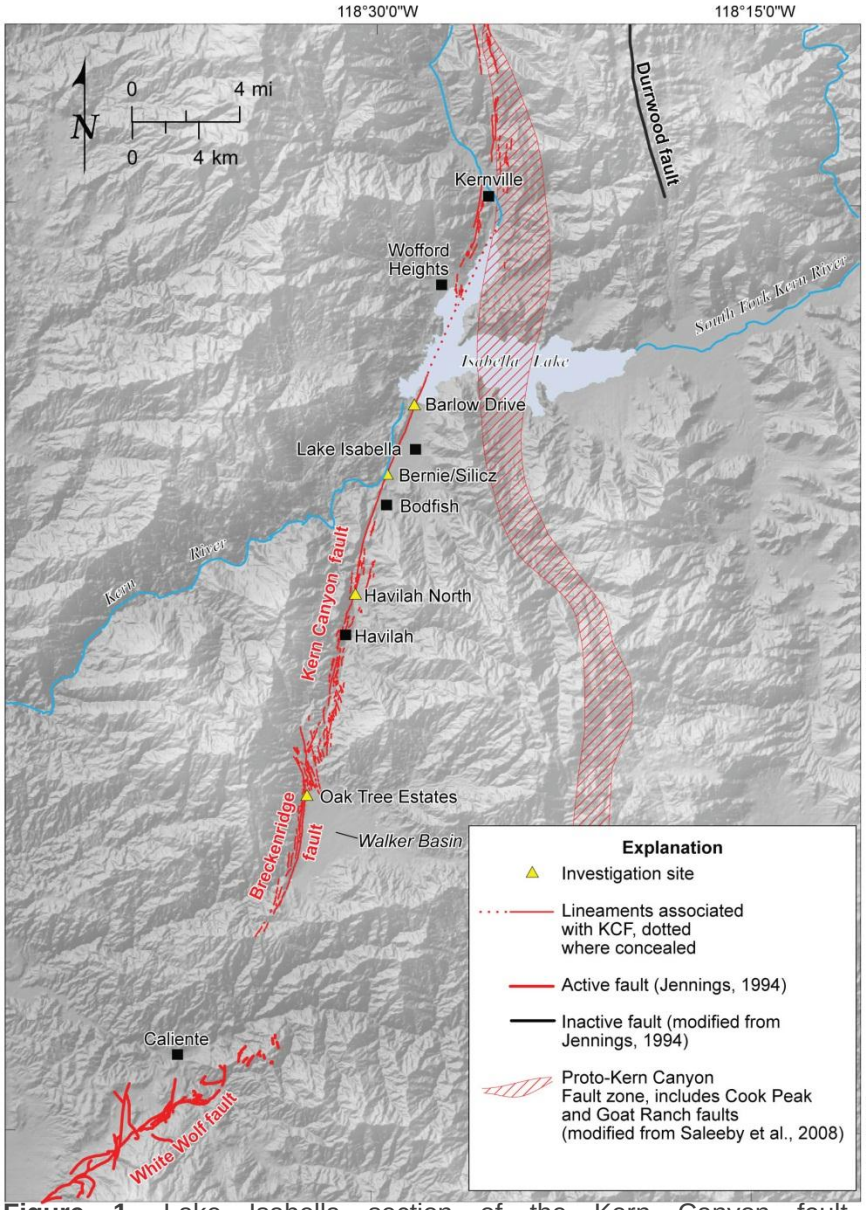

(A)

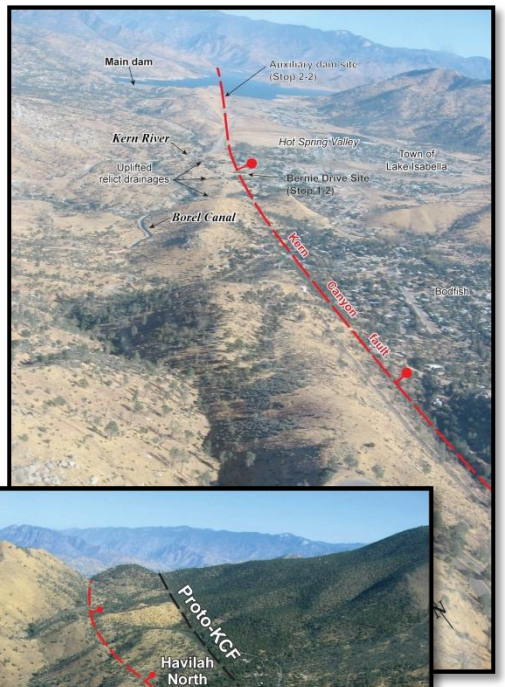

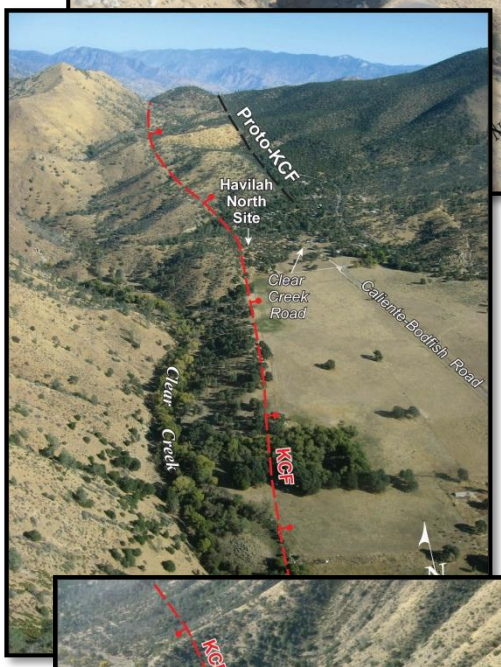

(B)

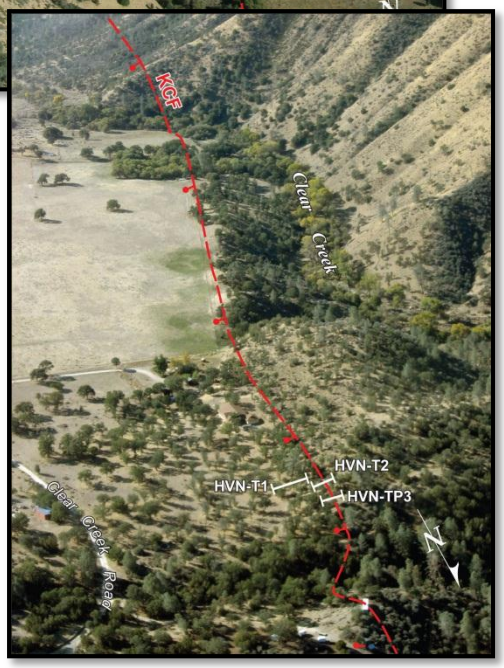

(C)

Figure 1. Lake Isabella section of the Kern Canyon fault. Photo A looks north and shows ponded alluvium in Hot Spring Valley at **Stop 1-2** (Bernie Drive paleoseismic site) and **Stop 2-1** (Auxiliary Dam).

Photo B looks north and show ponded alluvium in Havilah Valley at the North Havilah trench site and the opposite side of the prominent saddle at the south end of Hot Spring Valley. Photo C looks south across a similar area as photo B.

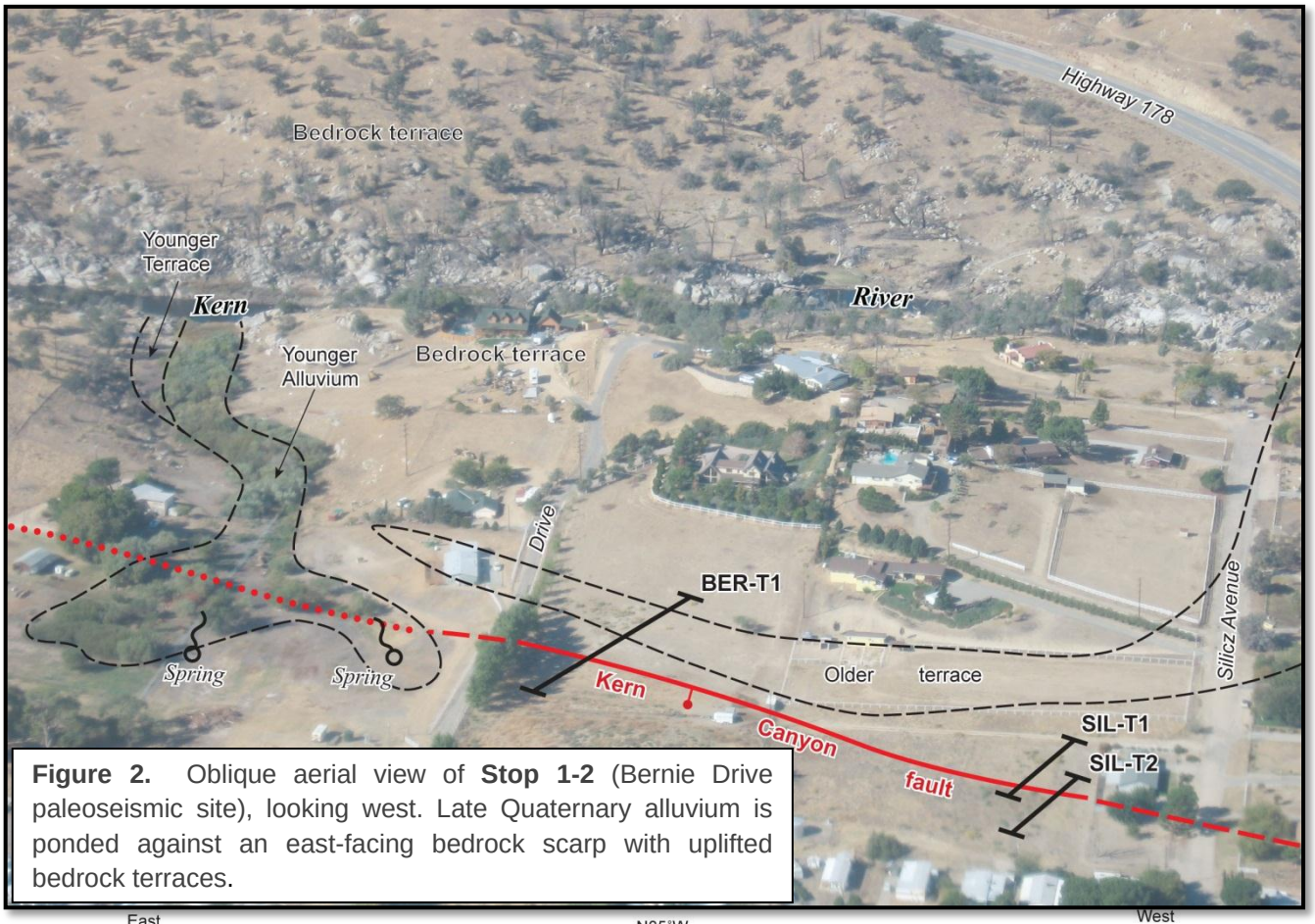

Figure 2. Oblique aerial view of **Stop 1-2** (Bernie Drive paleoseismic site), looking west. Late Quaternary alluvium is ponded against an east-facing bedrock scarp with uplifted bedrock terraces.

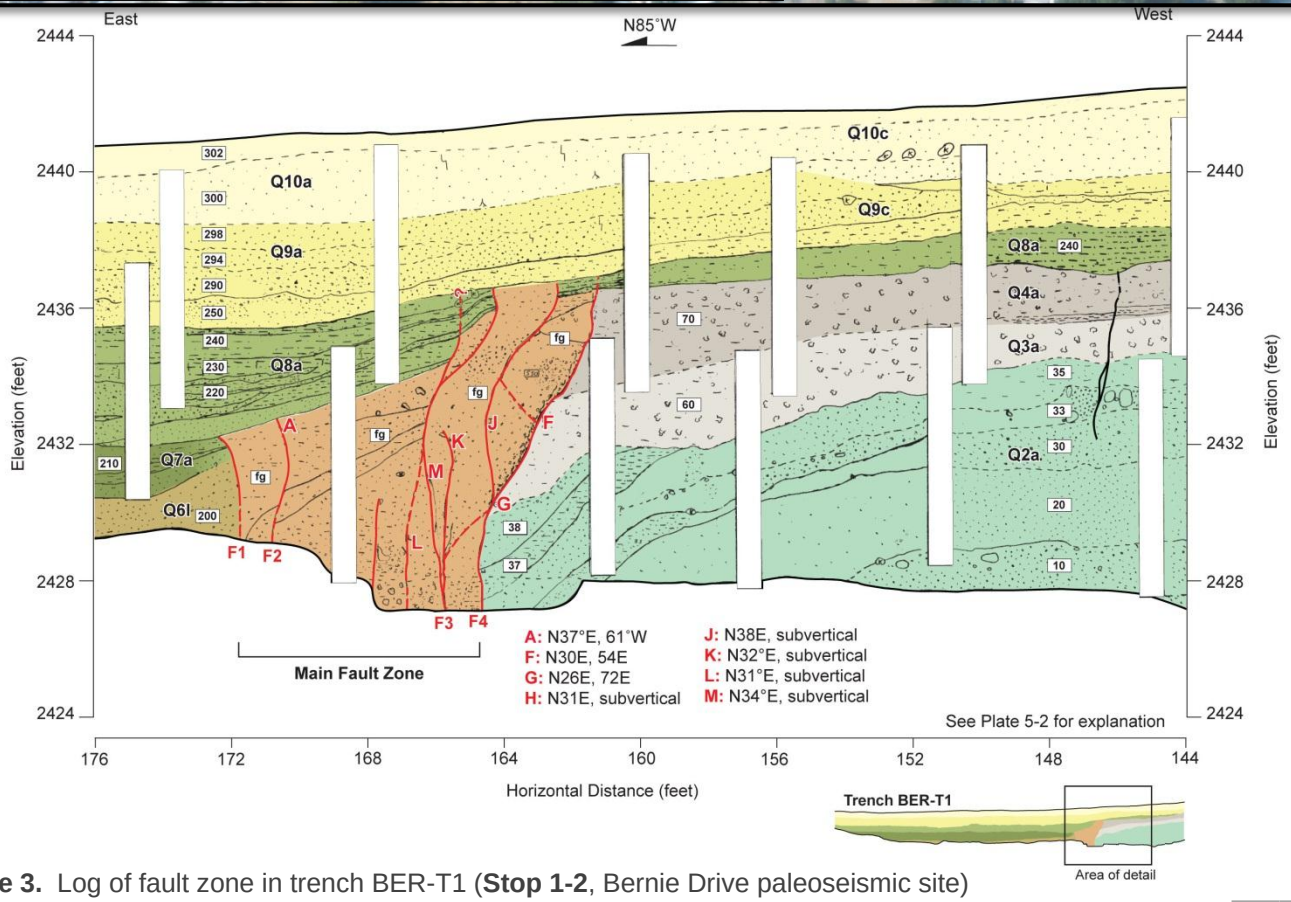

Figure 3. Log of fault zone in trench BER-T1 (**Stop 1-2**, Bernie Drive paleoseismic site)

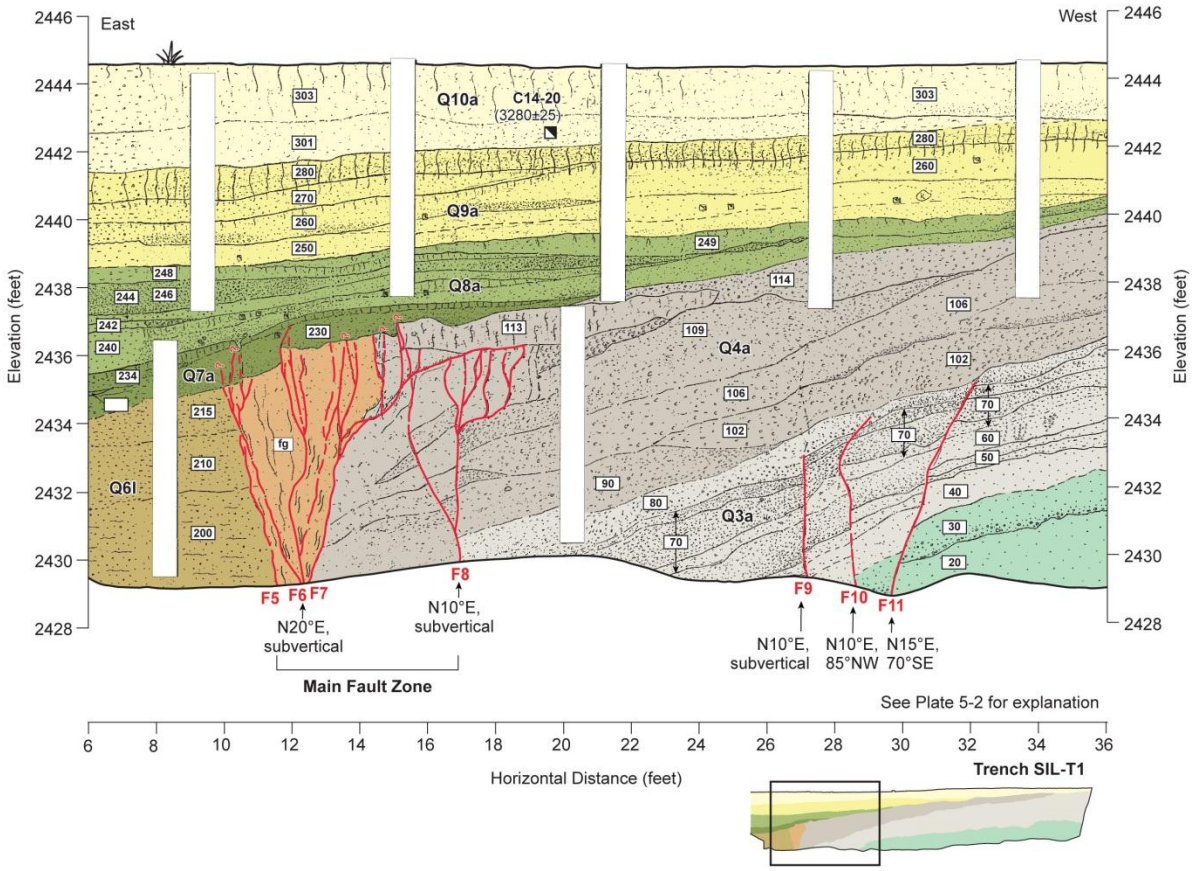

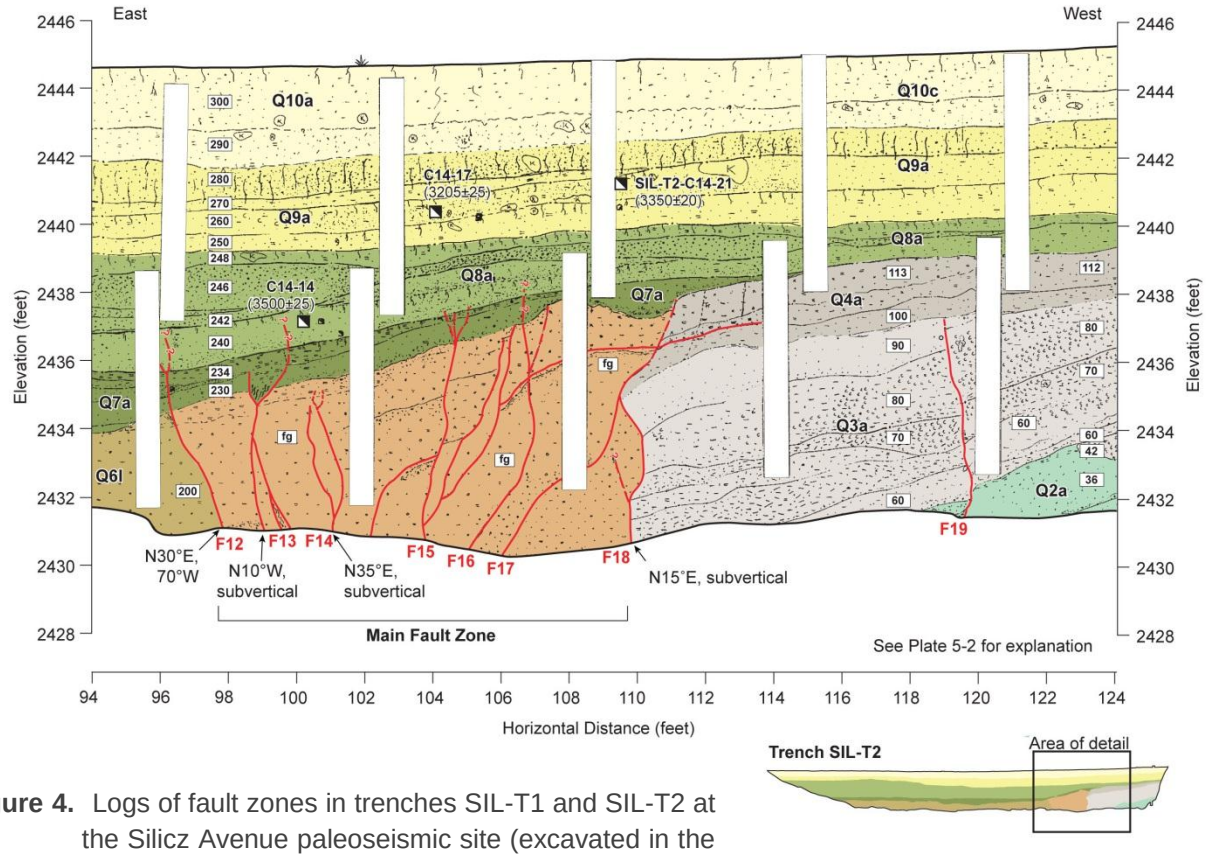

Figure 4. Logs of fault zones in trenches SIL-T1 and SIL-T2 at the Silicz Avenue paleoseismic site (excavated in the adjacent parcel to the north of **Stop 1-2**)

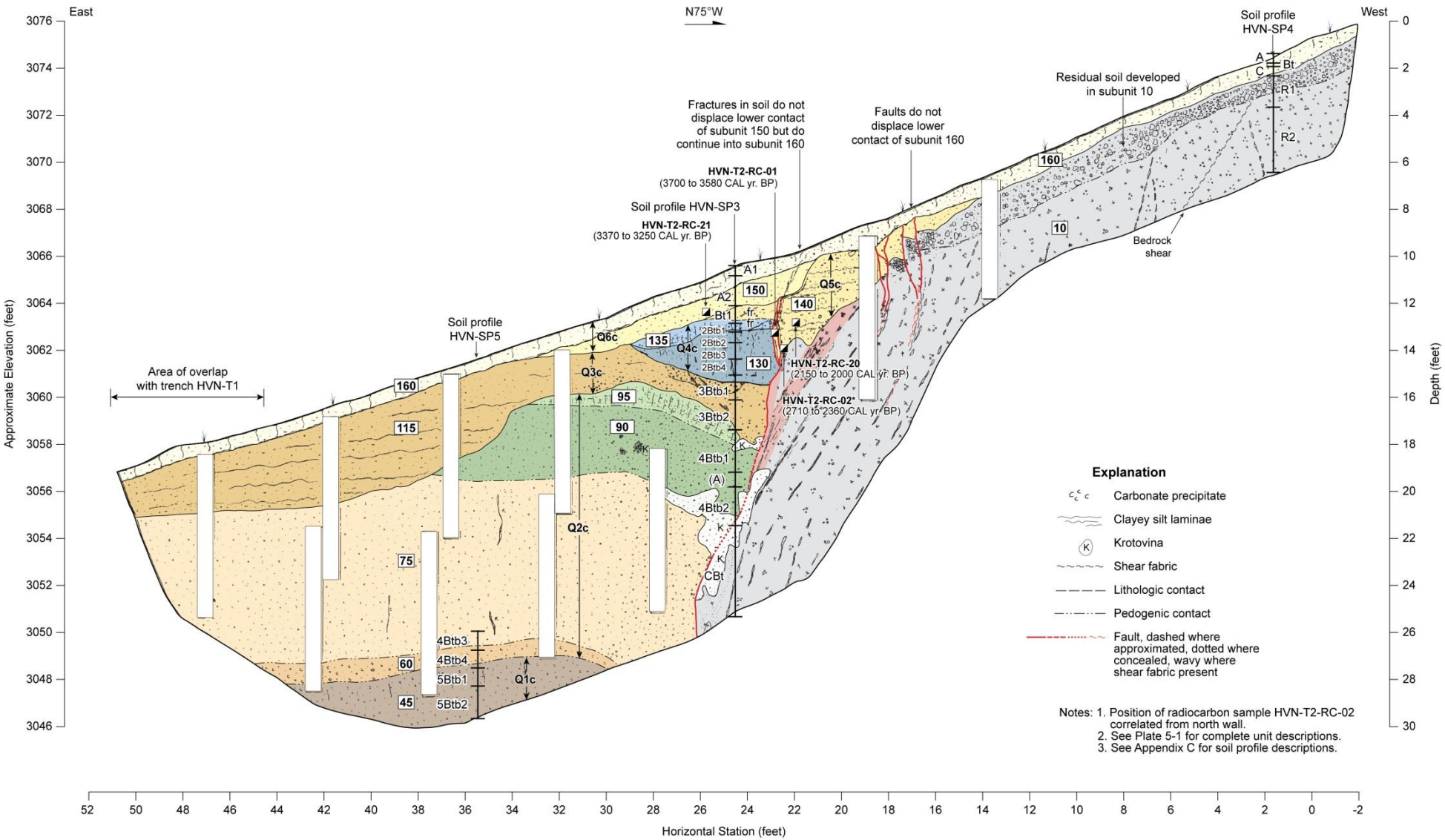

Figure 5. Log of fault zone exposed in trench HVN-T1 at the North Havilah paleoseismic site (see Figure 1 for location)

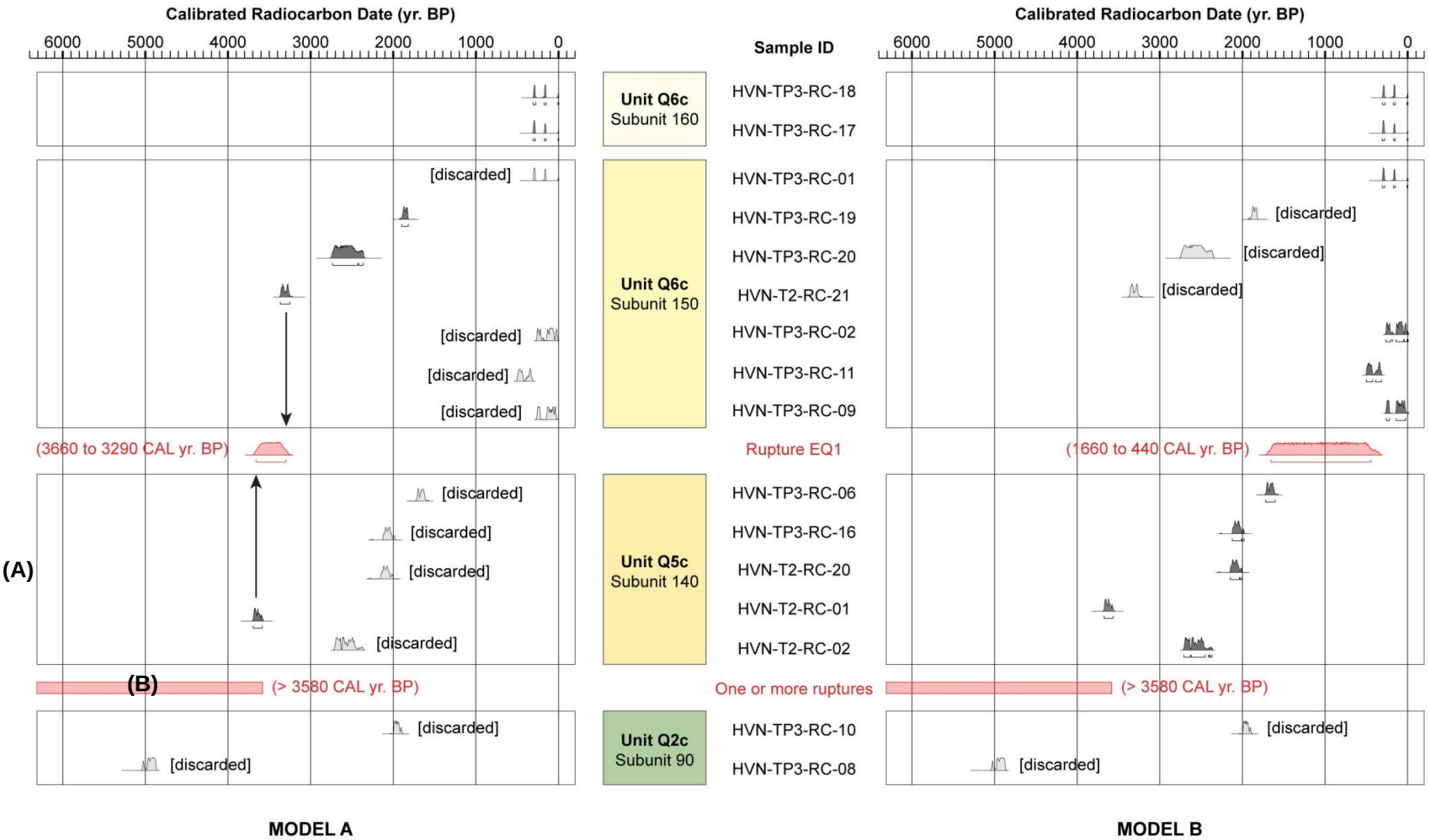

Figure 6. Stratigraphic models for radiocarbon results and event chronology from North Havilah paleosiesmic site (see Figure 1 for location)

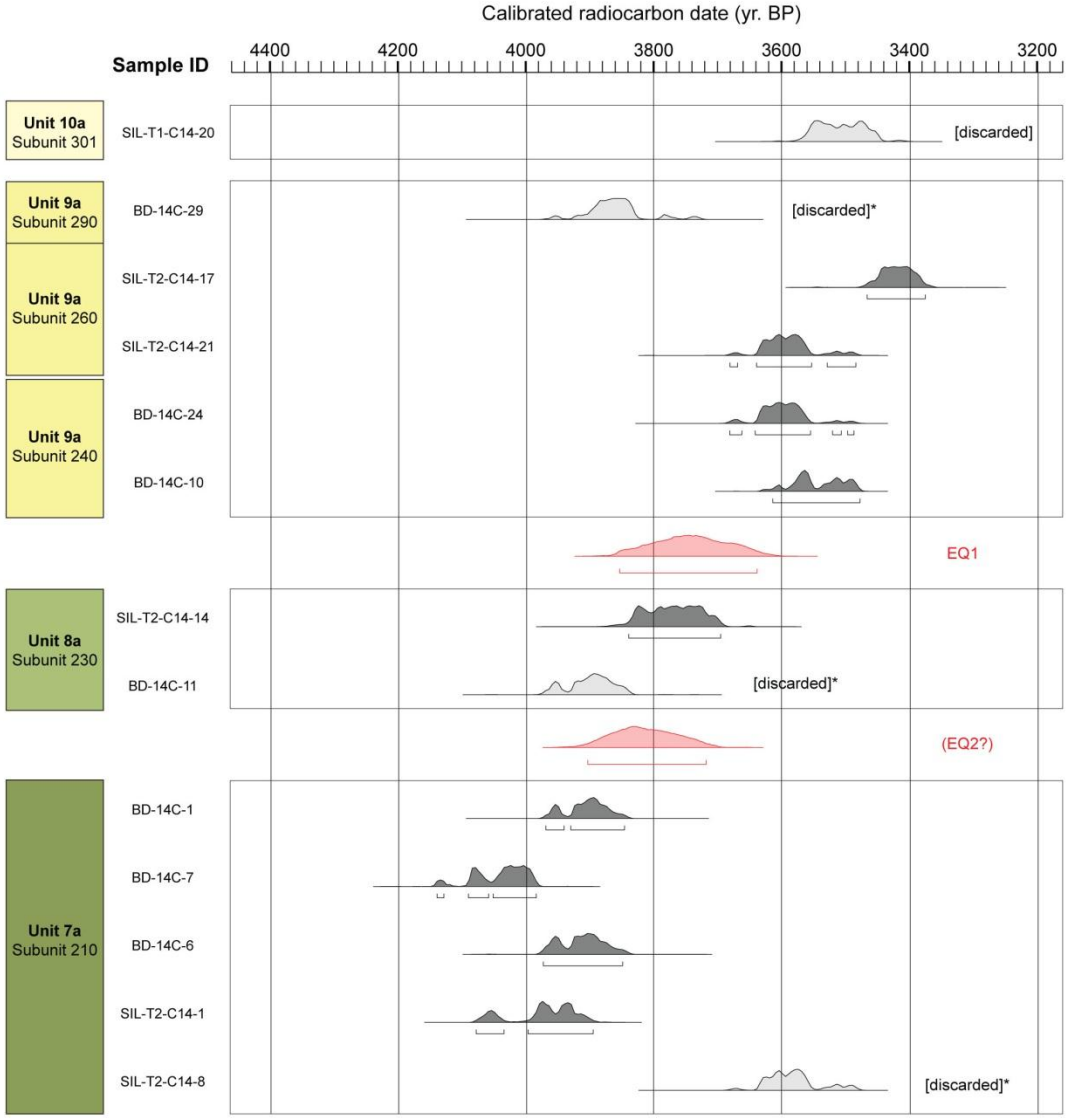

Figure 7. Stratigraphic model for radiocarbon results and event chronology from Bernie Drive paleoseismic site (**Stop 1-2**)

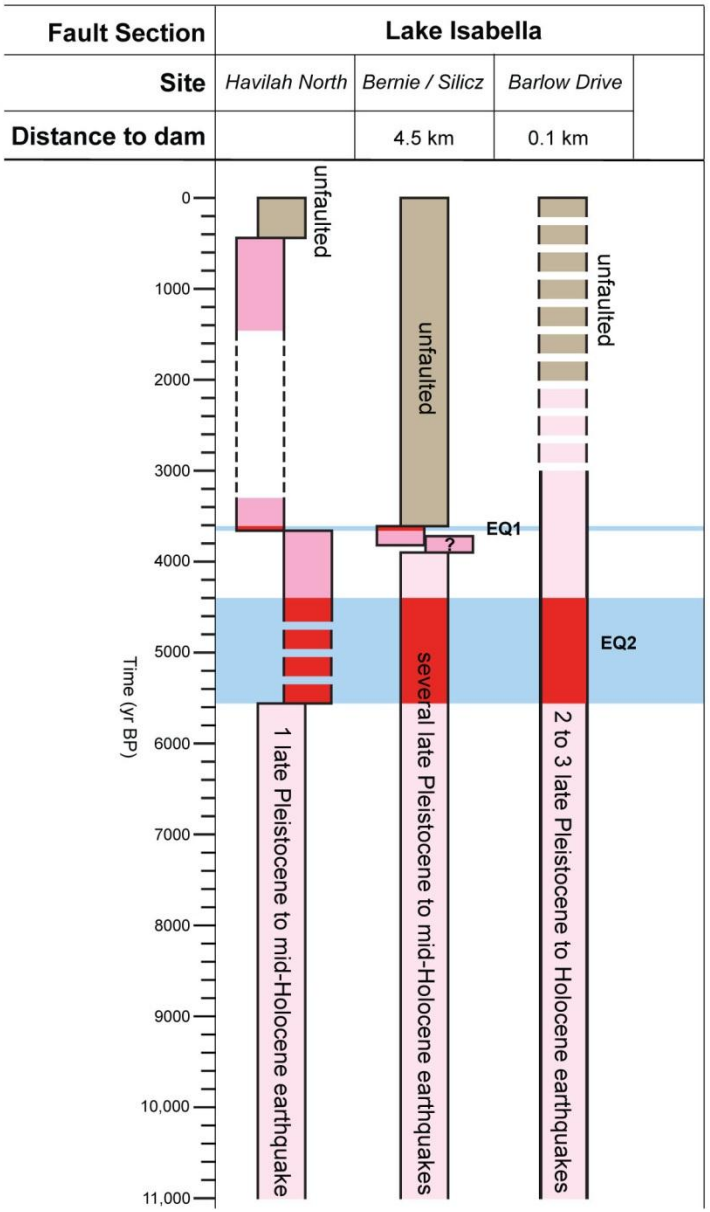

Figure 8. Earthquake chronology for the Lake Isabella section of the Kern Canyon fault

Road Log C-C′

Bernie Drive paleoseismic site (Stop 1-2) to Corral Creek paleoseismic site (Stop 1-3)

22.6 miles, 50 minutes

Mileage		Lat./Long.
0.0	**From the intersection of Bernie Drive and Reeder Drive, head south toward Chain Avenue (reset odometer)**	**35.6045° -118.4894°**
0.1	**Turn LEFT onto Chain Avenue**	**35.6030° -118.4899°**
0.3	**Take the 1st LEFT onto Lake Isabella Boulevard**	**35.6029° -118.4860°**
2.1	**Turn LEFT onto Kernville Road (becomes Wofford Heights Boulevard/CA-155)**	**35.6267° -118.4741°**
3.9	On the right you can see the Isabella Project Main Dam and the emergency spillway along the right side. Several flights of inset bedrock terraces are present on both sides of the river here	35.6373° -118.4820°
5.1	To the left is a good vantage of Engineers Point, an east-facing bedrock scarp of the KCF. Before the dams were built, the confluence of the Kern and South Fork Kern Rivers was located at the north tip of this bedrock ridge, as was the now-flooded agricultural town of Isabella	35.6594° -118.4779°
7.2	Cresting over this low saddle there is a good view across the lake of a prominent alluvial fan (Cyrus Flat) incised into a linear bedrock ridge. The linear valley behind this ridge is the approximate trace of the proto-Kern Canyon fault zone which accommodated right-lateral shear of ductile granite in the Cretaceous. The fan is graded to the Kern River Valley, one indication that the ridge and linear valley behind it has formed from erosional processes and not from active uplift.	35.6868° -118.4670°
8.8	**Stay on this road and continue forward through Wofford Heights toward Kernville**	**35.7069° -118.4563°**
10.7	A delta has formed where the Kern River meets Isabella Lake. Before impoundment, the reach of river between Riverkern and the Kern-South Fork Kern confluence the geomorphology was dominated by braided river channel in a broad, low relief alluvial plain.	35.7222° -118.4338°
13.5	**Turn LEFT onto County Rd 521/Sierra Way (becomes M-99 /Kern River Highway)**	**35.7558° -118.4176°**
15.6	Penstocks of the Kern River No. 3 Powerhouse, built in 1921 and operated by Southern California Edison. The take out for this powerhouse is 15 river miles upstream at Fairview Dam and flows through a series of long adits and cut-and-cover canals.	35.7763° -118.4358°

17.3	Just past Riverkern and the Tulare County line is the top end of the Kern River Valley—up-river from here the geomorphology records river incision into broad Pleistocene alluvial fans deposited on bedrock pediments, like the one across the river.	35.7974° -118.4510°
19.2	Across the river you can see a very prominent series of imbricated boulder levees inset against the incised fan and bedrock pediment	35.8237° -118.4611°
21.1	**Turn RIGHT off of the paved road onto a steeply climbing dirt road roughly 1.3 miles past the Chico Flat Campground (which is on the left)**	**35.8449° -118.4495°**
21.6	***From here forward the road is narrow and parking is limited*. If you need to consolidate vehicles then turn RIGHT into a clear area and jump in with old friends or make new ones.**	**35.8496° -118.4481°**
22.2	**Continue carefully down the unpaved road. It becomes one lane and after that you should turn LEFT toward the creek crossing.** The very coarse alluvial terraces on your left are inset into the bedrock pediment that you're driving along. These terraces are only a few meters thick. Right after the creek crossing is an excellent terrace exposure with a Pleistocene soil profile—you can walk back down here from the trench site in a few minutes if you want to.	**35.8513° -118.4375°**
22.6	**Pull forward as far as you can and park. Try park past the two dirt spur roads on your right—those are our turn arounds**	**35.8568° -118.4382°**
After Stop 1-3 you can reach Friday's camp by returning to M-99 (Kern River Highway) and turning RIGHT. Proceed 1.3 miles and turn LEFT into the Corral Creek Dispersed Camping Area		**35.8617° -118.4478°**

Stop 1-3a:

Record of Kern Canyon fault earthquakes at the Corral Creek paleoseismic site

Ashley Streig, *Fugro Consultants**

Keith Kelson, *Fugro Consultants*

Cooper Brossy, *Fugro Consultants*

**current affiliation: University of Oregon*

Abstract

The modern Kern Canyon fault (KFC) has been split into an eastern strand, located within the Proto-Kern Canyon fault zone and a western strand (Ross, 1986; Smith, 1964; Busby-Spera and Saleeby, 1990) and Nadin and Saleeby, 2008). Locally, the KCF is expressed as a prominent, east-facing break-in-slope where the western fault strand juxtaposes Mesozoic phyllite and quartzite on the west and Cretaceous granite on the east (Smith 1964; Ross 1986) (Figure 2). East of the fault, tributaries to Corral Creek have deposited late Quaternary sediments against an east-facing bedrock escarpment; west of the fault, deeply incised tributary valleys are cut into Mesozoic metamorphic bedrock and lack substantial late-Quaternary deposits.

The Corral Creek paleoseismic site crosses the western strand of the KCF, and is located in a zone of alluvial and debris-flow fan aggradation where Corral Creek and its local tributaries cross active strands of the KCF. The fault trace is expressed as east-facing bedrock scarps northwest and southeast of the site and is aligned with a vegetation lineament across the Corral Creek alluvial surface but has no geomorphic expression on this surface. Three trenches were excavated in 2009, by FWLA and URS, for the U.S. Army Corps of Engineers, and are labeled T1-A, T1-B and T1-C (Figure 3). Structural evidence for these four ruptures (designated EQ1 to EQ4, from youngest to oldest) includes upward fault truncations, warping and tilting of fine-grained and finely bedded stratigraphy, development of scarp-derived colluvium, and fissure-fill deposits. Trenches excavated at this site revealed evidence of four prehistoric earthquakes. The age of the most recent rupture (EQ1) is poorly constrained between about 3,700 and 600 years ago. The penultimate rupture (EQ2) is relatively well-constrained based on available radiocarbon dates, and occurred between 4,300 and 4,800 years ago. The third- and fourth-most-recent ruptures are poorly constrained in time; the third-most-recent rupture occurred during the middle Holocene (before 4,800 years ago) or possibly during the early Holocene, and the fourth-most-recent rupture occurred between the early Holocene to latest Pleistocene.

Trench Exposures

Two trenches were excavated across a Quaternary alluvial surface along Corral Creek, and a third trench was located south of the alluviated flat, exposing scarp-derived colluvium shed from the east-facing bedrock escarpment (Figure 2). The exposed bedrock is highly sheared weathered phyllite that exhibits a steeply east-dipping to vertical schistose foliation. The trenches exposed alluvium derived from granitic rocks in the tributary watershed east of the KCF, highly sheared colluvium derived from the metamorphic bedrock west of the KCF, and highly altered metamorphic bedrock. Five general phases of deposition are interpreted at the Corral Creek site; these phases are designated Q1 to Q5, with additional designators of “a” for alluvial deposits and “c” for

colluvial deposits (Figures 4 and 5). Cross section D–D‴ shows the primary stratigraphic units Q1 through Q5, and illustrates the deposition of young alluvium east of the western strand of the KCF (Figure 4).

Most Recent Earthquake

The most recent earthquake, EQ1, is expressed as upward fault terminations which are overlain by a scarp-derived colluvial unit (Q5c) and shearing of the underlying colluvial unit Q4c along the fault in T1-C (Figure 5). In trench T1-A and B we identify evidence of fracturing and warping of unit Q4a, which suggests the event occurred after deposition of the Q4 deposits (Figure 5). Unit Q4a shows about 1.1 m vertical separation across the western strand of the KCF. This displacement is a minimum vertical separation because the deposit dips to the west. This amount of separation is consistent with the thickness of unit Q4a (about 1.5 m). These relationships suggest that the vertical displacement of alluvial unit Q4a across the KCF is approximately 1.1 ± 0.61 m (Figure 4). Excavations show evidence that this deposit was deformed by the most-recent rupture and post-dates the EQ2 surface rupture. Radiocarbon analyses on charcoal samples from the upper part of alluvial unit Q4a indicate an age of 3,690 to 3,890 cal. yr BP. Given these ranges in displacement and age, this analysis yields a vertical slip rate of 0.28 ± 0.14 mm/yr since deposition of unit Q4a.

References

Busby-Spera, C.J., and Saleeby, J.B., 1990. Intra-arc strike-slip-fault exposed at batholithic levels in the southern Sierra-Nevada, California. Geology 18: 255–259.

Nadin, E., and Saleeby, J., 2008. Disruption of regional primary structure of the Sierra Nevada batholith by the Kern Canyon fault system, California. In: Ophiolites, arcs, and batholiths. ed. by Wright, J.E., and Shervais, J.W. Geological Society of America Special Paper 438 (doi: 10.1130/2008.2438[15]).

Ross, D.C., 1986. Basement–rock correlations across the White Wolf–Breckenridge–Southern Kern Canyon fault zone: Southern Sierra Nevada, California. U.S. Geological Survey Bulletin B1651, 25 pp.

Smith, Arthur R., 1964. Geologic map of California, Olaf P. Jenkins edition, Bakersfield sheet. Sacramento, Calif.: California Division of Mines and Geology, scale 1:250,000.

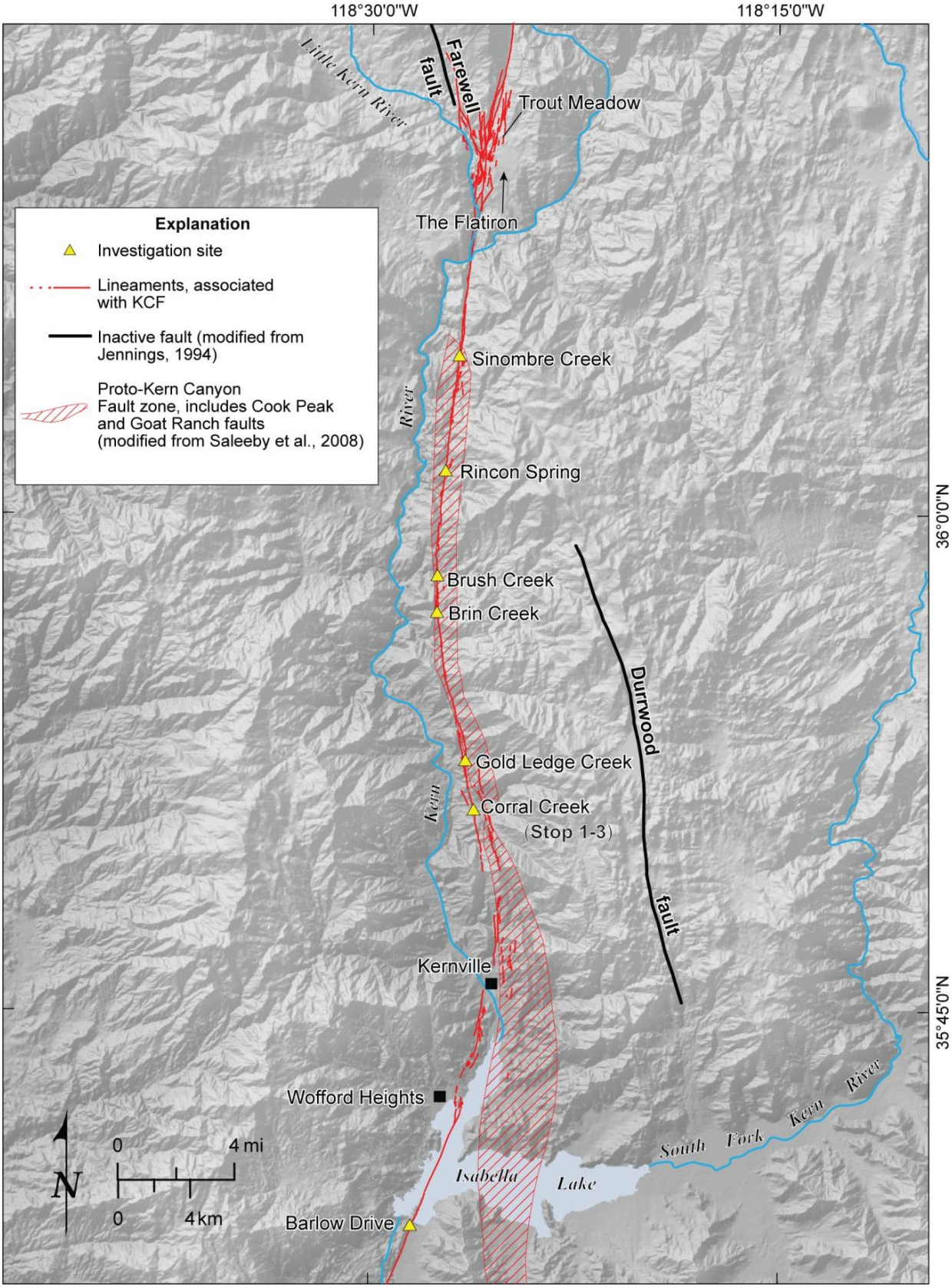

Figure 1. Investigation sites along the South Kern Canyon section of the Kern Canyon fault

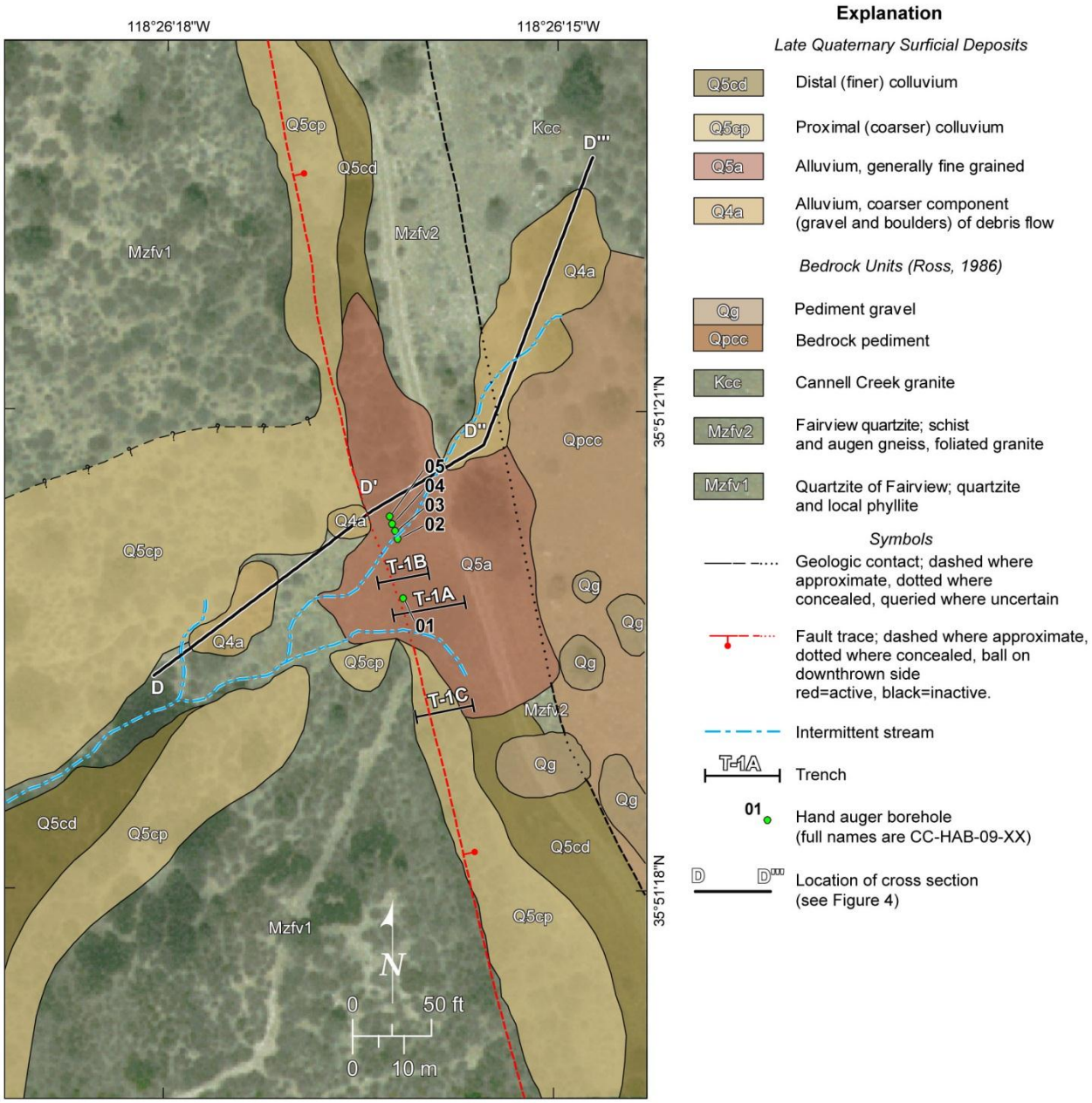

Figure 2. Geologic map of the Corral Creek paleoseismic site (**Stop 1-3**)

Figure 3. Oblique aerial photo of the Corral Creek paleoseismic site (**Stop 1-3**). Late Quaternary alluvium is ponded against an east-facing bedrock scarp with an uplifted bedrock pediment incised by ephemeral streams. Inset photo of vegetation lineament in ponded alluvium.

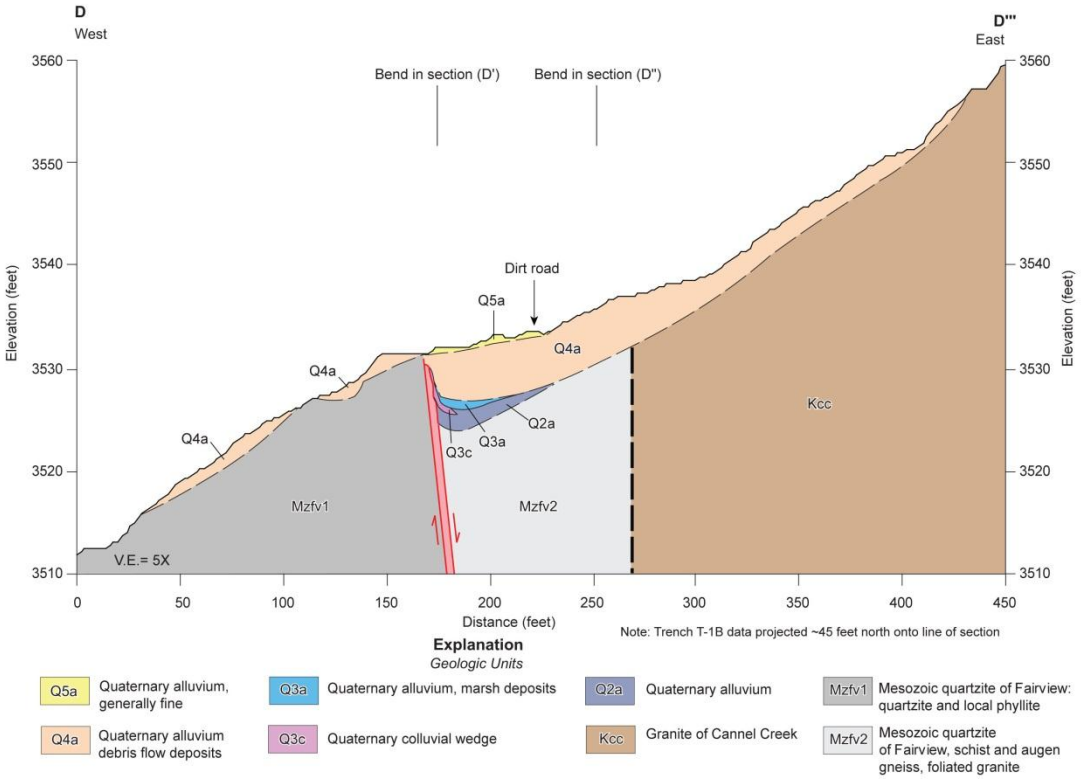

Figure 4. Cross section D-D''' across the Kern Canyon fault at the Corral Creek paleoseismic site (**Stop 1-3**) showing vertically displaced pediment and ponded alluvium

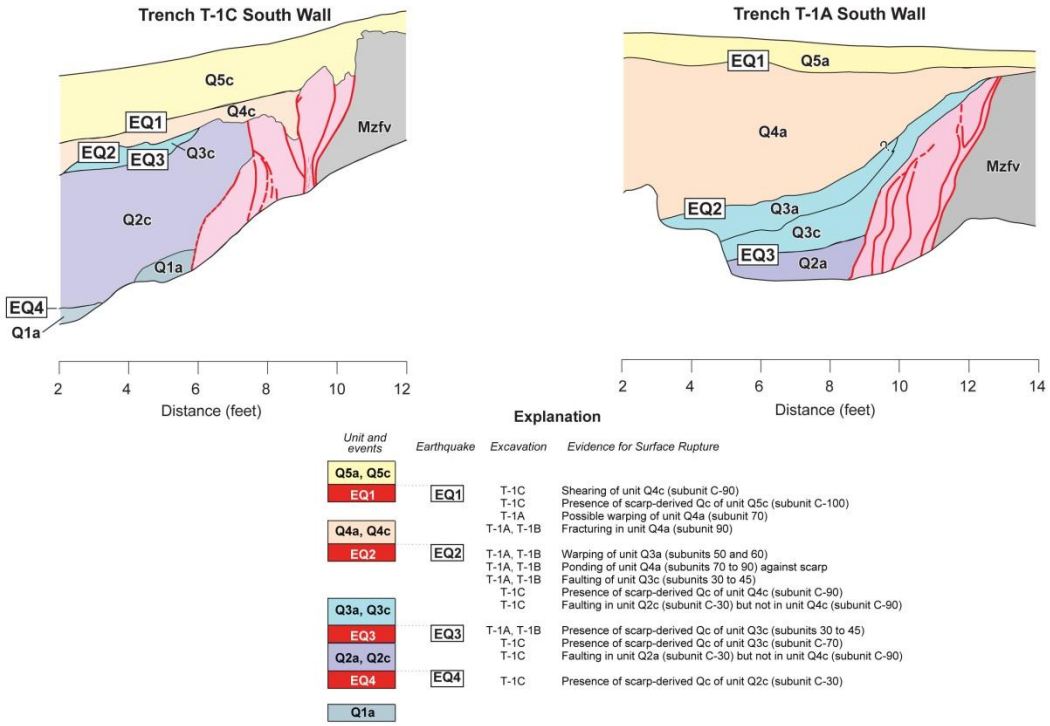

Figure 5. . Earthquake stratigraphy and interpreted horizons at the Corral Creek paleoseismic site (**Stop 1-3**). Trench T1-C exposed faulted colluvium and trench T1-A exposed faulted alluvium.

Stop 1-3b

Soil-Profile Development Principles Applied to an Investigation of the Kern Canyon Fault at Corral Creek, Kern County, California

Janet M. Sowers, *Fugro Consultants*

Paula Maat, *URS Corporation*

Overview

As part of a 2010 study of the Kern Canyon fault (URS, 2010), soil profile development was characterized in key exposures to help understand landscape evolution, and the nature, sequence, and timing of geomorphic and faulting events. The presence of a soil-profile indicates a period of landscape stability, and the geometry of the soil mantle reveals the shape and extent of that landscape surface. The characteristics of a soil profile are a function of the climate, the organisms, the relief, parent material from which the soil developed, and the time of development. (Jenny 1941)

Soil = f (cl, o, r, p, t, …)

Thus, soil features may give clues to past environments, sometimes indicating genesis under conditions different from the present. In addition, the degree of soil-profile development of a soil is a function of the time of landscape stability; thus, soils can provide age constraints for the deposits that host them.

Twenty-eight soil profiles were described at six trenching sites along the Kern Canyon fault. Soil-profile locations were selected collaboratively by the site geologist and the soil scientist and were often selected to address specific issues. Soil profiles were described using standard soil description methods (Birkeland 1999; Schoenberger et al. 2002) and data were entered on a data capture form. A sketch was made and a photograph taken of each profile.

Assessments of ages based on soil profile development were made in part by comparison of the soil profile features to dated soils in the region. Studies of soils and weathering features in glacial moraines in the southern Sierra Nevada were conducted by Burke and Birkeland (1979), Birkeland et al. (1980), Bursik and Gillespie (1993), and Berry (1994). Studies of soils on Sierra-derived alluvial fans in the San Joaquin Valley include Harden and Marchand (1980), Marchand and Allwardt (1981), and Harden (1982; 1987). Page and Sawyer (2007) describe and review existing data on colluvial and alluvial soils in the Sierra Nevada foothills.

Soils at Corral Creek

At the Corral Creek site, we studied four soil profiles-- two in road cut exposures (CC-1 and CC-2) and two in the trenches (CC-3 and CC-4). Both profiles in the road cut were developed in alluvium/debris flow deposits of unit Qfcc1. This unit is a thick widespread unit that forms a high terrace along the creek extending from the trench site to the mouth of the canyon where it is truncated by incision of the Kern River. The Qfcc1 terrace is measureably displaced across the fault, thus its age is key to interpretation of movement on the fault.

Soil Profile CC-1 is developed in cobbly granitic alluvium/debris flow deposits. We note that the surface rolls over slightly toward

the road, so 1 to 2 ft. of the original deposit may be eroded at this location. The surface of the fan at this location is at an elevation of 3490 ft, approximately 45 feet above the level of the creek bed, as determined from the LiDAR-derived contour map.

Profile CC-1 is developed in a 135-cm-deep exposure of loamy sand containing 50 to 75 percent cobbles and boulders. The soil has a well-developed A horizon with a dark grayish brown color (10YR 4/2), granular structure, and roots. The color fades with depth and transitions to a Bw horizon at 77 cm. In the Bw, the sandy matrix is a more oxidized color (10YR 5.4), exhibits a subangular blocky structure, and is slightly cemented with either clay or silica.

The cobbles and boulders in the exposure of Profile CC-1 are slightly to highly weathered. .In a count of 50 clasts, 36% were judged slightly weathered, 38% moderately weathered, and 26% highly weathered. Fresh cobbles and boulders did not occur in the subsurface, but were common above the ground surface. The degree of weathering of the subsurface clasts may be a useful age parameter.

We compared the degree of grussification of the clasts in this soil profile with published data for granitic clasts in glacial moraines of the eastern Sierra (Table 1). The data show that the clasts in this soil profile are more similar in degree of grussification to those of Tahoe-age moraines than to those of Tioga-age moraines.

Table 1. Comparison of Subsurface Grussified Clasts (Cobbles and boulders)

Site	Percent grussified subsurface clasts (>5 cm diameter)
Qfcc1 at Corral Creek	64% (sum of moderately and highly weathered clasts)
Tioga Moraines:	
Green Creek[1]	10 to 20
McGhee Creek[2]	0
Pine Creek[2]	<10
Bishop[2]	0 to 50
Tahoe Moraines:	
Green Creek[1]	80 to 90
McGhee Creek[2]	25 to 60
Pine Creek[2]	15 to 80
Bishop[2]	60 to 80

1. Burke and Birkeland, 1979
2. Berry, 1994

Soil profiles CC-3 and CC-4 were described in two paleoseismic trenches excavated across the Kern Canyon fault. Both are relatively young soil profiles developed in sandy granitic alluvium parent material ponded behind the scarp of the fault. Buried A-horizons suggest multiple episodes of faulting. Their features are consistent with the radiocarbon age of 4,500 to 4,800 cal yr BP for the laminated silty pond deposits at the base of CC-3.

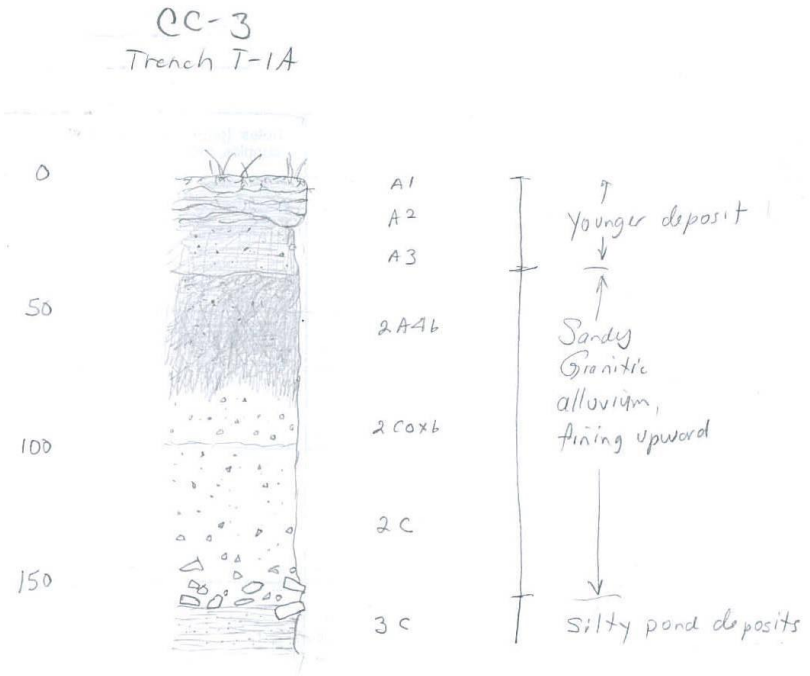

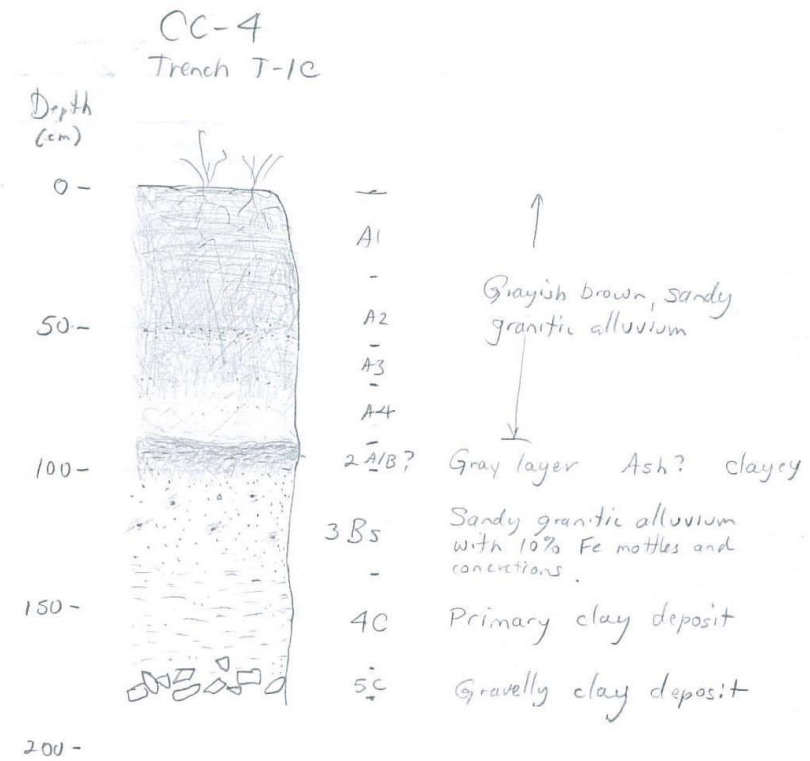

Stop 1-3c:

History of human occupation in the Kern River Valley

Jay Rehor, *URS Corporation*

Prehistory

The prehistory of the Kern River Valley, and the southern Sierra Nevada in general, is poorly understood with few large-scale archaeological studies. In addition, the depositional setting—with few areas of significant Holocene sedimentation—and a natural environment not conducive to preservation, makes reconstruction of cultural chronologies difficult. The earliest evidence for human occupation in California dates to the terminal Pleistocene ca. 13,000 years ago. Sites dating to the Pleistocene-Holocene transition are found surrounding the Southern Sierra, typically associated with lakes in the Southern San Joaquin Valley to the west and the Mojave Desert to the south and east. However, such early evidence has yet to be identified in the Kern River area.

The earliest identified cultural period in the Southern Sierra Nevada dates between 6,000 and 3,000 years ago, and is referred to as the Lamont Phase. This period is thought to have been characterized by warm, dry climatic conditions which encouraged the expansion of pinyon-juniper zones upslope. Prehistoric peoples in the southern Sierra seem to have adopted an economy revolving around hunting (from base camps) with some utilization of pinyon nuts. Technologically, this phase is distinguished by Pinto style points and the utilization of basalt for flaked-stone tools. While there are no confirmed Lamont Phase sites in the southern Sierra, a few Pinto-style spear points have been identified in the Kern River Valley, and indicate use of the area during that time.

During the Canebrake Phase—the next identified cultural period dating between 3,000 and 1,400 years ago—higher elevations were occupied and the economy of prehistoric people is seen to shift towards a greater exploitation of pinyon nuts as well as the harvesting of various bulbs and seeds, coincident with an increasing presence of millingstones in archaeological sites.

The subsequent Sawtooth Phase (until approximately 650 years ago) is marked by a continuing shift in favor of pinyon utilization. The transition from Elko to Rose Spring style projectile points is believed to represent the technological shift toward use of the bow and arrow. Obsidian is increasingly used for flaked-stone artifacts. Milling implements include manos, millingstones, and bedrock mortars. Shell beads too are known in Sawtooth Phase sites. The Chimney Phase—from 650 years ago until historic European contact—is characterized by a similar economy to that practiced previously, though sites suggest a more intensive and perhaps sedentary occupation, transitioning from seasonal camps to permanent or semi-permanent villages. Projectile points shift from Rose Springs to the Desert Series (Desert Side-Notched and Cottonwood Triangular). Beads, including glass beads from protohistoric sites, are not uncommon, and pottery (Owens Valley Brownware) appears.

Ethnography

Ethnographically, the Kern River Valley includes lands traditionally utilized by two Native American groups: the Kawaiisu and the Tubatulabal. Both peoples speak Uto-Aztecan languages, common to the Great Basin and southern deserts, though the two languages are

largely unintelligible; the Kawaiisu speaking a Numic dialect, while the Tubatulabal spoke Tubatulabalic. The boundary (if any) between the groups has not been well defined. The Tubatulabal resided primarily in the Kern River Valley and along the forks of the Kern. Seasonal forays were made into the Piute Mountains for hunting and the gathering of pinyon nuts. The Kawaiisu were located to the south of the Tubatulabal, occupying the Tehachapi Mountains and Walker Basin. Zigmond (1938) wrote that "most informants placed the boundary line between the two tribes a few miles south of the South Fork of the Kern River and the augmented Kern, and running parallel to them" (i.e., just south of the Isabella Project Main Dam).

Due to the biotic diversity within the Kern River area, the Tubatulabal were able to sustain a fairly large population and establish semi-permanent hamlets along the South Fork of the Kern River, many of which were covered by the waters of Lake Isabella. From February to sometime in August, the Tubatulabal focused their efforts on utilizing resources present within the valley—gathering seeds, greens, juniper berries and the nuts of the foothill pine, and hunting game. In late summer and fall, they tended to move to higher elevations, focusing on pinyon resources on the western slopes of the Sierra and on acorns in the Greenhorn Mountains. Groups returned to their hamlets at the start of winter.

Tubatulabal rock art is very abundant in the Kern River Valley and quite distinctive. Pictographs (painted with natural pigments) tend to be abstract, with curvilinear or angular shapes. Anthropomorphic or zoomorphic figures are uncommon, though there is a panel in the Piutes which appears to depict a mounted horseman. Generally, rock art is believed to have served a variety of functions ranging from the depiction of actual events both terrestrial and astronomical to serving magical purposes (e.g., hunting or fishing magic). Much of the rock art is believed to have been created by shamans who invoked spirits and were empowered by them. Important ceremonies included the toloache (an infusion of Datura) ritual and the mourning ceremony and were similar to those practiced by the Kawaiisu.

There is some disagreement as to where Kawaiisu lands ended and Tubatulabal lands began: Zigmond (1938), for example, claimed that Kawaiisu lands extended north to the area around Owens Peak, while Voegelin (1938) suggested that the Tubatulabal controlled Walker Pass and areas north. Merriam claimed that the Panamint Shoshone and Kawaiisu shared control of the western slope of Walker Pass, but that the Tubatulabal controlled the pass itself.

Based on ethnographic accounts, it is known that the Kawaiisu occupied a rich mythological landscape. This invisible world was filled with identifiable beings and anonymous non-beings, mythical giant creatures and great sky images, many associated with elements of the natural landscape. Rituals were oriented around important life events such as puberty. Death involved an elaborate set of rituals. A day following an individual's death, the body would be wrapped and placed in a cleft of rock. Periodically, ceremonies commemorating a number of deceased persons were held. These ceremonies involved the construction of a sacred enclosure within which images of the dead would be burned. Such occasions were celebrated with dancing and feasting.

History

The region was first visited by Europeans in 1776, when a party led by Spanish missionary Fr. Francisco Garces contacted the Tubatulabal in the southern Kern River Valley (Smith, 1978). The Kern River was then known as the "Rio

Bravo de San Felipe." Captain Joseph Reddeford Walker traveled through the Kern River valley in 1834 while searching for the northernmost snow-free pass over the Sierra. Walker pass is named after him. Captain Walker led numerous parties through the pass in subsequent years. When gold was discovered in the northern Sierra Nevada in 1848, Walker pass became one of the routes used to cross the Sierra by gold seekers. By 1850, Euro-American settlement in the Kern River Valley had begun.

Settlement within the valley increased rapidly after 1853, when gold was discovered in Greenhorn Gulch by Richard Keyes, and the town of Keysville sprang up. Over the next few years the Greenhorn area was swarming with would-be millionaires looking for the next big gold strike, but with little luck. A second Kern River gold rush was started in 1860, when Lovely Rogers discovered gold at the Big Blue mine, near present day Wofford Heights. Legend has it that Rogers was chasing his mule and picked up a rock to throw at it, when gold flecks in the rock caught his eye. The rush for gold forced out the inhabitants of the Indian village of Tulonoya, next to the site of the original Kernville (now inundated by Isabella Lake).

The third, and perhaps largest of the mining booms began in Havilah (south of present day Lake Isabella) in 1864. In 1866 Havilah became the seat of the newly formed Kern County, but lost the county seat to Bakersfield in 1874. By the late 19th century, as gold mines dried up and the profitability of mining decreased, the focus of the Kern River Valley economy shifted towards ranching and agriculture.

The development of electricity and harnessing of the Kern River began in 1906, with the opening of the Edison Electric Company's Kern River Canyon powerplant. Several hydroelectric plants were built along the river in the early 20th century, supplying power to growing cities of southern California. The towns of the Kern Valley were hopping as power company workers swarmed. A good road from the Kern Valley to Bakersfield along the Kern River connecting the power projects was clearly needed and was built piecemeal over several years. It was finally completed in 1926.

In 1948, the U.S. Army Corps of Engineers began construction of the Lake Isabella Dam. The dam was completed in 1953. Evidence of many periods of the Kern River Valley's history were buried under the rising waters of the reservoir, including numerous large prehistoric village sites, rock art sites, and the historic towns of Kernville and Isabella. However, various archaeological remnants of all of these periods can be found throughout the valley.

Surrounding the Corral Creek trench location you will notice several buildings and structures related to the Edison Company Camp #5, which was built in support of the construction of the Kern River 3 hydroelectric aqueduct in the 1920s. In addition, several mining prospect pits in the Corral Creek area were dated to the late 19th century, based on associated blasting caps and other artifacts found on site. Finally, during excavation of the Corral Creek seismic trenches for the Kern Canyon fault study, a single battered river cobble was uncovered in the trench. The cobble was likely used as a pestle by prehistoric Native Americans. The pestle was found at the contact between a paleosol and a colluvial wedge from the fault scarp, which buried it. Unfortunately, the pestle was non-diagnostic and could not be associated with a particular time period but, is evidence of seismic activity along the fault during the Holocene (i.e., the period of human occupation).

Road Log D-D′

Corral Creek Camping Area (Friday night camp) to Rincon overlook (Stop 2-1)

24.0 miles, 55 minutes

Mileage		Lat./Long.
0.0	**Turn LEFT out of the Corral Creek Campground onto M-99 (Kern River Highway) (reset odometer)** To the left is a good example of a bedrock pediment with thin alluvial cover now incised by the modern stream. This geomorphology is typical of Kern Canyon between Kernville and Goldledge campground (roughly 10 river miles).	**35.8617°** **-118.4478°**
0.8	North of the Goldledge Campground the terrace surfaces are located higher along the canyon walls and are primarily bedrock surfaces—the alluvial fan cover and bedrock pediments common just down canyon are generally absent.	35.8716° -118.4548°
4.9	Between here and Johnsondale Bridge the Kern River is incised into metamorphic bedrock. Beyond the deeply incised water gap immediately ahead the canyon walls are very steep and the bedrock terraces common north of Goldledge are absent. The river maintains an impressive degree of inherited sinuosity through this upcoming reach and coincides with an upstream decrease in river gradient visible on the longitudinal profile.	35.9153° -118.4864°
6.1	Johnny McNally's: home of the 40 oz Porterhouse. This is legit. The dated gold rush dioramas in the lobby are an added bonus.	35.9265° -118.4939°
8.0	Fairview Dam, take out point for the Kern River No. 3 Powerhouse.	35.9455° -118.4770°
10.7	Johnsondale bridge, the only river crossing north of Kernville. The road turns to climb up along the South Creek drainage.	35.9682° -118.4866°
11.2	Waterfall! (good flow in August this year, hopefully still running by FOP time).	35.9723° -118.4923°
13.3	The road has climbed about 270 m from Johnsondale Bridge and now enters a more forested terrain. The gradient of South Creek flattens slightly here, suggesting that the fluvial system upstream from here is graded to a higher base level that has not yet adjusted completely to the deep incision occurring at lower elevations.	35.9692° -118.5143°
15.5	**Turn RIGHT onto Forest Route 22S82** This road winds for the next 10 miles around a broad embayment inset into the towering domeland terraine above. This was probably at one time a relatively contiguous erosional surface that projected below the 3.5 Ma basalt flows capping bedrock terraces along the shoulder of Kern Canyon.	**35.9828°** **-118.5425°**
17.9	**Bear right to stay on Forest Route 22S82**	**36.0065°** **-118.5391°**
24.0	**Arrive at Stop 2-1. Park close in line on the right margin of the road, taking up the right lane, and gather near the roadcut. We'll have a very short walk up the adjacent hill so bring along some fluids if you're dehydrated from last night.**	**36.0409°** **-118.4893°**
We're taking up a lane of traffic here, and there is vehicle traffic on this road, so be careful. After we finish at this stop there are several pullouts on the road ahead where we can all turn around to head back down.		

The Flatiron

View south along upper Kern Canyon and the Kern Canyon fault from near Junction Meadow, Sequoia Nat'l Park

left photo 2009 (Lutz)
right photo 1903 (G.K. Gilbert)

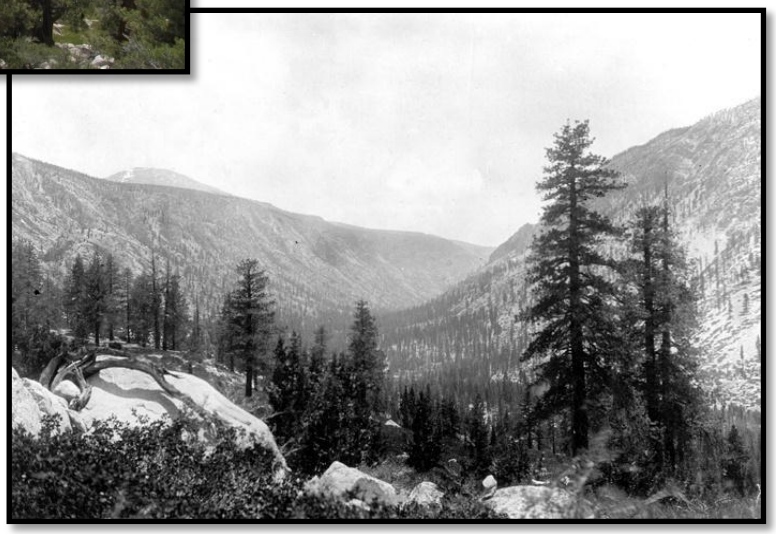

Stop 2-1a: Structural and Geomorphic Control on Landscape Evolution by the Kern Canyon Fault near the Little Kern River Valley, Tulare County, California

Keith Kelson, *Fugro Consultants*

Dave Simpson, *URS Corporation*

Ronn Rose, *US Army Corps of Engineers*

Colin Amos, *Fugro Consultants**

John Baldwin, *Fugro Consultants***

Julia Kelson, *Dartmouth College*

*currently: University of California, Berkeley

**currently: Lettis Consultants International

Abstract

The Holocene-active Kern Canyon fault (KCF) exerts first-order control on patterns of late Quaternary deformation, volcanism, and drainage within the southern Sierra Nevada. The 135-km-long KCF is a long-lived, reactivated geologic structure, and deep incision and drainage localization of the Kern River along the KCF reflect both current and earlier phases of deformation. We mapped late Quaternary strands of the KCF using geologic field mapping, aerial photography and lidar-derived digital elevation models to assess fault displacements and rupture segmentation. Structural segments of the KCF are marked by fault step-overs and/or complex intersections with ancient, inactive faults. Locally, the KCF and intersecting faults controlled the location of Pliocene volcanism, which in turn affected Plio-Pleistocene drainage development in the Little Kern River Valley (LKRV) and the Kern River Canyon upstream of the town of Kernville. More recently, late Quaternary movement has produced prominent east-facing fault scarps and aligned drainages that locally control hillslope and tributary sediment-transport processes. The KCF displaces a 3.5-Ma basalt flow underlying the "Flatiron", a broad intermontane plateau near the confluence of the Kern and Little Kern Rivers that coincides with the structurally complex intersection of the Farewell fault and the KCF.

The Pliocene basalt flanking Kern Canyon and within the adjacent LKRV reveals a dominant structural (fault) control on the location of eruptive centers. Basalt flows emanating from eruptive centers paralleling the KCF on the Flatiron and the Farewell fault in the LKRV indicate that both faults affected the pattern of shallow crustal processes. Three-dimensional exposures within the LKRV reveal basalt flows as much as 165 m thick filling a steep-sided, incised paleo-valley, which has since been re-incised by the present-day Little Kern River. The uppermost surface of the LKRV basalt has ~30 m of west-down displacement across the Farewell fault, and ~125 m of east-down separation across the KCF. Using a late Quaternary slip rate of 0.3 +/- 0.1 m/ka from paleoseismic trenching, separation of the basalt suggests initiation of east-down normal movement on the KCF between ~300 and 600 ka. Detailed geologic mapping and analysis of remote-sensing imagery delineates basalt remnants that record the Pliocene Kern River elevation and provides information on the history and rate of Kern River incision. Basalt remnants flank the canyon as far as ~15 km downstream of the Flatiron, and exhibit a southerly gradient (20 m/km) comparable with the modern channel. The heights of basalt remnants above the Kern River suggest a post-3.5 Ma incision rate into granitic rocks of about 0.09 m/ka.

Introduction

The boundary between the South Kern Canyon section of the Kern Canyon fault (KCF) and the north-striking North Kern Canyon section is near the confluence of the Kern River and the Little Kern River in an area known as the "Flatiron" (as labeled on the USGS Hockett Peak quadrangle) (Figure 1). South of the Flatiron, the KCF strikes about N09°E along a nearly linear, single strand for 25 km from Brush Creek to the Flatiron (Figure 1); north of the Flatiron, the KCF strikes essentially due north for at least 30 km within the linear upper Kern River Canyon (Figure 2). In addition to this change in fault strike, the Flatiron area is identified as a fault section boundary because of an intersection with the Farewell fault, the presence of multiple volcanic vents, and local complexities in the fault pattern. This collection of relatively anomalous geologic features all within one small area along the KCF indicates that geologic processes have affected (or been affected by) the behavior of the Kern Canyon fault zone near the Flatiron over long periods of geologic time.

The Flatiron area has been a subject of geologic reconnaissance and mapping for over 100 years, beginning with an early Sierra Club field trip that included Andrew Lawson and G.K. Gilbert (Lawson, 1904). Lawson acknowledged the presence of "lava sheets" on the Little Kern Plateau (i.e., the Flatiron) and correlated this surface with the Chagoopa Plateau flanking the northern part of the glaciated upper Kern River Canyon. Webb (1936) subsequently completed reconnaissance mapping of "a series of lava flows" on the Flatiron and within the Little Kern River valley and reported that the geomorphic surfaces on the two sides of the fault are at corresponding elevations and the basalt flows are not deformed by the Kern Canyon fault. Subsequent radiometric dating of this basalt by Dalrymple (1963) returned an age of roughly 3.5

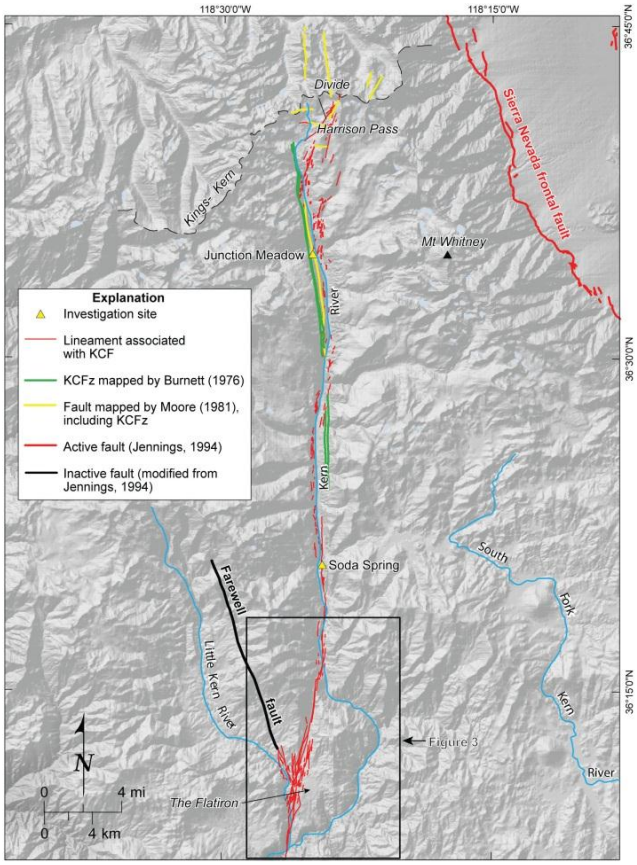

Figure 1. Investigation sites along the South Kern Canyon section of the KCF

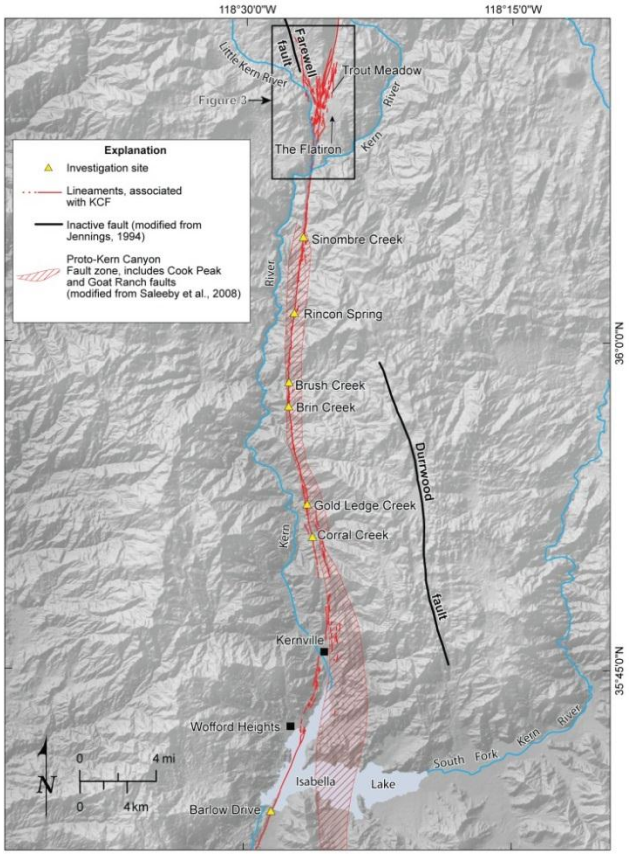

Figure 2. Investigation sites along the North Kern Canyon section of the KCF

Ma—this date has been cited by subsequent workers who inferred it to represent the minimum age of last activity along the KCF (Burnett, 1976; Moore and du Bray, 1978; du Bray and Dellinger, 1981).

However, recent investigations related to the Isabella Project have documented deformation of this basalt by the KCF (Page, 2005; URS, 2007; 2008; Kelson et al., 2010). Field observations in September 2007 document shear fabric in the basalt along the western edge of the Flatiron, collinear with a series of broad, east-facing fault scarps on the Flatiron surface along the northward projection of this shear zone. These observations represent the first definitive evidence for post-3.5 Ma displacement along the KCF in the upper Kern Canyon

Geologic Units

Geologic mapping of the Flatiron and the Little Kern River valley documents the pattern of faulting along the KCF and the Farewell fault and provides a basis for interpreting this location as a possible fault-section boundary. Previous workers (Webb 1946; du Bray and Dellinger 1981) show that the KCF deforms pre-Quaternary granites overlain locally by Tertiary basalt and younger surficial deposits. The Little Kern River basalt is up to 150-m-thick and filled a steep-walled paleovalley that roughly coincides with the modern position of the Little Kern River channel (Webb 1946). Several volcanic vents have been identified as probable sources for this basalt, including volcanic centers on both sides of the Little Kern River near its confluence with Fish Creek and one directly southeast of Burnt Corral Meadow (Figure 3). The uppermost surfaces of the basalt flow locally radiate away from these vents. Although the exact location of the basalt sample dated by Dalrymple (1963) is not precisely known, it is generally assumed that the 3.5 Ma date represents the age of the uppermost basalt flow on the Flatiron.

The northwestern extent of the basalt is less than about 1 km northwest of a vent near Burnt Corral Meadow, where it overlies thin gravel containing granitic and metamorphic cobbles and boulders deposited in the ancestral Little Kern River valley (unit Tgo, Figures 3 and 4a). Down the Little Kern River, the basalt thickens to about 120 m (Figure 4b), which corresponds to a progressive downstream deepening and steepening of the paleovalley, indicating that it had a steeper gradient than the present-day Little Kern River. Excellent three-dimensional exposures within the Little Kern River valley show the axis of the filled paleovalley trending about S30°E and with an average gradient of 1.5 degrees (Figure 3). Where the paleovalley intersects the Farewell fault and the KCF near Trout Meadow Creek the thickness of the basalt is about 165 m (Figure 4c).

Both margins of the basalt-filled paleovalley intersect a zone of deformation near the Flatiron that includes the Farewell fault and the KCF (Figure 3). The southwestern margin of the paleovalley projects across the Little Kern River near Trout Meadow Creek (Figure 3) and is exposed on the eastern margin of the Flatiron. This east-dipping paleovalley margin is prominently exposed along the east side of the Little Kern River, where the sheared granitic rocks contrast obviously with inset basalt flows (Page, 2005). The northeastern margin of the Little Kern River paleovalley is exposed near Trout Meadow Creek (Figure 3), and projects into the fault zone on the southern side of Trout Meadow Creek (Figure 3). East of the KCF, the uppermost surface of the basalt has a maximum elevation of about 1950 m in the central part of the Flatiron (Figure 3), which is about 50 m higher than the uppermost basalt surface in the

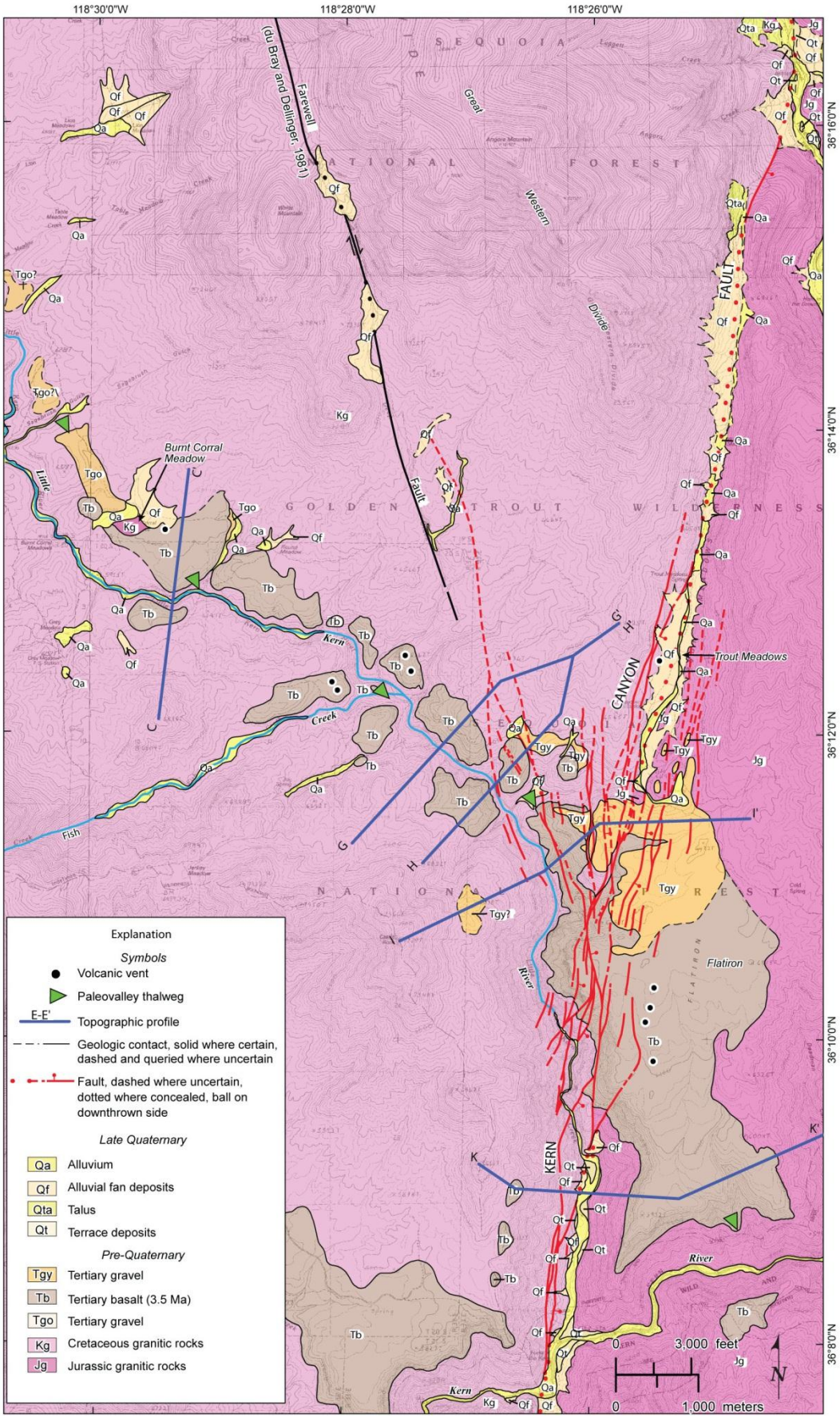

Figure 3. Geologic Map of the Flatiron Area

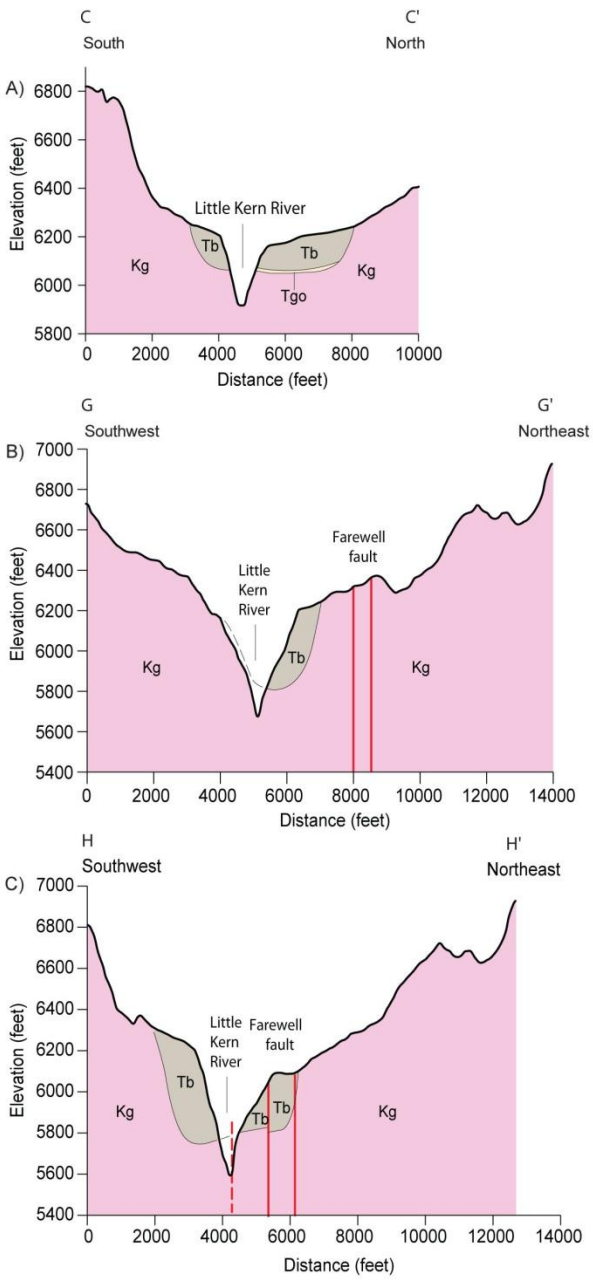

Figure 4. Cross sections C-C′, G-G′, and H-H′ across the Little Kern River. See Figure 3 for explanation of geologic units.

Little Kern River valley, west of the KCF. On the Flatiron, the basalt surface is at 1,800 m and slopes gently southward toward the Kern River canyon. Remnants of the Little Kern basalt are preserved along the flanks of the modern Kern River Canyon from the Flatiron southward for 25 km, nearly to the confluence of Brush Creek and the Kern River.

In the northern part of the Flatiron the basalt is overlain by about 25 m of gravel mapped as a Quaternary glacial deposit by Du Bray and Dellinger (1981), with an aggradational surface that ranges from 1,920 to 1,950 m elevation (unit Tgy; Figure 3). Remnants of this gravel are inset into the bedrock walls of the Trout Meadow valley (Figure 3) where they slope to the south and merge with the broader, unconfined deposit on the Flatiron, indicating deposition in a south-flowing fluvial system. This presumably records flow along the ancestral Kern River when it tracked southward through the Trout Meadow valley before incision of the modern canyon.

This post-basalt gravel extends across most of the KCF in the northern part of the Flatiron (Figure 3) and has at least 25 m of east-down vertical separation across the main strands of the KCF (Figure 5). Remnants of similar gravel occur high on the western flank of the Little Kern River valley at about 2,040 m elevation (Figure 5) and may have been deposited by the same post-basalt ancestral Kern River that previously occupied Trout Meadow.

Faults

The intersection of the Farewell and Kern Canyon faults is a complex zone of deformation that affects the 3.5 Ma basalt and younger deposits. The KCF at southern end of the Flatiron near the confluence of the Kern and the Little Kern rivers (Figure 3) is associated with a relatively narrow zone of fault-related springs, east-facing bedrock scarps, tonal lineaments, and highly fractured, sheared, and mylonitized granite along the eastern wall of the steep, rugged Little Kern River valley (URS, 2008) (Figure 3). Northward from the confluence of the Kern and Little Kern rivers, the zone of deformation associated with the KCF is progressively more complex with proximity to the Farewell fault. Within the south-trending part of the Little Kern River valley, the KCF strikes

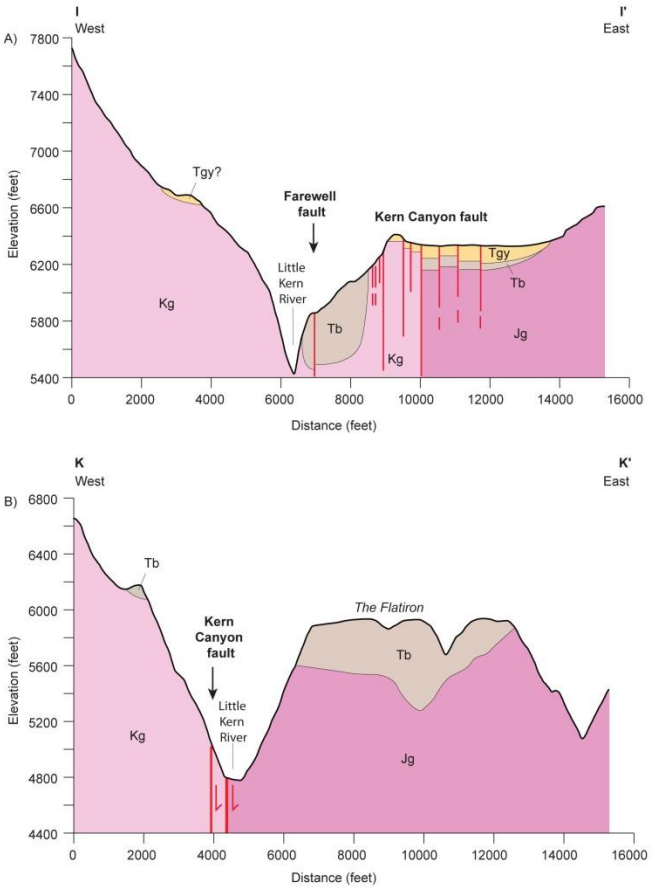

Figure 5. Cross sections I-I′ and K-K′ across the Little Kern River. See Figure 3 for explanation of geologic units.

north-northeast and splinters into northeast-striking splays that cut the basalt and extend onto the Flatiron surface. The geomorphic expression of these splays decreases north of the Flatiron. As first noted by Page (2005), the primary zone of deformation traverses the eastern wall of the Little Kern River valley about 4 km north of the confluence with the Kern River (Figure 6) and consists of multiple east-down strands in a 1.1-km-wide zone that displaces granite, basalt, and overlying alluvial gravel (Figure 3). Topographic profiles by URS (2007) documented at least three east-facing scarps developed in the basalt on the Flatiron surface and at least 15 m of east-down displacement.

The Farewell fault is a northwest-striking structure mapped by Matthews and Burnett (1965) and du Bray and Dellinger (1981) that continues about 40 km along the flank of the Great Western Divide and projects southeast toward an intersection with the KCF along the western margin of the Flatiron. Du Bray and Dellinger (1981) showed bedrock evidence for right-lateral slip along the southern part of the Farewell fault along a vertical or steeply dipping fault plane. The northern part of the Farewell fault traverses the high-altitude Farewell Gap, which forms the drainage divide between the Little Kern River and the Kings River. At Farewell Gap the fault is a wide shear zone within metamorphic bedrock that continues northwestward to Mineral King and shows evidence for substantial ductile and brittle deformation with dextral displacement (Busby-Spera and Saleeby, 1987).

The KCF intersects the Farewell fault about 5 km north of the Kern River where multiple fault strands continue to northwest along the Farewell fault and deform the Little Kern River basalt. The faulting is characterized by a series of left-stepping en echelon fault strands within a zone that widens decreases in geomorphic expression to the northwest. The fault displacements are defined by deformation of bedded basalt flows and are difficult to identify northward from the KCF where the Farewell fault is within granitic rocks. Possible fault-related geomorphic features (e.g., saddles, aligned drainages, bedrock scarps, vegetation alignments) are expressed in granitic rocks along the Farewell fault, though there is no evidence of late Quaternary deformation. The Farewell fault is associated with the linear stream valley of Deep Creek and continues through a prominent pass between White Mountain and Angora Mountain (Figure 3) in sheared granitic bedrock. Though no evidence of late-Quaternary displacement was observed along the Farewell fault, it seems likely that brittle deformation along the KCF has taken advantage of northwest-oriented structural fabric in rocks previously deformed by the Farewell

fault. North of the Flatiron the KCF includes several fault strands in the southern part of Trout Meadows (Figure 3). The Trout Meadows valley is narrower northward and appears to contain a less-complex pattern of faulting than near the Flatiron. At the northern end of the Trout Meadows valley the KCF is a single steeply east-dipping strand that strikes N08°E where it enters the Kern River Canyon. At the intersection with this canyon, orientation of the KCF changes to due north along the North Kern Canyon fault section (Figure 2).

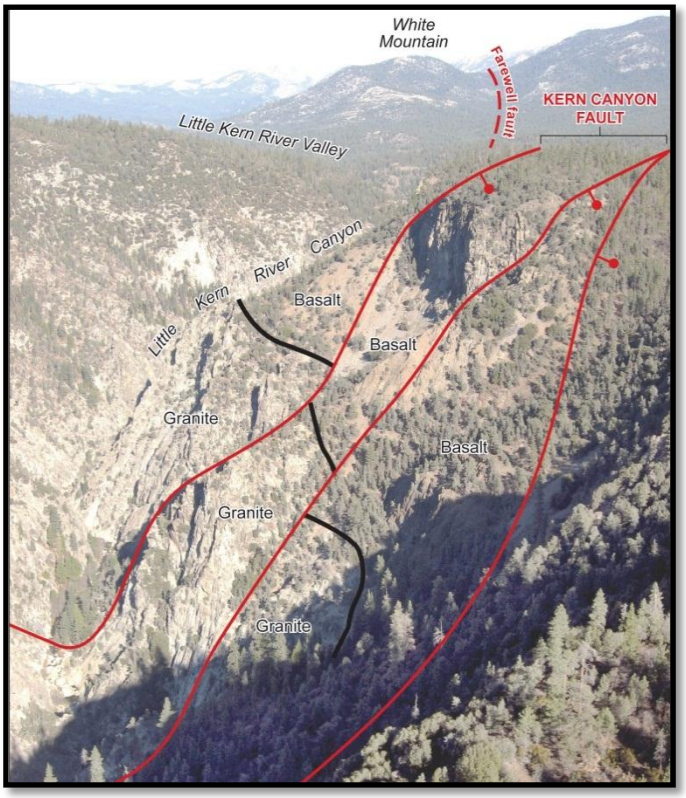

Figure 6. View northwest across the KCF toward the Little Kern River Valley and the Farewell fault.

Interpretation of Fault Segmentation

Several geologic relationships in the Flatiron area indicate that the Flatiron area forms the boundary between the South Kern Canyon and North Kern Canyon fault sections. First, the Flatiron area is associated with a change in the overall strike of the KCF, from a north-northeast (N08°E) strike south of the Flatiron to a due-north strike north of the Trout Meadows valley.

Second, the intersection of the KCF and the Farewell fault along the western margin of the Flatiron surface is characterized by a complex pattern of fault splays and en echelon fault steps (Figure 3). Geologic mapping of Tertiary volcanic flows and gravel deposits indicates that the Farewell fault and the KCF are structurally connected and that the fault pattern is related to long-term interaction between these faults. Although there is no evidence for late Quaternary displacement on the Farewell fault northwest of the KCF, the presence of this major crustal discontinuity appears to influence the pattern of surface ruptures and may locally accommodate brittle deformation within the complex fault intersection.

Third, the Kern Canyon and Farewell faults appear to be linked at a deep crustal level as shown by the numerous basaltic eruptive centers near the KCF on the Flatiron plateau and along the Farewell fault within the Little Kern River valley (Figure 3). These vents likely represent structural control of volcanism at the junction of the Farewell and KCF faults and suggest that the intersection of these two faults is a long-lived structural feature that extends through the seismogenic crust. The presence of the broad basalt-capped Flatiron surface at the fault intersection is related to the presence of these vents and the broad, low-lying Tertiary valley or basin within which the basalt was deposited. The geomorphic development of this broad Tertiary valley can be reasonably attributed to tectonic basin-forming processes that are probably related to long-term tectonic interaction of the Kern Canyon and Farewell faults over the past several million years.

Fourth, the geologic information from the Flatiron area provides a means to estimate the long term slip rate on the KCF, because the Little Kern

River basalt and overlying alluvial deposits are present on both sides of the fault. Several small remnants of basalt are preserved on the western side of the Little Kern River valley at elevations of about 1,880 m (Figures 3 and 5). The elevation of the basalt on the eastern side of the KCF near the southern end of the Flatiron is 1,795 m, indicating an east-down displacement across the fault of 85 m. However, because the small remnant west of the KCF probably is a preserved remnant of an originally thicker deposit, the base of the deposit may be a better measure of net vertical tectonic displacement. The base of the basalt remnant has about 155 m of east-down separation. Using a date of 3.5 Ma for the basalt (Dalrymple, 1963), the data provide a long-term slip rate of 0.045 mm/yr. Also, geologic mapping shows the possible presence of an isolated gravel deposit on the western side of the KCF at an elevation of about 2,055 m (Figures 3 and 5). If this gravel is correlative with the gravel overlying the basalt in the northern part of the Flatiron at an elevation about 1,930 m (Figure 5), then the east-down vertical displacement across the KCF is about 125 m. This gravel is less than 3.5 Ma because it overlies the Little Kern River basalt, but the offset of this gravel provides another long-term slip rate estimate of about 0.036 mm/yr. This long-term range of 0.036 to 0.045 mm/yr is an average over the past 3.5 million years and represents a minimum rate for the active KCF because the timing of displacement initiation is not known.

As noted previously, the uppermost surface of the Little Kern River basalt east of the KCF has a maximum elevation of about 1,950 m in the central part of the Flatiron (Figure 3). This elevation is about 50 m higher than the uppermost basalt surface in the Little Kern River valley which is at 1,900 m elevation. Possible explanations for this are (1) the possible presence of additional, unrecognized volcanic vents east of the KCF such that the basalt on the Flatiron was derived locally rather than from the vents identified in the Little Kern River valley, or (2) net *west*-down displacement across the combined Kern Canyon and Farewell faults over the past 3.5 Ma. This latter case is possible if the Farewell fault accommodated west-down displacement in the late Tertiary, after deposition of the basalt and gravel but before initiation of east-down displacement on the KCF. If so, then the total east-down displacement along the KCF of the Little Kern River basalt (and overlying gravel) is equal to the differences in elevation across the KCF of the basalt and gravel, plus the possible 50 m of west-down, post-3.5 Ma Tertiary displacement. The total net vertical tectonic displacement in this case ranges from 175 to 205 m. Using a maximum age of 3.5 Ma yields a minimum slip rate of 0.050 to 0.059 mm/yr. If a constant rate of 0.3 mm/yr is assumed for the late Quaternary KCF, the post-3.5 Ma faulting initiated about 580 to 686 ka.

The Kern River Paleovalley

Overall, the presence of the 3.5-Ma basaltic deposits and vents in the Little Kern and Kern valleys represent the locations and elevations of the ancestral Little Kern and Kern Rivers. Through additional mapping from 2009 to 2011, this basalt and similarly elevated gravel deposits have been delineated from their northernmost exposure near Burnt Corral Meadow in the Little Kern River valley, downstream for approximately 25 km to the Kern River Canyon narrows near Rincon Springs Creek (Figure 7). Many of the small basalt remnants cap isolated hilltops south of the Flatiron, as mapped by Matthews and Burnett (1965). Columnar basalt is common in the exposures. These basalt remnants are spatially associated with nearby coarse gravel deposits or bedrock strath surfaces. As shown on Figure 7, the margins of this paleovalley are

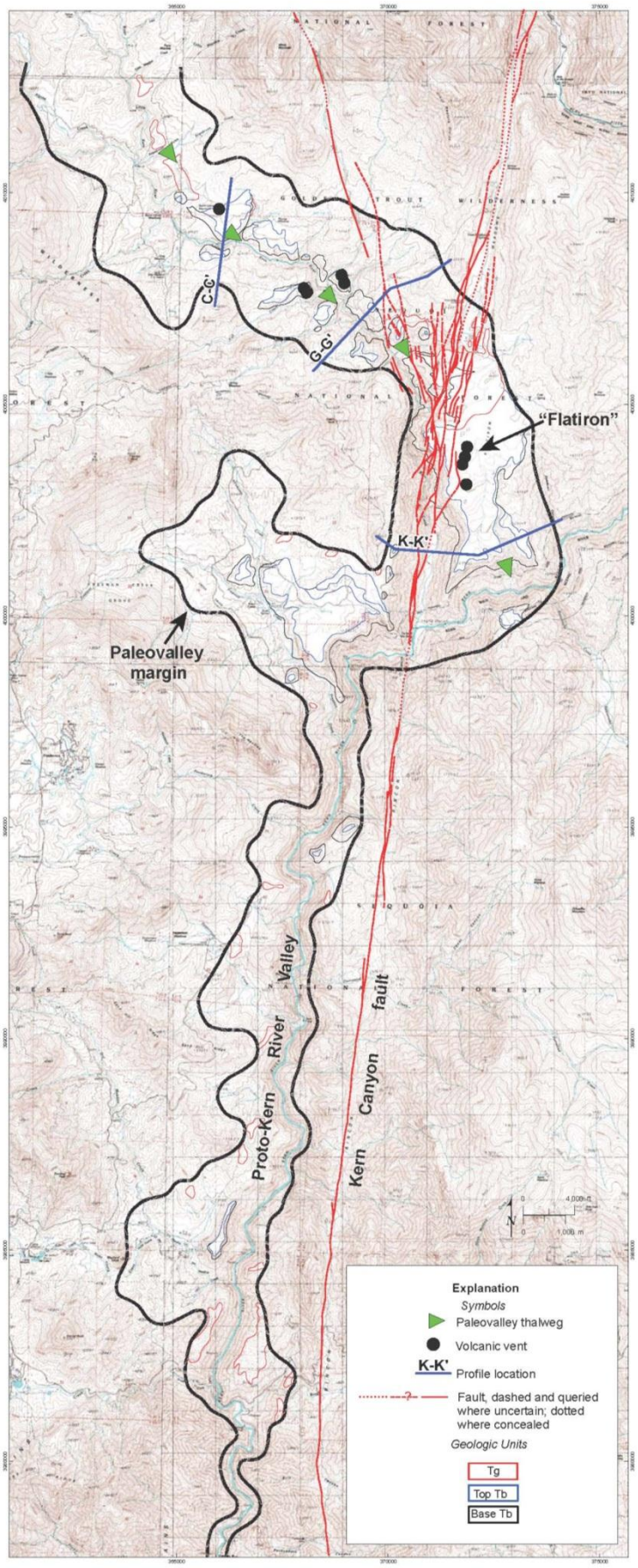

Figure 7. Map of basalt and gravel remnants in the Little Kern and Kern River valleys near the Flatiron and Rincon Springs Creek.

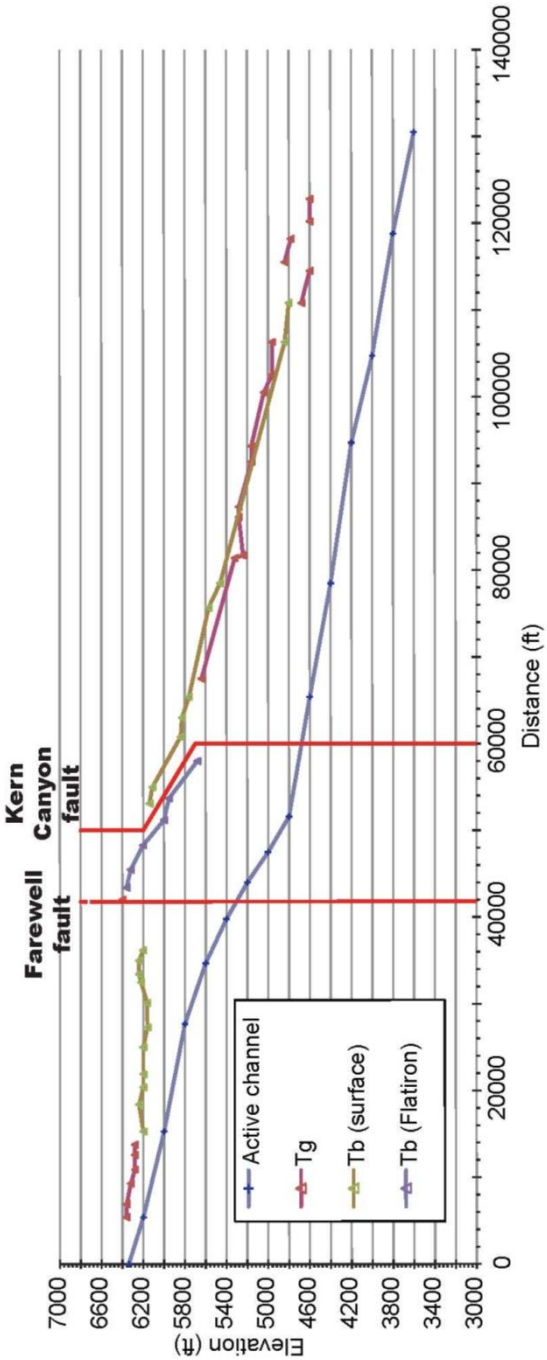

Figure 8. Topographic profiles of basalt and gravel remnants in the Little Kern and Kern River valleys near the Flatiron and Rincon Springs Creek. The Flatiron is the basalt surface between the Farewell and Kern Canyon faults, in this depiction.

mapped on the basis of fairly continuous western and eastern breaks-in-slope. The paleovalley is generally about 1 to 3 km wide, although it is much wider at Flatiron and in the present valley embayment occupied by Freeman Creek and Lloyd Meadow (Figure 7).

Topographic profiles of the basalt surfaces and spatially associated gravel deposits or strath surfaces are shown on Figure 8. The paleovalley gradient from these profiles is approximately 20m/km southward below the Flatiron, which is comparable to the present-day gradient on the Kern River. Upstream of the Farewell and Kern Canyon faults, the present gradient of the top of the basalt is nearly horizontal, which may have some interesting causes. One possible explanation is that the uppermost basalt strata resulted from ponding against the west-facing fault scarp of the Farewell fault; however, this would require that the basalts on both sides of the fault are not correlative. Another possibility is that the basalt reflects westward tilting, perhaps related to movement on either the Farewell or Kern Canyon faults. The steep southeastward gradient of the base of basalt (the paleovalley thalweg) argues against this possibility; the paleovalley thalweg actually plunges steeper than the current, very steep present-day Little Kern River. Alternatively, the low gradient of the upper basalt on the western side of the Farewell fault may reflect deposition that was contemporaneous with west-down displacement on the Farewell fault. This is consistent with the field observations that the basalt is thicker on the western side of the Farewell fault. Subsequent east-down movement on the Kern Canyon fault is indicated by the east-facing scarps in the basalt and younger deposits, also suggesting that the current episode of KCF displacement post-dates movement on the (now inactive) Farewell fault.

References

Burnett, J.L., 1976. Kaweah Peaks pluton and its relationship to the age of the Kern Canyon fault: Tulare County, California. California Division of Mines and Geology Map Sheet 35.

Busby-Spera, C.J., and Saleeby, J.B., 1987. Geologic guide the Mineral King area, Sequoia National Park, California: Pacific Section, Society of Economic Paleontologists and Mineralogists Field Trip Guidebook, 44 p.

Dalrymple, G.B., 1963. Potassium-argon rates of some Cenozoic volcanic rocks of the Sierra Nevada, California. Geological Society of America Bulletin 74: 379–390.

Du Bray and Dellinger, 1981. Geologic map of the Golden Trout Wilderness, southern Sierra Nevada, California. U. S. Geological Survey Map MF-1231A, scale 1:48,000.

Kelson, K.I., Amos, C.B., Simpson, D.T., Baldwin, J.N., Rose, R., Ticci, M., Kelson, J., Salesky, E., and Chipman, J., 2010, Structural and geomorphic control on landscape evolution by the Kern Canyon fault, southern Sierra Nevada, California: American Geophysical Union, Fall Meeting 2010, abstract #EP53B-0611

Kelson, K.I., Simpson, D.T., Rose, S.R., and Serafini, D.C., 2010, Seismic hazard characterization of the Kern Canyon fault for Isabella Dam, California: Proceedings, United States Society on Dams 2010 30th Annual Meeting, Sacramento, April, 2010, p. 295-310: http://ussdams.com/proceedings/2010Proc/295-310.pdf

Lawson, A.C., 1904. The geomorphogeny of the upper Kern Basin. University of California Publications in Geological Sciences, Bulletin 3: 291–376.

Matthews, R.A., and Burnett, J.L., 1965. Geologic map of California, Fresno Sheet. California Division of Mines and Geology, scale 1:250,000.

Moore, J.G., and du Bray, E., 1978. Mapped offset on the right-lateral Kern Canyon fault: Southern Sierra Nevada, California. Geology 6: 205–208.

Page, W.D., 2005. Reconnaissance along the Kern Canyon fault and inspection of the Little Kern basalt flow: Kern County, California. Consultants report prepared for Dam Safety Assurance Program, US Army Corps of Engineers, Sacramento, California; 6 pp. plus figures.

URS (URS Corporation), 2007. Quaternary fault study of the Rincon section of the Kern Canyon fault, California. Unpublished report prepared for U.S. Army Corps of Engineers, Sacramento, California, February 12.

URS (URS Corporation), 2008. Kern Canyon fault assessment, phase II: Kern and Tulare counties, California. Unpublished report prepared for U.S. Army Corps of Engineers, Sacramento, CA, March 21.

Webb, R.W., 1936. Kern Canyon fault, southern Sierra Nevada. Journal of Geology, 44: 631–638.

Webb, R.W., 1946. The geomorphology of the Middle Kern River Basin: Southern Sierra Nevada, California. Geological Society of America Bulletin 57: 355–382.

Stop 2-1b:
Late-Quaternary slip rate on the northern Kern Canyon fault

Colin Amos, *Fugro Consultants* *

Keith Kelson, *Fugro Consultants*

Dylan Rood, *Lawrence Livermore Nat'l Lab*

David Simpson, *URS Corporation*

Ronn Rose, *U.S. Army Corps of Engineers*

*currently: University of California, Berkeley

We will discuss a series of moraines deposited at the late Pleistocene glacial terminus in the northern Kern River canyon at Soda Spring. These moraine crests are displaced by the northern Kern Canyon fault and were characterized using airborne lidar data coupled with 10Be exposure dating of moraine boulders. This study provides the first slip rate estimate for the northern Kern Canyon fault. Adapted from Amos et al. (2010).

The significance of the Kern Canyon fault (KCF) as a first-order geologic structure within the southern Sierra Nevada has been recognized for over a century (Lawson, 1904; Webb, 1946; Ross, 1986). Previous investigations of the KCF underscore its importance as a late Cretaceous and Neogene shear zone in the tectonic development of the southern Sierra Nevada (e.g., Busby-Spera and Saleeby, 1990; Nadin and Saleeby, 2008). Study of the late Quaternary history of activity, however, has been confounded by the remote nature of the KCF and deep along-strike exhumation within the northern Kern River drainage, driven by focused fluvial and glacial erosion.

As part of the seismic safety study for the Lake Isabella dams, the U.S. Army Corps of Engineers commissioned an airborne lidar survey to collect high-resolution topographic data spanning the entire ~140 km length of the KCF. Here, we describe a site along the northern KCF (Soda Spring, Figure 1), where lidar data enabled identification and characterization of displaced glacial moraines as definitive evidence for late-Quaternary movement along the KCF.

The northern Kern River canyon represents a remarkable physiographic and geomorphic feature bisecting the southern Sierra Nevada, separating the Great Western Divide from the Kern Plateau to the east (Figure 1). Soda Spring marks the geomorphic boundary between the relatively broad, U-shaped glacial valley of the northern Kern River

The northern Kern River canyon represents a remarkable physiographic and geomorphic feature bisecting the southern Sierra Nevada, separating the Great Western Divide from the Kern Plateau to the east (Figure 1). Soda Spring marks the geomorphic boundary between the relatively broad, U-shaped glacial valley of the northern Kern River

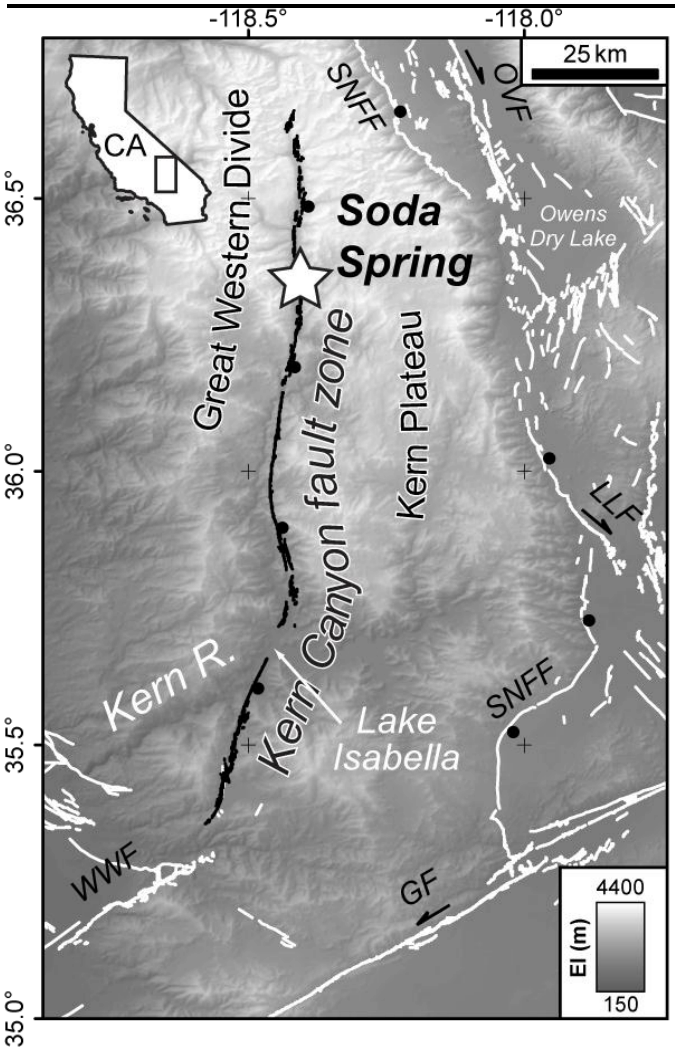

Figure 1. Overview map of the Kern Canyon fault zone showing the surface trace mapped from the lidar data. Other major Quaternary active faults in the southeastern Sierra Nevada region are abbreviated as follows: GF – Garlock Fault; LLF – Little Lake Fault; OVF – Owens Valley Fault; SNFF – Sierra Nevada Frontal Fault; WWF – White Wolf Fault. Arrows indicate the slip sense of predominately strike-slip faults, while the black ball shows the downthrown side of predominately normal faults.

canyon and the comparatively narrow gorge to the south.

Glacial landforms at Soda Spring were first identified by Lawson (1904) and later described by Matthes (1960), who correlated them with the Wisconsin, or Last Glacial period. Detailed mapping of glacial deposits and landforms at Soda Spring was completed using color orthophotos and hillshade images derived from the lidar topography (Figure 2).

Our mapping reveals three generations of nested terminal and recessional moraines and associated outwash surfaces, as well as extensive late Pleistocene alluvial fans, fluvial terraces, and colluvial deposits (Figure 2). The relative size, geomorphic character, and position of moraines features within the landscape supports correlation with the Tioga, Tahoe, and pre-Tahoe glaciations, using the existing nomenclature of glacial subdivisions in the Sierra Nevada (e.g., Gillespe and Zehfuss, 2004).

At Soda Spring, hillshade images computed from the bare-earth lidar topography reveal roughly north-south striking scarps along the KCF directly west of the Kern River (Figures 2 and 3). Where it intersects the Tahoe moraine loop, the fault trace has an average strike of ~N10°E before branching into two subparallel, north-striking splays. The bare-earth hillshade image reveals both splays as prominent lineaments forming east-facing scarps ~3-5 meters high where they intersect the Tioga moraine (Figure 3). The westernmost of these splays juxtaposes an isolated bedrock knob against moraine material, while the eastern strand displaces the moraine crest before disappearing beneath active Kern River alluvium to the north (Figure 2). Continuity of both the Tahoe and Tioga moraine loops across the fault suggests that slip on the northern KCF is predominantly normal with little or no lateral component of displacement.

The lidar topography provides a means to quantify fault displacement from the offset Soda Spring moraine crests. Topographic profiling across the eastern fault strand where

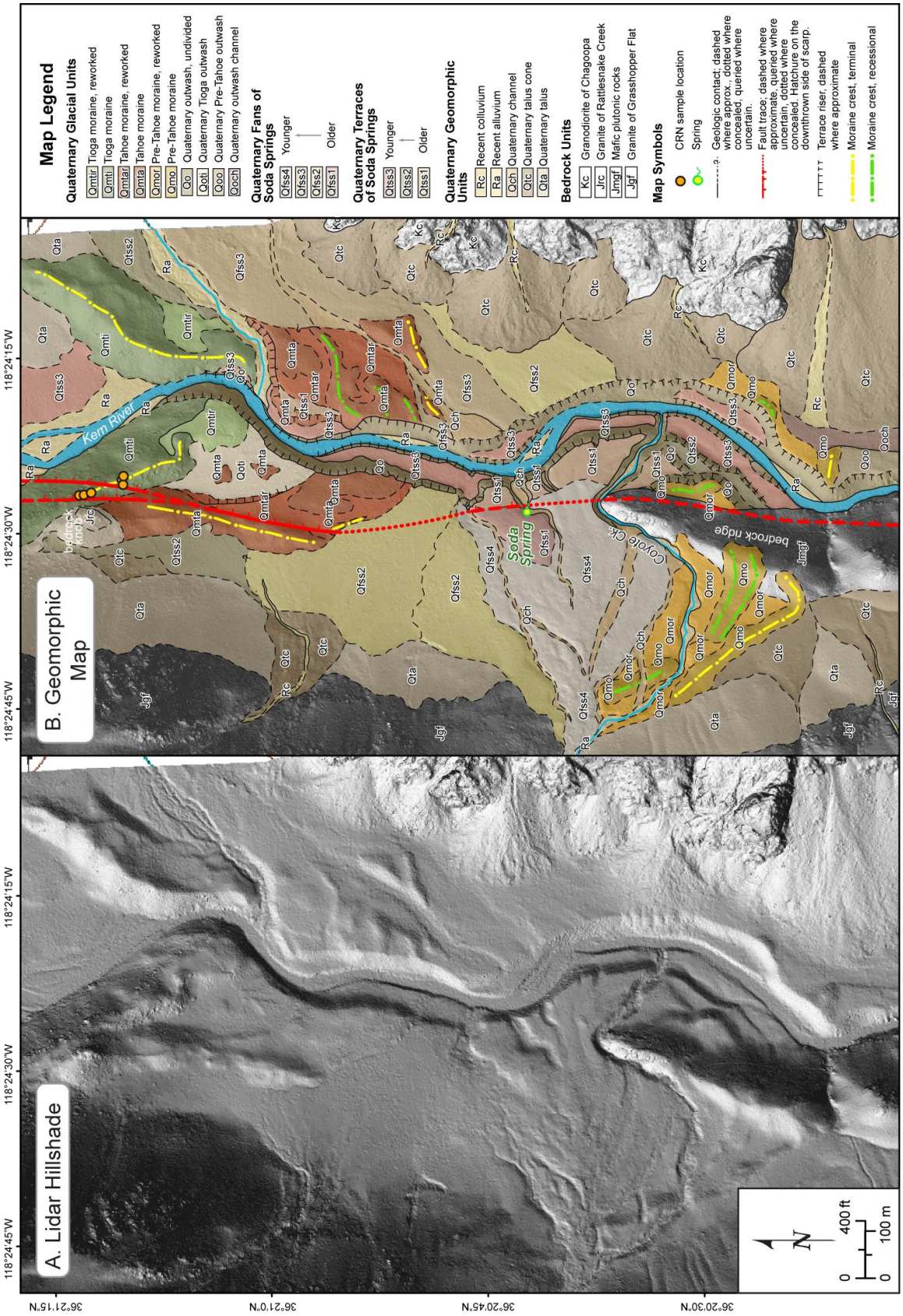

Figure 2. A) Bare-earth hillshade image from the lidar data and B) the results of geologic and geomorphic mapping of the northern Kern Canyon fault at Soda Spring. Bedrock units are reported by Moore and Sisson (1984).

it intersects the Tioga moraine crest suggests 2.6 ± 0.4 m of vertical separation, corresponding to 2.8 +0.6/-0.5 m of normal fault slip given a range of dips from 60° to 90° (Figure 4A). Given the lack of intact moraine crest preserved across the adjacent western fault strand, this value represents a minimum estimate of total fault displacement.

The late Quaternary slip rate along the KCF is calculated using measurements of cosmogenic ^{10}Be from six granitic boulders on the displaced Tioga moraine. Three large and intact boulders were sampled on each side of the fault to minimize the effects of post-depositional erosion, modification, or burial (Figure 5). The calculated exposure ages form a relatively tight cluster, ranging between 17.4 ± 0.4 and 18.7 ± 0.4 ka. A composite probability distribution function of the six exposure dates reveals an approximately normally distributed spread of ages centered on a mean of 18.1 ± 0.5 ka (Figure 6A).

Using a Monte Carlo simulation to calculate the normal-sense fault slip rate yields values of at least ~0.1 – 0.2 mm/yr at 95% confidence (Figure 6B).

This result provides the first clear documentation of late Quaternary activity on the northern KCF. Rates of normal-fault slip on the northern KCF measured at Soda Spring are comparable to Holocene vertical slip-rates of ~0.2-0.3 mm/yr measured for the Sierra Nevada frontal fault (Le et al., 2007) bounding the Owens Valley to the northeast.

References

Amos, C.B., Kelson, K.I., Rood, D.H., Simpson, D.T., Rose, R.S., 2010. Late Quaternary slip rate on the Kern Canyon fault at Soda Spring, Tulare County, California. Lithosphere, 2(6), 411-417.

Busby-Spera, C.J., Saleeby, J.B., 1990. Intra-arc strike-slip-fault exposed at batholithic levels in the southern Sierra-Nevada, California. Geology, 18(3), 255-259.

Gillespe, A.R., Zehfuss, P.H., 2004. Glaciations of the Sierra Nevada, California, USA. In: J. Ehlers, P.L. Gibbard (Eds.), Quaternary Glaciations - Extent and Chronology, Part II, pp. 51-62.

Lawson, A.C., 1904. The Geomorphogeny of the upper Kern Basin. University of California Publications in Geological Sciences, Bulletin, 3(16), 291-376.

Le, K., Lee, J., Owen, L.A., Finkel, R., 2007. Late quaternary slip rates along the Sierra Nevada frontal fault zone, California: Slip partitioning across the western margin of the Eastern California Shear Zone-Basin and Range Province. Geol. Soc. Am. Bull., 119(1-2), 240-256.

Maheo, G., Saleeby, J., Saleeby, Z., Farley, K.A., 2009. Tectonic control on southern Sierra Nevada topography, California. Tectonics, 28(Tc6006).

Matthes, F.E., 1960. Reconnaissance of the geomorphology and glacial geology of the San Joaquin Basin, Sierra Nevada, California. U.S. Geological Survey Professional Paper, 329.

Moore, J.G., Sisson, T.W., 1984. Geologic Map of the Kern Peak quadrangle, Tulare County California, U.S. Geological Survey Geologic Quadrange Map GQ-1684.

Nadin, E.S., Saleeby, J.B., 2008. Disruption of regional primary structure of the Sierra Nevada batholith by the Kern Canyon fault system, California. In: J.E. Wright, J.W. Shervais (Eds.), Ophiolites, Arcs, and Batholiths: Geological Society of America Special Paper 438. Geological Society of America Special Paper.

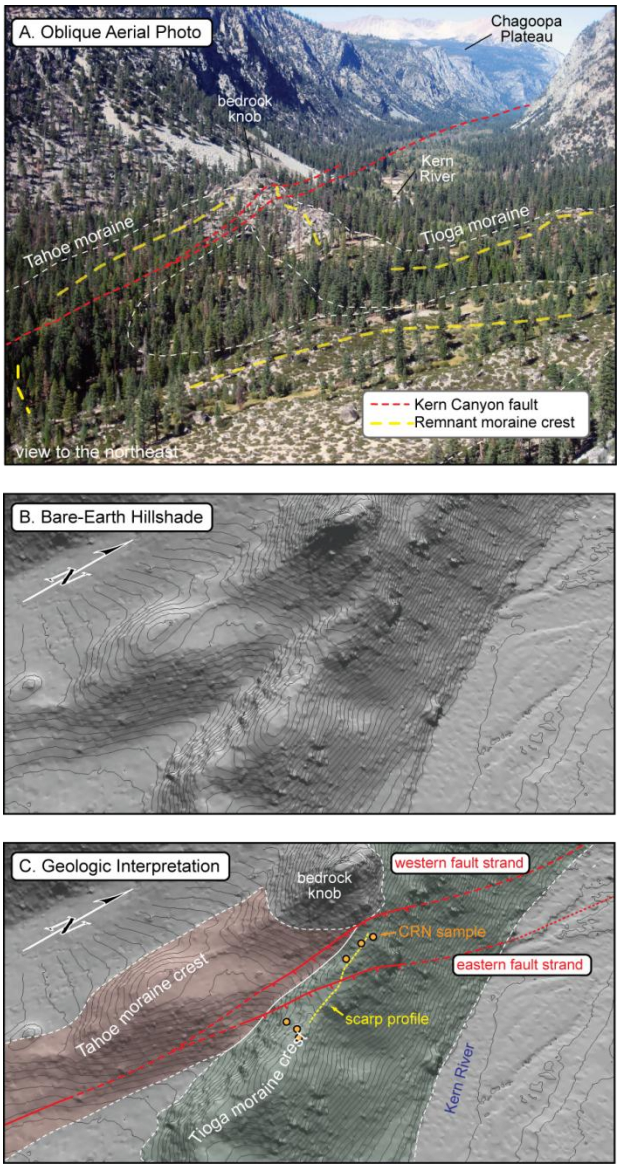

Figure 3. A) Oblique aerial image of the Soda Spring site near the intersection of the northern KCF with the Tioga and Tahoe moraines. The fault trace continues northward from Soda Spring along the floor of the U-shaped northern Kern Canyon. B) and C) Oblique perspective view of the offset Tioga moraine crest from bare-earth lidar hillshades. Scale varies in this perspective, but the scarp profile in C is ~ 90 m long. 5 ft elevation contours are also shown in each image.

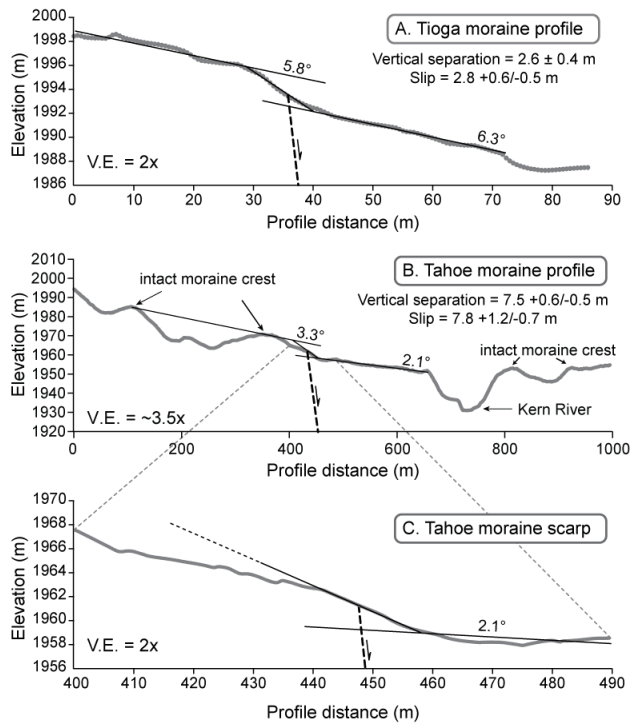

Figure 4. Topographic profiles extracted from the lidar topography showing regressions through intact portions of the (A) Tioga and (B) Tahoe moraine crests used in estimating vertical separation and displacement of these features across the KCF. C) A topographic scarp shown at the same scale as A separates uplifted Tahoe moraine to the west from relatively subdued moraine topography across the fault to the east.

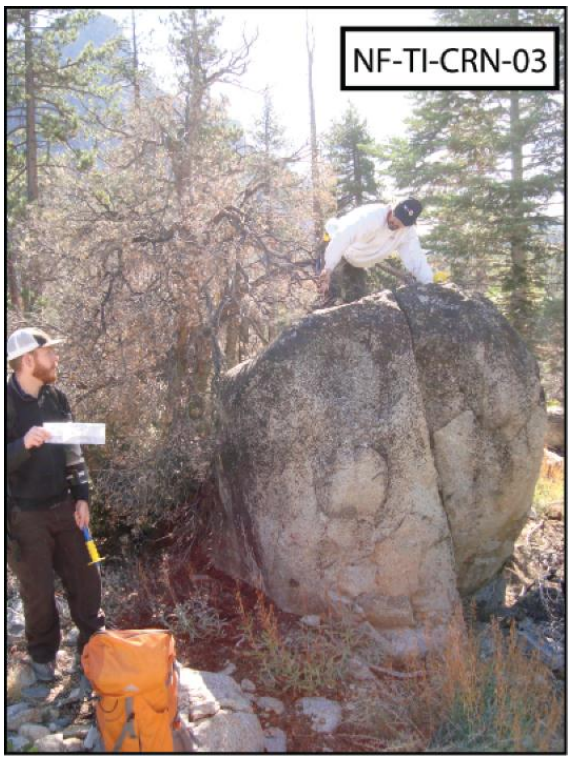

Figure 5. Boulder sampling at Soda Spring for cosmogenic ^{10}Be on the Tioga moraine crest.

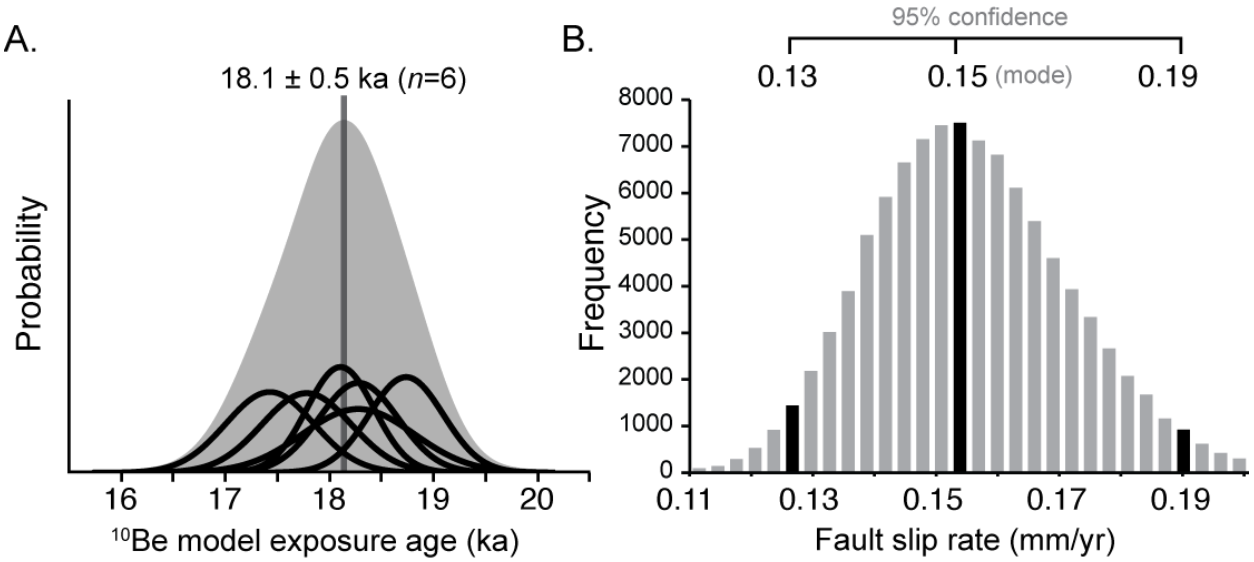

Figure 6. A) Composite relative probability density function of six exposure ages measured from cosmogenic ^{10}Be on Tioga moraine boulders. The peak age (18.1 ± 0.5 ka) represents a mean of all exposure ages. B) Histogram of predicted fault slip rates (100,000 trials) for the offset Tioga moraine showing the mode and associated 95% confidence intervals output from the Monte Carlo simulation.

Road Log E-E′

Rincon overlook (Stop 2-1) to Isabella Auxiliary Dam (Stop 2-2)

44.4 miles, 90 minutes

Mileage		Lat./Long.
Drive ahead on Forest Route 22S82, there are unpaved turnouts where you can turn your vehicle around		
0.0	**Reset your odometer as you pass Stop 2-1** This road winds for the next 10 miles across a broad pre-3.5 Ma relict landscape inset below a towering granite domeland terraine.	**36.0409°** **-118.4893°**
6.2	**Bear left to stay on Forest Route 22S82**	**36.0065°** **-118.5391°**
8.5	**Turn LEFT onto M-99 (Kern River Highway)**	**35.9828°** **-118.5425°**
10.7	The road descends about 270 m from here to Johnsondale Bridge and now passes back into scrub brush terrain. The gradient of South Creek steepens here where steep bedrock channels are more common that alluvial streams.	35.9692° -118.5143°
12.8	Waterfall. Yeah, yeah, knickpoints…big deal…	35.9723° -118.4923°
13.3	Johnsondale bridge—between here and mile 19.1 the Kern River is incised deeply into metamorphic bedrock and maintains an impressive degree of inherited sinuosity.	35.9682° -118.4866°
16.0	Fairview Dam, take out point for the Kern River No. 3 Powerhouse.	35.9455° -118.4770°
19.1	Between here and the Goldledge campground the canyon widens slightly, enough to preserve remnants of old bedrock terraces. The longitudinal profile steepens here where the Kern River exits the reach in metamorphic bedrock.	35.9153° -118.4864°
23.2	At Goldledge campground the canyon widens further, and the geomorphology is dominated by bedrock pediments with thin alluvial fan cover, all incised by the modern streams.	36.0409° -118.4893°
24.0	I didn't point this out on the way up, but there are some good exposures of a bedrock pediment surface cut on metamorphic bedrock along the left side of the road here. The pediment is incised by stream cuts that are backfilled with granitic boulders, and these are in turn capped by a relatively thin fan deposit.	35.8505° -118.4516°
27.4	Across the river you can see a very prominent series of imbricated boulder levees inset against the incised fan and bedrock pediment	35.8237° -118.4611°
29.3	Top of the braided alluvial section of the Kern River. Before impoundment, the reach of river between here and the Kern-	35.7974° -118.4510°

	South Fork Kern confluence the geomorphology was dominated by braided river channel in a broad, low relief alluvial plain.	
30.9	Penstocks of the Kern River No. 3 Powerhouse, built in 1921 and operated by Southern California Edison. The take out for this powerhouse is 15 river miles upstream at Fairview Dam and flows through a series of long adits and cut-and-cover canals.	35.7763° -118.4358°
33.1	**Turn LEFT onto Kernville Road (becomes Wofford Heights Blvd)**	**35.7558° -118.4176°**
35.9	A delta has formed where the Kern River meets Isabella Lake. Across the lake you can see a prominent alluvial fan (Cyrus Flat) incised into a linear bedrock ridge. The linear valley behind this ridge is the approximate trace of the proto-Kern Canyon fault zone which accommodated right-lateral shear of ductile granite in the Cretaceous. The fan is graded to the Kern River Valley, one indication that the ridge and linear valley behind it has formed from erosional processes and not from active uplift.	35.7222° -118.4338°
37.5	**Stay on this road and continue forward through Wofford Heights toward Lake Isabella (road becomes CA-155)**	**35.7069° -118.4563°**
41.5	To the left is a good vantage of Engineers Point, an east-facing bedrock scarp of the KCF. Before the dams were built, the confluence of the Kern and South Fork Kern Rivers was located at the north tip of this bedrock ridge, as was the now-flooded agricultural town of Isabella	35.6594° -118.4779°
43.4	**After crossing the Kern River at the Main Dam, turn LEFT onto Ponderosa Drive**	**35.6351° -118.4814°**
44.2	**Bear RIGHT at the U.S. Forest Service complex (onto Barlow Drive)**	**35.6441° -118.4765°**
44.4	**Park in the large open lot at the Stop 2-2: Isabella Project Auxiliary Dam**	**35.6440° -118.4738°**

Stop 2-2a:
Assessment of seismic hazard to the Isabella Project dams

Keith Kelson, *Fugro Consultants*

Andrew Lutz, *Fugro Consultants**

Ronn Rose, *U.S. Army Corps of Engineers*

Dave Simpson, *URS Corporation*

Ozgur Kozaci, *Fugro Consultants*

David Serafini, *U.S. Army Corps of Engineers*

*Currently: Lettis Consultants International

Introduction

Our investigation of seismic hazard to the Isabella Project dams utilized numerous geologic and paleoseismic techniques to characterize the poorly understood KCF, and develop well-constrained data on fault behavior for quantitative seismic hazard analyses. The program has resulted in a solid paleoseismic database that includes new information on fault location, activity, recent rupture chronology, and fault slip rate. These datasets are necessary for developing a defensible seismic source characterization of the KCF, and consequently for developing estimates of strong ground motions at the two dams.

The 135-km-long, north-striking Kern Canyon fault (KCF) has produced multiple surface-rupturing earthquakes within the past several thousand years with east-down displacement and little or no lateral offset. Field-based geologic and stratigraphic data suggest coseismic displacements of about 0.4 to 1.0 m and a late Quaternary slip rate of about 0.1 to 0.3 mm/yr. Possible rupture segments of the fault are interpreted based on a surface-rupture chronology determined from paleoseismic trenching, as well as by fault geometry and sense of slip derived from field and LiDAR-based mapping and analysis of instrumental seismicity. Paleoseismic evidence suggests possible contemporaneous surface ruptures on some adjacent fault sections, but also possible non-contemporaneity (i.e., the fault probably exhibits single-segment and multi-segment rupture behaviors). These analyses support the occurrence of surface-rupturing earthquakes with magnitudes ranging from **M**6.5 to perhaps **M**7.5. These findings represent a significant improvement to the characterization of seismic hazard (e.g., strong ground motions, surface rupture) to the dams, and will be used for analyses of probable failure modes, dam stability and, if needed, remedial design.

Late Quaternary fault segmentation

Both deterministic and probabilistic seismic hazard assessments (DSHA and PSHA, respectively) require evaluation of possible earthquake ruptures on specific fault segments. To estimate the magnitudes and likelihoods of surface-rupturing earthquakes along the KCF, we consider various scenarios in which ruptures occur along one or more sections of the fault. These scenarios are developed based on an understanding of the geologic complexity (i.e., the *physical* characteristics) of the KCF, as well as the timing and amounts of past surface ruptures (i.e., the *behavioral* characteristics). For the development of a segmentation model for the Kern Canyon fault, several fault *sections* are identified from the physical characteristics of the fault. These fault sections may or may not represent possible earthquake-rupture *segments*, which represent the behavioral characteristics of the KCF as a seismic source. Physical characteristics include changes in geometry and structure, such as changes in strike, presence of restraining bends or extensional steps, jogs, branching or intersection

points with other faults or fault strands, and major changes in lithology along the fault. Behavioral considerations incorporate timing, rupture length, and displacements that occurred during past earthquakes, and represent information obtained by paleoseismic studies.

Our fault segmentation model of the KCF is based on data that address how the various physical fault sections rupture as independent (solitary) fault segments or as dependent (linked) multi-section ruptures. The segmentation model is intended to represent the likely KCF ruptures during late Quaternary time (i.e., approximately the past 125,000 years). The fault sections considered in this hazard analysis, from north to south, are three sections of the Kern Canyon fault: the North Kern Canyon, South Kern Canyon, and Lake Isabella fault sections, and the Breckenridge fault (Figure 1). These sections form the basis for developing multiple earthquake rupture scenarios, estimating likely earthquake magnitudes and recurrence, and thus evaluating expected strong ground motions at the dams. Our investigations were developed specifically to obtain well constrained data on the physical and behavioral characteristics of these four fault sections and the five section boundaries. The physical characteristics of the sections were defined based on analysis of pre-existing geologic, seismologic, and geophysical data, geomorphic and geologic mapping along the KCF and Breckenridge faults, and consideration of regional seismotectonic models. The behavioral characteristics were defined based on detailed investigations at several sites, which were selected specifically for characterizing each of the fault sections (URS, 2008). The most promising sites on each of the four fault sections were investigated so that data are available for evaluating behavioral characteristics of all four sections. As noted earlier, geologic and logistical conditions strongly influenced the number of available promising sites on each section.

Late Quaternary fault characteristics

We completed detailed field investigations to assess late Quaternary rupture chronology, amount and direction of coseismic slip, and long-term average fault slip rate. These data were collected on each of the fault sections to assess the likelihood that adjacent sections do or do not rupture together during large-magnitude earthquakes. For example, if adjacent fault sections are separated by a relatively weak boundary (i.e., a minor change in fault strike) and have comparable rupture chronologies, then it is judged likely that the two fault sections rupture during the same (large) earthquake. If adjacent fault sections exhibit distinct differences in rupture chronology or slip rate, they are deemed more likely to rupture during separate (smaller) earthquakes. Through this approach, we developed a basis for interpreting the likelihood of various rupture scenarios.

Earthquake rupture chronology

Detailed paleoseismic information on the number and timing of geologically recent earthquake ruptures is available from several of the sites on the South Kern Canyon and Lake Isabella fault sections. Investigations of the North Kern Canyon fault section and the Breckenridge fault did not yield data on the timing of specific paleoearthquakes.

On the South Kern Canyon section, investigations at Rincon Spring (Figure 1) included excavation of three shallow trenches across the east-facing fault scarp and exposure of faulted and unfaulted latest Pleistocene (ca. 50 to 11 ka) and Holocene (post-11 ka) surficial deposits. The trenches targeted coarse-grained debris-flow deposits emplaced by high-energy flows crossing the KCF from east to west, as well as colluvial deposits derived from the uplifted

western side of the fault. The Brush Creek site included a single trench that exposed a well-developed shear zone in bedrock and faulted late Pleistocene and Holocene alluvial deposits. The Corral Creek site investigation included two short trenches into alluvium trapped on the eastern side of the fault, one short trench into colluvium shed from the east-facing fault scarp, and hand-auger boreholes to help identify buried strata east of the fault. At these sites, the ages of deposits were estimated from radiocarbon analysis of charcoal fragments, optically stimulated luminescence (OSL) analysis of sandy materials, and/or relative soil-profile development. From the site geomorphic mapping, trenching, drilling, and age-dating, these sites all indicate the occurrence of three Holocene surface-rupturing earthquakes, including two between about 2,000 and 5,000 years ago and one more than about 7,000 years ago. Within the analytical uncertainties related to stratigraphic correlations, laboratory age dates, and fault-related features, these ruptures appear to have occurred on the entire South Kern Canyon fault section.

On the Lake Isabella fault section (Figure 1), the Barlow Drive site included two trenches that exposed colluvium shed from the east-facing escarpment along the main fault trace, and eight shallow boreholes that define deeper strata. The Bernie/Silicz site included three trenches into fine-grained, well-bedded alluvial sediments deposited across the fault, as well as completion of several shallow boreholes to identify late Pleistocene deposits buried on the downthrown, eastern side of the fault. The Havilah North site included three excavations that exposed faulted and unfaulted colluvial deposits derived from the uplifted western side of the fault. The ages of deposits at these sites were estimated from radiocarbon analysis of charcoal fragments, OSL analysis of sandy materials, and/or relative soil-profile development. Based on the various investigations, these sites all indicate the occurrence of at least two, and perhaps as many as four, Holocene surface-rupturing earthquakes (during the past 11,000 years). Within the analytical uncertainties as noted above, these ruptures appear to have occurred at all three of the sites on the Lake Isabella section but may or may not be the same Holocene ruptures interpreted along the South Kern Canyon section.

Sense and amount of coseismic displacement

The geomorphic expression of the KCF along its entire length indicates that the sense of coseismic displacement is primarily down on the east, along a near-vertical, east-dipping normal fault. The fault trace is nearly straight where it traverses rugged topography (indicating a near-vertical dip), and fault scarps developed in late Quaternary surficial deposits all face to the east, indicating primarily east-down displacement, along the four fault sections.

Along the South Kern Canyon section, the fault trace is associated with some left-deflections in drainage channels, although the amount of purported left-slip would be highly inconsistent with the likely ages of the channels and the fault slip rate based on other analyses (see below). The left-deflections are instead a result of uplift on the western side of the fault, and north- or southward deflections of west-flowing drainages along the east-facing fault scarps. There are no well-developed indicators of fault slip direction in any of the trench exposures, with the exception of micro-fabric shearing in bedrock exposed in the Brush Creek trench. These trench relationships suggest primarily normal, east-down displacement, and are consistent with local and regional geomorphic indicators. The amount of coseismic displacement during individual ruptures is estimated based on several trench exposures, as measured by the total net vertical

tectonic displacement, which represents the sum of individual brittle (fault) displacements and off-fault tilting and warping.

Colluvial stratigraphy exposed in the Havilah North and Barlow Drive sites suggest that the two most-recent ruptures averaged about 1.1 m of east-down displacement; the net vertical tectonic displacement at the Bernie/Silicz site is estimated to be about 0.8 to 0.9 for both mid-Holocene ruptures. On the South Kern Canyon section, the Rincon Spring, Brush Creek, and Corral Creek sites all yielded estimates of about 0.4 to 1.7 m for net vertical tectonic displacement during recent ruptures. Collectively, these values suggest earthquake magnitudes in the range of **M**6.7 to 7.0 based on worldwide empirical relationships (Wells and Coppersmith, 1994).

Fault slip rate

The slip rate on the KCF during the Holocene is approximated by the amount of net vertical tectonic displacement produced during the past one or two ruptures, as indicated from the trench exposures at the Bernie/Silicz and Barlow Drive sites on the Lake Isabella section and the Corral Creek, Brush Creek, and Rincon Spring sites on the South Kern Canyon section. As noted above, these sites suggest approximately 0.4 to 1.7 m of net vertical tectonic displacement within the past approximately 5,000 years, yielding a short-term slip rate of about 0.1 to 0.4 mm/yr. The long-term slip rate (over the past 20 ka) from the Corral Creek site is 0.1 to 0.3 mm/yr, which is consistent with the short-term rate at this site. A maximum long-term slip rate is estimated on the Breckenridge fault from analyses at the Oak Tree Estates site, which suggests net vertical tectonic displacement of about 4 m on an alluvial-fan surface that is estimated to be about 20 to 50 ka. These data yield a rate of about 0.1 to 0.2 mm/yr, although detailed mapping of undeformed alluvial fans elsewhere along the Breckenridge suggest that this rate probably is a maximum and/or that the rate decreases dramatically south of Oak Tree Estates (Figure 1). On the North Kern Canyon section, detailed mapping, topographic profiling, and age-dating of a late Tioga-age (18 ka) glacial moraine at Soda Spring (Amos et al., 2010) show about 3 m of net vertical tectonic displacement, yielding a slip rate of about 0.1 to 0.2 mm/yr. Regional geomorphic mapping suggests that the slip rate probably decreases north of the Soda Spring site (Figure 1). The overall pattern of slip rate values presently available suggest, at this time, that the rate may be highest (as much as about 0.4 mm/yr) along the central fault sections (i.e., the Lake

Isabella and South Kern Canyon), and probably decreases gradually northward on the North Kern Canyon section and decreases abruptly southward on the Breckenridge fault.

Earthquake rupture scenarios

Detailed investigations of the fault sections and their boundaries provide a basis for interpreting possible earthquake rupture scenarios. Geologic and geomorphic mapping suggests that the complex boundary between the Breckenridge fault and the Lake Isabella section (“Piute Pass”, Figure 1) does not contain through-going fault strands, and probably represents a rupture-termination point. In contrast, a step-over in the fault at Kernville between the Lake Isabella and South Kern Canyon sections is only about 1 to 2 km wide and may not always inhibit rupture propagation. The boundary between the South Kern Canyon and North Kern Canyon sections (the “Flatiron”, Figure 1) contains fault-strand stepovers and intersections with other regional faults (i.e., the Farewell fault and possibly the Durrwood fault zone), but may or may not be a persistent rupture termination point. The northernmost end of the late Quaternary KCF, which probably is between Junction Meadow and the Kings-Kern Divide (“Harrison Pass”, Figure

1), coincides with a broad and complex zone of northeasterly striking faults in the Upper Kern Basin that probably inhibits earthquake ruptures on the north. Paleoseismic data from sites on all four sections address the relative likelihood of ruptures occurring on shorter, independent sections or as longer, multi-section ruptures.

The long-term slip rates for the two central sections of the KCF are comparable (approximately 0.1 to 0.4 mm/yr), and geomorphic expression of the fault is consistently strong along these two sections. The long-term slip rate on the North Kern Canyon section (about 0.1 to 0.2 mm/yr) maybe lower than the South Kern Canyon section, suggesting a that some ruptures may not extend northward past the Flatiron boundary (Figure 1). The long-term slip rate on the Breckenridge fault is also consistent with this range, but is poorly constrained at this time (pending laboratory age estimates of faulted deposits). The geomorphic expression of the Breckenridge fault in late Quaternary surficial deposits is considerably less than that along the KCF, suggesting that some ruptures may not extend southward past the Piute Pass boundary. Geologic mapping indicates that the fault stepover at the Piute Pass section boundary is significant and may inhibit through-going ruptures between the KCF and the Breckenridge fault. The section boundaries at Kernville and The Flatiron coincide with intersections with significant inactive fault strands, although the size and geometries of these intersections appear to not favor persistent rupture terminations over long time periods.

On the basis of available paleoseismic data from all of the detailed site investigations and regional analyses, a total of nine reasonable rupture scenarios are interpreted for the combined Kern Canyon and Breckenridge faults (Figure 3). These include an “unsegmented” scenario in which the entire 153-km-long Kern Canyon-Breckenridge fault system ruptures, three scenarios in which the fault system ruptures in two different segments (some composed of multiple fault sections), three scenarios in which the fault system ruptures in three segments, and one scenario in which all four fault sections rupture independently. The segmentation model also includes one scenario consisting of a “floating”, 50-km-long rupture that could occur anywhere along the KCF (or Breckenridge fault). Paleoseismic data on the timing of past ruptures suggest that the Lake Isabella and South Kern Canyon sections may rupture both dependently and independently. The similar long-term slip rates between these two sections and the North Kern Canyon section also suggest that ruptures may occur both dependently and independently. Using all the available information, preliminary weightings were assigned for the nine possible rupture scenarios (Figure 3) and used in DSHA and PSHA calculations (URS, 2009). The segmentation models suggest that 50% of the earthquakes on the KCF involve ruptures that are more than 50 km long and extend beneath the Auxiliary dam. Such ruptures probably are in the range of **M**6.5 to 7.5 (Wells and Coppersmith, 1994), and likely will generate surface faulting beneath the dam embankment. Of the scenarios that involve rupture of the Lake Isabella section, the weighted mean magnitude is about **M** 6.7.

Earthquake maximum magnitude

Seismic source characteristics for deterministic seismic hazard analysis (DSHA), which are required by some regulatory agencies, include a source-to-site distance and a maximum earthquake magnitude. Because the Isabella Auxiliary dam overlies the KCF (Figure 2), the source-to-site distance is 0 km. For a DSHA, the maximum earthquake magnitude is a judgment based on known characteristics of specific fault, in conjunction with the understanding of regional

geologic relationships and comparisons with faults in similar seismotectonic settings. Using information developed primarily from this investigation, the maximum magnitude for the KCF is judged to be **M**7-1/2. As summarized above, the KCF likely ruptures more than one fault section during large earthquakes, and rupture of the entire, unsegmented 153-km-long scenario cannot be precluded. The calculated magnitude value for this scenario is **M**7.51, which has a relatively low weighting of 0.05. For the case in which the three sections of the KCF rupture (about 135 km long, with a weighting of 0.10), the mean maximum magnitude is calculated to be **M**7.45. However, the final interpretations on the behavior of the KCF are not yet complete, and we acknowledge that there is significant aleatory uncertainty in the magnitude calculations (as much as 0.3 magnitude units).

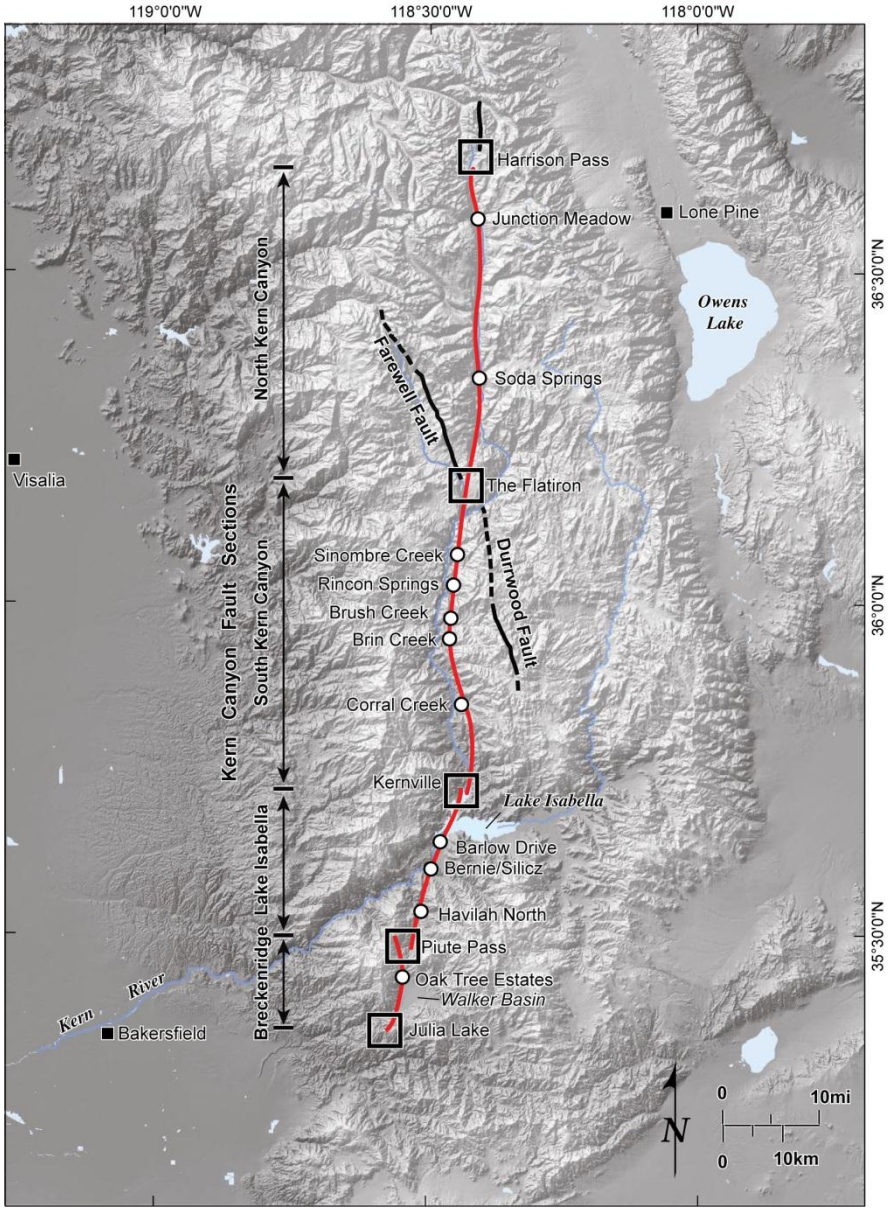

Figure 1. Hillshade rendering of the southern Sierra Nevada and surrounding region, showing location of the Isabella dams, primary fault sections of the Kern Canyon fault, and detailed investigation sites.

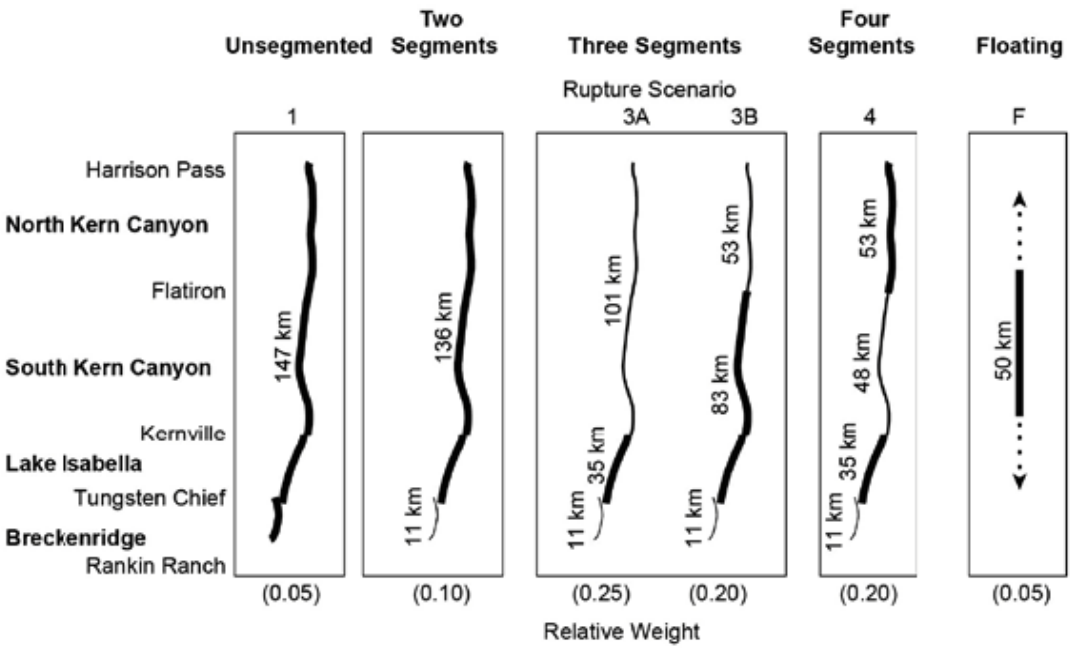

Figure 2. Schematic segmentation model for the Kern Canyon fault, showing fault sections and section boundaries, eight scenarios involving segmented and unsegmented ruptures along these fault sections, and surface-rupture lengths for each scenario rupture. Relative weights interpreted for each rupture scenario in parentheses. The ninth scenario is a 50-km-long rupture ("floating earthquake") anywhere along the fault system.

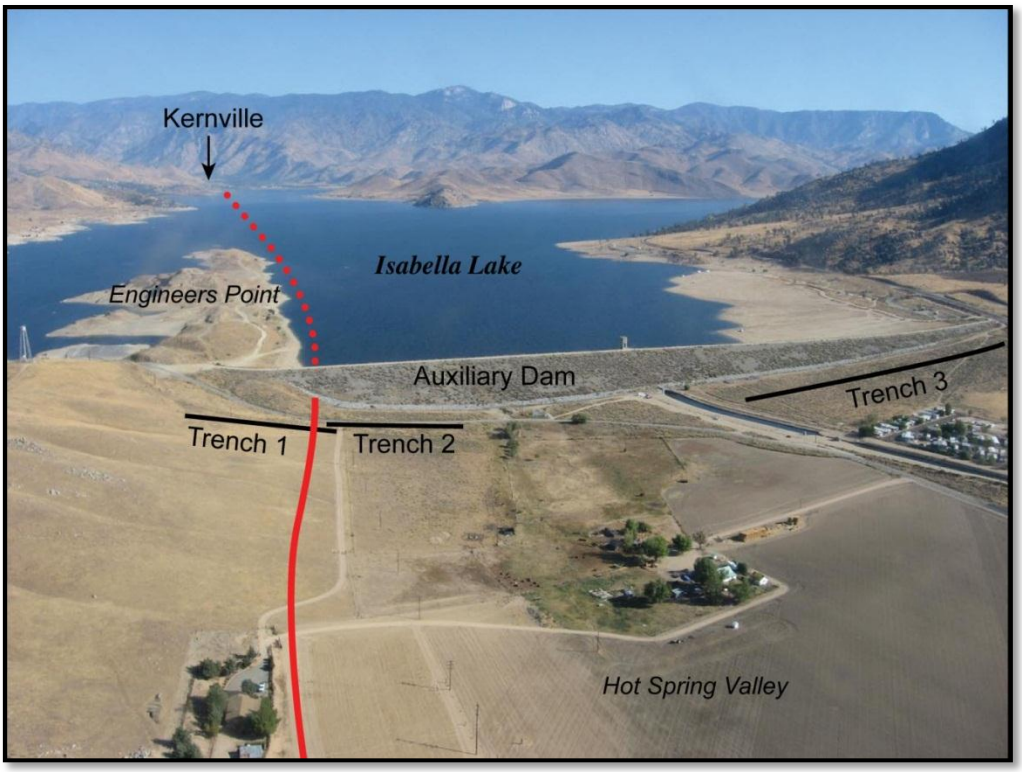

Figure 3. Oblique photo of the Isabella Auxiliary dam (**Stop 2-2**), looking north along Hot Spring Valley toward Isabella Lake and the Kern Plateau. The Kern Canyon fault continues beneath the Auxiliary dam on the left side of photograph, along the eastern side of Engineers Point.

Stop 2-2b:
Fault displacement hazard analysis for the Isabella Auxiliary Dam

Andrew Lutz, *Fugro Consultants**

Keith Kelson, *Fugro Consultants*

Steve Thompson, *Fugro Consultants**

*Currently: Lettis Consultants International

Abstract

Trench exposures and a shallow boring transect were completed at the Auxiliary Dam to constrain the width and location of the Kern Canyon fault and to characterize the style and distribution of vertical deformation during a large-magnitude earthquake. The paleoseismic data from these investigations indicate that 2.2 to 5.0 ft of east-down displacement has occurred during each of the last two surface ruptures. This displacement occurred along two fault strands (A and B) within a zone of deformation that intersects the Auxiliary Dam at a roughly 75-degree angle between dam stations 53+25 and 54+75.

Uncertainty in the distribution of deformation across the fault zone during the past two ruptures is represented by two surface-displacement scenarios, which anticipate that 40 percent to 100 percent of the total deformation is expected to be accommodated along fault strand B and that 0 percent to 60 percent of the total deformation is expected to be accommodated by folding and tilting with minor brittle faulting across the rest of the fault zone. Deposits exposed outside of this zone of deformation are unfaulted and are not expected to experience vertical deformation during a large-magnitude earthquake.

The expected future coseismic displacement at the Auxiliary Dam was calculated by determining the aleatory and epistemic uncertainties within the paleoseismic data. The resulting upper limit (of the 97.5 percent confidence interval) is 6.8 ft of east-down displacement. We consider this value to represent the best estimate of expected coseismic displacement for design considerations. A similar range of displacement estimate values was generated by using an alternative, scenario-based approach and a global earthquake-rupture data set. This second analysis resulted in a value of 5.0 ft for the mean and a value of 13.2 ft as the upper limit (of the 84 percent confidence interval). These data are generally consistent with the range developed from the paleoseismic data.

Width and location of faulting at the Isabella project Auxiliary Dam

The Kern Canyon fault intersects the right abutment of the Isabella Auxiliary Dam along the western margin of Hot Spring Valley, where the fault is associated with a prominent east-facing bedrock escarpment (Median Ridge/Engineers Point) (Figure 1). Although bedrock faults were identified in trenches and borings performed during pre-construction site characterization (USACE, 1948), the presence of active, late-

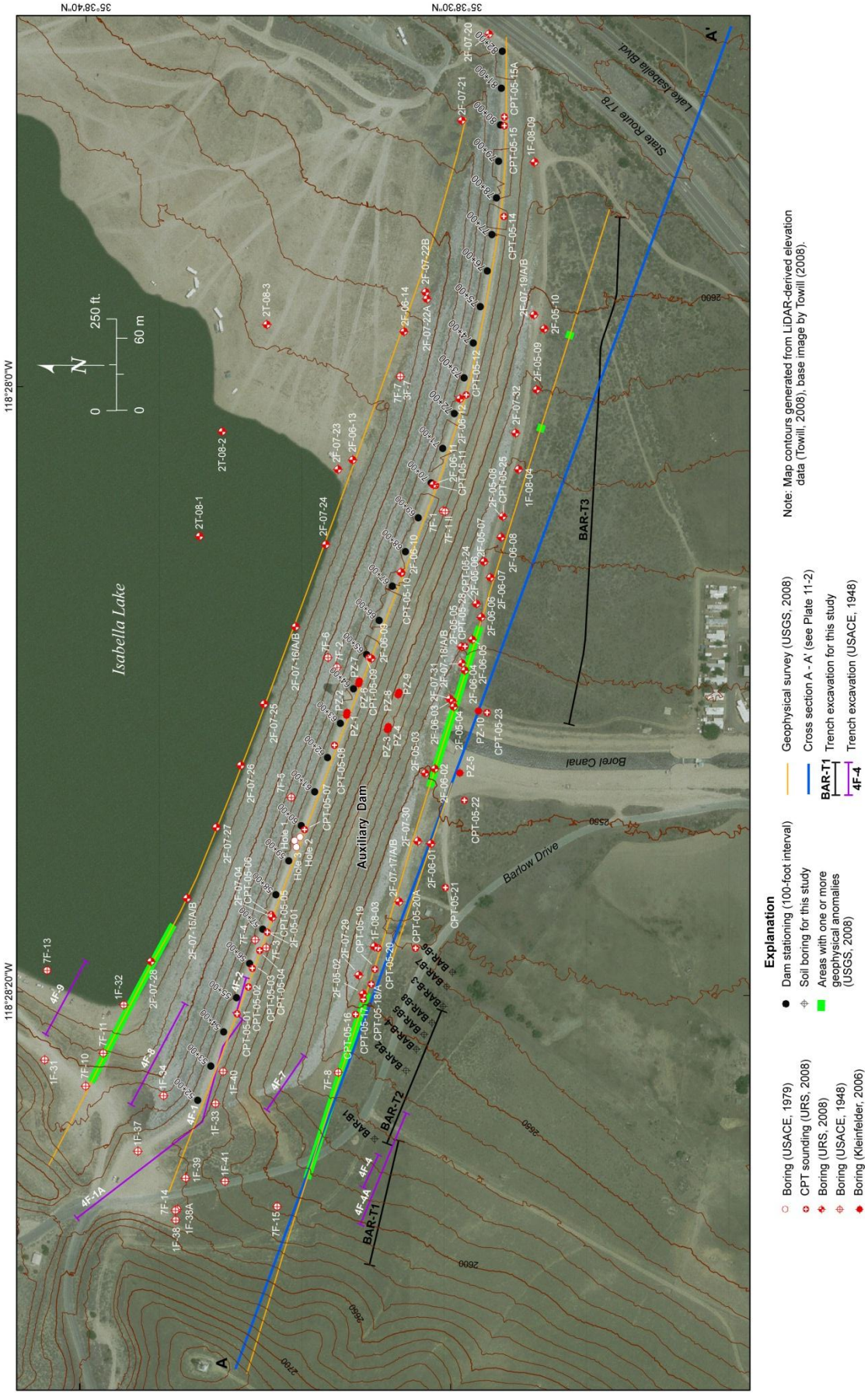

Figure 1. Investigation map of the Isabella Project Auxiliary Dam site

Quaternary deformation was not recognized. Paleoseismic evidence, some of which has been presented during the course of this trip, shows that the Kern Canyon fault has produced large surface-rupturing earthquakes in the past 11,000 years, and site specific data collected during the same study was used to identify the zone of active deformation and provide constraints on the position of the active faults and zones of secondary deformation beneath the Auxiliary Dam embankment. In addition, borehole and trench data from USACE (1948) and later work (URS, 2006) were analyzed and suggest that at least two (inactive) fault strands are present beneath the Auxiliary Dam and displace the top of bedrock but do not deform deposits at or near the surface.

Hot Spring Valley is an asymmetric basin underlain by alluvial-fan deposits that grade gently westward from catchments on the eastern side across to the valley axis near the eastern base of Median Ridge. A structure contour map of the bedrock surface using elevation data from borings and trenches shows that the bedrock surface slopes gently from east to west beneath Hot Spring Valley (Figure 2). Bedrock exposed at the surface east of the Auxiliary Dam is part of a pediment surface that slopes about 10 degrees to the west from the eastern valley margin to an elevation of 2,488 ft in boring 2F-07-19. Under the right abutment, the bedrock elevation steps up abruptly on the west between dam stations 53+50 and 56+50. This 300-ft-wide zone of displacement of bedrock represents the zone of long-term deformation in Hot Spring Valley and is generally consistent with the results of trenching investigations (Figure 1) as well as anomalies identified in geophysical data (USGS, 2009).

Trenches BAR-T1 and BAR-T2 were excavated near the right abutment of the Auxiliary Dam from the mid-slope of Median Ridge to near the axis of Hot Spring Valley (Figures 1 and 2). Trench BAR-T1 intersected two active fault strands (A and B) within an 80-ft-wide zone of deformation (Figure 3). This zone has accommodated 7.2 ± 2.7 ft of net vertical displacement over the past two earthquakes and a minimum of 31 ft in late-Quaternary time (combined with results from boring BAR-B1). The zone of secondary deformation in trench BAR-T1 spans from 10 ft west of fault strand A to 20 ft east of fault strand B. Trench BAR-T2 exposed colluvial deposits that are laterally continuous across its entire length and demonstrate an absence of late-Quaternary deformation between the fault strands exposed in trench BAR-T1 and the axis of Hot Spring Valley. The basal contact of unit Q7c represents the event horizon for the two most-recent earthquakes at the Barlow Drive Site and is undeformed where exposed in trench BAR-T2 from stations +0 to +200.

Deposits exposed in trench BAR-T3 indicate that coseismic deformation has not occurred near the left abutment of the Auxiliary Dam during Holocene time (past 11,000 years). Alluvial-fan deposits in trench BAR-T3 are laterally continuous over tens to hundreds of feet and are not faulted, warped, or tilted; there is no evidence of broad-scale folding or earthquake-induced liquefaction.

Though not presented in detail here, constraints provided by trench, borehole, and geophysical data indicate that the 80-ft-zone of fault deformation identified in trench

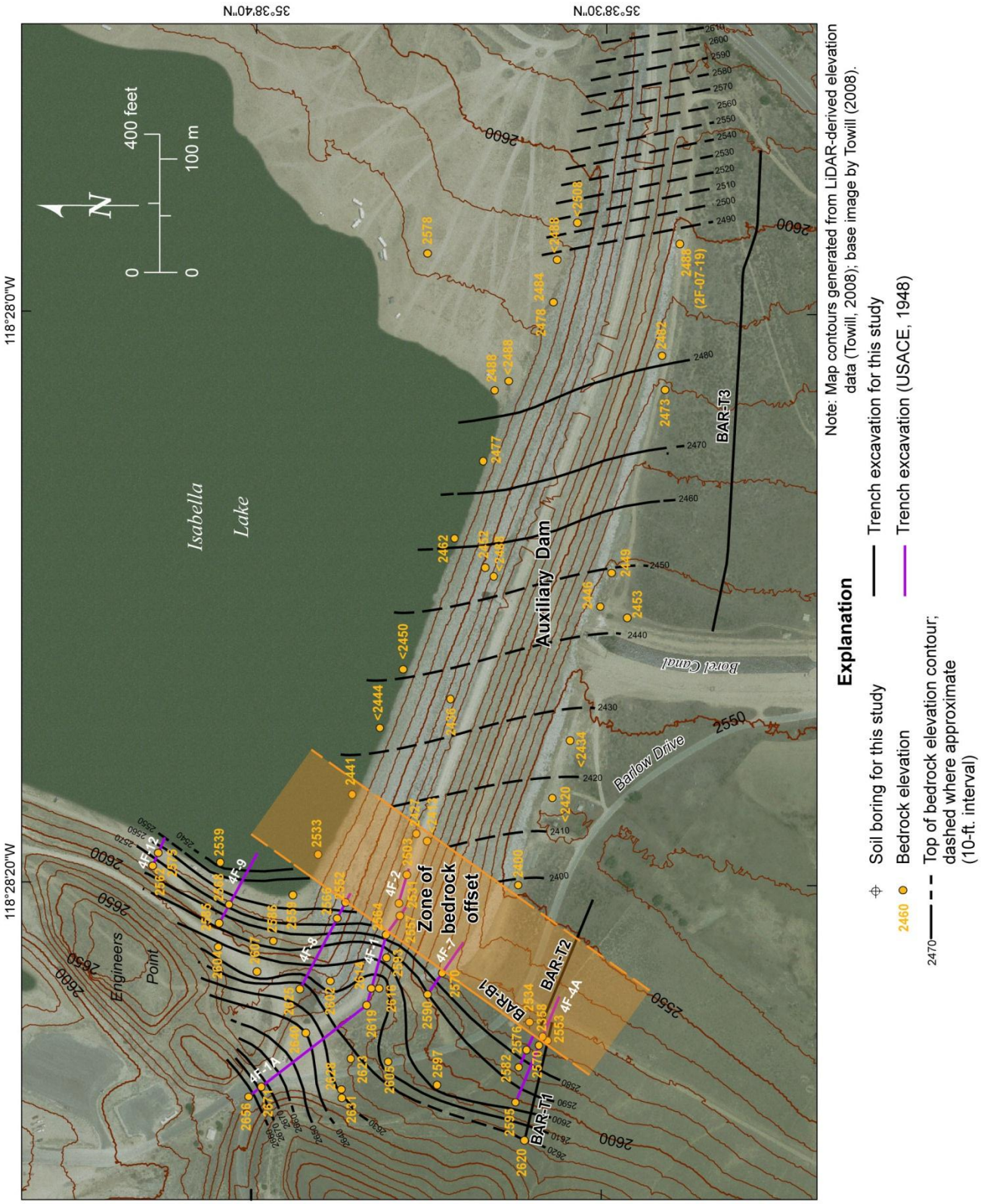

Figure 2. Top of Bedrock Structure Contour Map

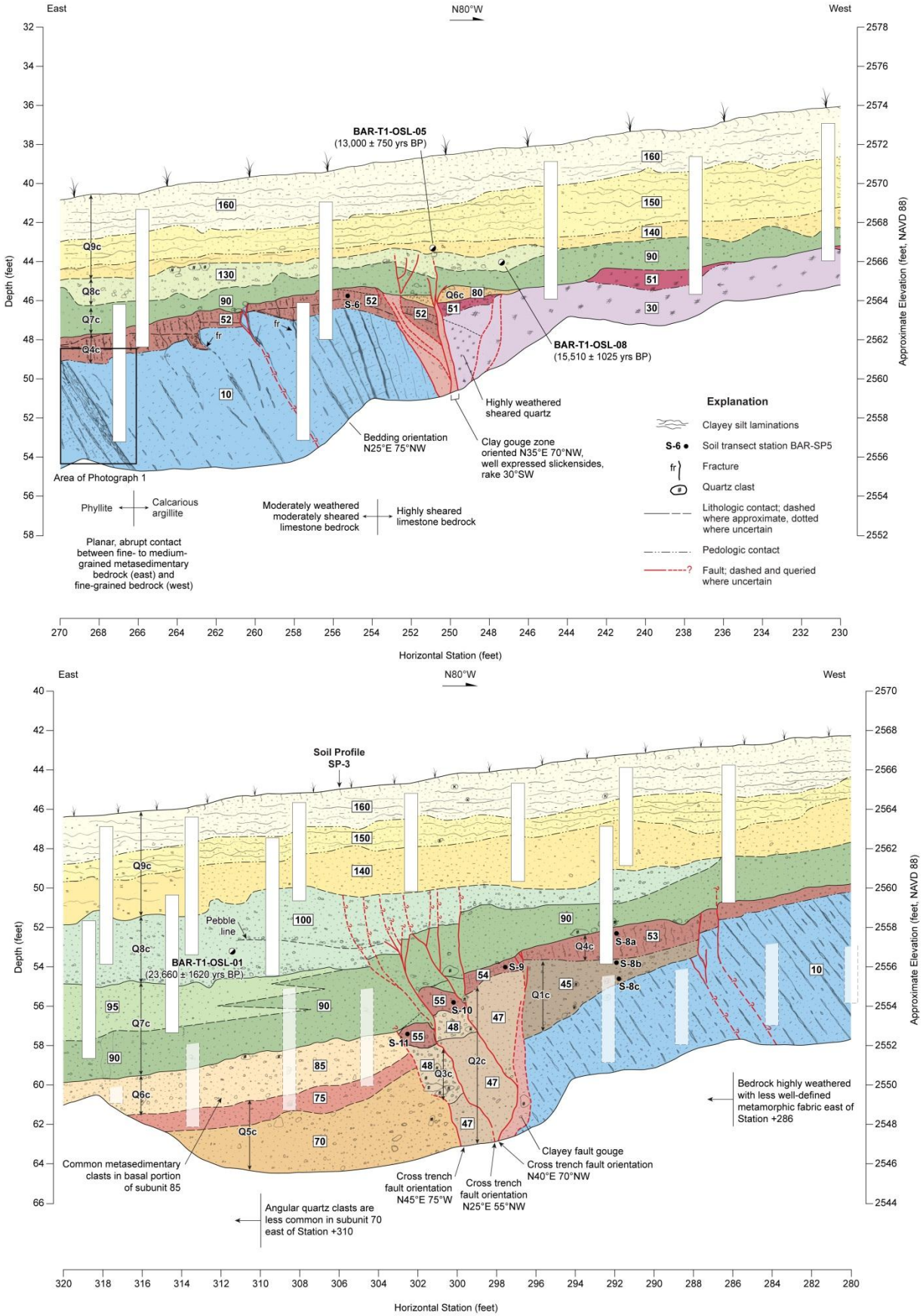

Figure 3. Log of fault zones A (above) and B (below) exposed in trench BAR-T1

Fault Displacement Hazard Analysis

Subsurface investigations at the Barlow Drive site identified an 80-ft-wide zone of primary fault deformation, which indicates possible surface rupture hazard within a 150-ft-wide zone at the latitude of the Auxiliary Dam crest (Figure 4). The detailed data from the Barlow Drive site provide qualitative data about the relative degree of deformation accommodated by individual fault strands or within areas between faults. Although the trench data cannot predict whether the majority of future coseismic displacement will be accommodated by distributed deformation across this zone or by brittle faulting along a discrete fault plane, the relationships in trench BAR-T1 and borehole BAR-B1 provide a reasonable (and probably representative) analog for the pattern of deformation that would likely occur beneath the dam during a large earthquake on the Lake Isabella section of the KCF.

Fault Displacement Distribution

The geologic and geomorphic data from subsurface investigations at the Barlow Drive site show clear evidence for vertical deformation on the KCF at the Auxiliary Dam. There is no compelling site-specific evidence for significant strike-slip movement at the Barlow Drive site or at any other location along the KCF. Future deformation beneath the dam is therefore estimated to be accommodated by net east-down displacement on the fault zone, with a distribution of deformation that will include one or more of the patterns observed in trench BAR-T1, including (from west to east):

- Minor eastward tilting and folding directly west of fault strand A
- Minor east- or west-down vertical displacement on fault strand A
- Eastward tilting and possible minor but distributed faulting in the area between fault strands A and B
- East-down faulting and possible locally complex faulting along fault strand B
- Minor eastward tilting and folding directly east of fault strand B

The above analysis of fault zone characteristics was combined with geologic judgment to develop two scenarios (1 and 2) for expected displacement beneath the dam. These two end-member displacement scenarios consider uncertainty with regard to the relative contribution of brittle faulting and block tilting and folding to the expected amount of net vertical tectonic displacement. In displacement scenario 1, coseismic deformation is distributed over most of the fault zone, with some brittle faulting along fault strand B. In displacement scenario 2, coseismic deformation is concentrated in a single location (along fault strand B). Though not described in detail here, faults C and D are not included in either displacement scenario because they are not considered capable faults and are not expected to rupture during the next earthquake. These scenarios are represented in Figure 5 as histograms that show the partitioning of expected coseismic deformation in a generalized way relative to the Auxiliary Dam stationing. and Figure 6 shows the cumulative density functions for both scenarios.

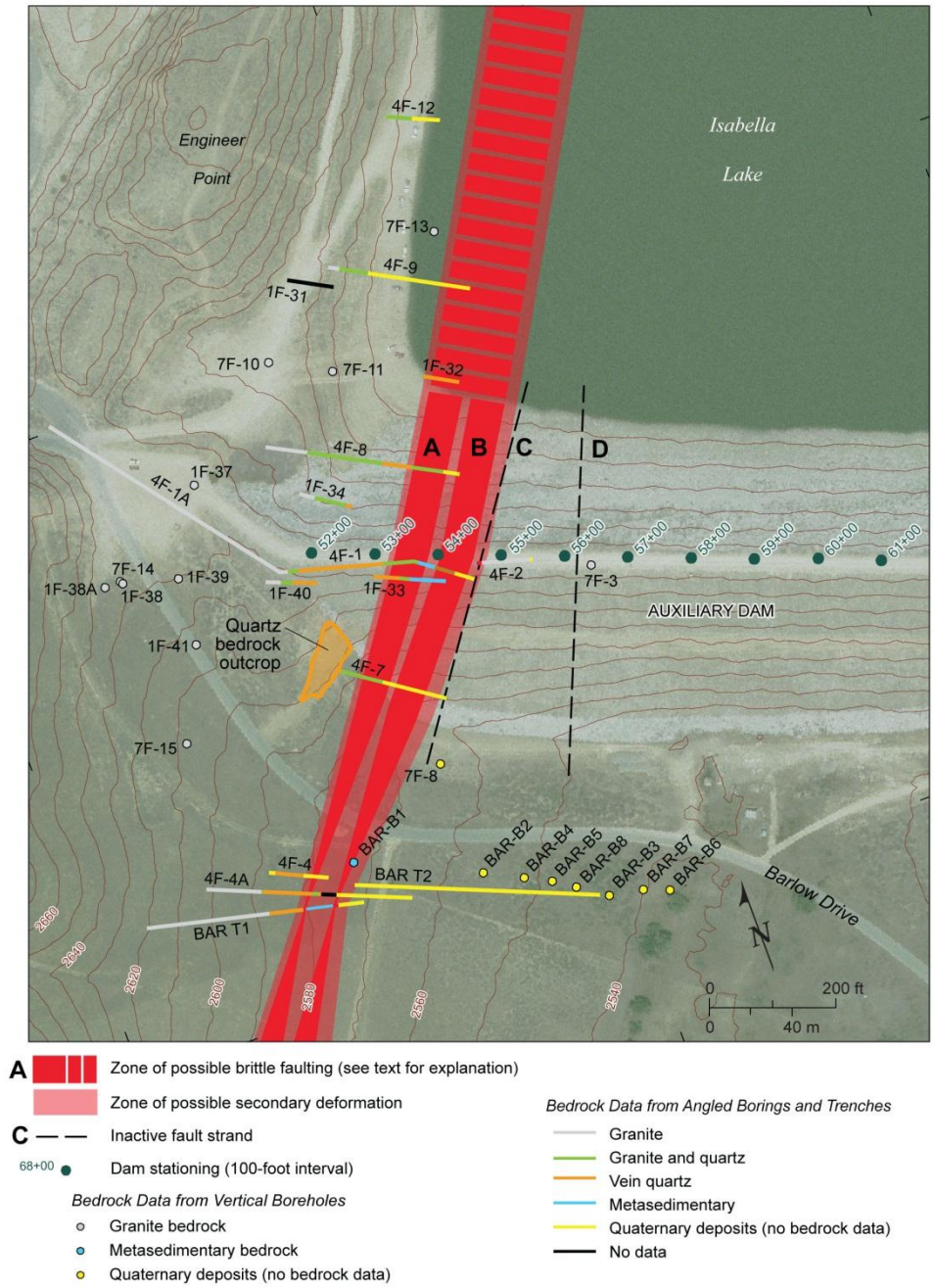

Figure 4. Zones of possible fault rupture and deformation at the Isabella Project Auxiliary Dam

Consideration of displacement scenario 1 (Figures 5 and 6) is based on field observations that fault strand A produced east-down or west-down deformation over the past two earthquakes and accommodated broad-scale eastward tilting of the area between fault strands A and B. Displacement scenario 1 also includes vertical displacement that is localized along fault trace B as a percentage of the total net vertical tectonic deformation. Displacement scenario 1 was developed using measurements of vertical displacements during the past two earthquakes from

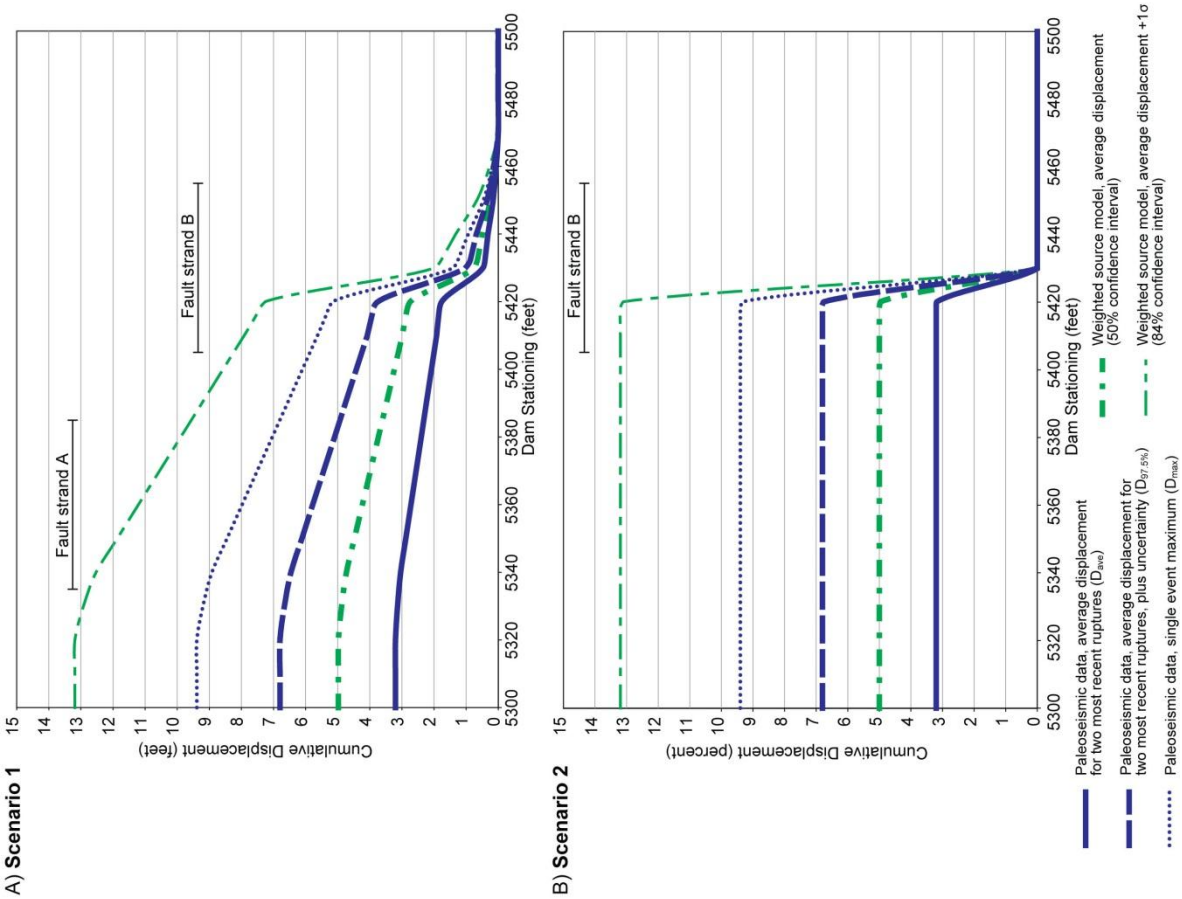

Figure 5. Distribution of Expected Deformation as a Percent of Total Displacement

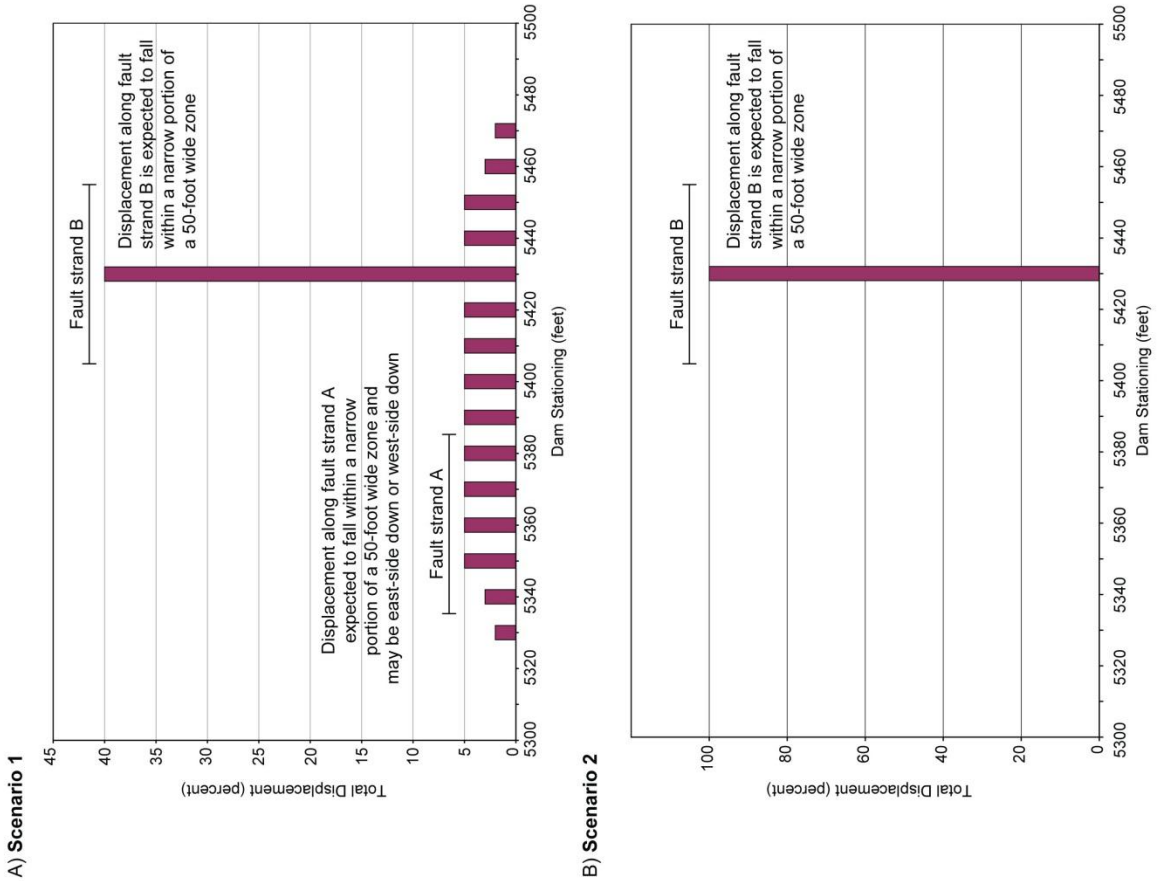

Figure 6. Probability Density Functions for Cumulative Displacement

trench BAR-T1 at the Barlow Drive site. From these data, fault B is expected to accommodate 40 percent of the total slip during a future rupture, and the remaining 60 percent of the total slip is expected to be distributed equally across the remaining width of the fault zone (likely reducing slightly toward on the edges of the fault zone). Fault strand A is not expected to accommodate any more displacement than the adjacent areas; however, slip along this fault could occur as either east- or west-down displacement.

Displacement scenario 1 is generally consistent with field observations of deformation documented along the KCF. However, inherent variability in near-surface earthquake ruptures and a relatively sparse worldwide database of the pattern of rupture within a given fault zone suggest that the actual distribution of coseismic deformation in future earthquakes could be substantially different than the scenario described above. The data do not preclude the possibility that all of the east-down coseismic displacement on the KCF at the Auxiliary Dam may occur specifically on a single fault strand and that this localized deformation could occur anywhere within the active fault zone. However, field observations of a thick package of colluvium in contact with bedrock along fault strand B indicate that this fault strand has accommodated the majority of localized deformation during the past several surface ruptures and is most likely to accommodate the majority of brittle faulting in a future earthquake. Displacement scenario 2 (Figures 5 and 6) reflects the possibility that all of the vertical deformation will be localized within this prominent zone of brittle faulting.

Displacement Estimates

This analysis considers two general approaches for estimating net displacement across the KCF at the Auxiliary Dam: (1) an approach that combines paleoseismic data with a consideration of the uncertainty related to event-to-event slip variability and, (2) a scenario-based fault displacement hazard analysis. Both approaches are deterministic in nature and are based on empirical data from worldwide data sets of historical earthquake rupture amounts, as described below.

In Approach 1, paleoseismic data documented in trench BAR-T1 show that the past two surface-rupturing earthquakes at the Barlow Drive site produced 7.2 ft of east-down coseismic displacement, an average of 3.6 ft per earthquake (Table 1, Approach 1); these values are consistent with paleoseismic data from other sites along the KCF. In the following analysis, the amount of vertical displacement produced by the past two earthquakes is referred to as the total displacement (D_t), and the per earthquake average is referred to as the average displacement (D_{ave}). Although 7.2 ft is considered to be the best estimate for D_t, epistemic uncertainty is considered by measuring the upper (9.9 ft) and lower (4.5 ft) limits of D_t, which also represent (respectively) the upper and lower boundaries of the 2σ confidence interval (Table 1, Approach 1). This upper limit for D_t yields a D_{ave} value of 5.0 ft (Table 1), though this value does not necessarily represent the maximum displacement during a single rupture.

Although the paleoseismic data provide robust constraints on the best estimate and

upper limit values for D_t, these data include significant uncertainty about whether or not the majority of the observed deformation was produced by only one of the two most recent ruptures (that is, whether displacement during the past two ruptures varied significantly from the values for D_{ave} presented above). The minimum constraint on slip-per-event during the past two ruptures from the Barlow Drive site indicates that the second-most-recent (penultimate) earthquake produced at least 0.5 ft of vertical displacement that was accommodated by brittle faulting along fault strand B. Subtracting 0.5 ft from the preferred and absolute maximum D_t results in single event maximums (D_{max}) of 6.7 ft and 9.4 ft, respectively, for the most-recent rupture (Table 11-2). These values for D_{max} are similar to the range of displacements calculated from the global earthquake data set using Approach 2.

In Approach 1, calculation and judgment of the average and maximum values for single event displacement (D_{ave} and D_{max}) provide a strong characterization of epistemic uncertainty in the paleoseismic data. However, because these calculations were performed using a relatively small data set of ruptures (n=2), it is important to also incorporate the aleatoric uncertainty represented by individual rupture characteristics. Analysis by Hecker and Abrahamson (2004) of a composite worldwide data set of slip from historical ruptures indicates that the amount of slip produced by a surface-rupturing earthquake is influenced by variability in slip pattern through time and variability in slip as a function of earthquake magnitude. From this analysis, Hecker and Abrahamson (2004) characterize the uncertainty in the amount of slip related to event-to-event variability as a coefficient of variability of 0.41. Because this coefficient of variation describes the value of one standard deviation divided by the mean, then the application of the best estimate D_{ave} determined from trench observations (3.6 ft) results in a standard deviation of 1.48 ft due to aleatoric uncertainty (i.e., the coefficient of variability). Assuming that the standard deviation due to epistemic uncertainty lies halfway between the best estimate (3.6 ft) and the upper limit (5.0 ft) value of D_{ave}, then combining the epistemic and aleatory uncertainties results in a total sigma (σ_T) of $(1.48^2 + 0.7^2)^{1/2} = 1.6$ ft. Therefore, the upper limit of displacement for expected coseismic rupture at the 97.5 percent confidence interval ($D_{97.5\%}$) is 6.8 ft (Table 2).

In Approach 2, the estimation of expected displacement along the KCF at the Auxiliary Dam considers a range of rupture scenarios and the uncertainties in estimating displacement based on the Wells and Coppersmith (1994) global empirical data set, with additional constraints on aleatoric uncertainty from Wesnousky (2008). The scenario earthquakes considered for this approach are those described in Section 10.4. Table 11-4 presents the rupture scenarios (expressed as rupture source, weight, and surface rupture length) that involve the Lake Isabella section of the Kern Canyon fault. The estimated rupture magnitudes for each source are derived from fault rupture area–magnitude empirical relations developed by Wells and Coppersmith (1994). The range of expected displacements on the KCF from the rupture scenarios shown in Table 11-4 was

Table 1. Approach 1: Epistemic Analysis of Paleoseismic Data (n=2)

	Total Displacement during the Past Two Ruptures D_t	Average Displacement per Rupture $D_t/2$ (D_{ave})	Minimum Displacement per Rupture 0.5 ft	Maximum Displacement per Rupture D_t-0.5 (D_{max})
Best estimate	7.2 ft	3.6 ft	0.5 ft	6.7 ft
Upper limit	9.9 ft	5.0 ft	0.5 ft	9.4 ft

Table 2. Approach 1: Aleatoric Analysis of Paleoseismic Data

Total sigma	Ave per Event	$D_{2.5\%}$	$D_{97.5\%}$
$\square_T$	D_{ave}	D_{ave} - 2*$\square_T$	D_{ave} + 2*$\square_T$
1.6 ft	3.6 ft	0.4 ft	6.8 ft

Table 3. Empirical Approach Using Wells and Coppersmith (1994), SRL-AD Relation

Rupture Source	Weight	SRL	AD	D - 1σ	D + 1σ
Unsegmented	0.05	146 km	9.8 ft	3.7 ft	25.5 ft
SKC+LI+B	0.00	93 km	6.6 ft	2.5 ft	17.2 ft
LI+SKC+NKC	0.15	135 km	9.1 ft	3.5 ft	23.8 ft
SKC+LI	0.30	82 km	5.9 ft	2.3 ft	15.4 ft
LI+B	0.00	45 km	3.5 ft	1.3 ft	9.1 ft
LI	0.45	34 km	2.7 ft	1.0 ft	7.1 ft
Floating	0.05	50 km	3.8 ft	1.5 ft	9.9 ft
Total:	**1.00**	**Weighted average:**	**5.0 ft**	**1.9 ft**	**13.2 ft**

Notes:

Total log(σ) of 0.42 used in the analysis. Total uncertainty combines Wells and Coppersmith (1994) SRL-AD regression uncertainty (0.36) and aleatory variability of rupture about the average (0.21) from Wesnousky (2008).

Wells and Coppersmith (1994) all-slip-types SRL-AD (average displacement) relation has higher correlation coefficient and lower standard deviation than normal-fault relation.

Wells and Coppersmith (1994) all-slip-types SRL-MD (maximum displacement) relation yields comparable numbers to the D + 1σ values above.

Wells and Coppersmith (1994) SRL-AD results comparable to Wesnousky (2008) SRL-AD results.

estimated by using surface rupture length–maximum displacement (SRL-MD) and surface rupture length–average displacement (SRL-AD) relations developed by Wells and Coppersmith (1994) (Table 11-2). The weighted average of these values is 5.0 ft (Table 11-4), which reflects the relative likelihood of the different earthquake scenarios (Table 10-2). Also, the SRL-AD values were modified as follows to account for the likelihood that surface displacement at the site will be either more or less than the average displacement. Where the SRL-AD relation is an estimate of average surface displacement, the standard deviation does not include the variability of surface displacement along the length of the fault rupture; this variability needs to be considered to evaluate displacement at various probabilities of exceedance.

Analysis of along-strike displacement variability for earthquake surface ruptures by Wesnousky (2008) estimated the ratio of the 84th percentile displacement to the median displacement to be 1.41, which is equivalent to a log standard deviation(s) of 0.21 log units. Adding this variability in log(AD) (s = 0.36) and the variability of displacement about the average (s = 0.21) results in a combined standard deviation in the log of displacement (log[D]) of $(0.36^2 + 0.21^2)^{1/2} = 0.42$. Incorporating this standard deviation into the SRL-AD relation of Wells and Coppersmith (1994) yields a value of 13.2 ft for AD plus 1σ.

References

Hecker, S. and Abrahamson, N. A., 2004. Low slip-at-a-point variability: Implications for earthquake-size distribution, fault rupture hazard, and ground-motion modeling: Basin and range seismic hazards summit II, Western States Seismic Policy council, 16-19 May 2004, Program and Abstracts, 21-22.

USACE (U.S. Army Corps of Engineers), 1948. Definite project report: Isabella project, Kern River, California, Part IV, Dams and Appurtenances.

USGS (U.S. Geological Survey), 2009. Geophysical characterization of Isabella Dam: Seismic refraction tomography, DC resistivity, self potential, and electromagnetics. Prepared for U.S. Army Corps of Engineers, Sacramento District, under inter-agency agreement no. W62N6M62694265.

URS (URS Corporation), 2006. Kern Canyon fault assessment study: Technical memorandum, Isabella Dam, Dam Safety Assurance Program, Lake Isabella, CA. Unpublished report prepared for U.S. Army Corps of Engineers, Sacramento, California, 6 p., plus figures.

Wells, D.L., and Coppersmith, K.J., 1994. New empirical relationships among magnitude, rupture length, rupture width, rupture area, and surface displacement. Seismological Society of America Bulletin, 84: 4: 974–1002.

Wesnousky, S.G., 2008. Displacement and Geometrical Characteristics of Earthquake SurfacenRuptures: Issues and Implications for Seismic-Hazard Analysis and the Process ofnEarthquake Rupture. Seismological Society of America Bulletin, 98: 1609-1632

Road Log F-F′

Isabella Auxiliary Dam (Stop 2-2) to Little Lake fault (Stop 2-3)

63.4 miles, 100 minutes

Mileage		Lat./Long.
0.0	**Turn LEFT on Barlow Drive (reset your odometer)**	**35.6440° -118.4738°**
1.4	**Turn LEFT onto Wofford Heights Boulevard**	**35.6298° -118.4798°**
1.6	**Turn LEFT to merge onto CA-178 (toward Ridgecrest)**	**35.6277° -118.4778°**
9.2	After passing around the south margin of Isabella Lake along the north flank of Cooke Peak, the road gains a low saddle and then enters the South Fork Kern River valley. This valley is characterized by coalesced alluvial fans on the south side that are graded to valley level, and steep, incising drainages that descend from the Kern Plateau to the north. Over the next 15 miles we'll pass through three bedrock narrows that cause the valley to step northeast in what resembles an en echelon pattern in map view. It' possible that the geomorphology of this valley is still heavily influenced by topography generated in late Cenozoic time by north-south extension in the "Isabella breakaway zone" between the Kern Plateau and the Scodie Mountains, as described by Maheo et al. (2009). Modern microseismicity indicates east-west extensional strain through this area, implying that the local strain field has shifted significantly since the time this prominent tectonic fabric was generated.	35.6357° -118.3827°
27.8	**Turn LEFT onto Chimney Creek Scenic Byway**	**35.7486° -118.1126°**
32.4	At this turn is an outstanding view of the Scodie Mountains. If we were a smaller group it would be great to stop here for a view of the relict plateau developed on top of the Scodie Mountains (possibly/likely equivalent to the Kern Plateau landscape) and the relict topography of the "Isabella breakaway zone" between these two features. But there's still plenty else to see today.	35.7696° -118.0859°
34.4	Saddle between Canebrake Creek and Chimney Creek drainages. You may have noticed Lamont Peak on your right coming up the hill. At the first impression this looks like very rugged terrain, but the stream profile of Chimney Creek is less steep here than it is a few miles downstream where it descends to South Fork Valley, probably because of a significant degree of	35.7885° -118.0710°

	inherited sinuosity incised into the bedrock channels. This reach of creek may be incising through an intermediate erosional landscape that has not yet adjusted to change in base level (e.g., Clark et al., 2005).	
36.9	**Bear RIGHT at the road junction** We're now in Lamont Meadow, a relatively large expanse of ponded alluvium inset into the Kern Plateau. There is a knickpoint at the mouth of this meadow where Chimney Creek is actively incising, but the stream gradient does not change until several more miles downstream.	**35.8149°** **-118.0539°**
38.7	The road turns to climb out of Lamont Meadow near the head of the valley. About 3 miles further up valley the stream gradient is distinctly lower than in Lamont Meadow, a gradient more representative of the subdued topography of the Kern Plateau.	35.8388° -118.0432°
41.8	By this point you will start to notice that we've passed into a distinctly different landscape that where we've been all w eekend. The hillslopes are relatively subdued, and the weathering profiles exposed in road cuts are deep and imply a degree of landform stability that is absent in the rapidly incising gorges at lower elevations.	35.8614° -118.0193°
42.1	Cresting a saddle here you will have a fleeting view of the peneplain of the Kern Plateau, notable for the numerous flat-topped hills (relatively) that rise to consistent heights of about 8000 ft.	35.8651° -118.0175°
42.5	**Turn RIGHT onto Kennedy Meadows Road (becomes 9 Mile Canyon Road)**	**35.8693°** **-118.0132°**
43.2	At this point we cross over the drainage divide between the San Joaquin Valley and Indian Wells Valley, and begin a (nine-mile) descent down Nine Mile Canyon. If the day is clear you'll have outstanding views of Indian Wells and Searles Valleys.	35.8598° -118.0061°
45.0	Impressive example of debris flow boulder levees)pointing right at you!)	35.8582° -117.9847°
50.0	Valley crossing for the LADWP aqueduct	35.8469° -117.9262°
51.5	Beginning the ninth mile of Nine Mile Canyon. Note the deeply embayed rangefrint and absence of clear fault expression as you cross into the valley.	35.8371° -117.9049°
53.1	**Turn LEFT onto US-395 (northbound)** We'll be following along the basalt exposed in this stream (river?) cut until we reach our next stop, just ahead ten minutes.	**35.8420°** **-117.8753°**

63.3	**Turn LEFT at Little Lake Road**	**35.9314° -117.9077°**
63.4	**Continue 0.1 mile and park along the dirt road**	**35.9322° -117.9095°**

Walk south for ~500 m along the abandoned rail bed, observing tectonic-geomorphic features (e.g., shutter ridges, spring lines, etc.) along the Little Lake fault before climbing an isolated knob of basalt to gain a view of the Little Lake wash. Depending on our time, we will take our discussion to Fossil Falls, **Stop 2-3B** [35.97028/ -117.90802], by driving ~3 miles north to Cinder Rd. and exiting right off of the highway. From there, we will follow the signs to Fossil Falls and park along the dirt access road after turning around at the Fossil Falls trailhead.

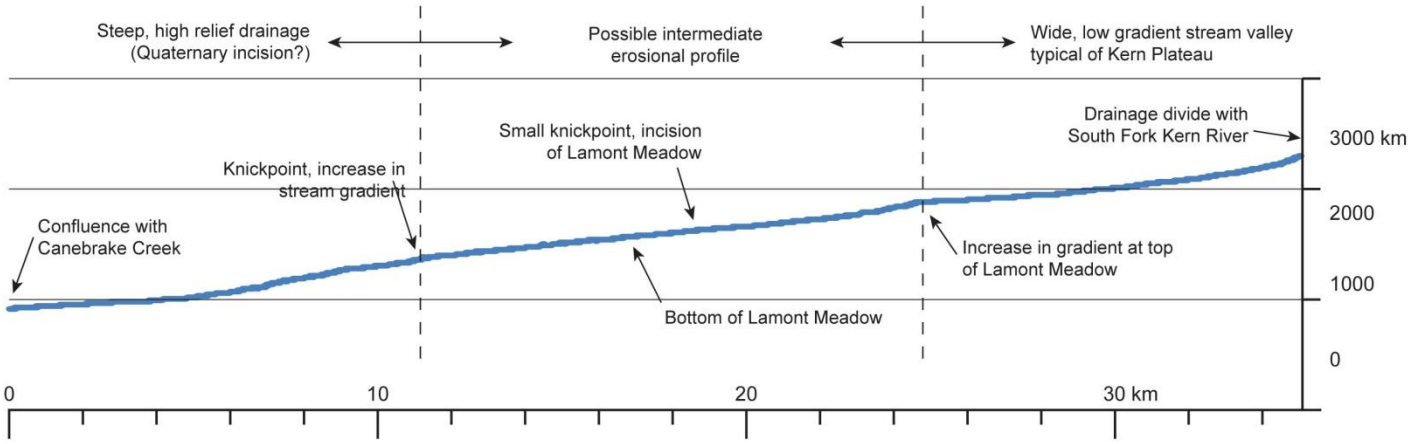

Longitudinal Profile of Chimney Creek. Profile starts at the confluence with the Canebrake Creek. Vertical exaggeration is 15x.

Road Log G-G′

Little Lake fault zone (Stop 2-3) to Black Mat site (optional Stop 2-4)

9.4 miles, 15 minutes

Mileage		Lat./Long.
0.0	**Turn LEFT on US-395 northbound (reset your odometer)**	**35.9316° -117.9080°**
2.9	Turn right here to go to Fossil Falls if you're headed that way, otherwise continue north on US-395.	**35.9772° -117.9229°**
3.8	Red Hill cinder cone on the right.	35.9835° -117.9257°
8.3	**Turn RIGHT on Coso Road. Coso Ranch, tonight's camp, is on the other side of the highway.**	**36.0458° -117.9471°**
9.3	**Arrive at Stop 2-4, park along road.**	**36.0541° -117.9322°**

That's the end of Saturday's road trip. If you need any supplies you can get them at the store here, it's the only place around for miles.

Stop 2-3:

LATE-QUATERNARY TECTONIC, GEOMORPHIC, AND VOLCANIC INTERACTIONS IN THE LITTLE LAKE AREA

Colin Amos, *University of California, Berkeley*

Burch Fisher, *University of California, Santa Barbara*

Dylan Rood, *Lawrence Livermore National Laboratory*

Angela Jayko, *U.S. Geological Survey*

Roland Burgmann, *University of California, Berkeley*

We will visit two locations to discuss active faulting and the history of fluvial downcutting and Quaternary volcanism in the Little Lake area. ***Stop 2-3A*** *will focus on fault slip rates in this portion of the eastern California shear zone. Time permitting, we will then continue on to* ***Stop 2-3B****, where we will explore the Fossil Falls area.*

The dextral Little Lake fault (Figure 1) represents one in a distributed network of active strike slip and normal faults east of the Sierra Nevada in California. Together, this network, termed the eastern California shear zone (ECSZ) or Walker Lane belt, accommodates roughly one quarter of Pacific – North American plate translation (Dokka and Travis, 1990). A curious feature of the ECSZ is the apparent mismatch between interseismic strain measured from GPS (~12 ± 2 mm/yr, Sauber et al., 1994) and summed geologic slip rates spanning the zone, which total ~6 ± 2 mm/yr across south of the Garlock fault (Oskin et al., 2008). Individual structures within this zone, such as the Blackwater fault, also show pronounced rate discrepancies, where interseismic strain measured from radar interferometry (up to ~7 mm/yr, Peltzer et al., 2001) outpaces Quaternary-averaged rates of fault slip (~0.5 mm/yr, Oskin and

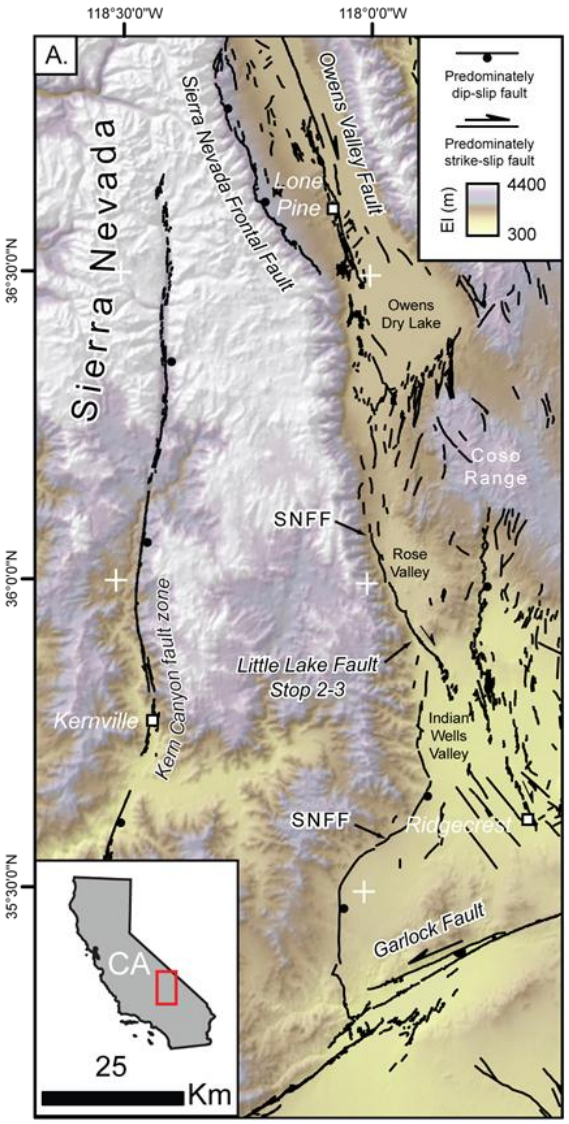

Figure 1. Regional tectonic map of the southeastern Sierra Nevada of California.

Iriondo, 2004). Comparatively little is known about how this dextral shear in the ECSZ is transferred and partitioned onto structures north of the Garlock fault in the Indian Wells and Rose Valley areas (Figure 1). At **Stops 2-3A** and **2-3B**, we will discuss new measurements of displaced Quaternary landforms cut by the Little Lake fault and new constraints on Quaternary fault slip-rates based on ^{10}Be exposure dating that bear on this discrepancy.

The Little Lake fault separates the Coso Range to the east from the Sierra Nevada, where the western edge of the ECSZ impinges upon the southeastern corner of the Sierra Nevada block. As the southern Owens Valley fault terminates to the north, a releasing stepover transfers strain across the Coso Range onto active faults in the Indian Wells Valley (Unruh et al., 2002), including the Little Lake and Airport Lake faults.

Little Lake refers to the small freshwater pond (formerly "Little Owens Lake") now occupying the paleo drainage channel of Pleistocene Owens River, as it coursed southward toward the Indian Wells Valley and China Lake. A former outpost, filling station, and hotel at Little Lake are now gone after being bypassed by Hwy 395 during four-laning in the 1960s. Duffield and Smith (1978) elegantly summarize the history of fluvial downcutting and basaltic volcanism through the Little Lake spillway. They recognize three Quaternary basalt flows in the Little Lake area that interacted with drainage from Owens Lake. Eruption of the youngest of these flows, the basalt of Red Hill, resulted in the creation of Fossil Falls, a series of stepped, dry waterfalls upstream of Little Lake, which we will visit as part of **Stop 2-3B**. We contribute to this story by mapping and characterizing a series of fluvial terraces and deposits within Little Lake wash (Figure 2) that record outburst flooding as a result of this youngest eruption. Recognition that the margins of this landform are cut by the Little Lake fault also provides new slip-rate information for this structure.

Figure 2. View across Little Lake wash where the Little Lake fault intersects a prominent terrace within the paleo-Owens River drainage.

Terrace deposits within Little Lake wash consist of predominately basaltic boulders and roughly 10-20% felsic granitic clasts. The total thickness of this deposit is on the order of several meters, resting unconformably on a subhorizontal strath eroded into the basalt of Red Hill. This

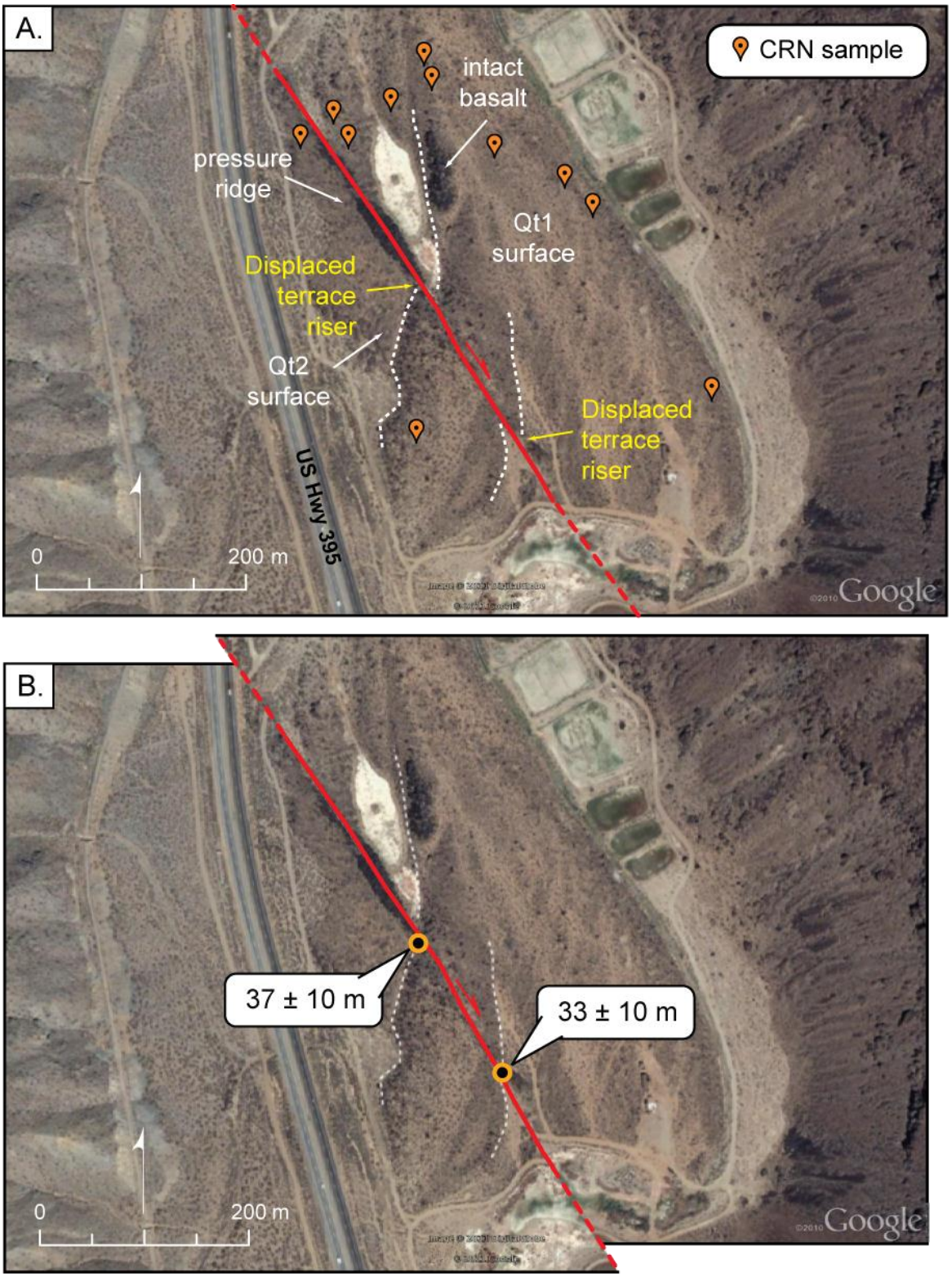

Figure 3. (A) Google Earth image of Little Lake wash highlighting offset of the Qt1/Qt2 terrace riser, as well as the location of ^{10}Be samples collected from meter-scale felsic boulders on these surfaces. (B) Reconstructed offset along the Little Lake fault suggests between ~33 and 37 m of dextral riser displacement based on this image. A nominal uncertainty of 10 m was assigned based on the average riser width.

strath is visible beneath the relatively thin veneer of boulders present on the lower Qt2 surface and also along a prominent pressure ridge formed on the Little Lake fault. The underlying strath is not exposed below the Qt1 terrace. As described in Fisher et al. (in review), these offsets were originally identified and characterized using Google Earth imagery (Figure 3), yielding dextral displacement estimates of ~33-37 m.

Subsequent surveying using terrestrial laser scanning (TLS) yields lateral displacement measurements ranging between 30-42 m (Figure 4), in good agreement with estimations based on Google Earth imagery. This measurement incorporates the maximum and minimum distance range of riser midpoints grouped on either side of the Little Lake fault.

Preliminary results of ^{10}Be exposure dating for felsic boulders on both the Qt1 and Qt2 terrace surfaces indicate a relatively tight cluster of exposure ages centered at ~65 ka (Figure 5). The age distributions for each surface are indistinguishable from one another, suggesting a similar depositional age for each terrace level. One possible explanation for these overlapping ages is that the relatively thin veneer of boulders on the Qt2 surface represents the erode d remnants of the Qt1 terrace deposit, formed during the waning stages of flow during this depositional event. In any case, similarity in ages between these two surfaces provides tight constraints on the dextral slip rate for the Qt1/Qt2 riser. Sampling these age and slip distributions to calculate fault slip rates yields an average rate of 0.6 ± 0.1 mm/yr over the past ~65 ky (Figure 6).

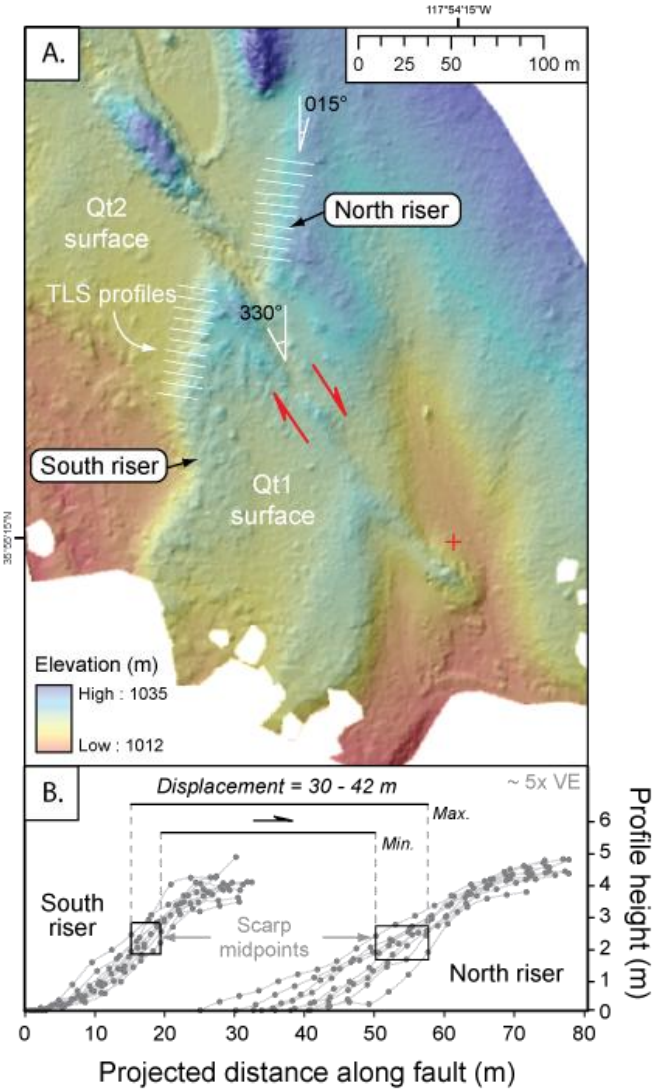

Figure 4. (A) 50-cm digital elevation model derived from terrestrial laser scanning overlain on a hillshade image of the displaced terrace surface in Little Lake wash. (B) Topographic profiles along the western terrace riser used to reconstruct the total dextral offset of this feature. Individual profiles were extracted perpendicular to the average riser orientation (015°), and were then rotated as a group 45° clockwise onto a plane parallel to the local fault strike (330°). Locations for each profile are presented in A.

Similarity between this slip rate and that estimated from offset of the older basalt flows at Little Lake (0.6 mm/yr; Roquemore, 1980) suggest relatively sustained, modest rates of dextral displacement at the 10^4 – 10^5 yr-timescales, clearly outpaced by much shorter-term geodetic estimates of interseismic strain.

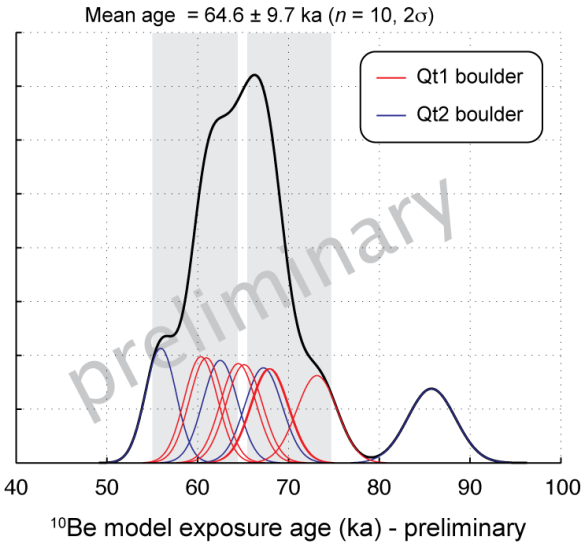

Figure 5. Preliminary surface exposure dating results for boulders sampled on the Qt1 and Qt2 terrace surfaces. A pronounced peak centered at a mean age of 64.6 ± 9.7 ka

Our surface exposure dating results also agree well with ^{3}He exposure dating on the Red Hill basalt from Cerling (1990). Using recalculated production rates and the online exposure-age calculator from from Goehring et al. (2010), this ^{3}He concentration suggests eruption prior to 72.1 ± 4.0 (1σ). Close correlation with our dating results indicates widespread erosion of the Red Hill basalt within the Little Lake spillway at ~65 ka, possibly during a major outburst flood event following breach of the upstream lava dam. Although the youngest recalculated ^{3}He ages from Cerling (1990) suggest younger erosion and scour of the Red Hill basalt at Fossil Falls at ~19 ka, our results suggest that major erosion of the Red Hill basalt, and possibly formation of the falls itself, occurred earlier, likely closely linked in time to disruption of the Owens River drainage by eruption of this lava.

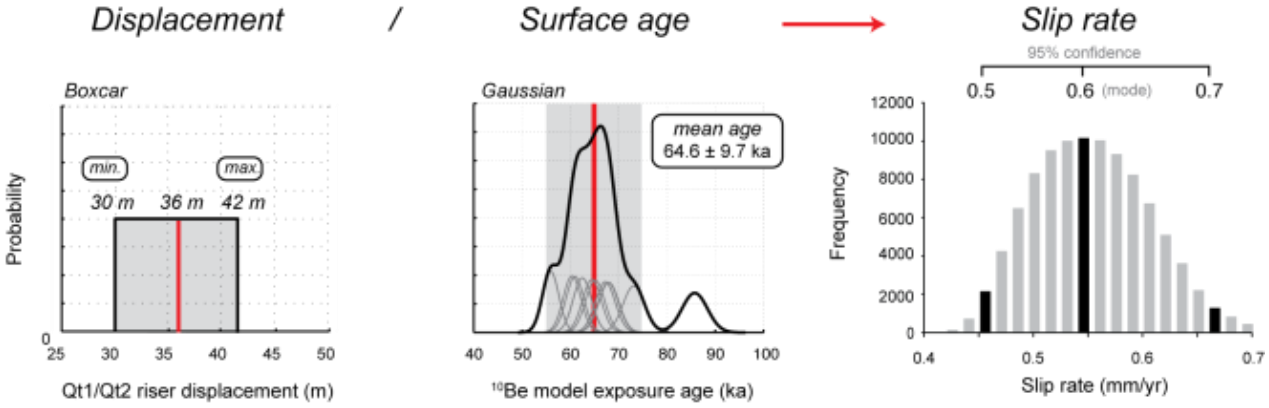

Figure 6. Dextral fault slip rates for the Qt1/Qt2 terrace riser are calculated using a Monte Carlo simulation (100,000 trials) sampling a boxcar distribution of fault slip measured from TLS surveying and a peak age approximated by a normal distribution centered at 64.6 ± 9.7 ka (2□). Reported slip rates (0.6 ± 0.1 mm/yr) represent the mode and associated 95% confidence intervals of the resultant histogram of slip rate values.

References

Cerling, T.E., 1990. Dating geomorphologic surfaces using cosmogenic He-3. Quaternary Res., 33(2), 148-156.

Dokka, R.K., Travis, C.J., 1990. Role of the Eastern California shear zone in accommodating Pacific-North-American plate motion. Geophys. Res. Lett., 17(9), 1323-1326.

Duffield, W.A., Smith, G.I., 1978. Pleistocene history of volcanism and Owens River near Little-Lake, California. Journal of Research of the Us Geological Survey, 6(3), 395-408.

Fisher, G.B., Amos, C.B., Bookhagen, B., Burbank, D.W., Godard, V., in review. Channel widths, landslides, faults, and beyond: The new world order of high-spatial resolution Google Earth imagery. Geomorphology.

Goehring, B.M., Kurz, M.D., Balco, G., Schaefer, J.M., Licciardi, J., Lifton, N., 2010. A reevaluation of in situ cosmogenic (3)He production rates. Quaternary Geochronology, 5(4), 410-418.

Oskin, M., Iriondo, A., 2004. Large-magnitude transient strain accumulation on the Blackwater fault, Eastern California shear zone. Geology, 32(4), 313-316.

Oskin, M., Perg, L., Shelef, E., Strane, M., Gurney, E., Singer, B., Zhang, X., 2008. Elevated shear zone loading rate during an earthquake cluster in eastern California. Geology, 36(6), 507-510.

Roquemore, G., 1980. Structure, tectonics, and stress-field of the Coso-Range, Inyo-County, California. J. Geophys. Res., 85(NB5), 2434-2440.

Sauber, J., Thatcher, W., Solomon, S.C., Lisowski, M., 1994. Geodetic Slip Rate for the Eastern California Shear Zone and the Recurrence Time of Mojave Desert Earthquakes. Nature, 367(6460), 264-266.

Unruh, J.R., Hauksson, E., Monastero, F.C., Twiss, R.J., Lewis, J.C., 2002. Seismotectonics of the Coso Range-Indian Wells Valley region, California: Transtensional deformation along the southeastern margin of the Sierran microplate. In: A.F. Glazner, J.D. Walker, J.M. Bartley (Eds.), Geologic Evolution of the Mojave Desert and Southwestern Basin and Range: Geologial Society of America Memoir, pp. 277-294.

Stop 2-4:

The Rose Valley Black Mat, Salt Wells Spillway and Owens River System, Rose Valley to China Lake

In central Rose Valley, late Pleistocene and early Holocene deposits record the terminal stage of the last glacial-pluvial and onset of Holocene aridity. The section exposed in the quarry **Stop 2-4A** records the last outflow across the Haiwee sill from pluvial Owens Lake, the Younger Dryas climate event and Holocene xerophytic landscape. **Stop 2-4B** highlights ^{14}C *Anadonta* and gastropod shell ages from the Salt Wells sill, China Lake. The shell ages are described in context of previous work on the terminal late Pleistocene Searles Lake highstand by G.I. Smith and others. At **Stop 2-4C** we discuss the regional implications of the fluvial-marsh deposits, disintegration of the paleo Owens River and overflow from the Owens and China Lake spillways. **Stop 2-4D** highlights the emergence of Clovis culture on the early Holocene landscape following deposition of the Rose Valley Black mat.

Stop 2-4a:

Rose Valley Black Mat, Caltrans Quarry Pit

Angela Jayko, *U.S. Geological Survey*

Jack McGeehin, *U.S. Geological Survey*

Jack Meyer, *Far Western Archeology*

Late Pleistocene Owens Lake lowered below the 1145 m LGM spillway at the Haiwee sill (Gale, 1914) forming a closed basin lake by ~14.5-14.75 ka which persists today (Bacon et al., 2006; Orme and Orme, 2008). Flow in the Owens River below the sill also terminated as a consequence of lower discharge. This transition is preserved in a fluvial to marsh transition recorded at the Coso Junction quarry pit, Rose Valley. The site provides a minimum limiting age for termination of Owens River flow from the late Pleistocene glacial Owens Lake to Indian Wells Valley-China Lake to the south (Fig. 1). Black mats, which record the last vestiges of late Pleistocene 'spring-fed' streams and wetlands in now arid valleys of the southern great basin, were dated and explicitly described in the Amargosa and Las Vegas area by Quade et al., 1998 (Fig. 2). The Rose Valley black mat has yielded two bulk sediment ages of 11,400 and 11,365 cal BP on the carbonaceous horizon (black mat) at the top of the fluvial-paludal section (Table 2; ^{14}C ages calibrated using IntCal09, Reimer et al, 2009).

The base of the quarry exposure consists of a well-rounded cobble conglomerate with diverse clast types derived from the Sierra Nevada and Coso Range. This is succeeded by ~3 m of silty sand with abundant fine branching rhizoliths that that form a lace-like network on weathered surfaces. A wetlands assemblage of mollusks including: [1]*Helisoma cf. ammon* (Gould), [2]*Succinea cf. rusticana* (Gould), [3]*Physa cf. humerosa* (Gould), [4]*Fossaria cf modicella (Say)?*, [5]*Gyraulas cf circumstriatus* (Tryon)? or *parvus* (Lea), [6]*Lymnaea cf. stagnicola (Say),*

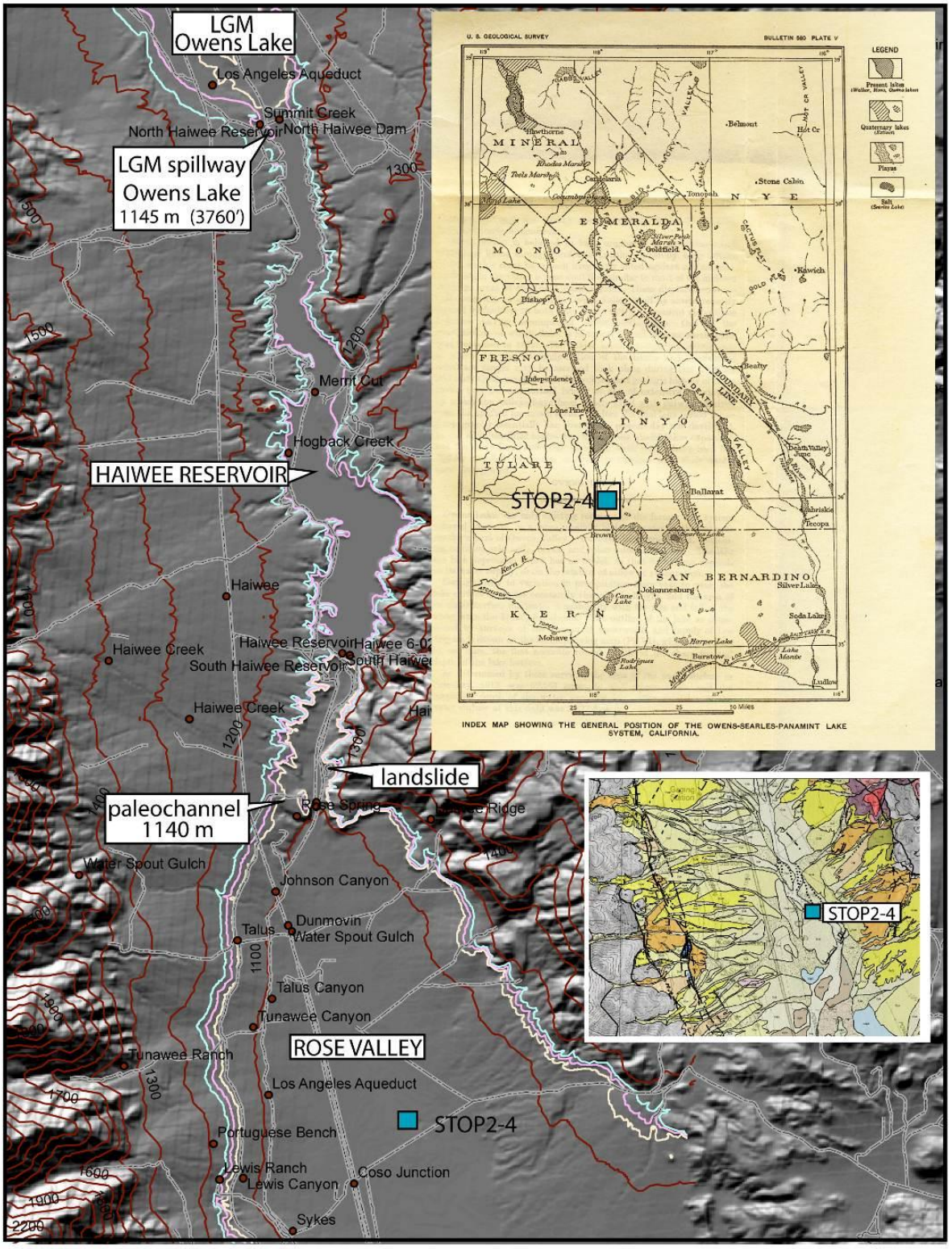

Figure 1. Location of Coso Junction quarry pit, Rose Valley and Stop 2-4

Inset map: Pleistocene Owens River system from Gale, 1914. During LGM (OIS-2) lakes connected between Owens and Panamint V. OIS-6 lakes connected between Lake Russell, Mono basin and Lake Manly, Death Valley.

Lower inset map: Surficial deposits map showing channel and active washes. Quarry pit is located within an old axial channel that runs the length of the valley.

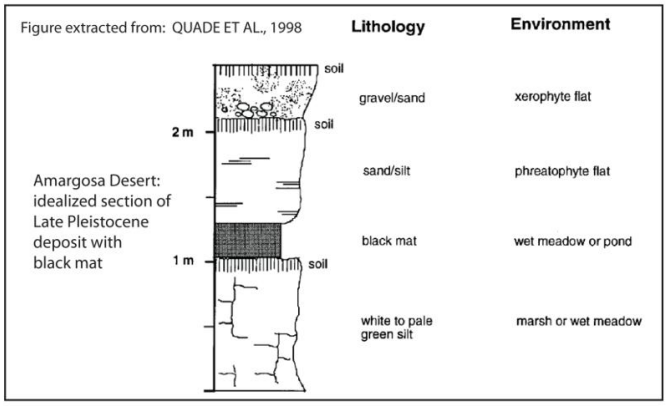

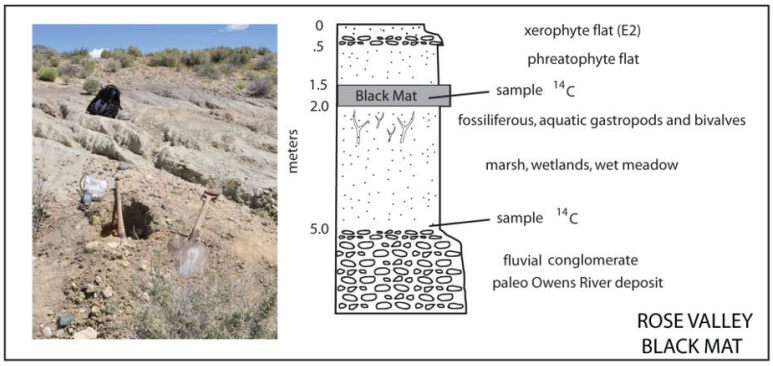

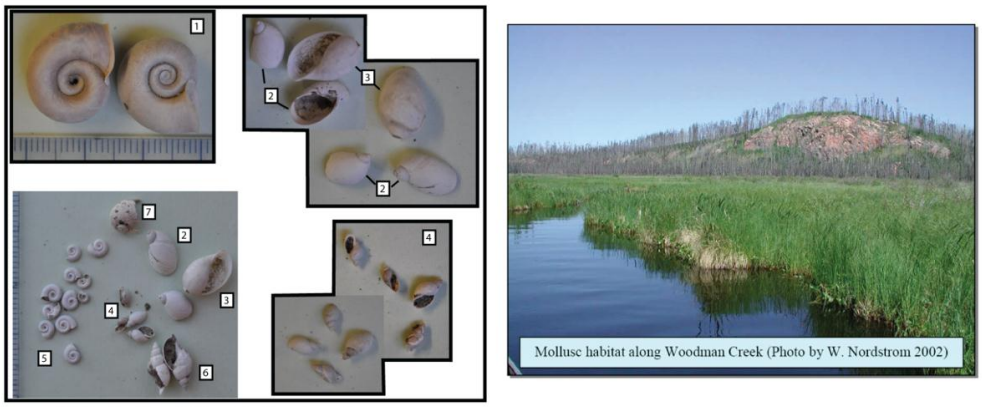

Mollusks, Rose Valley black mat section

Figure 2. (top) Idealized stratigraphic section with a black mat reproduced from Quade et al. (1998).
(center) Generalized stratigraphic section of the Rose Valley black mat at the Coso Junction quarry pit. Photo of the exposure at the quarry pit showing location of 14C samples (Table 1).
(bottom) Photo plate showing mollusks collected from upper part of the silty sand unit under the black mat horizon. Photo on right may resemble the late Pleistocene environment.

[7]*Vorticifex (parapholyx) effusa* (Lea), and *Pisidium, sp* (Fig 2, photos 1-7) were found in the upper part of the silty-sand and below an ~20-40 cm thick, notably dark carbonaceous layer, the black mat. The black mat is overlain by ~1 m of silt which is succeeded by a thin, ~ 0.5 m horizon of poorly sorted alluvial material and upper cap of eolian sand and pebbles.

Physa, Gyraulas and *Lymnae* are found in ponds and marshes associated with submerged and emergent wetlands vegetation (Clark, 1981; Taylor, 1985; Koehler, 1995). *Vorticifex*

(parapholyx) effusa (Lea) is found living today in water bodies from Lake Tahoe northward (Hanna, 1963). At this latitude, modern *Gyraulas circumstriatus* lives at ~1100 m higher elevation than the site and 1600m higher than occurrences in Panamint Valley (Taylor, 1985).

The succession above the fluvial conglomerate correlates with the marsh or wet meadow, wet meadow or pond, phreatophyte flat, and xerophyte/xerophytic flat units of Quade et al., (1998). The conglomerate at the base of the section is interpreted as a paleo Owens River channel. An organic horizon in the lower part of the rhyzolithic and fossil-bearing silt above the conglomerate, ~ 470 cm from the surface was dated as 13,250 ± 50 ka (Meyer et al., 2010). The coarse clast supported, cobble conglomerate at the base of the exposed section is interpreted as a paleo Owens River that was deposited concurrent with overflow at the Haiwee spillway. The 13,250 ± 50 cal BP (Meyer, et al., 2011) on the base of the marsh/wetlands silt-sand deposit provides a proxy for the minimum constraining age of change from open to closed basin conditions in Owens Lake. There are, however several indicators that the Haiwee spillway was inactive earlier, by~ 14.5-15 ka (Bacon et al, 2006) and discussed in **Stops 2-4b** and **2-4c**.

Stop 2-4b:

Anadonta and gastropod ^{14}C ages from the Salt Wells Spillway, China Lake, CA

Angela Jayko, *U.S. Geological Survey*

Jack Meyer, *Far Western Archeology*

Sandy Rogers, *Maturango Museum*

The Salt Wells spillway at 665 m elevation accommodates overflow from China Lake into Searles Lake via Salt Wells Valley. Late Pleistocene fluvial and lacustrine deposits near the spillway formed in response to initiation and termination of overflow from Owens Lake, and to the waxing and waning of the greater Owens River system (Smith, 2009). The Pleistocene highstand of China Lake is constrained by the Searles Lake spillway onto Panamint Valley at 690 m (2264') elevation via the Randsburg Wash spillway. As Searles Lake rose during glacial-pluvial expansions it captured higher elevation lakes and watersheds including China Lake (Gale, 1914; Smith, 2009) until it reached its spillway limited highstand.

This short note provides five new radiocarbon dates on freshwater mussels, *Anodonta sp*. collected in the upper Salt Wells Valley spillway area from the Naval Air Weapons Station, China Lake by Kaldenberg (2006) and a gastropod collected by Meyers et al., 2010. The anadonta locality is described as "in Salt Wells Valley west on the road between CLP [presumably the China Lake Pilot Plant] and the ammunition storage areas [presumably the Main Magazines], near the high-water overflow between the two dry lakes". The exact collection location is unknown, but was probably within a 1-km radius of UTM 447515E/3949727N (NAD83) (Fig 1). Smith (2009) mapped upper Pleistocene lacustrine deposits (units B (24-15 ka) and C (13.5-10.5 ka)), in the area indicated as the sample locality.

Anodonta lives in rivers and fresh water lakes (cf. Firby, 1997), so their occurrence corresponds to a time when China Lake was either spilling into Searles Lake and Searles was a closed basin, or else Searles Lake was higher than the Salt Wells spillway. Five bivalve samples yielded calibrated ^{14}C ages of 14.4 ± 100 to 16.9 ± 70 ka with three ages about 15.0 ka cal yr BP (Table 1).

The gastropod *Helisoma (Carinifex) newberryi* (Manuel Palacios-Fest per. comm.) dated at 13,387 cal yr BP and associated with *Anadonta* occurs in a beach deposit overlying a wave cut bench at 652 m (2140') in Salt Wells Valley, Searles basin providing a minimum limiting age for overflow from Searles Lake via the Randsburg spillway into Panamint Valley (Meyer et al., 2010).

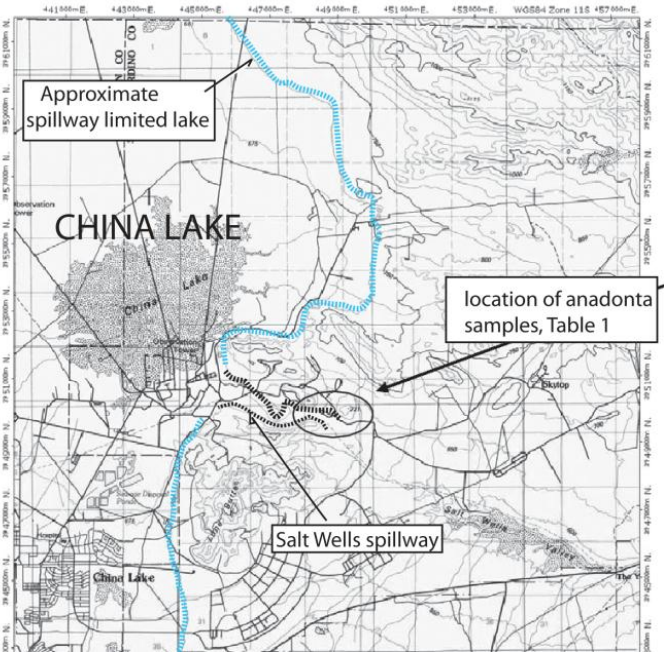

Figure 1. Map showing the location of anadonta sp collected from the Salt Wells spillway, pluvial China

CHINA LAKE OUTLET AGES							
LAB NUMBER	sample description	C14 AGE	error	*delta* 13C	calibrated age	Dated on	source
Beta-280686	gastropod, China Lake outlet	11500	50	-8	13,387	07/13/2010	Meyer et al., 2010
Beta-211384	anadonta, China Lake outlet, Salt Wells Valley	12450	90		15,008	01/18/2006	Kaldenberg, 2006
Beta-211385	anadonta, China Lake outlet, Salt Wells Valley	12480	60		15,150	01/18/2006	Kaldenberg, 2006
Beta-211387	anadonta, China Lake outlet, Salt Wells Valley	12030	100		14,400	01/18/2006	Kaldenberg, 2006
Beta-211388	anadonta, China Lake outlet, Salt Wells Valley	12440	70		15,026	01/18/2006	Kaldenberg, 2006
Beta-211389	anadonta, China Lake outlet, Salt Wells Valley	13800	70		16,877	01/18/2006	Kaldenberg, 2006

Stop 2-4c:

Closed basins and abandoned sills along the late Pleistocene Owens River, CA

Angela Jayko, *U.S. Geological Survey*

Jack Meyer, *Far Western Archeology*

Outflow from the Haiwee sill and open basin conditions in Late Pleistocene Owens Lake can be inferred from downstream deposits in Rose, China-Searles Lake and Panamint Valleys.

Studies of lake levels from several basins in the region including Lake Mojave, Lake Manly in Death Valley, Lake Gale in Panamint Valley and Owens Lake indicate a short period of aridity around 18.5 ka (Benson et al., 1999; Anderson et al., 2003; Wells et al., 200; Bacon et al., 2006; Jayko et al., 2008; Fig 2-4C) and Owens Lake temporarily dropped below its sill (Bacon et al., 2006). This was followed by a pluvial and rising lake levels around 14.5-15.5 ka.

This pluvial was of short duration and lakes receded again around 15.5-15.0 with Owens Lake closing for the last time until present (Bacon et al., 2006). The Owens River fluvial conglomerate exposed in the Rose Valley quarry (Stop 2-4A) is not directly dated. Overflow conditions in basins downstream and discharge volumes required for overflow of Searles Lake into Panamint Valley provide possible constraints.

The late Pleistocene *Anadonta* from the Salt Wells spillway, China Lake indicates overflow into Searles basin, or depending on the shell sample elevation (Table S2-4), integration of Searles Lake with China Lake.

Although ^{14}C dates on lacustrine shell can give maximum ages caused by inherited carbon, the 16.8-14.4 ka ^{14}C dates for a freshwater China Lake at or near its spillway are in good agreement with a spillway limited Searles lake at ~15.5 ka determined from Pleistocene deposits in Searles Valley (Smith et al., 1983, Smith, 2009) and termination of Owens River Flow into Panamint Valley by ~14700-15100 cal BP (Jayko et al., 2008, calibrated using IntCal09). Searles Lake was still large, but ~ 38 m (124')' below its 690 m spillway by 13,387 cal yr BP (Meyer et al., 2010), and ~13 m below the Salt Wells spillway. Other climate proxies from Owens Lake, Panamint Lake, and from the termination of large glaciers in the Sierra Nevada (Clark and Gillespie, Phillips et al.) also indicate transitional conditions and significant melt runoff by 14-15 k

Wetlands and marsh conditions persisted between ~13.4 and 11.5 ka ^{14}C Rose Valley marsh (Fig S2-4C). Similar conditions persisted which until 10,520 ± 140; 10,020 ± 120 ^{14}C yr B.P; (calibrated age ~ 11.5-12.0 ka) at about the same elevation in Panamint Valley where a 'black mat' deposit originally noted by E.L Davis adjacent to Lake Hill. Fossils at the Lake Hill site were described by Taylor (1985).

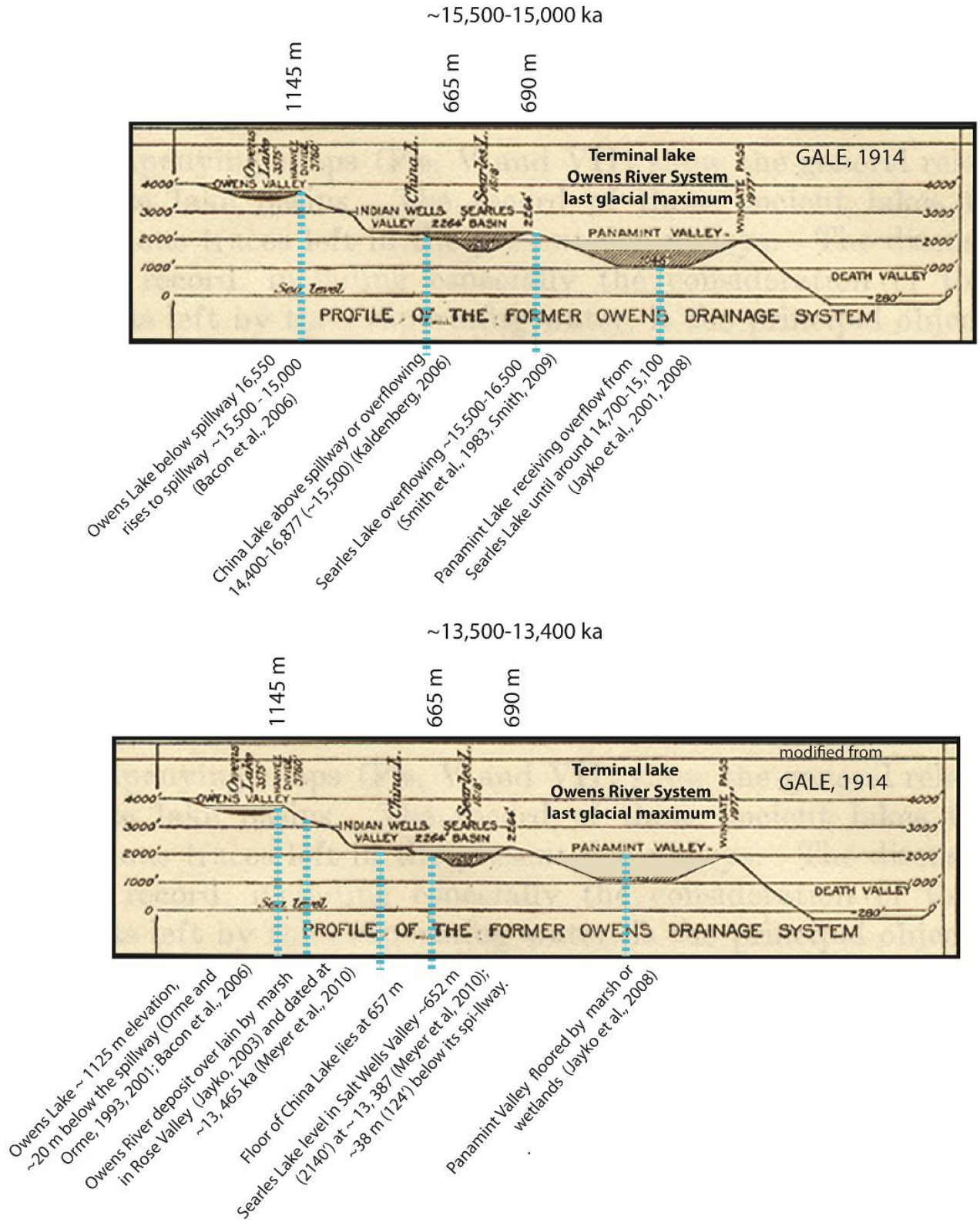

Figure 1. Profile showing the extent of the Owens River system during the last glacial maximum. Panamint Valley is the terminal lake. The headwaters are Adobe and Long Valley. Last time the Owens River was integrated between Mono Lake and Death Valley was during OIS-6.

Stop 2-4d
The Borden Collection and the insights it provides on ancient lifeways in Rose Valley, Eastern California, CA

Sandy Rogers, *Maturango Museum*

Archaeological research has been conducted in the Coso Range in support of geothermal exploitation. Paleo-Indian artifacts have also been reported from the area by avocationalists. One such group, Ferris Borden and colleagues of the ASA, surveyed Rose Valley intensively in the late 1960's. However, after his death his collection vanished until 2008, when it was delivered to the Maturango Museum for cataloging and curation. Only rough cataloging has been completed, but it is clear that it contains one of the largest extant assemblages of Paleo-Indian tools from eastern California. The bulk of the collection seems to come from the disused Caltrans gravel pit just north of the Gill Station Road, and was probably a salvage operation by Borden. This area corresponds to CA-INY-1799. The collection (~3,700 artifacts) is heavily weighted toward the Paleo-Indian period and contains 216 Great Basin Stemmed points, 46 Great Basin Concave-Based points (including 6 fluted points) (Figure 1), and 26 crescents (Figure 2). At least 296 core-based scraping tools are included crescents (Figure 2). The quantity and variety of tools suggest intensive hunting and processing of faunal resources in the area at a time when the area was composed of marshes and lakes. Obsidian hydration rates (c.f. Ambrose and Stevenson, 2004, Stevenson and Scheetz, 1989; Stevenson et al. 1998, 2000; Zhang et al. 1991; Zhang and Behrens 2002; Rogers 2008b) on a sample of the GBCB points (N = 14) average 12,643 $\pm$ 1000 cal BP, and are consistent with a Paleo-Indian age (Figure 3). The hydration dating analysis employs temperature-dependent diffusion theory (Rogers 2007); the specific algorithms are described in Rogers (2011a). Flow-specific hydration rates are used (Rogers, 2011b).

Figure 1. Photo showing representative examples of four Holocene cultures in the Borden collection, oldest at the top and youngest at the bottom. Concave fluted base, top right is considered Clovis.

Figure 2. Middle and Late Holocene tools from the Borden collection.

Chronometrics:
Obsidian Dates

- Hydration rims measured on 14 GBCB/fluted points or point bases
  - 12 Coso obsidian (WSL, WCP, JR, SLM), 2 Fish Springs
  - Ages computed with source-specific rates, temperature corrected for site elevation and burial depth
- Age
  - Mean: 12,643 cal BP
  - Sample standard deviation: ± 1000 yrs

Figure 3. Age of Great Basin concave base and fluted points inferred from thickness of hydration rinds.

References

Ambrose, W. R., and C. M Stevenson, 2004, Obsidian Density, Connate Water, and Hydration Dating. Mediterranean Archaeology and Archaeometry 4(2):5-16.

Anderson, D. E., and Wells, S. G., 2003, Latest Pleistocene lake highstands in Death Valley, California, in Enzel, Y., Wells, S. G., and Lancaster, N., eds., Paleoenvironments and paleohydrology of the Mojave and southern Great Basin Deserts: Geological Society of America Special Paper 368, p. 115-128.

Bacon, S. N., Burke, R. M. Pezzopane, S. K. and Jayko, A. S., 2006, Last Glacial Maximum and Holocene Lake Levels of Owens Lake, Eastern California. Quaternary Science Reviews 25: 1264-1282.

Duffield, W. A., and Bacon, C. R., 1981, Geologic map of the Coso volcanic field and adjacent areas, Inyo County, California: U.S. Geological Survey Miscellaneous Investigations Series, I-1200, 1 plts, 1:50,000 scale.

Firby, J.R., Sharpe, S.E., Whelan, J.E., Smith, G.R., and Spauling, W.G., Paleobiotic and isotopic anlysis of mollusks, fish, and plants from core
OL-92: Indicators for an open or closed lake system: geological Society of American Special Paper 317, p.

121-125.

Gale, H. S., 1914b, Salines in the Owens, Searles, and Panamint Valleys, southeastern California: U. S. Geological Survey Bulletin 580-L, p. 251-323.

Hanna, G.D., 1963, Some Pleistocene and Pliocene freshwater mollusca from California and Oregon: California Academy of Sciences, v 43, 20 p.

Jayko, A.S., surficial deposits of the Darwin Hills 30' x60' Quadrangle, Inyo County, CA: U.S. Geological Survey, scale 1:100,000.

Jayko, A. S., Forester, R. M., Kaufmann, D. S., Phillips, F. M., Yount, J. C., McGeehin, J., Mahan, S. A, 2006, Late Pleistocene lakes, Panamint Valley, California, in Reheis, M.C., Hershler, R., and Miller, D.M., eds., Late Cenozoic Drainage History of the southwestern Great Basin and Lower Colorado River region: Geological Society of America, Special Paper 439, p. 150-184.

Kaldenberg, R. M., 2006, Radiocarbon dates from Anodonta sp., Charcoal, and Haliotis sp. shell found near the overflow between Lake China and Lake Searles, Beta Radioanalytic Lab, Inc., results. NAWS Memorandum to file, dated Jan. 18, 2006. Copy on file, Maturango Museum.

Koehler, P.A., 1995, late Pleistocene Mollusks from the Dolomite Site, owens Lake Playa, California: verliger, v. 38, p. 312-318.

Meyer, J., Rosenthal, BF., Byrd, B.F., and Young, D.C., Constructing a regional historical context for terminal Pleistocene/early Holocene archaeology of the the north –central Mojave Desert: DO legacy Resource management Program, 195 p.

Orme, A.R., and Orme, A.J., 1993, Late Pleistocene oscillations of Lake Owens, eastern California: Geological Society of America Abstracts with Programs v. 25, p. 129-130.

Orme, A.R., and Orme, A.J., 2000, Deformation of late Pleistocene shorelines at Owens Lake, eastern California: tectonic and hydrologic implication: Geological Society of America Abstracts with Programs v. 32, p. A333.

Orme A.J., and Orme, A.R., 2008, late Pleistocene climate and tectonic impacts on Owens Lake levels and linkages, in Reheis, M.C., Hershler, R., and Miller, D.M., eds., Late Cenozoic Drainage History of the southwestern Great Basin and Lower Colorado River region: Geological Society of America, Special Paper 439, p. 207-225.

Quade, J., Forester, R.M., Pratt, W.L., and Carter, C., 1998, Black mats, spring fed-streams and late-glacial age recharge in the southern Great Basin: Quaternary Research, v. 49, p. 129-148.

Rogers, A.K., 2007, Effective Hydration Temperature of Obsidian: A Diffusion-Theory Analysis of Time-Dependent Hydration Rates. Journal of Archaeological Science 34:656-665.

Rogers, A.K., 2009, Anodonta, sp. Shell ages from Salt Wells valley, naval Air Weapons station, China Lake: Working Manuscript MS 62, Maturango Museum, 5p.

Rogers, A.K., 2011a, Chronological Analysis by Obsidian Hydration Dating (OHD): Theory and Algorithms. Maturango Museum Working Manuscript MS70, Rev D, Dated 22 March 2011. Maturango Museum, Ridgecrest.

Rogers, A.K., 2011b, Flow-Specific Hydration Rates for Coso Obsidian: An Analytical Study. Maturango Museum Working Manuscript MS82, Rev B, Dated 20 March 2011. Maturango Museum, Ridgecrest. Smith, G.I., 2009, Late Cenozoic geology and lacustrine history of Searles Valley, Inyo and San Bernadino Counties, CA: U.S. Geological Survey Professional Paper 1727, 115p.

Stevenson, Christopher M., E. Knauss, J. J. Mazer, and J. K. Bates, 1993, The Homogeneity of Water Content in Obsidian from the Coso Volcanic Field: Implications for Obsidian Hydration Dating. Geoarchaeology 8(5):371-384.

Stevenson, Christopher M., J. J. Mazer, and B. E. Scheetz, 1998, Laboratory Obsidian Hydration Rates: Theory, Method, and Application. In: Archaeological Obsidian Studies: Method and Theory. Advances in Archaeological and Museum Science, Vol. 3, M. S. Shackley, ed., pp.181-204. New York: Plenum Press.

Stevenson, C.M., Gottesman, M, and Macko, M., 2000, Redefining the Working Assumptions for Obsidian Hydration Dating.: Journal of California and Great Basin Anthropology 22(2):223-236.

Stevenson, C.M., and Scheetz, B.E. , 1989, Induced Hydration Rate Development of Obsidians from the Coso Volcanic Field: A Comparison of Experimental Procedures. In: Current Directions in California Obsidian Studies, R. E. Hughes, ed., pp. 23-30. Contributions of the University of California Archaeological Research Facility No. 48. Berkeley: University of California.

Taylor, D.W., 1985, Evolution of freshwater drainages and molluscs in western North America: in Smiley C.J., eds., Late Cenozoic history of the Pacific northwest, California Academy of Sciences, p. 265-321.

Taylor, D.W., 1986, Fossil molluscs from the Lake Hill archeological site, Panamint valley, southern California: Contributions of the Great Basin Foundation Number 2, p.42-54.

Wells, S.G., Brown, W. J., Enzel, Y., Anderson, R. Y., and McFadden, L. D., 2003, Late Quaternary geology and paleohydrology of pluvial Lake Mojave, Southern California *in* Enzel, Y., Wells, S. G., and Lancaster, N., eds, Paleoenvironments and paleohydrology of the Mojave and southern Great Basin Deserts: Geological Society of America Special Paper 368, p. 79-114.

Zhang, Y., Stolper, E.M. and G.J. Wasserburg, 1991, Diffusion of Water in Rhyolytic Glasses. Geochimica et Cosmochimica Acta 55:441-456.

Zhang, Y, and Behrens, H., 2000, H_2O Diffusion in Rhyolitic Melts and Glasses. Chemical Geology v. 169, p.243-262 .

Road Log H-H′

Saturday night camp to Owens Lake (Stop 3-1)

20.5 miles, 25 minutes

Mileage		Lat./Long.
0.0	**Turn LEFT on US-395 northbound (reset your odometer)** As you drive north from camp you can see a discontinuous series of compound scarps developed in older alluvial fan deposits. These scarps are commonly delineated by the trees that grow around fault-line springs.	**36.0456°** **-117.9481°**
11.6	On the left just past Sage Flats Road is the Sage Flat paleoseismic site, trenched by Amos and Lutz in 2010 who found evidence for two late Pleistocene surface rupturing earthquakes but no evidence of rupture during the 1872 Owens Valley earthquake.	**36.2098°** **-117.9793°**
16.8	**Turn RIGHT in Olancha onto CA-190.**	**36.2822°** **-118.0061°**
20.5	**Continue for 3. 7 miles and park along the right shoulder of the highway.**	**36.3194°- -117.9633°**

Stop 3-1a:

Historic shorelines and the 1872 Owens Valley earthquake: A rupture segment east of Dirty Socks Spring

Angela Jayko, *U.S. Geological Survey*

Burt Slemmons, *University of Nevada, Reno*

Eutizio Vitorri, *Italian Agency for Environmental Hazards*

Gary Carver, *Humboldt State Univ., Emeritus*

We were hoping Burt Slemmons, emeritus UNR could make it for this morning's stop. Burt recognized the significance ofthe surface rupture exposed at the 'Dirty Socks Spring' site (Slemmons p. 52 in Hill, 1972; Slemmons et al., 2008), mentored Carver and Vittori, and continues efforts to understand the fault segment in relation to historical data and new lidar elevation models. This stop is divided into two parts: **STOP 3-1A** *summarizes evidence for dextral strike-slip faulting north of HWY 190 based on offset of late Holocene to historic beach deposits (Vitorri et al., 1993).* **STOP 3-1B** *makes a traverse across offset mid-early Holocene beach and lacustrine deposits south of the HWY 190 where a late Holocene channel is beheaded along the Owens Valley fault and where spectacular colonial tufa rosettes are well preserved on wave cut late Pleistocene and early Holocene benches.*

The 1872 earthquake ruptured at least ~87 km with an estimated magnitude **M**7.5-7.7 (Ellsworth, 1990; Beanland and Clark, 1994) or ~**M**7.4-7.5 (Bakun, 2006) using a point source model. The Bartlett Springs to Dirty Socks Spring segment adds an additional ~26 km for a potential ~113 km rupture length (Vittori et al., 1993; Slemmons et al., 2008; **Figure 1**).

Establishing the location and elevation of historic shorelines is of fundamental importance for interpreting the recency of offset berms north of HWY 190 and therefore potential 1872 surface rupture south of the Owens Dry Lake. The 3597' (1096.3 m) elevation of the 1872 shoreline was surveyed by Mulholland, and in following years by the Los Angeles Water Commission (Gale, 1914). The 1872 shoreline was the highest historic level measured and 30' (9.1 m) higher than 1913 levels following agricultural development in Owens Valley (tabulated in Gale, 1914; **Figure 2)**. The lake elevation was reported as 1095 m in a report prepared for the city of Los Angeles (Lee, 1915) and fluctuated between 1090 m and 1087 m prior to 1913 (Gale, 1914; Lee, 1906, 1912, 1915).

The Carthage Wharf site (Gale, 1914) south of Cartago, which was used for steamboat shipping in the 1870's (Chalfant, 1921) lies at about 1095 to 1096 m elevation based on modern DEM's and topographic maps. The Swansea wharf, originally 106 m long, was left emergent following the 1872 seismic event (Hobbs, 1910; Chalfant, 1921; Beanland and Clark, 1994). An additional 46 meters of wharf was built following the 1872 earthquake (Chalfant, 1921). Based on historic maps, the wharf was at about 1093 m on its west side and 1096 m on its east side, consistent with ~3 m drop in shoreline elevation reported by Gale (1914).). The lake dried forming the present playa surface after diversion of the Owens River water via the Los Angeles aqueduct in the early 1900's. **Figure 3** shows the 1913 shoreline and a 'historic' shoreline mapped by the Los Angeles Water Commission georeferenced using mile section corners and Earthscope lidar data. Note that the mapped historic shoreline terminates at the projected trace of the southern Owens Valley fault.

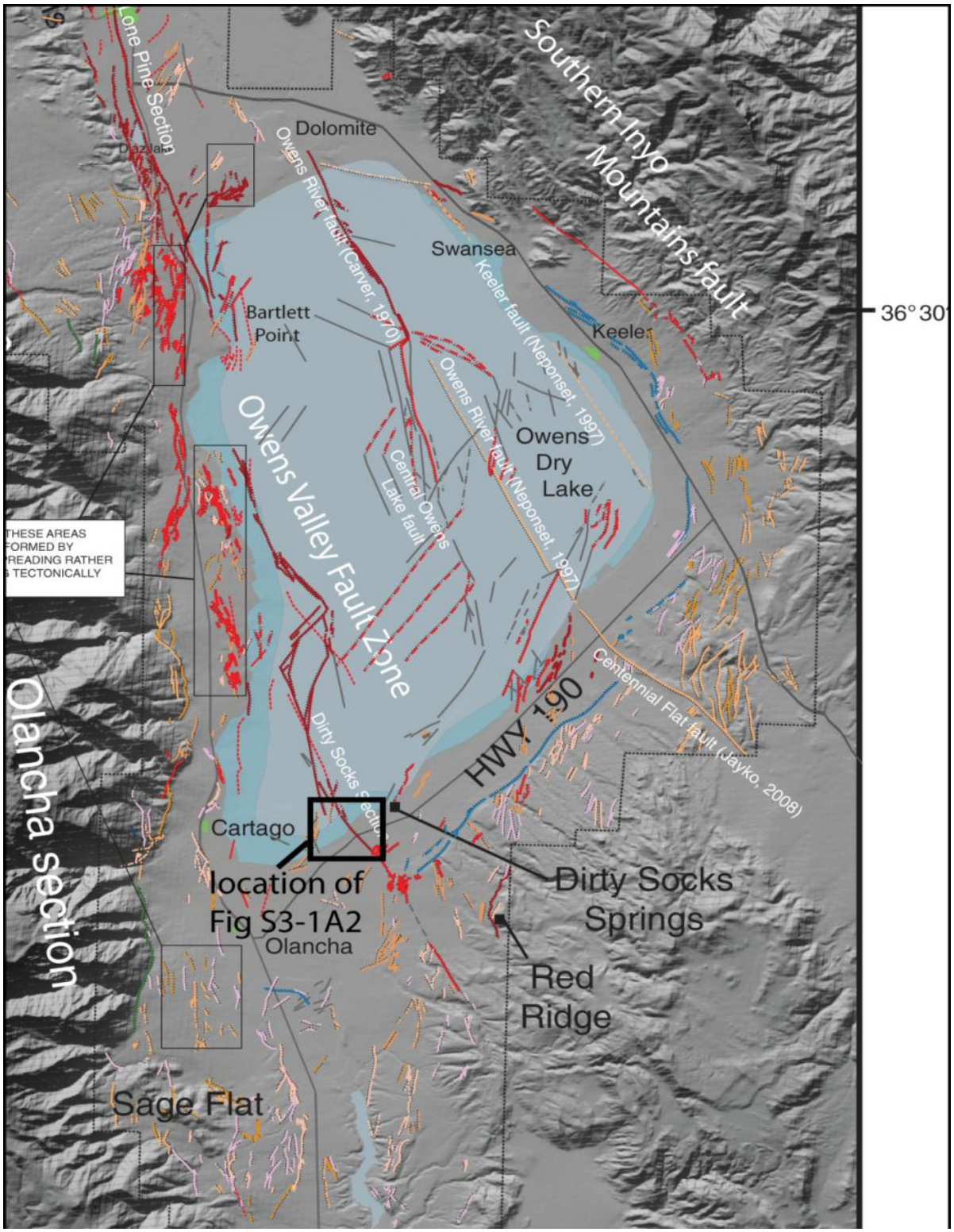

Figure 1. Southern part of the Quaternary Fault and Lineament map Owens Valley, Slemmons et al., (2008) with location of Figures 2 through 4 highlighted. There is a strong geomorphic lineament south of the mapped traced where the fault continues into the Cactus Flat area and apparently links to a transtensive mountain graben within the Coso Range (Jayko, 2009).

Figure 2. Los Angeles water commission map of 1913 shoreline and 'historic' shoreline georeferences with Stinson (1977) Keeler 15' Quadrangle.

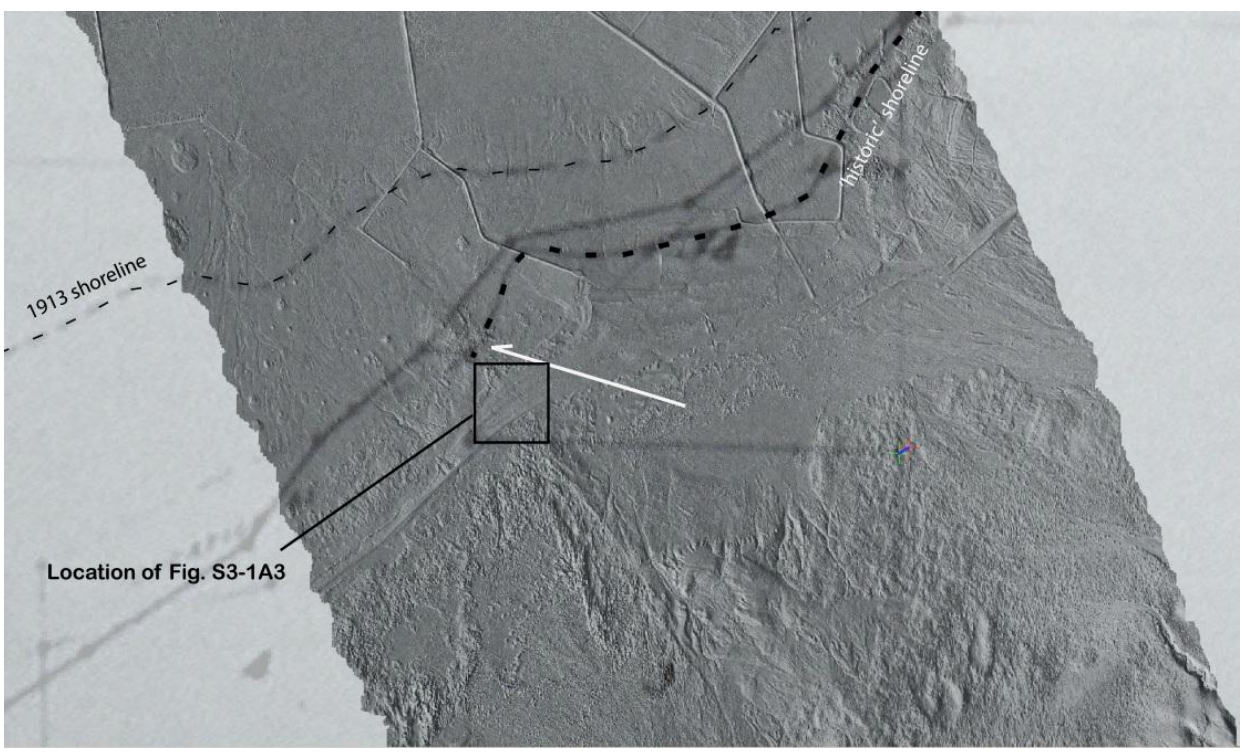

Figure 3. Los Angeles Water Commission map showing 1913 shoreline-dashed and historic shoreline solid (highlighted with heavy dash), survey line (with points) and mile sections overlain on earthscope lidar data. Note that the historic shoreline terminates at the projected trace of the southern Owens Valley fault.

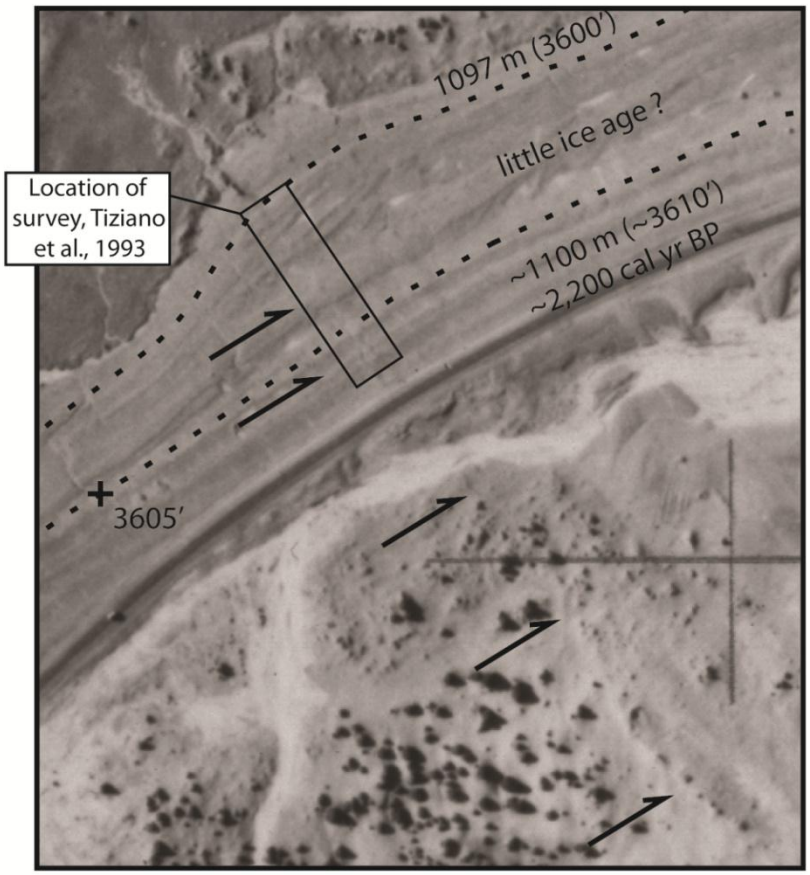

Figure 4. 1967 low sun-angle photo of late Holocene and historic shorelines west of Dirty Socks spring, southern Owens Valley. Arrows show location of 1872 (?) fault scarp north of HWY 190. Box shows location of survey (Vittori et al., 1993). As mapped, the 1913 version of the historic shoreline is north of the 3600'contour (1097 m) on the Vermillion Canyon 7.5' quadrangle.

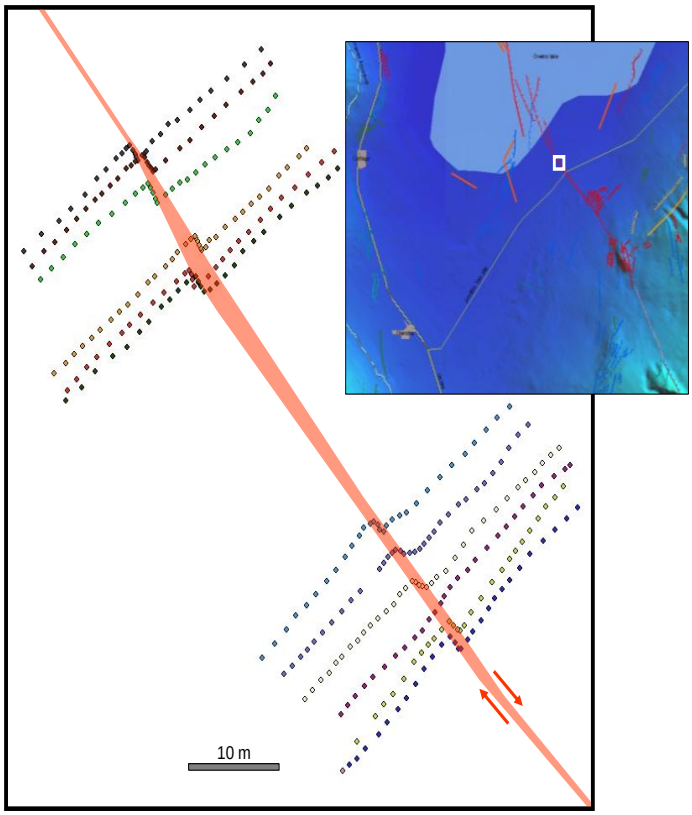

Figure 5. Beach berm crest and inflections, surveyed by Vittori et al., (1993) reproduced from Slemmons et al. (2008). Southern profile lines are probably the ~1101 m (~3610') shorelines ~2200 cal yr BP (Beanland and Clark, 1994, compiled in Bacon et al., 2006). Northern profile lines are probably little ice age to historic.

Stop 3-1b:

Late Pleistocene lake deposits and the 1872 rupture south of HWY 190

Angela Jayko, *U.S. Geological Survey*

Eutizio Vitorri, *Italian Agency for Environmental Hazards*

Burt Slemmons, *University of Nevada, Reno*

South of HWY 190, the Dirty Socks segment of the Owens Valley fault clearly cuts terminal Pleistocene and early Holocene lake deposits between 1097 m and 1180 m elevation. The lacustrine features offset along the fault scarp are dated by correlation with recessional and highstand glacial-pluvial events summarized in Bacon et al., 2006 and highlighted below. There is also one ^{14}C from the locality (Figure 1) although ten additional samples collected from berms and lake deposits have been submitted 03/2011 for AMS dating.

During the early Holocene (~11,500 to 10,500 y.b.p) the shoreline of Owens Lake rose to about 1110 to 1120 m elevation following a brief, very late Pleistocene dry period (Bacon et al., 2006). The shoreline remained between about 1120 and 1125 m elevation until about 7,600 cal yr BP. The Altithermal, a warming event between about 7,500 and 4,300 y.b.p. caused alpine glaciers to recede, alpine tree line to rise and lake levels fall (cf. Davis, 1999; Doerner and Carrara, 2001; Benson et al., 2002). Maximum aridity occurred after deposition of the Mazama Ash at 6730 ^{14}C yr B.P. (Doerner and Carrara, 2001). The Owens Lake was mainly desiccated and either receded to lower elevations than the historic lake stand or dried (Benson et al., 1997; 2002; Smith et al., 1997). A late Holocene highstand at ~ 3600 ka produced a distinctive shoreline at ~1108 m elev.

Figure 1 shows the location of sample GPS 021-04 with the corrected ^{14}C cal yr BP age of ~12,800 (Intcal09, Reimer et al., 2009) on *Anadonta sp*. shell. Sites in the photos below are from north of the 1108 shoreline and dirt road in the air photo image. Several shallow exposures show the fault trace at the surface with dune sand juxtaposed against lake deposits. Figure 1 through 4 show field and shallow pit exposures of the Dirty Socks segment, Owens Valley fault. Figure 2 shows generalized map of surficial deposits on earthscope lidar base.

WW	SAMPLE ID	MATERIAL	REGION	$\delta^{13}C$	^{14}C AGE	±	DATED ON
WW5220	**GPS 021-04**	shells	Owens V.	0	10,710	40	03/30/05

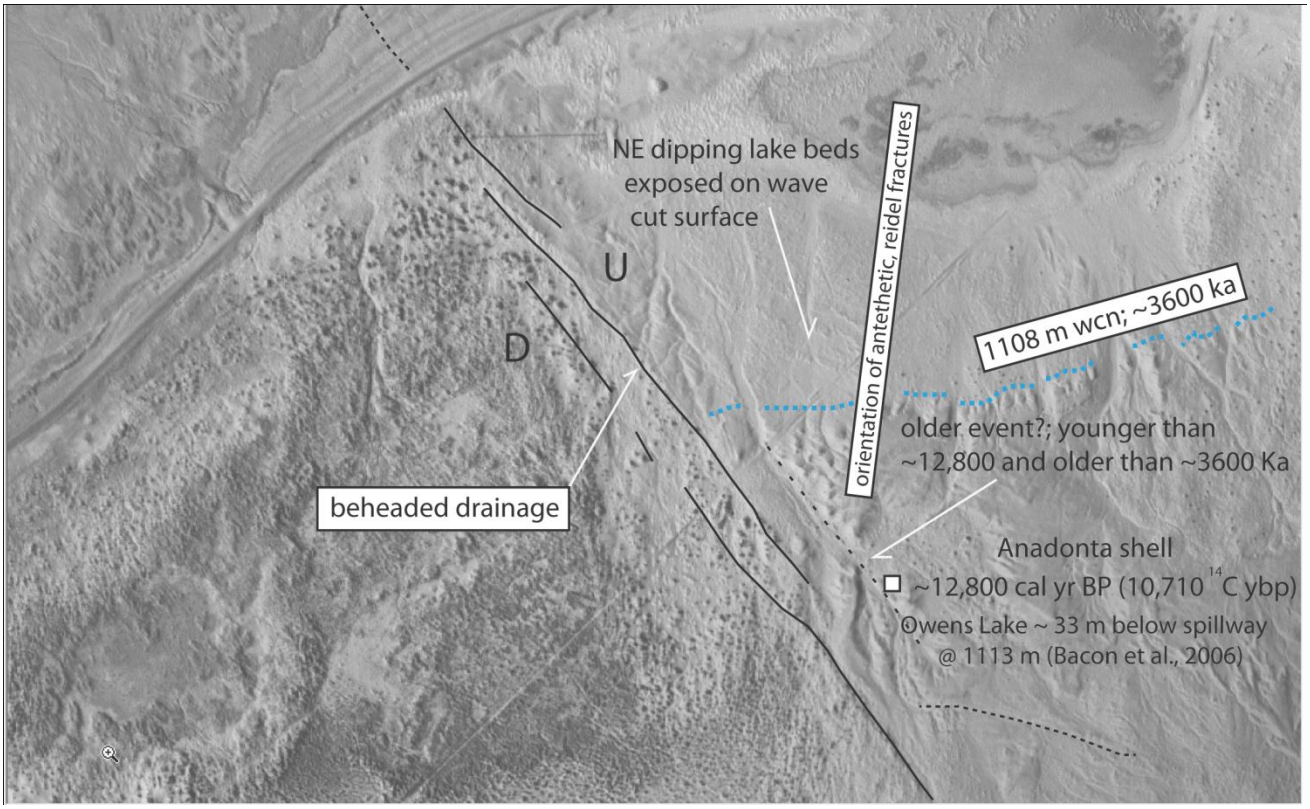

Figure 1. 1:12,000 scale low sun angle air photo over lain on earthscope lidar data. Image shows the southern rupture between the historic strandline of Owens Lake and early Holocene nearshore and beach deposits. North to the top. Sites in **Figures 2 and 3** are located north of the beheaded drainage and west of the 'U'. The 1108 m shoreline-dashed blue- (~3600 ka) makes a wavecut notch into older lake deposits. We'll park south of the highway and look at the beheaded channel, cut by the Dirty Socks segment of the Owens Valley fault which ruptured in 1872. There are also deformed and tilted lake deposits exposed on the 1108 m wavecut platform east of the fault which show evidence for long term deformation along the fault segment. We'll walk south across the 1108 m wavecut notch an up onto early Holocene and late Pleistocene shallow nearshore and beach deposits. These deposits sit a couple meters higher than the surface west of the fault and likely record offset from an earlier event along the fault trace. For those interested we can also traverse south across the 1145 m lacustrine abrasion surface, the 1160 m shoreline and across the deformed 1180 m shoreline on the pop-up. South of the pop-up, delta foresets deposited at the 1160 m shoreline are exposed in a wash cut. However the fault is not obvious in wash cuts or geomorphology south of the pop-up until you reach the northern Coso Range.

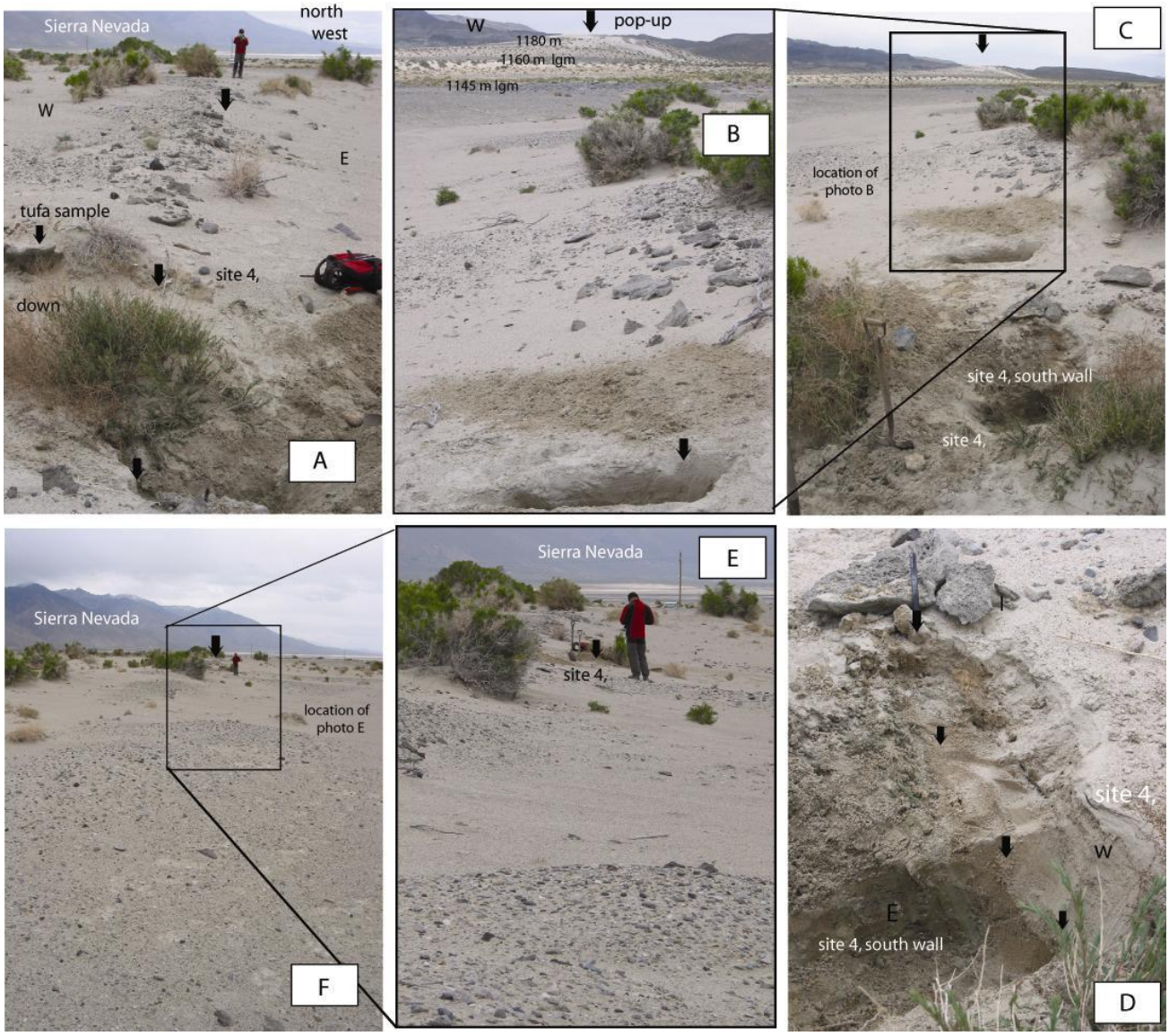

Figure 2. Photo A – view looking north along the Dirty Socks segment of the historic, 1872 rupture south of Highway 190. Photo B- view looking south along the fault scarp towards the dune-capped pressure ridge which deforms the 1180 OIS-6 and 1160 m OIS-2 shorelines. Arrow at base of photo B shows location of pit 2 (site 4). Photo C shows an expanded view to the south with site 4 more clearly visible. Photo D shows view of south wall of site 4 with fault trace delineated by clay gouge separating green-olive lake deposits from eolian deposits in shallow pit and surface of fault exposed towards the south. Photo E shows location of site 4; view looking towards the north. Pole along road in the background of the photo. Photo F shows distal view of site 4 looking towards the north. Dark arrow pointing down show location of site 4 pit.

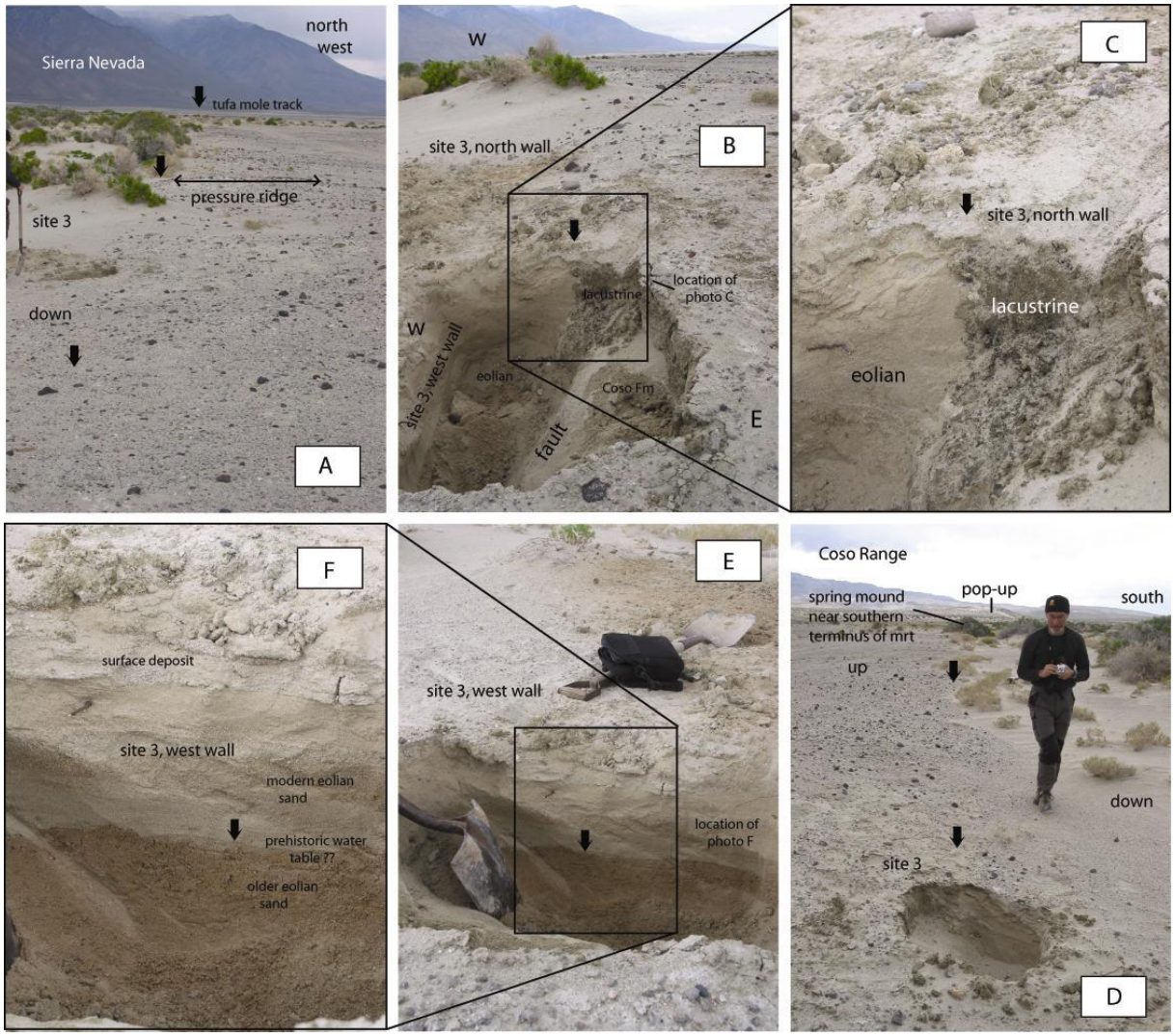

Figure 3. Photo A - view looking north along fault trace rupture (Heavy arrows pointing down at fault), note shovel located at site 3 pit shown in photo B. There appears to be a subtle mole track or pressure ridge along the fault trace. Photos B and C show the fault exposed in a shallow pit at site 3; photos B & C looking towards the north. Photo D site 3 pit, view looking towards the south. Note the pop-up (large pressure ridge to the south). Photos E and F of deposits on the west side of the fault in pit at site 3.

Figure 4. Photo looking south of HWY 190 towards the pop-up and Owens Valley fault (reproduced from Slemmons et al., 2008)

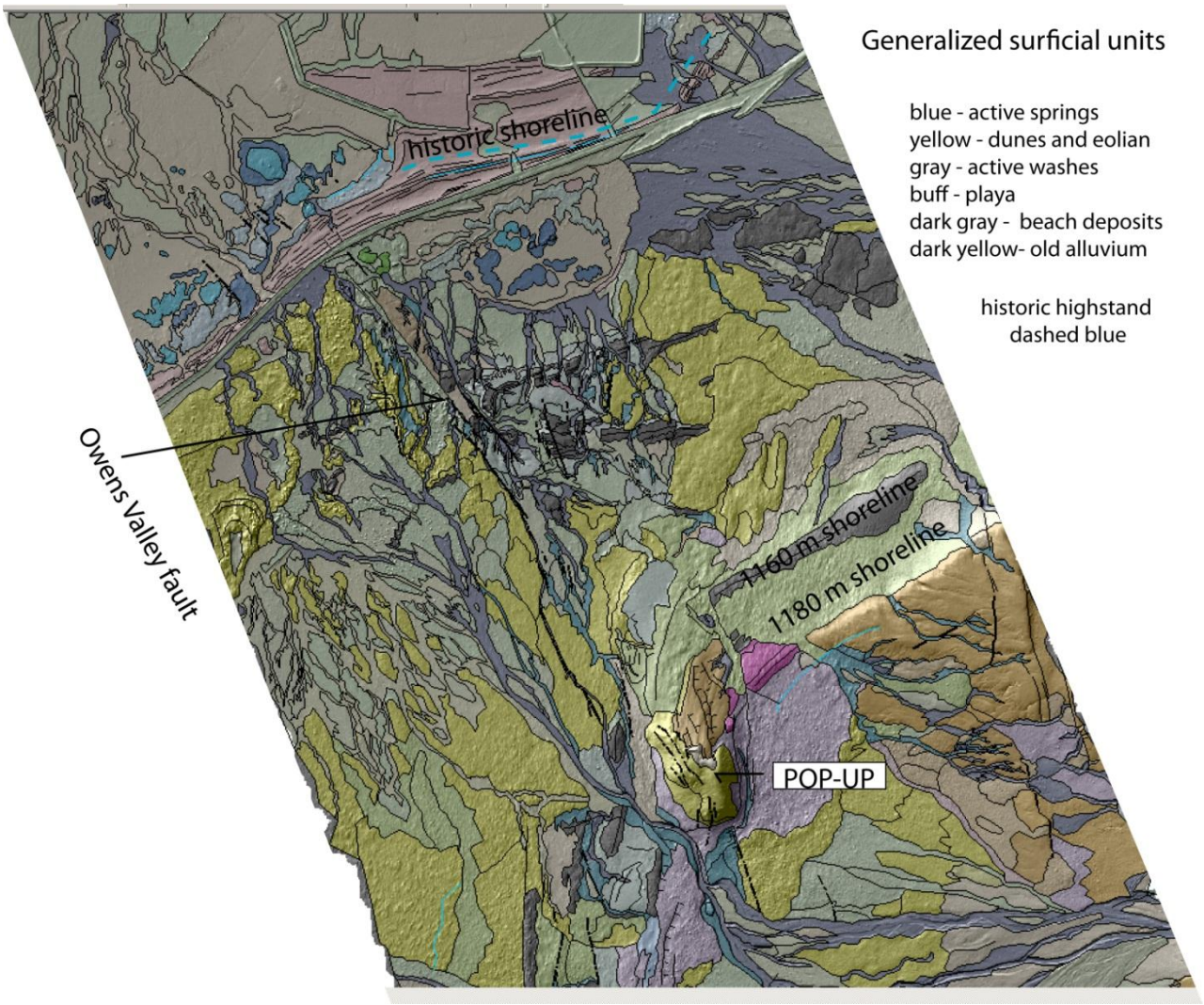

Figure 5. Preliminary map of late Pleistocene and Holocene surficial deposits on earthscope lidar base. Main units shown in legend.

References (Stops 3-1 a and 3-1b)

Bacon, S. N., Burke, R. M. Pezzopane, S. K. and Jayko, A. S., 2006, Last Glacial Maximum and Holocene Lake Levels of Owens Lake, Eastern California. Quaternary Science Reviews 25: 1264-1282.

Bakun, 2006, MMI attenuation and historical earthquakes in the basin and range province of western North America : Seismological Society of America, v. 96, p. 2206-2220.

Beanland, S. and M. M. Clark,1994, The Owens Valley fault zone, eastern California, and surface rupture associated with the 1872 earthquake, U.S. Geological Survey Bulletin1982, 29 p.

Benson, L.V., Kashgarian, M., Rye R., Lund, S.P., Smoot, J.P., Kester, C., Mensing, S., Meko, D., and Lindstrom, S., 2002, Holocene multidecadal and multicentennial droughts affecting northern California and Nevada: Quaternary Science Review, v. 21, p. 659-682.

Carver, G. A., 1970, Quaternary tectonism and surface faulting in Owens Lake basin, California: Reno, University of Nevada, Mackay School of Mines Technical Report AT2, 103 p.

Davis, O.K., 1999, Pollen analysis of Tulare Lake, California: Great Basin-like vegetation in central California during the full-glacial and early Holocene: Review of Palaeobotony and Palynology, v. 107, p. 249-257.

Doerner, J.P. and Carrara, P.E., 2001, Late Quaternary vegetation and climate history, Long Valley area, west-central Idaho, USA: Quaternary Research, v. 56, p. 103-111.

Gale, H. S., 1914, Salines in the Owens, Searles, and Panamint Valleys, southeastern California: U. S. Geological Survey Bulletin 580-L, p. 251-323.

Hill, M. R., 1972, A centennial- The great Owens Valley earthquake of 1872: California Geology, v. 25, p. 51-54.

Hobbs, W. H., 1910, The earthquake of 1872 in Owens Valley, California: Beitr. Geophysics., v. 10, p. 352-385.

Hough, S. and Hutton, K., 2008, Revisiting the 1872 Owens Valley, California earthquake: Bulletin Seismological Society of America, v. 98, p. 931-949.

Jayko, A.S., Surficial deposits of the Darwin Hills 30' x60' Quadrangle, Inyo County, CA: U.S. Geological Survey, scale 1:100,000.

Lee, C.H., 1912, An Intensive study of the water resources of a part of the Owens Valley, California: U. S Geological Survey Water Supply Paper 294, 135 pp.

Lee, C.H., 1915, Report on hydrology of Owens Lake Basin and natural soda industry as affected by the Los Angeles Aqueduct Diversion: Unpublished supplement to the 'Final Report of Los Angeles Aqueduct Water Supply Investigations to Owens Valley' submitted by Lee, C.H., to William Mulholland, chief engineer, Los Angeles Aqueduct, June 10, 1911.

Lee, W.T., 1906, Geology and Water Resources of Owens Valley: U. S Geological Survey Water Supply Paper 181, p. 28 pp.

Reimer et al., 2009, Intcal09 and Marine09 radiocarbon age calibration curves, 0-50,000 years cal BP: Radiocarbon, v. 51, p. 1111-1150.

Slemmons, D.B, Vittori, E., Jayko, A.S., Carver, G.A., and Bacon, S.N., 2008, Quaternary Fault and Lineament Map of Owens Valley, Inyo County, Eastern California: Geological Society of America Map and Chart Series 96, 25 pp. 2 sheets, scale:1:100,000.

Stinson, M. C., 1977, Geologic map and sections of the Keeler 15' Quadrangle, Inyo County, California: California Division of Mines and Geology, Map Sheet 38, scale 1:62,500.

Vittori, E., Michette, A. M., Slemmons, D. B., and Carver, G., 1993, Style of recent surface deformation at the south end of the Owens Valley fault zone, eastern California: Geological Society of America Abstracts with Programs, v. 25, p. 159.

Stop 3-2:

The Oak Creek Debris Flows of July 12, 2008, Independence, Inyo County, CA

Dave Wagner, *California Geological Survey*

Margie DeRose, *Bureau of Land Management and U.S. Forest Service*

Jim Stroh, *The Evergreen College, Emeritus*

Introduction

On July 12, 2008 tropical moisture moved westward across southwestern United States to southern California where it caused thunderstorms and local pockets of intense rain. In the late afternoon, a cell of intense rain was centered on the Oak Creek drainage just north of Independence in Inyo County, California. This area had been burned in an intense, lightning-sparked range fire in July 2007. Around 5 pm, water, sediment, and debris began moving down tributaries in the Oak Creek drainage area, eventually concentrating in the north and south forks of Oak Creek. At about 5:30 pm a hyperconcentrated flow destroyed a motor home parked at the Oak Creek campground on the north fork of Oak Creek, and its sole occupant jumped into the flow but he managed to survive.

By then, the Mt. Whitney Fish Hatchery had been severely damaged along with several Fish and Game employee residences. The Inyo County Register (July 15, 2008) reported that along Oak Creek, 25 homes were destroyed and another 25 were damaged to some extent. Relatively few people were home and amazingly there were no serious injuries or fatalities among the residents. At 5:30 pm, the Independence Volunteer Fire Department received reports of flooding and propane leaks and responded along with Cal Fire personnel to find mud flowing across Highway 395. Boulder-rich debris flows also moved down the south fork of Oak Creek destroying the Bright Ranch. Fortunately, no one was there at the time. Debris flows from the south fork merged with sand-rich hyperconcentrated flows from the north fork near the fish hatchery and filled the channel of Oak Creek. Mud flowed east of Highway 395 through the Ft. Independence Indian Reservation

Remains of the main house at the Bright Ranch on the south fork of Oak Creek.

Mud along north fork of Oak Creek. Mt. Whitney Fish Hatchery in the background. Photo by Ken Babione

eastward, almost reaching the Los Angeles Aqueduct. Highway 395 was closed during the evening and night of July 12 and was subject to restricted travel for over a week.

Extent of the Flows

Rilling of slopes and scouring of stream channels extend up to 3000 m elevation on the escarpment of the Sierra. From the high country, mud moved through the Oak Creek drainage, onto alluvial fans and out into Owens Valley, a distance of over 16 km with 1800 m of relief. Slopes are veneered with aeolian sand, decomposed granite, and ash from last year's fire and the channels are filled with sandy, bouldery sediment that is both fluvial and alluvial. Source areas for the south fork of Oak Creek are underlain by glacial till so flows moving down this part of the drainage contained more and bigger boulders than those in the north fork.

Water and sediment moved down the narrow canyons of the North Fork drainage as a hyperconcentrated flow (40-70 % sediment by weight). At the apex of the fan of the North Fork of Oak Creek the channel turns sharply south and the flow spread across the fan carrying boulders, logs and trees. Flows continued down the channel of the North Fork of Oak Creek which turns east and heads for the Mt. Whitney Fish Hatchery. Just upstream from the hatchery, the debris flow (70-90% sediment by weight) from the south and north forks merged and headed east through the hatchery and destroying homes . Flows then crossed Highway 395, passed through the Ft. Independence Reservation and came to rest in the flat lands west of the Los

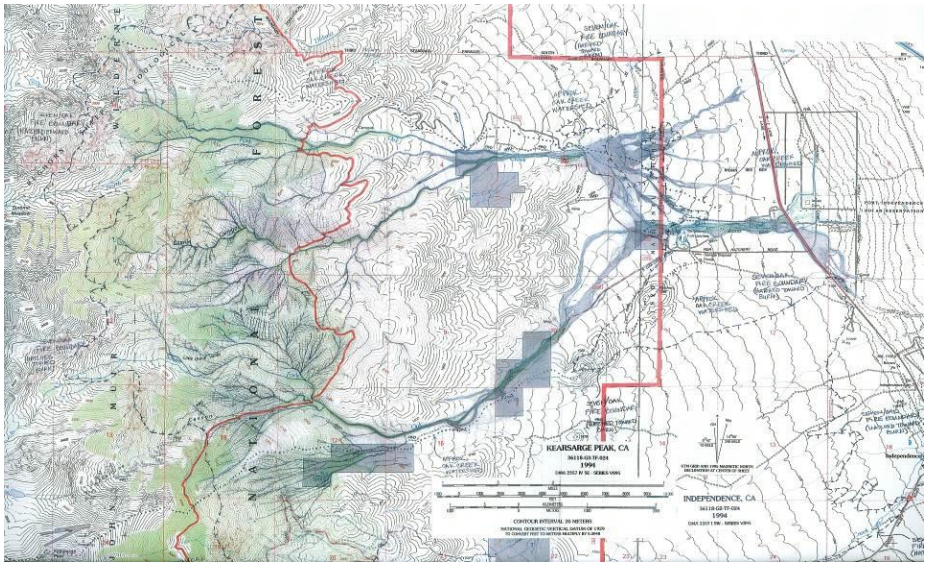

Map of the Oak Creek water-sediment flows of July 12, 2008 and their source areas.

Hyperconcentrated flow from the North Fork of Oak Creek. The Mt. Whitney Fish Hatchery is at the left side of the photo. Flows from the north and south forks of Oak Creek merged just upstream from the hatchery. Photo by Ken Babione.

The man who surfed the flow

At about 5:30 on July 12, 2008, Don Rockwood was preparing dinner in his motor home parked at the Oak Creek campground when a tree crashed through the wall of his motor home. Moments later the motor home came apart and Rockwood jumped into the flow to escape. An accomplished body surfer, he began ride the flow. As he surfed the flow for hundreds of meters, he saw his pickup truck, also swept away, bearing down on him from behind. He was

Don Rockwood, who surfed over a mile in the flow. Photo from the Inyo County Register.

able to steer sideways, avoiding the truck, and managed to reach shallower and slower mud where he was able to stand. A wave, about three feet high, swept him away again, submerging him and smashing him against a rock. Now, suffocating, he thought the end was near but the mud slowed and he was able to stand again, making his way to the Fish Hatchery Road. Most of his clothing had been torn away and his shoes were gone. He knew there would be people at the fish hatchery so he began to walk along the road but soon it became impassable due to flowing mud, probably from the South Fork of Oak Creek. Lightning began to strike nearby and he was shivering so he looked for shelter but there was none. Rockwood decided he must make it to the hatchery so he picked up a branch to use as a pole and headed through the flow toward the hatchery. Mud was up to his chest but he made it through, emerging caked with mud, astonishing a group of fire fighters. He was quickly airlifted to the hospital and treated for major lacerations but otherwise he was ok.

Don Rockwood's truck.

Observations by Don “Rock” Rockwood:

- First “wave” was about 3 feet high; hit his motor home at about 5:30 pm.
- Second “wave,” about 8-12 feet high, hit moments later, destroying the motor home so he jumped into the mud and body surfed about a mile until it slowed enough for him to stand.
- Third “wave,” about 3 feet high, knocked him off his feet; he surfed about another 0.5 mile before he was able to stand.
- After the three “waves” there was a steady flow of mud. Rain had stopped but there were lightning strikes nearby.

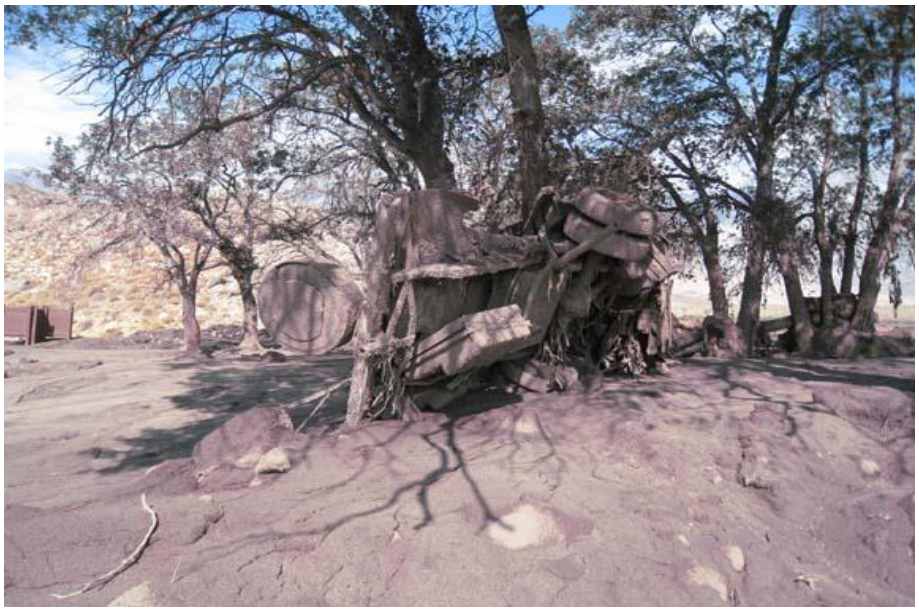

Remains of Don Rockwood's motorhome

North Fork of Oak Creek

The largest single source area for the flow is drained by an unnamed tributary to the North Fork of Oak Creek, here informally referred to as the middle fork of Oak Creek. Extensive rilling occurred on the slopes at elevations mostly between 2000 and 2800 m. Deep incision and scouring in the middle fork is apparent above 2200 m elevation and becomes more pronounced downstream. Below 2000 m elevation incision is typically 5 to 15 m; usually bedrock is exposed at the thalweg. Headward and sideward erosion in the form of slumping is ongoing. Deposits exposed in the walls of the new channel are both fluvial boulder gravel and alluvial debris flows attesting to a history of events such as this one. Calculations based on run-up (superelevation) around channel bends suggest the largest surge was traveling about 12 miles per hour.

Rilling of slopes in Charlie Canyon. Photo by J. DeGraf, USFS

Granitic boulder (~1 cubic m) that came to rest against a tree trunk on the middle Fork of Oak Creek

Bends in the channel of the middle fork of Oak Creek where speed of the flow was estimated by measuring run-up (superelevation).

Deeply incised channel of the middle fork of Oak Creek. Note run up of mud above the new channel

South Fork of Oak Creek

The South Fork of Oak Creek has a different channel morphology than the north fork. It is much wider, as much as 300 to 400 m in places. It had three major sources areas that collectively rival the size of middle fork. Extensive rilling occurred on the slopes below Onion Valley, Sardine Canyon and above Tub Springs. Most of the rilling occurred between 2000 and 2800 m elevation. This area is underlain by boulder-rich glacial till, so the water-sediment flows that moved down the south fork carried more and bigger boulders than in the north fork giving rise to a more complex flow regime. The leading edges of the flows were debris flows with boulder snouts which clogged the stream channel forcing the south fork into a new channel. Hyperconcentrated flows followed the bouldery debris flows and overtopped the boulder plugs. A second avulsion forced sediment out across the fan of the South Fork of Oak Creek.

Sediment from north and south fork of Oak Creek merged west of the Mt. Whitney Fish Hatchery. The South Fork of Oak Creek was forced into a new channel closer to the mountain front. The old channel marked by vegetation near the top of the photo is now abandoned. A second avaulsion caused sediment to flow across the fan of the south fork but it eventually joined Oak Creek just west of the fish hatchery. Photo by Ken Babione.

Damage to homes and Highway 395

Twenty-five homes along Oak Creek just east of the Mt. Whitney Fish Hatchery were reportedly destroyed (Inyo Register, July15, 2008). They were situated very close to the creek and were battered by boulders and logs.

Home destroyed along Oak Creek

Mud and debris filled the Oak Creek channel and new channel was established to the south. The creek was diverted back to its original channel soon after the event by CALTRANS allowing residents to reach their homes. Mud flowed across Highway 395 and through the Ft. Independence Indian Reservation damaging another 25 homes. Mud and water flowed across the highway for days requiring traffic detours or escorts to pass through the area.

Mud flowing across Highway 395 requiring CHP escorts to guide traffic through. Photo by Ken Babione

Acknowledgments

We would like to acknowledge the assistance of those who contributed to this very preliminary investigation: Ken Babione, Don Bright, Dan Holland (CALTRANS), Cheryl Seath (BLM), Lynn Oliver (USFS), Jerry De Graff (USFS), Todd Ellsworth (USFS), Inyo County Sherriff's Department, Inyo County Volunteer Fire Department, and CAL FIRE. Wagner would like to thank Don Rockwood for the interview about his experiences.